

The human immune response to viral vectored vaccine regimens against Ebola virus and Sudan virus in clinical trials



Rebecca Anne Makinson

Linacre College

University of Oxford

A thesis submitted for the degree of

Doctor of Philosophy

Michaelmas Term 2024

Word count: \approx 40,000 (excluding tables, figure legends, references and appendix)

Abstract

Ebola disease (EBOD), caused by viruses of the *Orthoebolavirus* genus, poses a significant public health threat, with the majority of outbreaks caused by the Ebola and Sudan virus species. EBOD is a viral haemorrhagic fever characterised by symptoms including fever, fatigue, internal and external bleeding, and a high case fatality rate of 48.5%. Effective control of Ebola virus and Sudan virus requires a combination of robust public health measures, effective therapeutics and efficacious vaccines. The 2014-2016 Ebola virus epidemic accelerated vaccine efforts towards Ebola virus, ultimately leading to the licensure of two WHO-approved vaccines, rVSV-ZEBOV and Ad26.ZEBOV/MVA-BN-Filo, which were then deployed for use in future outbreaks. However, at the time of writing no vaccines have been approved for use against Sudan virus. This thesis aims to address longstanding questions in the development of vaccines against orthoebolaviruses. First, it evaluates the durability of several key vaccine candidates targeting Ebola virus: the approved Ad26.ZEBOV/MVA-BN-Filo regimen, as well as the experimental candidates cAd3/MVA-BN-Filo and cAd3-EBOZ/Ad26.ZEBOV in UK volunteers and cAd3/MVA-EBO Z in both UK and Senegalese volunteers. Evaluating the durability of Ebola virus vaccines is essential when considering immunisation strategies to incorporate prophylactic immunisation of at-risk individuals such as healthcare or laboratory workers. Durability was assessed between 43 and 62 months, depending on the vaccine, with good durability observed in antigen-specific IgG as well as T cell responses. At the time of writing, this represents the longest term follow-up of any Ebola virus vaccine. In some volunteers, a third ebolavirus vaccine dose in the form of an Ad26.ZEBOV boost was administered between 43 to 48 months after the original prime-boost vaccines. Ad26.ZEBOV induced a strong anamnestic response and boosted T cells and IgG titres to levels above those enumerated at baseline. In a previous study, the immunogenicity of the cAd3-EBOZ/MVA-EBO Z vaccine differed between a UK and Senegalese cohort but data from this thesis indicate these differences were no longer observed following the Ad26.ZEBOV boost. Secondly, this thesis measured the immune response to the glycoproteins from both Ebola virus and Sudan virus induced by vaccination with the novel bivalent vaccine, biEBOV, in a first in-human dose escalation trial. biEBOV was found to be immunogenic towards the glycoprotein from both species, although it did not induce a neutralising antibody response against pseudotyped lentiviruses expressing the Sudan virus

glycoprotein. Together, these findings provide new insight into the durability of potential prophylactic ebolavirus vaccines, and on the development of biEBOV, a key candidate multivalent Sudan and Ebola virus vaccine.

Acknowledgements

This thesis would not have been possible without the incredible support and collaboration of many people. First and foremost, I am deeply grateful to Professor Teresa Lambe, Professor Katie Ewer, Professor Sir Adrian Hill and Dr Amy Flaxman for their outstanding project supervision and mentorship. I am inspired by your work and feel incredibly fortunate to have had the opportunity to learn from each of you.

Starting a DPhil in a pandemic was never going to be straightforward but it was made infinitely easier with the support of the Jenner Institute COVID-19 clinical trial team. Jamie Fowler, Jeremy Aboagye, Federica Cappuccini, Leila Godfrey, Sandra Belij-Rammerstorfer, Marta Ulaszewska, Dr Hannah Sharpe and Danny Wright - thank you for the Friday quiz days, socially distanced lunches and becoming my “lab family” when pandemic restrictions kept us from our own.

A further thanks go to Alex Sampson for his assistance with setting up the pseudotyped lentivirus assays and for providing plasmids and cell lines and to Dr Elizabeth Clutterbuck for her assistance and protocols for the memory B cell ELISpots. My thanks also go to the clinical teams who conducted the study set up and trial visits and to Janssen for donating the Ad26.ZEBOV vaccine used as the delayed booster. This thesis would also not be possible without the participation of the volunteers in Oxford, London and Dakar.

Lastly a huge thank you to my lovely family – thank you for encouraging me to study science at university, for all your encouragement throughout every stage of my career but most importantly for your unwavering moral support over the last four years. I have never been in any doubt that you will be proud of me no matter which path I take through life.

Table of Contents

1. Introduction	22
Orthoebolaviruses and Ebola disease	22
Genome organisation	25
sGP/GP gene products	26
Filovirus Tropism	28
Ebola virus (EBOV)	29
Treatments	29
Vaccines targeting EBOV	30
rVSV-ZEBOV (Ervebo)	32
Ad26.ZEBOV/MVA-BN-Filo (Zabdeno/Mvabea)	33
cAd3-EBO Z (+/- MVA-BN-Filo or MVA-EBO Z)	35
Vaccine Induced Immune Correlates of protection	35
Sudan virus (SUDV)	37
Treatments	37
Vaccines targeting SUDV	38
ChAdOx1 biEBOV	39
Correlates of protection	39
Thesis Aims and Outline	40
2. Materials and Methods	42
Materials	42
Reagents	42
Antigens	47
Plasmids	47
Buffers, solutions, and cell media	48
Methods	48
Immunology	49
Whole Blood Separation – isolation of PBMC and plasma	49
PBMC cryopreservation	49
Serum collection	49
PBMC thawing	50
Anti-EBOV GP and anti-SUDV GP total IgG ELISA	50
Avidity ELISA	51

CMV ELISA	52
Plasma Heat Inactivation	53
Pseudovirus Neutralisation assay	53
Memory B Cell Culture	54
Memory B Cell ELISpot	55
Peptide Preparation	55
Ex-vivo IFN- γ ELISpot assay	56
Peptide Mapping	57
In silico HLA restriction predictions	57
Flow Cytometry with Intra-cellular Cytokine Staining (ICS).....	58
Molecular Biology	61
Endonuclease Restriction Digests	61
Agarose Gel Electrophoresis	61
Agarose Gel Extraction.....	61
DNA ligation	62
DNA concentration quantification	62
Bacterial Transformation.....	62
Plasmid DNA preparations	63
Plasmid Sequencing.....	63
Production of Lentiviral Pseudotypes.....	63
Titration of Lentiviral Pseudotypes	64
Western Blotting.....	64
DNA extraction from PBMC	65
HLA typing.....	65
Image creation	66
Statistics.....	66

3. Durability of the immune response to three cAd3-EBO Z prime-boost regimens and the administration of an Ad26.ZEBOV boost in UK volunteers. 67

Introduction 67

Study-Specific Methods 68

 REVOLVE clinical trial design..... 68

Results 71

 Recruitment

 Humoral Immunology

 T Cell immunology.....

Discussion 84

Conclusions	87
4. Durability of cAd3-EBO Z/MVA-EBO Z and the administration of a delayed Ad26.ZEBOV boost in Senegalese adults.....	89
Introduction	89
Human Cytomegalovirus.....	89
EBL06 Clinical Trial	90
Objectives:.....	91
Study-Specific Methods	92
RESOLVE clinical trial design.....	92
REVOLVE clinical trial design	93
Results	93
Recruitment	93
Humoral Immunology	94
Binding IgG Antibodies.....	94
T cell immunology.....	97
Responses in Senegalese volunteers compared to UK volunteers.	103
CMV and vaccination response	104
Discussion	109
Comparisons between the UK and Senegalese Volunteers	112
CMV positivity and Immunogenicity to ebola vaccination.....	113
Conclusions	116
5. Durability of the Immune Response to Ad26.ZEBOV /MVA-BN-Filo up to 46 months post-prime.....	117
Introduction	117
EVOLVE Study.....	117
Objectives	118
Study Specific Methods	118
PRISM clinical trial design	118
Results.....	119
Recruitment	119
Durability to EBOV	120
Humoral Immunogenicity	120

Memory B cells.....	122
Durability of T Cell Responses	123
Durability of immune responses to SUDV.....	126
Humoral Responses	127
T cell responses	128
Discussion	135
Durability to EBOV	135
Durability to SUDV	136
SUDV T cell peptide mapping	137
Conclusions	140
6. <i>First-in-human immunogenicity data against a bivalent orthoebolavirus vaccine targeting both Ebola virus and Sudan virus (ChAdOx1 biEBOV)</i>.....	141
Introduction	141
Methods.....	142
EBL07 Trial Study Design.....	142
Objectives.....	143
Results.....	143
Recruitment	143
Humoral Immunogenicity to biEBOV.....	144
T Cell Immunogenicity to biEBOV	147
Discussion	150
Conclusion.....	154
7. <i>Summary of Findings, Implications and Future Directions</i>	155
Durability	155
Future directions for durability work.....	159
Multivalent vaccines.....	160
Future directions for multivalent vaccine work	161
8. <i>Supplementary Chapter</i>.....	163
Set-up and Qualification of an ELISA to measure anti-SUDV IgG	163
Introduction	163
Materials and Methods	164

Anti-SUDV GP IgG ELISA procedure	164
Antigen	164
Standard Pool & Positive Control	164
Test Samples	164
Parameter definitions.....	165
Linearity	166
Precision	168
Robustness	169
Comparability of matched plasma and serum.....	169
Sample stability from repeated freeze-thaw cycles.....	170
Assay cut-off	171
Ongoing Assay Monitoring.....	173
Discussion	174
Supplementary Figures and Tables	192

List of Tables

Table 1.1: Outbreaks of Ebola Disease in humans, subdivided by virus species. Source data obtained from Centers for Disease Control and Prevention (CDC) [26] accessed March 24 th 2024.....	23
Table 1.2: A snapshot of some of the key vaccine candidates targeting EBOV which are currently in or have completed human clinical trials. Vaccines which are studied as part of this thesis are underlined.	31
Table 1.3: A list of the vaccine candidates targeting SUDV which are currently being evaluated in human clinical trials. rVSV-SUDV is included despite not yet entering clinical trials as the WHO has prioritised it for clinical testing as the basis of the efficacy of rVSV-ZEBOV. Vaccines which are studied as part of this thesis are underlined.....	38
Table 1.4: A summary of the trials and parent trials which are the focus of this thesis. Long-term follow-up data is available for EVOLVE (in the PRISM trial), EBL01, EBL04, EBL05 (in the REVOLVE trial) and EBL06 (in the RESOLVE trial). EBL07 is not a long-term follow-up trial and instead assesses the immunogenicity of ChAdOx1 biEBOV up to a maximum of 364- days post vaccination.....	41

Table 2.1: Materials and reagents used in this thesis	42
Table 2.2: Antigens used for in-house ELISA assays and their source.....	47
Table 2.3: Plasmids used to create pseudotyped lentiviruses viruses and their source.	47
Table 2.4: Intracellular and extracellular stains for the ICS panel.....	60
Table 3.1: Volunteer demographics in the REVOLVE clinical trial. Age on the date first clinical trial visit for REVOLVE is shown.	72
Table 4.1: Volunteer demographics for the RESOLVE clinical trial. Age on the date of the first clinical trial visit for RESOLVE.....	94
Table 4.2: Volunteer demographics in the RESOLVE and REVOLVE clinical trials. Age on the date first clinical trial visit for RESOLVE or REVOVLE is shown.....	105
Table 4.3: CMV serostatus data at the time of enrolment into parent study and at the time of administration of Ad26.ZEBOV boost (time of enrolment into the REVOLVE or RESOLVE clinical trials) stratified by country of recruitment.	106
Table 5.1: Volunteer Demographics at time of first PRISM visit by subgroup. Age is recorded at the time of enrolment into the PRISM study. Prime and boost vaccinations were administered as part of the EVOVLE clinical trial.....	120
Table 6.1: Demographic information for the EBL07 clinical trial. Data is presented as n (%) or range (median).	144
Table 7.1: A summary of the EBOV GP IgG seropositivity rate in vaccine regimens as measured across multiple chapters of this thesis.....	157
Table 7.2: A summary of the T cell response to peptides spanning EBOV GP as measured by ELISpot using freshly isolated PBMC.....	158

List of Figures

Figure 1.1: Schematic of the genome organisation of SUDV and EBOV. The single stranded RNA genome contains seven genes which are represented by boxes. Non-coding and intergenic regions are shown as a black line. Three open reading frames and proteins are

available in the GP gene, indicated here by asterisks, and are generated through transcriptional editing (further detail is available in section 0). The RNA genome schematic was informed by previously published images [27, 32] and the figure was generated for this thesis using BioRender.com. 26

Figure 3.1: Schematic showing the outline and vaccination schedule for the EBL01, EBL04 and EBL05 parent trials and the REVOLVE clinical trial. Blood draws for the boosted and unboosted groups are depicted as red droplets in a time course table. 70

Figure 3.2: anti-EBOV GP IgG as measured by in house standardised ELISA. Circles denote volunteers who received an Ad26.ZEBOV boost in the REVOLVE trial, squares denote volunteers who opted out of an Ad26.ZEBOV boost and are 'unboosted'. Dark blue shapes represent volunteers recruited from EBL01, green shapes represent volunteers recruited from EBL04 and light blue shapes represent volunteers recruited from EBL05. In all cases lines represent geometric means and bars show 95% confidence intervals. A) Durability of ELISA titres and rates of seropositivity at the first time point in all volunteers by original trial. B) ELISA units over time in boosted and unboosted EBL01 and EBL04 volunteers. In boosted volunteers, Ad26.ZEBOV was administered at D0. Shapes show geometric means C) ELISA units at the final time point (365 days after enrolment in REVOLVE) in EBL01 and EBL04 volunteers who did and did not receive an Ad26.ZEBOV boost. Asterisks show statistical significance with Mann Whitney test. **** P<0.0001. 74

Figure 3.3: anti-EBOV GP IgG as measured by in house standardised ELISA measured over the three vaccinations in the parent and current study. A. EBL01 volunteers (vaccine schedule: cAd3-EBOZ, MVA-BN-Filo, Ad26.ZEBOV) B. EBL04 volunteers (vaccine schedule cAd3-EBOZ, MVA-BN-Filo, Ad26.ZEBOV). 75

Figure 3.4: Avidity of IgG antibodies to EBOV-GP. Individual data points were expressed as an IC50 and shown here as scatter dot plots. Asterisk shows significant difference as determined by two-tailed Wilcoxon paired test *, P=0.0425. 76

Figure 3.5: Pseudoneutralisation of EBOV GP-bearing lentiviral pseudotypes at day of, and 7 days post-boost. Shapes represent neutralisation IC50 with lines showing median. A) IC50 in EBL01 and EBL04 boosted volunteers at long term follow-up/time of Ad26.ZEBOV vaccination and 7 days post boost Asterisks show statistical significant as measured by Wilcoxon signed rank test ***P=0.005. B) Correlation between pseudoneutralisation IC50

and antigen specific binding IgG with aggregated data from day of boost and 7 days post boost..... 77

Figure 3.6: EBOV GP-specific IFN- γ T cell responses as measured in PBMC by IFN- γ ELISpot. Circles denote volunteers who received an Ad26.ZEBOV boost in the REVOLVE trial, squares denote volunteers who opted out of an Ad26.ZEBOV boost and are 'unboosted'. Dark blue shapes represent volunteers recruited from EBL01, green shapes represent volunteers recruited from EBL04 and light blue shapes represent volunteers recruited from EBL05. In all cases lines represent geometric means and bars show 95% confidence intervals. A) Durability of the T cell response at the first time point in all volunteers by original trial. B) T cell response over time in boosted and unboosted EBL01 and EBL04 volunteers. In boosted volunteers, Ad26.ZEBOV was administered at D0. Shapes show geometric means C) T cell response at the final time point (365 days after enrolment in REVOLVE) in EBL01 and EBL04 volunteers who did and did not receive an Ad26.ZEBOV boost. Asterisks show statistical significance with Mann Whitney test. *** $P= 0.0006$ 79

Figure 3.7: EBOV GP-specific IFN- γ T cell responses as measured in PBMC by IFN- γ ELISpot over the three vaccinations in the parent and current study. A. EBL01 volunteers (vaccine schedule: cAd3-EBOZ, MVA-BN-Filo, Ad26.ZEBOV) B. EBL04 volunteers (vaccine schedule cAd3-EBOZ, MVA-BN-Filo, Ad26.ZEBOV). 80

Figure 3.8: Heat map of responses to individual peptide pools spanning the EBOV GP at: A. 7 days after cAd3-EBOZ/MVA-BN-Filo (EBL01) cAd3-EBO Z/ MVA-EBO Z (EBL04), or cAd3-EBOZ/Ad26.ZEBOV (EBL05) vaccination or B. 7 days after Ad26.ZEBOV vaccination (REVOLVE clinical trial). Panel C shows fold change in SFC between responses 7 days after MVA boost in the EBL01, EBL04 and EBL05 trials and 7 days after Ad26.ZEBOV vaccination in the REVOLVE trial. Lines show median with whiskers showing range..... 81

Figure 3.9: ICS analysis in EBL01 and EBL04 boosted volunteers, 28 days after Ad26.ZEBOV vaccination. A. The proportions of CD4+ and CD8+ T cells that secreted any combination of interferon- γ , interleukin-2, and TNF in EBL01 or EBL04 volunteers 28 days after boosting with Ad26.ZEBOV. B. The proportion of CD8+ cells secreting CD107a (LAMP1)..... 83

Figure 4.1: Schematic showing the outline and vaccination schedule for the EBL06 (parent trial) and RESOLVE clinical trials..... 93

Figure 4.2: anti-EBOV GP IgG as measured by in house standardised ELISA. Triangles represent individual data points; lines show geometric means with bars showing 95%

confidence intervals. Arrows indicate time points where a vaccination was administered. Dotted line shows the seropositive cut-off. 96

Figure 4.3: Avidity of IgG antibodies to EBOV-GP. Individual data points were expressed as an IC50 and shown here as scatter dot plots. Significant difference was determined by two-tailed Wilcoxon test ($P=0.0634$). 97

Figure 4.4: EBOV GP-specific IFN- γ T cell responses as measured in PBMC by ELISpot. Triangles represent individual data points; lines show geometric mean with bars representing 95% confidence intervals. Arrows indicate time points where a vaccination was administered. 99

Figure 4.5: Heat map of responses to individual peptide pools spanning the EBOV GP at: A. 7 days after cAd3-EBO Z/ MVA-EBO Z vaccination (EBL06 trial) or B. 7 days after Ad26.ZEBOV vaccination (RESOLVE clinical trial). Panel C shows fold change in SFC between responses 7 days after MVA boost in the EBL06 trial and 7 days after Ad26.ZEBOV vaccination in the RESOLVE trial. Lines show median with whiskers showing range. 101

Figure 4.6: Results from flow cytometry with ICS. A. The proportions of CD4+ and CD8+ T cells that secreted any combination of interferon- γ , interleukin-2, and TNF 28 days after boosting with Ad26.ZEBOV. B. CD107a expression as a percentage of CD8+ T cells at 28 days after boosting with Ad26.ZEBOV. 102

Figure 4.7: Comparison between the primary immunology outcomes A. tIgG ELISA and B. IFN- γ ELISpot) between the UK and Senegalese cohorts receiving Ad26.ZEBOV boost as part of the REVOLVE and RESOLVE clinical trials. Lines show geometric means with bars showing 95% CI. Time on the x-axis represents time from Ad26.ZEBOV boost in days. 104

Figure 4.8: anti-CMV IgG units at the time of enrolment into the RESOLVE and REVOLVE studies as generated by ELISA. Dashed lines indicate the seropositive threshold set as 11 standard units as defined by the ELISA manufacturer's instructions. Red shapes represent volunteers that have seroconverted in the 4.25 years since they were last serotyped A. anti-CMV IgG titres stratified by country of recruitment. B. Relationship between CMV IgG titre and age in each population, triangles represent Senegalese volunteers, circles represent UK volunteers. No correlation was found between age and anti-CMV IgG (Spearman's rank analysis, all UK volunteers $r:-0.07$, $P=0.61$, Senegal $r:0.29$, $P=0.13$). 106

Figure 4.9: Effect of CMV serostatus on the peripheral T cell repertoire. T cell populations from isolated PBMC were assessed by flow cytometry in UK CMV-seropositive (CMV+) and

CMV-seronegative (CMV-) individuals as well as in Senegalese volunteers who were all CMV+. A. CD4+ as a percentage of CD3+ T cells B) CD8+ as a percentage of CD3+ T cells C) CD4:CD8 ratio. Volunteers below the dotted line have an inverted ratio. D) The mean relative prevalence of CD4+ T cell subsets by cohort and CMV serostatus. E) The mean relative prevalence of CD8+ T cell subsets by cohort and CMV serostatus. Associations between groups and T cell subsets were assessed by Kruskal-Wallis with Dunn's multiple comparisons post-hoc. *p < 0.05. 108

Figure 4.10: Immune responses stratified by CMV serotype in UK volunteers at day of Ad26.ZEBOV boost (cAd3-EBO Z / MVA-EBO Z long term follow-up) or at the peak measured response A. IgG titres at long term follow-up B. ELISpot responses at long term follow-up C. IgG titres at 7 days post boost D. ELISpot responses at 7-days post-boost. P numbers are shown above the plots as determined by Mann Whitney U test. 109

Figure 5.1: Schematic showing the outline and vaccination schedule for the subset of the EVOLVE (parent trial) and PRISM clinical trial groups presented in this chapter. EBOV = Ebola virus, SUDV = Sudan virus, TAFV = Tai Forest virus, MARV = Marburg virus. GP = glycoprotein, NP = nucleoprotein. 119

Figure 5.2: anti-EBOV GP IgG as measured by in house standardised ELISA. Shapes represent individual data points; circles, squares and triangles represent volunteers who originally received a 28, 56 and 84-day interval between their Ad26.ZEBOV prime and MVA-BN-Filo boost respectively. Lines show geometric means with bars showing 95% confidence intervals. The dotted line shows the seropositive cut-off (166 ELISA Units)..... 121

Figure 5.3: Pseudoneutralisation of EBOV GP-bearing lentiviral pseudotypes. Shapes represent neutralisation IC50 with lines showing median. A) IC50 by prime-boost interval at 40 months post vaccination. B) Correlation between pseudoneutralisation IC50 and antigen specific binding IgG..... 122

Figure 5.4: EBOV-GP specific IgG-BMEM response A. BMEM response at the two time points by prime-boost interval. Lines show median with bars showing interquartile range B. Time course from EVOLVE trial to PRISM cohort 3 trial for a subset of 18 volunteers for whom memory B cell ELISpots were carried out in the parent study. Shapes show medians with lines showing interquartile range. Asterisks indicate statistically significant differences determined by Friedman's test with Dunn's multiple comparisons post hoc ***p<0.0001. 123

Figure 5.5: T cell responses measured by IFN- γ ELISpot assay to peptides spanning the EBOV GP. Circles, squares and triangles represent volunteers who originally received a 28, 56 and 84-day interval between their Ad26.ZEBOV prime and MVA-BN-Filo boost respectively. A) Primary data generated from the PRISM C3 trial B) A time course from EVOLVE trial to PRISM cohort 3 trial for a subset of 24 volunteers for whom ELISpots were carried out on the same SOP for the original regimen. C) Heat map of responses to individual peptide pools in all volunteers spanning the EBOV GP at 40 months post-prime. 125

Figure 5.6: T cell responses to EBOV GP as measured by flow cytometry with ICS at the first time point (40 months). Lines show geometric mean with bars showing 95% confidence intervals. The dotted line shows the assay's LLoD. A) Percentage of CD4+ or CD8+ T cells producing any combination of IFN- γ , IL-2, or TNF in response to stimulation with peptides spanning the EBOV glycoprotein at the first time point by parent trial prime-boost interval dose. B) CD107a expression as % of CD8+ T cells by prime-boost interval. 126

Figure 5.7: anti-SUDV GP IgG measured by in house standardised ELISA. Shapes represent individual data points; circles, squares and triangles represent volunteers who originally received a 28, 56 and 84-day interval between their Ad26.ZEBOV prime and MVA-BN-Filo boost respectively. Lines show geometric means with bars showing 95% confidence intervals. The dotted line shows the seropositive cut-off (72 ELISA units). A) Responses at the two long term follow-up time points by prime-boost interval. B) Data from all groups combined at both time points and responses from orthoebolavirus naïve volunteers used as control samples. Asterisk indicates a statistically significant difference determined by Kruskal-Wallis with Dunn's multiple comparisons post hoc * P=0.0221 C) Anti-SUDV GP and anti-EBOV GP IgG at the first long term follow-up time point. Significant correlation was determined by Spearman's correlation test. 128

Figure 5.8: T cell responses measured by IFN- γ ELISpot assay to peptides spanning the SUDV GP. Circles, squares and triangles represent volunteers who originally received a 28, 56 and 84-day interval between their Ad26.ZEBOV prime and MVA-BN-Filo boost respectively. A) Responses at the two long term follow-up time points by prime-boost interval. B) Data from all groups combined at both time points and responses from orthoebolavirus naïve volunteers used as control samples. Asterisks indicate statistically significant differences determined by Kruskal-Wallis with Dunn's multiple comparisons post hoc *** P=0.0002 ***p<0.0001. C) Heat map of responses to individual peptide pools spanning the SUDV GP in

the ELISpot assay for all volunteers at 40 months post-prime. D) T cell responses to the SUDV GP and EBOV GP at 40 months post prime. Significant correlation was determined by Spearman's correlation test $**P=0.0015$ 130

Figure 5.9: Immunodominant regions of T cell recognition in the Sudan virus glycoprotein (SUDV Gulu). (A) The frequency of responders was calculated as the percentage of volunteers assayed for a peptide with an ELISpot response above the cut off (mean + 3 standard deviations of the negative controls of the sample set). The x-axis label indicates the position in the glycoprotein of the first amino acid in the peptide. Peptides spanning amino acids 351 - 514 were not tested at the individual multimer level as no responders were found to the mega pool. (B) 2D representation of the key domain organizations of the SUDV GP. SP = signal peptide, IFL= internal fusion loop TM= transmembrane domain. 132

Figure 5.10: Details of positive peptides identified in this work. A) Table detailing peptides and their percentage amino acid identity with other sequenced SUDV strains, and the other five orthoebolaviruses to show intra or inter-species conservation. The accession and sequence data for SUDV sequences used for analysis of intra-species conservation are: 1976 Nzara-Boniface: MH121162, 1976 Nzara-Maridi: MK952150, 1979 Maleo: KC242783, 2004 Yambio: MH121169, 2012 Kibaale: KC545389-91, 2012 Luwero: KC589025, 2011 Nakisamata: JN638998 and 2022 Mubende: WEY06140. Orthoebolavirus sequences for inter-species analysis are: EBOV: Q05320, BDBV: B8XCNO, TAFV: Q66810, RESTV: Q66799 and BOMV: A0A4D5SG72. B) UpSet plot to visualise the inter-species data from (A) all putative epitopes identified in peptides showing their conservation across the six members of the Genus Orthoebolavirus. On the x-axis, each column represents a different combination of species (rows), showing which peptides are part of a given combination (displayed by filled circles in the combination matrix). The bar height corresponds to the number of peptides identified to be 100% conserved with the given species combination. Each combination is mutually exclusive. The total number of peptides to be 100% conserved with each individual antigen is indicated as a horizontal bar at the bottom left of each subpanel. Plot was created with Python 3.13. 133

Figure 5.11: HLA allele frequency in the participants chosen for single peptide analysis (N=9) HLA class I frequency for A, B and C loci are shown in panels (A), (B) and (C), respectively. HLA class II frequency for DQ and DRB1 loci are shown in panels (D), (E) respectively..... 134

Figure 6.1: Infographic representation of ChAdOx1 biEBOV vaccine..... 143

Figure 6.2: Anti-filovirus IgG as measured by in-house standardised enzyme-linked immunosorbent assay (ELISA). Shapes represent geometric means with error bars showing 95% confidence intervals. Arrows indicate vaccination time points. A. Anti-EBOV GP IgG following one dose of biEBOV B. Anti-EBOV GP IgG following two doses of biEBOV administered at D0 and D84 C. Anti-SUDV GP IgG following one dose of biEBOV D. Anti-SUDV GP IgG following two doses of biEBOV administered at D0 and D84. 146

Figure 6.3: Pseudoneutralisation of EBOV GP-bearing lentiviral pseudotypes. Pseudoneutralisation of EBOV GP-bearing lentiviral pseudotypes as measured by in-house neutralisation assay. Shapes represent neutralisation IC50 with lines showing median..... 147

Figure 6.4: T cell responses to SUDV and EBOV GP as measured by flow cytometry with ICS. Lines show median. Percentage of T cells producing any of IFN- γ , IL-2, or TNF in response to stimulation with peptides spanning either the EBOV and SUDV glycoprotein at baseline (D0) and at 2 weeks post-vaccination (D14) and at two weeks post boost (D98) by dose. A) CD4+ T cell responses to EBOV GP peptides. B) CD4+ T cell responses to SUDV GP peptides. C) CD8+ T cell responses to EBOV GP peptides. D) CD8+ T cell responses to SUDV GP peptides. 149

List of abbreviations

Ad26	Human adenovirus serotype 26
aEU	Arbitrary ELISA unit
BDBV	Bundibugyo virus (<i>Orthoebolavirus bundibugyoense</i>)
Bmem	Memory B cells
BOMV	Bombali virus (<i>Orthoebolavirus bombaliense</i>)
CD	Cluster of differentiation
CFR	Case Fatality Rate
cGMP	Current Good Manufacturing Practice
ChAd3/cAd3	Chimpanzee Adenovirus type 3
CI	Confidence Interval
CMV	<i>Cytomegalovirus</i>
CoP	Correlate of Protection
CV	Coefficient of variation
DC-SIGN	Dendritic Cell-Specific Intercellular Adhesion Molecule-3-Grabbing Non-Integrin
DMEM	Dulbecco's Modified Eagle Medium
DMSO	Dimethyl sulfoxide
DPBS	Dulbecco's Phosphate Buffered Saline
DRC	Democratic Republic of the Congo
EBOD	Ebola disease
EBOV	Ebola virus (<i>Orthoebolavirus zairense</i>)
ELISA	Enzyme-linked immunosorbent assay
ELISpot	Enzyme-Linked Immunosorbent Spot
EMA	European Medicines Agency
EVD	Ebola Virus Disease
FACS	Fluorescence-Activated Cell Sorting
FCS	Fetal calf serum
FDA	Food and Drug Administration
FNA	Fine needle aspirate

FSC	Forward scatter
GMT	Geometric mean titres
GP	Glycoprotein
HIV	Human Immunodeficiency Virus
HLA	Human leukocyte antigen
HRP	Horseradish peroxidase
IC50	Half-maximal inhibitory concentration
ICS	Intracellular cytokine staining
IFN- γ	Interferon gamma
Ig	Immunoglobulin
IL-2	Interleukin-2
IQR	Interquartile range
LAMP1	Lysosomal-associated membrane protein 1
LLoD	Lower limit of detection
LLPC	Long-lived plasma cell
mAb	Monoclonal antibody
MARV	Marburg virus (<i>Orthomarburgvirus marburgense</i>)
MERS	Middle east respiratory syndrome
MHC	Major Histocompatibility Complex
MVA	Modified Vaccinia virus Ankara
MVA-BN-Filo	Modified Vaccinia Ankara-Bavarian Nordic multivalent Filovirus vaccine
MVA-EBO Z	Modified Vaccinia Ankara monovalent EBOV vaccine
NHP	Non-human primate
NPC1	Niemann-Pick C1 protein
OD	Optical Density
PBMC	Peripheral blood mononuclear cell
PFU	Plaque forming units
pVN	Pseudovirus neutralisation assay
QC	Quality control
RBD	Receptor Binding Domain

RESTV	Reston virus (<i>Orthoebolavirus restonense</i>)
RPMI	RPMI Roswell Park Memorial Institute media
RNA	Ribonucleic acid
RPM	Revolutions per minute
RT	Room temperature
SAGE	The Strategic Advisory Group of Experts on Immunization
SARS-CoV-2	Severe Acute Respiratory Syndrome Coronavirus 2
SEB	Staphylococcal Enterotoxin B
SFC	Spot forming cells
sGP	Soluble glycoprotein
SOP	Standard operating procedure
SP	Signal peptide
SSC	Side scatter
ssGP	Small soluble glycoprotein
SUDV	Sudan virus (<i>Orthoebolavirus sudanense</i>)
TAFV	Tai Forest virus (<i>Orthoebolavirus taiense</i>)
TCID	Tissue Culture Infective Dose
T _{CM}	Central memory T cell
T _{EM}	Effector memory T cell
T _{EMRA}	Effector memory T cells re-expressing CD45RA
tlgG	Total Immunoglobulin G
TIM1	T-cell immunoglobulin mucin receptor 1
TLR4	Toll-like receptor 4
T _N	Naïve T cell
TNF	Tumour Necrosis Factor
UK	United Kingdom
vp	Viral particles
VSV	Vesicular Stomatitis Virus
WHO	World Health Organization

Manuscript published from this thesis:

The following manuscript has been accepted for publication in the Lancet Microbe and includes work included in this thesis:

Jenkin D.*, **Makinson R.***, Sanders H., Sampson A., Platt A., Tran N., Dinesh T., Mabbett R., Lawrie A., Quaddy J., Poulton I., Berrie E., Cicconi P., Lambe T. **Safety and immunogenicity of a bivalent Zaire and Sudan ebolavirus ChAdOx1 vectored vaccine in adults: an open-label, non-randomised, first-in-human phase 1 clinical trial.** The Lancet Microbe.

* Joint first authorship

Statement of Authorship

This thesis has been composed by Rebecca Makinson and all work presented is that of Rebecca Makinson, unless stated otherwise. Clinical trials were designed by the clinical trials clinicians. Clinical trials regulatory and ethics applications, and clinical care and collection of demographic data were conducted by the clinical trials team, clinicians and research nurses. Design of immunological work, running of cellular and antibody assays, statistical analyses and interpretation were conducted by Rebecca Makinson. Clinical trial blood processing and ELISpots required for the primary clinical trial outputs were conducted by Rebecca Makinson and aided by clinical trials research assistants. For the RESOLVE study ELISpots and flow cytometry were conducted on site in Senegal by the IRESSEF team and then all plate reading, gating, QC, serology and formal analysis was conducted by Rebecca Makinson. Pseudotyped lentivirus assays for the EBL07 clinical trial were conducted by Alexander Sampson. All other assays were conducted by Rebecca Makinson.

1. Introduction

Orthoebolaviruses and Ebola disease

The genus *Orthoebolavirus*, (formerly known as *Ebolavirus*) is classified within the family Filoviridae and comprises of six known species: *Orthoebolavirus zairense* (Ebola virus [EBOV]), *Orthoebolavirus sudanense* (Sudan virus [SUDV]), *Orthoebolavirus bundibugyoense* (Bundibugyo virus, [BDBV]), *Orthoebolavirus taiense* (Tai Forest virus [TAFV]), *Orthoebolavirus restonense* (Reston virus [RESTV]) and *Orthoebolavirus bombaliense* (Bombali virus [BOMV]). Four species - EBOV, SUDV, BDBV and TAFV- are known to cause Ebola disease (EBOD) in humans (Table 1.1). Of the remaining two, RESTV causes lethal disease in non-human primates, shows mild virulence in pigs, but has been documented as avirulent in all known cases of exposed humans [1-4]. Finally, BOMV, identified in 2018 in the Bombali District of Sierra Leone among free-tailed bats, particularly the *Mops condylurus* and *Chaerephon pumilus* species, shares 55–59% nucleotide identity with other orthoebolaviruses. No naturally occurring BOMV isolates have been cultured to date, but infectious BOMV has been generated using recombinant DNA technology. While its glycoproteins have been proven to facilitate entry into human cells *in vitro*, there has been no evidence of BOMV infections in humans or other animals [5, 6].

Among the four viruses known to cause EBOD in humans, EBOV and SUDV have been the causative agents of 25 and 8 outbreaks respectively between 1976 to present-day, accounting for the vast majority of total orthoebolavirus outbreaks (Table 1.1) and therefore are the focus of this thesis. SUDV and EBOV are zoonotic and multiple species of bat are thought to be possible reservoir hosts responsible for spillover events [7-9]. Once a human is infected, human-to-human transmission occurs primarily through direct contact with bodily fluids of EBOD infected individuals, cadavers or fomites [10, 11]. Healthcare workers have historically been at particularly high risk due to their increased potential for exposure to infectious fluids [12].

EBOD has an incubation period of 2 – 21 days and presents similarly regardless of whether the infection is with SUDV or EBOV [13, 14]. The disease typically begins with a

nonspecific febrile illness, with fever, fatigue, muscle pain and malaise being the most common symptoms. These are then followed by severe gastrointestinal symptoms [15]. In some patients, who are often highly viraemic with dysregulated immune responses, both internal and external bleeding can occur, and EBOD can progress to a complex multiple organ dysfunction syndrome that may be fatal [16]. A subset of patients develop robust immune responses leading to clinical improvement [15]. However, recovery can be hindered by long-lasting clinical sequelae such as arthralgia, ocular and neurological complications [17] and/or virus persistence in immune-privileged sites, which can result in disease flares or the initiation of new chains of infection via sexual transmission [18-21]. Survivors have also been reported to experience a myriad of social issues due to the stigmatisation associated with the disease [22-24].

The mean case fatality rates (CFRs) in confirmed cases from 1976–2022 is 66.6% [95% CI 55.9–76.8] for EBOV and 48.5% [95% CI 38.6–58.4] for SUDV, although CFRs have been heterogenous across outbreaks [25].

Table 1.1: Outbreaks of Ebola disease in humans, subdivided by virus species. Source data obtained from Centers for Disease Control and Prevention (CDC) [26] accessed March 24th 2024.

Country	Cases	Deaths	Year
Bundibugyo virus			
Uganda	149	37	2007
Dem. Rep. of the Congo	36	13	2012
Sudan virus			
Sudan (present day South Sudan)	284	151	1976
Sudan (present day South Sudan)	34	22	1979
Uganda	425	224	2000
Sudan (present day South Sudan)	17	7	2004

Uganda	1	1	2011
Uganda	6	3	2012
Uganda	11	4	2012
Uganda	164	55	2022
Tai Forest virus			
Côte d'Ivoire (Ivory Coast)	1	0	1994
Ebola virus			
Zaire (present day DRC)	318	280	1976
Zaire (present day DRC)	1	1	1977
Gabon	52	31	1994
Zaire (present day DRC)	315	250	1995
South Africa	2	1	1996
Gabon	60	45	1996
Gabon	37	21	1996
Republic of Congo	57	43	2001
Gabon	65	53	2001
Republic of Congo	143	128	2002
Republic of Congo	35	29	2003
Dem. Rep. of the Congo	264	187	2007
Dem. Rep. of the Congo	32	15	2008
Dem. Rep. of the Congo	66	49	2014
Multiple countries*	28646	11323	2014-2016
Dem. Rep. of the Congo	8	4	2017
Dem. Rep. of the Congo	54	33	2018
Dem. Rep. of the Congo & Uganda	3470	2287	2018-2020

Dem. Rep. of the Congo	130	55	2020
Dem. Rep of the Congo	11	9	2021
Dem. Rep of the Congo	12	6	2021
Guinea	23	12	2021
Dem Rep of the Congo	1	1	2022
Dem Rep of the Congo	5	5	2022

*Countries with widespread transmission were Guinea, Liberia and Sierra Leone.

Countries with limited local cases were Italy, Mali, Nigeria, Senegal, Spain, the United Kingdom and the United States.

Genome organisation

The viral genomes of SUDV and EBOV are approximately 19 kb long, linear, non-segmented negative sense, single-stranded RNA containing seven genes: nucleocapsid protein (NP), polymerase cofactor viral protein 35 (VP35), matrix protein VP40, glycoprotein (GP), VP30, VP24, and the large RNA-dependent RNA polymerase (L), as shown in Figure 1.1 [27]. The genomes also contain short noncoding regions at the 3' and 5' ends, known as the 3' leader and the 5' trailer, which contain essential regulatory elements for genome replication and transcription [28, 29]. Of the gene products, GP has the lowest amino acid sequence identity and similarity between SUDV and EBOV [30, 31].

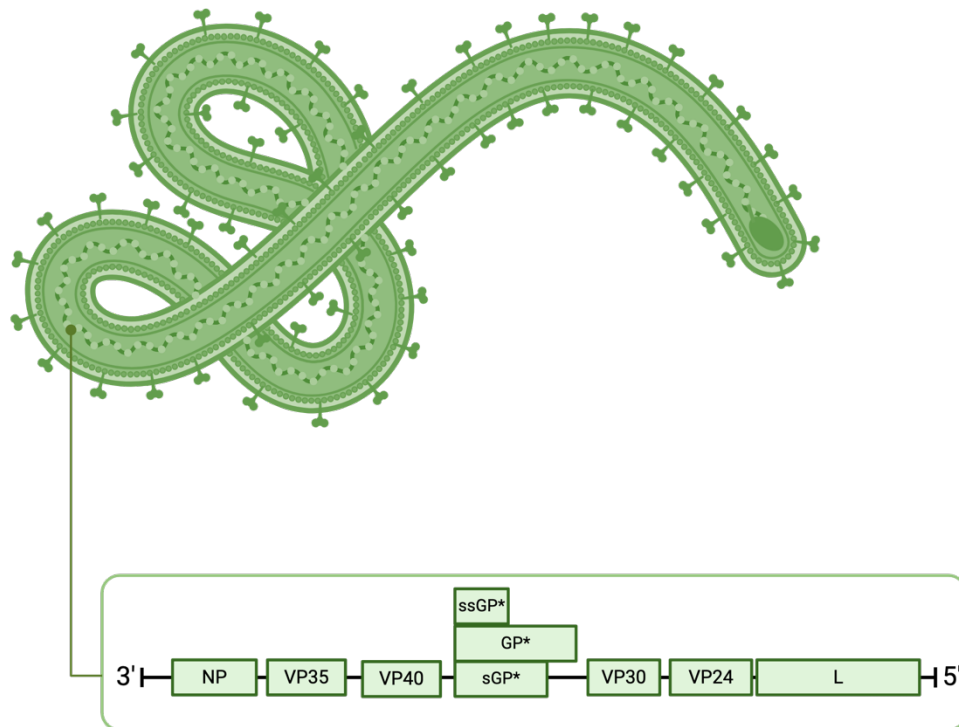


Figure 1.1: Schematic of the genome organisation of SUDV and EBOV. The single stranded RNA genome contains seven genes which are represented by boxes. Non-coding and intergenic regions are shown as a black line. Three open reading frames and proteins are available in the GP gene, indicated here by asterisks, and are generated through transcriptional editing (further detail is available in section 0). The RNA genome schematic was informed by previously published images [27, 32] and the figure was generated for this thesis using BioRender.com.

sGP/GP gene products

The GP gene encodes three proteins: soluble glycoprotein (sGP), structural viral membrane-anchored envelope protein (GP_{1,2}), and small soluble glycoprotein (ssGP), with the latter two being a product of a co-transcriptional editing strategy [33-35]. The transcripts are estimated to be produced in a 71:24:5 ratio (sGP:GP_{1,2}:ssGP) [34].

As the primary product of the GP gene, sGP is expressed from the non-edited mRNA species and is initially translated as a Golgi-specific precursor protein (pre-sGP) which is then cleaved by furin to yield the mature sGP and a small, non-structural, secreted protein termed Δ -peptide [36]. The 364 amino acid monomeric sGP forms homodimers that are secreted from infected cells [37].

For the mRNA species that encodes the structural membrane-anchored viral glycoprotein (GP_{1,2}) to be generated a 'stutter' event takes place during transcription. The L polymerase stutters at a specific 'editing site' where there are 7 consecutive uridines (U) leading to the insertion of an additional U [33]. This results in a frame shift, postponing the stop codon and producing a longer transcript that encodes the GP_{1,2} precursor. Initially, it is produced as a 676 residue pre-GP which is post translationally cleaved into the N-terminal GP₁ and the C-terminal GP₂ proteins by the protease furin [38]. The two proteins assemble via a disulfide bond to form heterodimers, which in turn assemble into homotrimers on the surface of the nascent virions as GP_{1,2}— hereon referred to in this thesis simply as GP.

For the mRNA species encoding the second non-structural glycoprotein, ssGP, to be produced, the addition of two extra Us, or the subtraction of a single U, occurs resulting in a frame shift to produce the shorter transcript [34]. The ssGP conformation is unknown but it is thought to be monomeric or dimeric and is secreted from the cell [34].

Full length GP is the sole surface expressed protein on the virion and it has a well-established function as the sole attachment factor in filovirus cell entry [39] which is further described in section 0. A growing body of literature has aimed to investigate the functions of sGP and ssGP due to the paucity of data. In cell line studies *in vitro*, EBOV quickly mutates to preferentially synthesise primarily GP (GP_{1,2}), but the virus reverts to a primarily sGP-producing phenotype *in vivo* in a Guinea pig model. This observation suggests that sGP provides a selective advantage within the host [40]. sGP has since been shown to act as an antigenic immune modulator, triggering immune activation and increasing vascular permeability [41]. As GP and sGP share 295 N-terminal residues, they share some mutual epitopes including those in the receptor binding domain (RBD)

and the glycan cap. It has therefore been hypothesised that sGP acts as an ‘antibody sink’, aiding the virus in immune subversion by sequestering antibodies and impairing the development of protective, neutralising antibody response [42]. However, more recent studies have demonstrated that antibodies that cross-react with sGP did not block viral neutralisation in assays where sGP was present [43]. Furthermore, antibodies specific for sGP drove neutrophil-mediated phagocytosis and predicted vaccine-mediated protection in vaccinated macaques [44]. The role of ssGP is still unknown [45].

Filovirus Tropism

EBOV and SUDV have a broad cellular tropism and are able to infect a range of cell types but primarily infect hepatocytes, endothelial cells, dendritic cells, macrophages and monocytes [46].

Filovirus entry is mediated by binding of the viral GP to multiple attachment factors on the host cell surface resulting in internalisation of viral particles, primarily by macropinocytosis [47]. Identified attachment factors include T cell immunoglobulin mucin receptor 1 (TIM1), dendritic cell-specific intercellular adhesion molecule 3-grabbing nonintegrin (DC-SIGN), and Toll-like receptor 4 (TLR4) on the host cell surface [48-51]. Following internalisation, viral particles are trafficked to the endosome. Upon acidification of the endosome, GP is cleaved by cellular cysteine proteases such as cathepsins, exposing the putative RBD of GP₁ [52] allowing binding to the late endosomal/lysosomal protein Niemann-Pick C1 protein (NPC1) receptor and facilitating the fusion of the viral membrane with the endosomal membrane [53, 54]. The viral nucleocapsid (containing the viral RNA genome) is released into the cytoplasm of the host cell and the viral negative-sense RNA genome replicates and is transcribed to generate mRNAs which are translated to viral proteins. Newly synthesized viral components are assembled and progeny virions bud, release and propagate the infection [55].

Ebola virus (EBOV)

Treatments

Current management of Ebola Virus Disease (EVD) primarily involves supportive care, focussing on managing fluid loss and rehydration with oral and intravenous fluids, as well as symptom management in Ebola Treatment Units [15, 56]. However, several therapeutics targeting EBOV have been developed and deployed either under compassionate use protocols or in clinical trials during outbreaks. Among these, the WHO strongly recommends two monoclonal antibody (mAb) treatments: mAb114 (Ansuvimab; Ebanga) and REGN-EB3 (Inmazeb) [57].

In a randomised controlled trial (PALM study; Clinical trial no. NCT03719586) conducted during an EBOV outbreak in the Democratic Republic of the Congo (DRC), both mAb114 and REGN-EB3 demonstrated superior efficacy compared to the control group (the monoclonal antibody ZMapp) [58]. mAb114 is an IgG1 monoclonal antibody isolated from a survivor of the Kikwit EVD outbreak in the DRC, 11 years after clinical infection. mAb114 interacts with the RBD of the GP₁ subunit of EBOV-GP_{1,2}, preventing its binding to the cell receptor protein Niemann-Pick C1. This action blocks endolysosomal escape and halts viral entry, even at low pH [59].

REGN-EB3 is a combination of three IgG1 monoclonal antibodies (REGN3470-REGN3471-REGN3479) which target non-overlapping epitopes in the glycan cap, RBD, and internal fusion loop of the EBOV GP respectively, resulting in viral neutralisation and activation of antibody dependent cellular cytotoxicity functions [60]. All three IgG1 antibodies were developed by immunising mice with humanised immune systems (Velocimmune[®] mice) [61].

Despite these advances in therapies over the years, the PALM study noted that 34% of total patients in the trial and 67% of patients who presented with higher viral loads at baseline (cycle threshold \leq 22) died despite receiving either REGN-EB3 or mAb114. There is clearly a need to develop more efficacious interventions. Further improvements should be made in aggressive supportive-care measures as well as ensuring

combination strategies use agents targeting non-overlapping sites of the GP with potentially complementary mechanisms of action to guard against viral escape [58, 62]. Finally, therapeutics cannot be effective if they are not available for use and access to therapeutics may be challenging, especially in resource-poor areas. Clinical grade mAbs are costly to manufacture and the pricing and supply of the aforementioned mAbs currently remain uncertain. It is crucial that these drugs are available where they are needed most: in regions where there is an active Ebola outbreak, or where the risk of outbreaks is high or very likely [57].

Vaccines targeting EBOV

The catastrophic and unprecedented 2014- 2016 West African Ebola virus epidemic fast-tracked countermeasures for EBOV. Prior to 2014, most EBOV vaccine candidates were stalled between the preclinical and clinical milestones on the path to licensure as a result of problems with funding clinical trials, a lack of interest from pharmaceutical companies, and competing priorities in public health [63].

There are now multiple vaccines targeting EBOV at various stages of clinical development. The majority of later-stage candidates are viral vectored vaccines, both replicative attenuated and non-replicative, but there are also candidate polypeptide, protein nanoparticle and DNA vaccines in the pipeline (Table 1.2). As the viral GP is the sole virally encoded surface-expressed protein and the cell surface attachment factor, it is the immunogen of the majority of products.

The development of vaccines against EBOV has historically been challenging as there are a host of practical and ethical challenges that come with conducting efficacy trials for vaccines targeting pathogens that cause rare and sporadic outbreaks. With this in mind, only two vaccines have been pre-qualified for use by the WHO: rVSV-ZEBOV and Ad26.ZEBOV/MVA-BN-Filo with human efficacy data available for rVSV-ZEBOV only [64] and Ad26.ZEBOV/MVA-BN-Filo receiving approval by bridging of animal data via 'the animal rule' [65, 66].

The World Health Organisation Strategic Advisory Group of Experts (WHO-SAGE) have recommended a ring-vaccination program that immunises those most at risk of disease, defined as contacts or contacts of contacts of an EVD patient, with a single dose of rVSV-ZEBOV (Ervebo, Merck). It is recommended that individuals identified as ‘lower-risk’ receive the EMA licensed and WHO pre-qualified Ebola vaccines, Ad26.ZEBOV and MVA-BN-Filo, administered in a heterologous prime-boost schedule. Lower risk individuals include ‘health workers and frontline workers in neighbouring areas and countries where the outbreak may spread’ as well as other groups such as ‘international responders who regularly support EVD outbreak response efforts and laboratory workers with possible exposure to Ebola virus’.

Table 1.2: A snapshot of some of the key vaccine candidates targeting EBOV which are currently in or have completed human clinical trials. Vaccines which are studied as part of this thesis are underlined.

Vaccine Name	Type of Vaccine	Species Targeted	Present Status	Key Reference(s)
rVSV-ZEBOV[®] (Ervebo)	Viral vector (rVSV)	EBOV	Phase III, FDA approved	[64]
<u>Ad26.ZEBOV/MVA-BN-Filo</u> <u>(Zabdeno/Mvabea)</u>	Viral vector (Ad26 and MVA)	EBOV, SUDV, MARV, TAFV	Phase III*, EMA licensed	[67, 68]
GamEvac-Combi	Viral vector (Ad5 and rVSV)	EBOV	Phase II, licensed under ministry of health of Russian Federation	[69]
Ad5-EBOV	Viral vector (Ad5)	EBOV	Phase II, approved by China Food and Drug Administration (CFDA)	[70]

<u>cAd3-EBO Z[§] (+/- Mvabea or MVA-EBO Z)</u>	Viral vector (cAd3)	EBOV	Phase II	[71]
DNA-EBOV	DNA vaccine	EBOV	Phase I	[72]
Ad26.Filo and MVA-BN-Filo	Viral vector (Ad26 and MVA)	EBOV, SUDV, MARV, TAFV	Phase I	[73]
rVSVN4CT1-EBOVGP1 (Vesiculovax)	Viral vector (rVSV)	EBOV	Phase I	[74]
<u>ChAdOx1 biEBOV</u>	Viral vector (ChAdOx1)	EBOV, SUDV	Phase I	Not available, Phase I data presented in Chapter 6
Ebola Virus Glycoprotein Nanoparticle Vaccine	Nanoparticle adjuvanted with Matrix M	EBOV	Phase I	[75]
INO-4202	DNA vaccine	EBOV	Phase I	[76]

[§]also known as rVSVΔG-ZEBOV-GP or V920. *Data from the phase III trial of Ad26.ZEBOV and MVA-BN-Filo in Sierra Leone is yet to be formally reported. [§]also known as CAd3-EBO-Z or cAd3-ZEBOV.

rVSV-ZEBOV (Ervebo)

rVSV-ZEBOV, marketed as Ervebo by Merck, is a live, attenuated recombinant vesicular stomatitis virus (rVSV) in which the gene for the endogenous envelope glycoprotein is replaced with that from the EBOV-Kikwit 1995 strain. The efficacy of rVSV-ZEBOV has been demonstrated in several rodent and non-human primate (NHP) models [77-81]. The vaccine has also demonstrated partial peri- or post-exposure efficacy in rhesus macaques when administered 20 to 30 minutes after exposure [82].

In a human efficacy trial (Ebola ça Suffit; Pan African Clinical Trials Registry number: PACTR201503001057193) conducted in Guinea, contacts and contacts of contacts of

individuals with EVD were grouped into clusters and these clusters were randomized to receive a single dose of the rVSV-ZEBOV vaccine at a dose of 2×10^7 plaque forming units (PFU) immediately or with a 21-day delay. At an interim analysis, no cases of EVD occurred 10 or more days after randomization among randomly assigned contacts and contacts of contacts vaccinated in immediate clusters. 16 cases were recorded in those receiving the vaccine with the 21-day delay. These results demonstrate that the rVSV-ZEBOV vaccine is indeed fast-acting and efficacious against EVD in humans with an estimated vaccine efficacy of 100% (95% CI 79.3–100.0, $P=0.0033$) [64, 83].

Following the successful efficacy results, over 300,000 individuals were immunized with Ervebo during the 2018 to 2020 DRC EBOV outbreak using a ring vaccination strategy. Real-world data from a retrospective observational study using data collected during this vaccination effort showed that rVSV effectiveness was 84% against EVD (95% credible interval 70–92) 10 or more days after vaccination. Vaccination status was self-reported [84].

The persistence of vaccine-induced anti-EBOV glycoprotein IgG antibodies has been assessed in an observational cohort study of the African and European phase 1 trials (NCT02287480, NCT02933931; NCT02296983 PACTR201411000919191), where groups were vaccinated with a single 3×10^5 PFU or $1\text{--}5 \times 10^7$ PFU dose of rVSV-ZEBOV. Antibody responses were shown to be sustained for at least 2 years across trial site location and dose ranges [85].

It is currently recommended that the rVSV-ZEBOV vaccine be delivered in outbreaks as part of a ring vaccination strategy. There is no natural market for the vaccine, and the vaccine must be secured through the global stockpile which has been operational since 2021. WHO-SAGE currently recommends a global EBOV vaccine stockpile containing 500,000 doses. This is estimated to be sufficient to avert outbreaks or epidemics of similar scale as the one experienced in 2014-2016.

Ad26.ZEBOV/MVA-BN-Filo (Zabdeno/Mvabea)

Ad26.ZEBOV/MVA-BN-Filo, marketed as Zabdeno and Mvabea by Janssen, is delivered as a heterologous regimen with a 56-day (8 week) prime and boost interval. The

Zabdeno component is derived from adenovirus serotype 26 (Ad26) and expresses the EBOV GP in place of the replication-essential adenovirus early 1 region. Unlike Ervebo, Zabdeno is unable to replicate in humans. MVA-BN-Filo (Mvabea, Bavarian Nordic) is a recombinant, replication-deficient, modified vaccinia Ankara–vectored vaccine expressing EBOV Mayinga GP as well as SUDV Gulu GP, Marburg virus Musoke GP, and TAFV nucleoprotein (dose 1×10^8 TCID₅₀) [86].

While protective efficacy against the other *orthoebolavirus* species targeted by the MVA-BN-Filo component has not yet been demonstrated, preclinical studies indicate a Zabdeno/Mvabea prime-boost immunization with an 8-week interval provided full protection to NHPs against an EBOV challenge [87].

Clinical trial data demonstrate that Zabdeno/Mvabea is safe. However, very rare cases of vaccine-induced immune thrombotic thrombocytopenia (VITT) have been reported in post-marketing campaigns for the Ad26.COV2.S vaccine which targets SARS-COV-2 and utilises the same Ad26 vector [88]. To date, no cases of VITT have been reported in any Ad26-vectored vaccines other than that targeting COVID-19, including the Ad26.ZEBOV, MVA-BN-Filo vaccine regimen [89]. Ongoing monitoring of these events should continue in both clinical trials and post-marketing surveillance.

Trials show the vaccine elicits strong anti-EBOV GP antibody responses along with both CD4+ and CD8+ T cell responses [68, 90]. In May 2019, WHO-SAGE recommended using this vaccine as part of efforts to contain the outbreak in the DRC. As a result, over 200,000 people in the DRC and Rwanda were vaccinated [91] but this study was not designed for efficacy. Therefore, the likelihood of clinical benefit of Ad26.ZEBOV, MVA-BN-Filo for European licensure under exceptional circumstances was based on an immunobridging approach. The primary analysis used anti-GP binding antibody concentrations from five studies conducted in eight countries across Africa, Europe and America to demonstrate a mean predicted survival probability of 53.4% with a lower limit 95% CI of 36.7% [86]. However, due to the high stringency of the NHP model, which is fully lethal, compared to the average human case fatality rate of 50 – 60%, this

survival probability should not be directly interpreted as clinical vaccine efficacy as it is likely an underestimate [86].

cAd3-EBO Z (+/- MVA-BN-Filo or MVA-EBO Z)

cAd3-EBO Z is a replication-deficient adenovirus chimpanzee serotype 3 vector expressing wild-type EBOV GP glycoprotein from the Zaire Mayinga strain. The virus contains deletions in the E1 and E4 region of the viral genome [92]. A single dose demonstrated efficacy in NHP challenge and durable protective efficacy was improved when boosted with MVA [93]. In clinical trials, cAd3-EBO Z has been tested as a single dose [92, 94, 95], as well as in a prime-boost regimen with MVA-BN-Filo (Mvabea) [71, 92] or MVA-EBO Z [96]. Head-to-head comparisons show the immune response from the cAd3-EBO Z was effectively boosted by MVA resulting in measured cellular and humoral immune responses higher than with cAd3-EBO Z alone [71], reinforcing the findings from the preclinical study.

Vaccine Induced Immune Correlates of protection

Immune correlates of protection (CoP) are “measurable markers that are statistically associated with vaccine efficacy” [97]. CoP can be divided into two categories: mechanistic, whereby “the measured correlate is directly responsible for protection”, and non-mechanistic, “a surrogate indicator which may contribute to, but is not exclusively involved in, protection” [98].

CoP for Ebola virus are likely to differ between natural infection and vaccine-induced immunity and may also vary depending on the vaccine type. A universal CoP applicable across all vaccines and routes of infection seems unlikely [98]. To date, identifying CoP against EVD in humans has been challenging, primarily because such studies can only be conducted during outbreaks, where the urgency of the situation complicates the planning and execution of clinical research. As a result, animal models, particularly NHPs, have so far been key in identifying correlates of protection against EVD and demonstrate a role for both antibodies and CD8+ T cells in mediating protection, depending on the vaccine platform.

For example, experiments with rVSV-ZEBOV vaccine in cynomolgus macaques with impaired immune responses due to simian-human immunodeficiency virus infection or depletion of CD4+ or CD8+ T cells showed that CD4+ but not CD8+ T cells were required at the time of vaccination for protection. This suggests that VSV-EBOV-mediated protection is primarily a result of the production of EBOV GP-specific antibodies, rather than T cell immunity [99]. However, transcriptomic analysis in samples from the same macaques shows gene expression differences between the CD8+ depleted and non-depleted animals upon vaccination indicate a potential minor regulatory role for CD8+ T cells in protection elicited by VSV-EBOV vaccination [100]. A more recent NHP study using a systems serology approach identified sGP-targeted antibody responses, especially those eliciting antibody-dependent neutrophil phagocytosis, as key correlates of rVSV-ZEBOV vaccine-mediated protection, surprisingly [44]. In post-hoc analysis of human trials, binding GP antibodies measured by ELISA (conducted on the Q2 Solutions Vaccines assay) to be 200 EU per mL or higher and two-times or more from baseline from 14 days after vaccination are estimated to be the most appropriate dichotomous correlate of protection [101].

Likewise, after Ad26.ZEBOV and MVA-BN-Filo vaccination the concentration of EBOV surface glycoprotein (GP)-binding antibodies as well as GP-neutralising antibody levels as measured by pseudoneutralisation assay were a strong predictor of survival after intramuscular challenge of cynomolgus macaques with EBOV [66].

Conversely, for cAd3-EBO Z/ MVA-EBO Z vaccines although acute protection associated strongly with antibody responses, long-term protection correlated with CD8+ T cell responses in NHPs challenged 10 months post-vaccination, specifically polyfunctional CD8+ T cells expressing a combination of TNF and IFN- γ [93].

Further evidence for the role of T cells in EVD protection comes from studies of rAd5-GP vaccine. In this study, passive transfer of high-titre polyclonal antibodies from vaccinated Ebola virus-immune cynomolgus macaques to naïve macaques did not confer protection against disease. However, depletion of CD8+ cells by a mAb *in vivo* abrogated protection in four out of five subjects, suggesting that CD8+ cells play a

major role in the immune protection induced by the rAd5-GP vaccine against Ebola virus infection in NHPs [102].

Aside from vaccine studies, the role of anti-EBOV binding and neutralising antibodies in protection against EBOV infection is also supported by successful outcomes from monoclonal antibody studies in both humans and NHPs [58, 103, 104].

Sudan virus (SUDV)

Due to the sporadic rate of SUDV outbreaks, research into SUDV has been more limited than research into EBOV. This has resulted in fewer available therapeutics and vaccines, with the existing interventions being at earlier stages in development. The 2022 outbreak of SUDV in Uganda was the first in a decade and prompted WHO and other organisations to focus on reviewing and consolidating existing evidence and support novel research against the virus [105].

Treatments

Despite their efficacy against EBOV, REGN-EB3 and mAb114 have a narrow therapeutic range and are not effective against SUDV [106]. Of the available therapeutics, two specifically target SUDV, while the others aim to be broad spectrum and target multiple orthoebolaviruses. Few products have human safety data, and none have human efficacy data [107].

During the recent outbreak in Uganda, the broad-spectrum two mAb cocktail MBP134 (Mappbio) and the antiviral Remdesivir were approved by the Ugandan National Regulatory Authority for compassionate use [107]. While both treatments have demonstrated efficacy in NHPs [108-110], no randomised controlled trials have been conducted in humans. In one observed case during the aforementioned Ugandan outbreak, a healthcare worker infected with SUDV received a combination of MBP134 and Remdesivir and survived [111].

Given that there is no known effective treatment for SUDV, developing new therapies and testing existing ones for safety and efficacy remains a key priority. MBP134 and

Remdesivir have been identified as priorities for testing in a clinical trial in a future outbreak [107].

Vaccines targeting SUDV

There are currently multiple anti-SUDV vaccines in the human clinical trial pipeline, although none have progressed past phase I or have human efficacy data. The most developed candidates are all viral vectored vaccines, and several are bi- or multivalent (Table 1.3). During the 2022 SUDV outbreak, three vaccines were prioritised by the WHO for trial they were: cAd3-SUDV, VSV-SUDV, and ChAdOx1 biEBOV which is bivalent and targets the GP of both EBOV and SUDV.

Table 1.3: A list of the vaccine candidates targeting SUDV which are currently being evaluated in human clinical trials. rVSV-SUDV is included despite not yet entering clinical trials as the WHO has prioritised it for clinical testing as the basis of the efficacy of rVSV-ZEBOV. Vaccines which are studied as part of this thesis are underlined.

Vaccine Name	Type of Vaccine	Species Targeted	Present Status	Key Reference(s)
cAd3-EBO S	Viral vector (cAd3)	EBOV	Phase I	[112]
<u>ChAdOx1 biEBOV</u>	Viral vector (ChAdOx1)	EBOV, SUDV	Phase I	Not available, Phase I data presented in Chapter 6
<u>Ad26.ZEBOV /</u> <u>MVA-BN-Filo*</u>	Viral vector (Ad26 and MVA)	EBOV, SUDV, MARV, TAFV	Phase III* Pre-clinical	[113]

(Zabdeno/Mvabea)				
Ad26.Filo / MVA-BN-Filo	Viral vector (Ad26 and MVA)	EBOV, SUDV, MARV, TAFV	Phase I	[73]
rVSV-SUDV	Viral vector (rVSV)	SUDV	Pre-clinical	Not available

*this vaccine is approved for use against EBOV, phase II data is available for EBOV, there is a paucity of data available on the immunogenicity to SUDV, which is encoded in the MVA-BN-Filo boost.

ChAdOx1 biEBOV

biEBOV uses the ChAdOx1 platform which is a replication-deficient simian adenovirus vector and encodes the GP from both SUDV and EBOV at the E1 locus and the E4 insertion site respectively. E1 and E4 expression cassettes both under the TetR-repressible cytomegalovirus promoter. ChAdOx1 as a backbone has been used to target multiple pathogens in human clinical trials [114-119], most notably it was the platform for the ChAdOx1 nCoV19 vaccine targeting severe acute respiratory syndrome coronavirus 2 (SARS-CoV-2) [120]. biEBOV has been tested in phase I trials in both the UK (NCT05079750) and Tanzania (NCT05301504). First in-human dose escalation data from the UK phase I clinical trial is presented in Chapter 6 of this thesis.

Correlates of protection

To date only one published study has aimed to assess correlates of protection for SUDV. This study showed that anti-SUDV GP binding antibody titres were a good predictor of survival in NHPs vaccinated with Ad26.Filo/ MVA-BN-Filo [113]. It is possible that the CoP for SUDV will present similarly to those for EBOV and vary depending on the vaccine platform. Further studies conducted as vaccine candidates progress through development will provide more insight into this.

Thesis Aims and Outline

Although remarkable success has been made in the field, knowledge gaps for vaccines targeting EBOV have been identified by WHO-SAGE including (i) the durability of immunity and the (ii) extent of cross-reactivity against non-EBOV species, such as SUDV [121]. Data evaluating the persistence of the immune response will be essential to inform the optimal immunisation policy for deployment of vaccines, including the potential to adapt immunisation strategies to incorporate prophylactic immunisation of at-risk individuals such as healthcare workers [122]. Therefore, this thesis uses samples from clinical trials conducted in Oxford, UK and Dakar, Senegal to evaluate the durability of the licensed Ad26.ZEBOV/MVA-BN-Filo regimen (PRISM trial, conducted in Oxford, Chapter 5) and the phase III candidate cAd3-EBO Z boosted with either Ad26.ZEBOV (REVOLVE trial, conducted in Oxford, Chapter 3), MVA-BN-Filo (REVOLVE trial, conducted in Oxford, Chapter 3) or MVA-EBO Z (REVOLVE & RESOLVE trials, conducted in UK or Senegal respectively, Chapters 3 & 4). As boosting volunteers would be a viable strategy for boosting immunogenicity in an outbreak scenario, a subset of volunteers who had previously been vaccinated with cAd3-EBOZ/MVA-BN-Filo or cAd3/MVA-EBO Z received a third dose of ebola virus vaccine in the form of Ad26.ZEBOV (REVOLVE trial, Chapter 3). All Senegalese volunteers who had received a prime-boost cAd3-EBOZ/MVA-EBO Z were also boosted with Ad26.ZEBOV (RESOLVE trial, Chapter 4). These studies assess the boosting capacity of Ad26.ZEBOV in UK and Senegalese volunteers as well as the durability of the original regimens.

Looking to the future, if the next generation of candidate filovirus vaccines are to come, they should ideally target multiple orthoebolavirus species for ease of manufacturing, stockpiling and deployment in an outbreak. A multivalent vaccine would also be ideal for prophylactic use to protect healthcare workers against multiple species. This thesis, therefore, also evaluates the novel bivalent vaccine biEBOV against both SUDV and EBOV in a phase I first-in-human clinical trial (EBL07 trial, conducted in Oxford, Chapter 6) and assesses the immune response to SUDV in individuals vaccinated with Ad26.ZEBOV / MVA-BN-Filo, which is currently approved only for EBOV (PRISM trial, conducted in Oxford, Chapter 5).

A summary of the clinical trials, and their parent trials, studied in this thesis is listed in Table 1.4.

Table 1.4: A summary of the trials and parent trials which are the focus of this thesis. Long-term follow-up data is available for EVOLVE (in the PRISM trial), EBL01, EBL04, EBL05 (in the REVOLVE trial) and EBL06 (in the RESOLVE trial). EBL07 is not a long-term follow-up trial and instead assesses the immunogenicity of ChAdOx1 biEBOV up to a maximum of 364- days post vaccination.

Trial	Parent Trial	Parent Trial Vaccines	Country of Recruitment	Thesis Chapter	Current Study Intervention
REVOLVE	EBL01	cAd3-EBO Z & MVA-BN-Filo	UK	3	Optional Ad26.ZEBOV boost and/or long-term follow-up only
	EBL04	cAd3-EBO Z & MVA-EBO Z	UK	3 & 4	
	EBL05	cAd3-EBO Z & Ad26.ZEBOV	UK	3	
RESOLVE	EBL06	cAd3-EBO Z & MVA-EBO Z	Senegal	4	Long term follow-up & Ad26.ZEBOV boost
PRISM (cohort 3)	EVOLVE	Ad26.ZEBOV & MVA-BN-Filo	UK	5	Long-term follow-up only
EBL07	N/A	N/A	UK	6	ChAdOx1 biEBOV vaccination

2. Materials and Methods

Materials

Reagents

Table 2.1: Materials and reagents used in this thesis

Material/Reagent	Company	Catalogue number
0.22 µm filters	Fisher Scientific	FDR-120-060Y
0.5 mL insulin syringe	BD BioSciences	037-7614
1.5 mL Eppendorf tubes	ThermoFisher Scientific	FB74031
10-250 kDa pre-stained protein standard	New England Biolabs	P7719S
12-well tissue culture plate	Corning	3737
15 mL Falcon tube	Sarstedt	554502
175 cm ² cell culture flask	Corning	431086
2-Mercaptoethanol	ThermoFisher Scientific	31350010
20 mL syringe	BD BioSciences	300613
24-well tissue culture plate	Corning	3738
25 cm ² cell culture flask	Corning	430639
4-nitro-phenyl-phosphate	Sigma-Aldrich	N2765-100TAB
50 mL Falcon tube	Sarstedt	547254
5 mL polypropylene FACS tubes	BD BioSciences	352063
5 mL syringes	BD BioSciences	309647
5 X Diethanolamine Buffer	Pierce	34064
6-well tissue culture plate	Corning	3736
7 mL Bijou tubes	Sigma Aldrich	Z645338

96-well U-bottom plate	BD BioSciences	353077
96-well V-bottom plate	BD BioSciences	511V96
Alkaline phosphatase (AP) substrate 3 component kit	Bio-Rad	170-6432
AL buffer	Qiagen	1038826
Anti-CD28	eBioScience	16-0289-81
Anti-CD49d	eBioScience	16-0499-85
Any kD Mini-PROTEAN® TGX Stain-Free Protein Gels	Bio-Rad	4568125
ArC Amine Reactive compensation beads	ThermoFisher Scientific	A10346
ATL buffer	Qiagen	939011
BCIP/NBT plus	Europa Bioproducts	NBTH-1000
Benzonase	Millipore	70664
Blocker™ Casein in PBS	Sigma Aldrich	37528
Bovine Serum Albumin	Sigma Aldrich	A7906-100G
BrightGlo Luciferase Assay System	Promega	E2620
Carbenicillin	Sigma Aldrich	C1613
Carbonate-Bicarbonate capsules	Sigma Aldrich	C3041
Casyton	OLS OMNI Life Science	5651808
CoolCell	Corning	432006
CpG-ODN 2006:	Invitrogen	tlrl-2006-5
Cryovials	ThermoFisher Scientific	CRY-960-130J
Dimethyl Sulfoxide (DMSO)	Sigma Aldrich	D2650

Distilled Water	ThermoFisher Scientific	15230089
DNA Gel Extraction Kit	New England Biolabs	T1020S
DSP DNA Midi Kit	Qiagen	937255
Dulbecco's Phosphate Buffered Saline	Sigma Aldrich	D8537-500ML
Dulbecco's Modified Eagle's Medium (DMEM) high glucose	Sigma Aldrich	D6546
ECL Plus Western Blotting Substrate	ThermoFisher Scientific	32134
Fixation/Permeabilization Solution kit	BD BioSciences	554714
Foetal Calf Serum	Gibco	10500-064
FuGENE Transfection Reagent	Promega	E2311
GeneRuler 1 kb ladder	ThermoFisher Scientific	SM0311
Goat-anti-human IgG	Millipore	401442
Goat Anti-Mouse IgG (H + L)-HRP Conjugate	Bio-Rad	1706516
GolgiStop™ Protein Transport Inhibitor (Containing Monensin)	BD BioSciences	554724
GolgiStop™ Protein Transport Inhibitor (with Brefeldin A)	BD BioSciences	555029
Halt Protease Inhibitor Cocktail	ThermoFisher Scientific	10516495
Human anti-cytomegalovirus IgG ELISA kit	Abcam	Ab108724
iBind™ Flex Solution Kit	ThermoFisher Scientific	SLF2020
IFN- γ antibody catcher (1-DIK)	Mabtech	3420-2A
IFN- γ antibody detector (7-1B6-Biotin)	Mabtech	3420-2A
Kanamycin	Sigma Aldrich	K0129

KpnI-HF Restriction Enzyme	New England Biolabs	R3142S
LB Broth powder	Sigma Aldrich	L3522
L-glutamine	Sigma Aldrich	G7513-100ML
Lectin from Phaseolus vulgaris (red kidney bean) (PHA-L)	Sigma Aldrich	L4144
Leucosep tubes	Greiner	227209
Lymphoprep	STEMCELL Technologies	G7513-100ML
MAIP ELISpot plates	Millipore	MAIPS4510
MEM Non-Essential Amino Acids	ThermoFisher Scientific	11140035
NotI-HF Restriction Enzyme	New England Biolabs	R3189S
Nunc 96 well LumiPlate white with lid	Fisher Scientific	10072151
NUNC Immuno Plates (442404)	ThermoFisher Scientific	DIS-971-030J
Opti-MEM	ThermoFisher Scientific	31985062
Paraformaldehyde	Alfa Aesar	43368
Penicillin (100U)/Streptomycin (100 µg)	Sigma Aldrich	P-0781
Phosphate buffered saline tablets	Sigma Aldrich	P4417-100TAB
Plasmid Midi Kit	QIAGEN	12143
Plasmid Mini Kit	QIAGEN	12123
Pokeweed Mitogen	Sigma Aldrich	L-9379
Proteinase K	Qiagen	19131
Red blood cell lysis solution	Qiagen	158904

RPMI-1640 medium	Sigma Aldrich	R0883-500ML
RIPA Lysis and Extraction Buffer	ThermoFisher Scientific	89900
Scal-HF Restriction Enzyme	New England Biolabs	R3122S
Sodium Azide (NaN ₃)	Sigma Aldrich	S2002
Sodium Pyruvate (100 mM)	ThermoFisher Scientific	11360039
Sodium thiocyanate (NaSCN)	Sigma Aldrich	80518
Staphylococcal enterotoxin B (SEB)	Sigma Aldrich	S4881
Staphylococcus aureus Cowans Strain Pansorbin cells (SAC)	VWR International Ltd	507861- 50
Sterile H ₂ O	Sigma Aldrich	W3500-500ML
Streptavidin-ALP	Mabtech	3420-2A
SYBR™ Safe DNA Gel Stain	ThermoFisher Scientific	S33102
Synthetic Peptides	ProImmune	N/A – custom order
T4 DNA ligase	New England Biolabs	M0202S
TAE Buffer (Tris-acetate-EDTA) (50X)	ThermoFisher	B49
Transfer pipette	Sigma Aldrich	Z350826
Trypan Blue solution 0.4%	Sigma Aldrich	T8154-100ML
TrypLE Express Enzyme (1X), no phenol red	ThermoFisher Scientific	12604013
Tween-20	Sigma Aldrich	9005-64-5
Gene Ruler 1kb	ThermoFisher Scientific	11571595
Nuclease-Free Water	New England Biolabs	B1500S
rCutSmart buffer	New England Biolabs	B6004S
OneComp eBeads	ThermoFisher Scientific	01-1111-42

Antigens

Table 2.2: Antigens used for in-house ELISA assays and their source.

Antigen	Source
Trimeric EBOV GP Accession: AHX24649.1	Made in-house, The Jenner Institute
Trimeric SUDV GP Accession: Q66814.1	Custom made for this project by The Native Antigen Company

Plasmids

Table 2.3: Plasmids used to create pseudotyped lentiviruses viruses and their source.

Plasmid	Function	Source
P8.91	HIV-1 lentivirus packaging plasmid	Donation from E. Wright, University of Sussex via Alexander Sampson.
pCSFLW	Reporter plasmid	Donation from E. Wright, University of Sussex via Alexander Sampson.
P299.SUDV	SUDV GP	Cloned for this thesis at The Jenner Institute.
P300.EBOV	EBOV GP	Cloned for this thesis at The Jenner Institute.

Buffers, solutions, and cell media

R0 medium: RPMI (Sigma) containing 1% sterile filtered Penicillin-Streptomycin (Sigma), 1% L- Glutamine (Sigma).

R10 medium: RPMI (Sigma) containing 1% sterile filtered Penicillin-Streptomycin, 1% L- Glutamine and 10% heat-inactivated, sterile-filtered foetal calf serum, pre-screened for low reactivity (Labtech International)

Complete DMEM medium: Dulbecco's Minimum Essential Medium (DMEM) containing 1% sterile filtered Penicillin-Streptomycin (Sigma), 1% L- Glutamine (Sigma) and 10% heat-inactivated, sterile-filtered foetal calf serum, pre-screened for low reactivity (Labtech International).

Complete RPMI 1640 medium: RPMI (Sigma) containing 10% FBS, 1% penicillin/streptomycin, 1 % L-glutamine, 1% non-essential amino acids, 1% sodium pyruvate and 0.1% 2-mercaptoethanol).

FACS buffer: PBS containing 0.1% BSA and 0.01% sodium azide.

Carbonate (coating) buffer: Carbonate-bicarbonate capsules (Sigma) dissolved in PBS (15 mM Na₂CO₃, 35 mM NaHCO₃, pH 9.3).

PBS/Tween (PBS/T): PBS (Sigma, P2194) with 0.5% Tween-20

TAE buffer: 50X concentrated TAE buffer diluted to 1X in dH₂O (40 mM Tris, 40 mM acetate, 1 mM EDTA pH 8.6).

Lysogeny broth (LB) agar: 37 g LB Agar powder dissolved in 1000 mL MiliQ water

Lysogeny broth (LB): 25 g LB broth powder dissolved in 1000 mL MiliQ water

Methods

Immunology

Whole Blood Separation – isolation of PBMC and plasma

Heparinised whole blood samples were stored at room temperature (RT) prior to processing within 4 hours of venepuncture. Peripheral blood mononuclear cells (PBMC) and plasma were separated from the heparinised whole blood by density centrifugation at 1000 x g for 13 minutes at RT in either leucosep tubes or 50 mL falcon tubes using Lymphoprep™ as a density gradient medium. Plasma samples were frozen in aliquots of 1.8 mL at -80 °C, PBMC were washed with R0 medium and resuspended in R10 medium. PBMC with significant erythrocyte contamination were incubated with 5 mL of red blood cell lysis solution for 5 minutes before a further wash and resuspension in R10 medium. Cell counts were determined using a CASY Cell Counter (Roche Innovatis AG).

PBMC cryopreservation

Following separation and use in any assays that required freshly isolated PBMC, PBMC were cryopreserved. PBMC were resuspended in foetal calf serum (FCS) and incubated at 4 °C for 30 minutes. An equal volume of FCS + 20% DMSO was then added to give a final solution of PBMC in FCS + 10% DMSO. 1 mL of cell suspension were added to each cryovial at a concentration of 6×10^6 – 12×10^6 PBMCs/mL. Cryovials containing cells were immediately distributed to CoolCells with a standardized controlled-rate of freezing of -1 °C/minute and stored for 12 to 72 hours at -80 °C before being transferred to either a vapour-phase liquid nitrogen tank at -196 °C or a freezer at -150 °C for long-term storage.

Serum collection

In trials requiring serum collection, as specified by the study specific protocol, approximately 9 mL of blood was drawn into BD Vacutainer® Serum tubes. The samples were centrifuged at 1800 rpm for 5 minutes at RT. Following centrifugation, two 1.8 mL

aliquots of serum were extracted using a transfer pipette and stored in cryovials at -80 °C until further use.

PBMC thawing

Cryopreserved PBMCs were thawed by immersion in a 37 °C water bath. Thawed cells were added dropwise into 10 mL of pre-warmed R10 in a Falcon tube. Cells were centrifuged at 1800 rpm for 5 minutes to remove 10% DMSO in FCS and resuspended in 2 mL of R10 containing 1 µL of 5925 U/mL benzonase per million cells. Cells were incubated at 37 °C with 5% CO₂ in a humidified incubator for 2 to 6 hours prior to use.

Anti-EBOV GP and anti-SUDV GP total IgG ELISA

Anti-EBOV GP and anti-SUDV GP total IgG antibodies were measured by a standardized in-house ELISA. Nunc ELISA plates were coated with 1 µg/mL of either SUDV GP trimer (UniProtKB: Q66814.1) or EBOV GP trimer (GenBank: AHX24649.1) in Dulbecco's PBS at 4 °C for 14 to 20 hours. After coating, plates were washed six times with PBS / 0.05% Tween and blocked with casein for 1 hour at RT. Thawed samples, diluted in casein, were added to the wells in triplicate and incubated for 2 hours at RT alongside an internal positive control, also in triplicate, and a two-fold ten-point serial dilution standard curve of pooled seropositive human plasma in duplicate. 4 wells were left blank with casein only. After washing as previously described, a secondary goat anti-human IgG conjugated to alkaline phosphatase (Sigma) was added at a dilution of 1:1000 in Casein for 1 hour at RT. Plates were washed a final time and developed using 4-nitrophenyl phosphate in diethanolamine buffer (Pierce). Optical density (OD) was read at 405 nm using an ELx808 microplate reader (BioTek Instruments). The OD values of the standard points were fitted to a four-parameter hyperbolic curve against the

arbitrary ELISA units. The OD values of the samples and the parameters of the standard curve were used to calculate arbitrary ELISA units for each sample. The internal control was used to standardise results between plates.

QC criteria were applied whereby samples with a coefficient of variation (CV) >20%, plates where the ELISA units of the internal control fell outside of the acceptable range and plates where the parameters of the standard curve (A, B, C and D) fell outside the acceptable range failed and samples were repeated. Seropositive cut-offs were determined within the assay set-up and are set as the mean plus 3 standard deviations of the response of unvaccinated controls.

The anti-SUDV ELISA was set-up and partially validated as part of this thesis. The full report is available in the supplementary section: Set-up and Qualification of an ELISA to measure anti-SUDV IgG.

Avidity ELISA

EBOV GP-specific total IgG antibody avidity of donor plasma was assessed by sodium thiocyanate (NaSCN)-displacement ELISA. Only samples with a detectable IgG titre above the seropositive cut-off on the respective tIgG ELISA were selected for avidity analysis. The assays were conducted as for tIgG ELISAs with the following deviations: plasma samples and a positive control plasma pool were diluted with casein normalised to an OD₄₀₅ of 1. Dilutions were calculated using the anti-EBOV or anti-SUDV GP tIgG titres generated from the tIgG ELISA. After incubation with sample, increasing

concentrations of NaSCN (Sigma-Aldrich) diluted in PBS were added at 50 μ L per well to each row down the plate at increasing concentrations (1 M, 2 M, 3 M, 4 M, 5 M and 6 M) except for the first row where only PBS was added. Plates were incubated for 15 minutes at RT before washing six times with PBS/T and incubating with the secondary antibody as per the ELISA methods, OD_{405} was measured using an ELx808 absorbance reader (BioTek) until an OD_{405} of 1 (0.8–1.2) was reached in the wells with PBS and plasma sample only and without NaSCN. Gen5 ELISA software v3.09 (BioTek) was used to plot the test sample OD_{405} against the concentration of NaSCN, and a spline function with smoothing factor 0.001 was fitted to the data. For each sample, the concentration of NaSCN required to reduce the OD_{405} to 50% of that without NaSCN (IC_{50}) was interpolated from this function and reported as a measure of avidity. Each plate contained a positive control of pooled seropositive plasma. A QC process was applied, whereby if the IC_{50} of the positive control did not fall within a pre-determined range (1.33 and 1.79) for EBOV, the plate failed QC. Any samples with a CV of >20% between the duplicates also failed QC. QC fails were repeated until the sample passed.

CMV ELISA

Anti-Cytomegalovirus (CMV) total IgG titres were assessed using a commercially available ELISA kit (Abcam) according to the manufacturer's instructions. Plates were pre-coated by the manufacturer with a native, inactivated preparation of the full host of viral proteins from all parts of the viral replication cycle. Test plasma samples were diluted 1:100 in sample diluent and 100 μ L of diluted plasma was added to duplicate wells of a pre-coated plate alongside positive, negative and 'cut-off' controls, also in duplicate. Samples were incubated for 1 hour at 37 °C before washing three times with 300 μ L of washing buffer per well. Following washing, a horseradish peroxidase (HRP)

labelled anti-Human IgG conjugate was added to the wells. Plates were incubated for 30 minutes at RT in the dark. After washing again as before, 100 μ L of TMB substrate was added per well and plates incubated for 15 minutes at RT, in the dark. An equal volume of stop solution was added per well and the absorbance was read immediately at 450nm using a BioTek ELx800 microplate reader. Arbitrary units and cut-off values were determined as per the manufacturer's instructions and used to classify plasma samples from participants as seropositive or seronegative for CMV.

Plasma Heat Inactivation

To prevent assay interference from complement factors, plasma samples were heat inactivated prior to testing on the pseudovirus neutralisation assay. Samples were thawed, equilibrated to RT, aliquoted into 200 μ L and heat inactivated at 56 °C for 30 minutes in a water bath.

Pseudovirus Neutralisation assay

Heat inactivated plasma were diluted to an initial 1:40 dilution in complete DMEM and serially diluted 2-fold in duplicate in white 96-well Nunclon Delta-Treated flat-bottom 96-well plates (Thermo Fisher) to a 1:2560 dilution. For SUDV assays, anti-SUDV mAb 16F6 (IBT BioServices) is used as an internal control as is diluted 2-fold from a starting concentration of 10 μ g/mL to 0.15625 μ g/mL in complete DMEM. For EBOV assays, mAb KZ52 (IBT BioServices) is diluted 2-fold and used as a positive control. For SUDV assays, pooled positive plasma was diluted 1:40, then 2-fold and used as a positive control. 50 μ L of PV containing supernatant diluted in complete DMEM to give 1×10^6 RLU equivalent

was added per well. The plate was centrifuged at $500 \times g$ for 10 seconds before incubation at 37 °C, 5% CO₂ for 1 hour. HEK293T/17 target cells were seeded at 1×10^4 cells per well and plates were incubated at 37 °C and 5% CO₂ for 48 hours. Six wells contain cell and virus only and six wells contain only cells. Cells are lysed and luciferase reporter gene activity was measured in relative light units (RLU) as described above in the Titration of Lentiviral Pseudotypes method. IC₅₀ values were calculated for the neutralization assays based on 4-parameter log-logistic regression dose-response curves after normalisation to 0% and 100% using the average of cell-only and cell-and-virus-only plate controls. Dose-response curves were fit using GraphPad Prism v10.0.3 IC₅₀ values for the internal plate control were used as a quality control criterion to pass or fail data from plates.

Memory B Cell Culture

Cryopreserved PBMC were thawed and resuspended in 96-well round-bottom culture plates at a final concentration of 2×10^5 cell/well in complete RPMI 1640 media (10% FBS, 1% penicillin/streptomycin, 1 % L-glutamine, 1% non-essential amino acids, 1% sodium pyruvate and 0.1% 2-mercaptoethanol). Cells were cultured at 37 °C, 5% CO₂, 95% humidity for 5 days with *Staphylococcus aureus* Cowan strain pansorbin cell suspension (SAC) at 1:5000 dilution (Calbiochem-Novabiochem), pokeweed mitogen at 1:6000 dilution (Sigma-Aldrich), and CpG oligonucleotide at a 1:40 dilution (ODN-2006; TCG-TCG-TTT-TGT-CGT-TTT- GTC-GTT, InvivoGEN). Memory B cells were harvested on day five and washed three times prior to stimulation in the memory B cell ELISpot assay.

Memory B Cell ELISpot

Wells in MultiScreen-IP filter plates, (Millipore) were coated with 5 µg/mL of EBOV Mayinga variant GP antigen, 5 µg/mL diphtheria toxoid tetanus toxoid (Statens Serum Institut), 10 µg/mL Goat anti-Human Ig polyclonal Secondary Antibody mix (Life Technologies), or PBS alone. Plates were blocked with complete media for 5 hours in the incubator before seeding with 2×10^5 PBMC per well in the EBOV antigen and TET wells. For the wells coated with the IgG mix, 2×10^4 and 2×10^3 PBMCs were seeded in duplicates. The plates were incubated overnight at 37 °C in 5% CO₂ and 95% humidity. Plates were washed 4 times with PBS-Tween and once with PBS. Bound immunoglobulin G (IgG) antibody was detected using an alkaline phosphatase conjugate at a 1:5000 dilution (Sigma-Aldrich) and an AP-conjugate substrate kit (nitroblue tetrazolium + 5-bromo-4-chloro-3-indolyl phosphate in dimethylformamide; Bio-Rad).

Peptide Preparation

Multimer (12 to 17mer) peptides overlapping by 11 amino acids spanning the length of the Sudan virus GP and SP or the Ebola virus GP and SP, were custom synthesised for this work by Proimmune, UK at a minimum purity of 70%. Peptides were reconstituted in DMSO to a concentration of 100 mg/mL and stored at -80 °C. For ELISpots and ICS assays, peptides were diluted to working concentrations in R10 prior to use. Sequences of peptides are detailed in the supplementary information (Table S 3, Table S 4, Table S 5).

Ex-vivo IFN- γ ELISpot assay

Fresh PBMC samples isolated within 4 hours of venepuncture, or cryopreserved PBMC, were used to perform Interferon- γ -linked enzyme-linked immunospot (ELISpot) assays to enumerate responses to the SUDV or EBOV glycoprotein antigen. Multiscreen 96 well IP ELISpot plates (Millipore) were coated with 10 $\mu\text{g}/\text{mL}$ of human anti-IFN- γ coating antibody (clone 1-D1K, Mabtech) in carbonate buffer for 8 to 72 hours at 4°C. After three washes with PBS, the plates were blocked with R10 media for 2 to 8 hours at RT. Freshly isolated PBMCs were added in duplicate or triplicate wells at 2.5×10^5 PBMCs in 50 μl per well, along with pools of multimer peptides spanning the relevant antigen at a final concentration of 2.5 $\mu\text{g}/\text{mL}$ (Proimmune) peptide pool layouts are detailed in the supplementary (Figure S 10, Figure S 11). Negative and positive controls were included for each sample using R10 without antigen and a mixture of staphylococcal enterotoxin B (SEB, 0.02 $\mu\text{g}/\text{mL}$) and phytohaemmagglutinin-L (PHA, 10 $\mu\text{g}/\text{mL}$), respectively.

The assays were incubated for 16 to 18 hours at 37°C with 5% CO₂. Plates were developed by removing cells and washing six times with PBS-Tween, followed by the addition of 1 $\mu\text{g}/\text{mL}$ of anti-IFN- γ detector antibody (7-B6-1-Biotin) to each well. After a 2 to 4 hour incubation, plates were washed again, and 1:1000 SA-ALP was added for 1 to 2 hours. After a final wash step, plates were developed using BCIP NBT-plus chromogenic substrate (Moss). The substrate remained in the wells until spots first became visible in the positive control wells at which point the reaction was halted by removing the substrate and washing plates with H₂O. Plates were tapped to remove excess water and left to dry overnight in the dark. The ELISpot plates were counted using an AID automated

ELISpot counter (AID Diagnostika, algorithm C), with identical settings for all plates. Spot counts were adjusted only to remove artifacts. Triplicate well responses were averaged, and the mean response of the unstimulated (negative control) wells was subtracted and were reported as spot forming cells (SFCs) /10⁶ PBMCs. If the % CV of triplicate wells was <50%, the anomalous data point was excluded and data was taken from the mean of duplicate wells. Quality control (QC) criteria were applied excluding results from further analysis if responses were >80 SFCs/10⁶ PBMCs in the negative control wells (PBMCs without antigen) or <800 SFCs/10⁶ PBMCs in the positive control wells. These values were empirically determined during assay validation.

Peptide Mapping

Samples from participants with the highest peak responses against the peptide pools were selected, considering sample availability, and tested against the individual constituent peptides of the respective pools to identify immunodominant peptides (n = 2 to 5 participants per pool) as per the *Ex-vivo* IFN- γ ELISpot assay described above with the following exceptions: Plates were coated with individual peptides at a concentration of 10 μ g/mL and 2 x 10⁵ PBMC were assayed per well. Responses were considered positive if they were greater than three standard deviations of the median of the negative control response for all volunteers (equivalent to 30.3 SFC/ 10⁶ PBMC).

In silico HLA restriction predictions

MHC Class I and class II alleles were analysed using NetMHCpan (v4.1) and NetMHCIIpan (v4.1) respectively to assign an HLA restriction element from each

volunteer to each of the positive peptides. HLA restriction and peptide binding strength were assigned for each peptide by predicting binding to all HLA molecules of the positive volunteer and reporting the lowest percentile rank score and associated HLA molecule. For HLA class I, rank score binding values less than 0.5% were considered predictive of strong binding of an epitope to an HLA allele, at this binding value, 95% of validated epitopes are identified with a specificity greater than 99%. Rank score binding values less than 2 were considered predictive of weak binding of an epitope to an HLA allele. For HLA class I alleles, rank score binding values less than 2% were considered predictive of strong binding of an epitope to an HLA allele and less than. A threshold of 10% was considered predictive of weak binding of an epitope to an HLA allele.

Flow Cytometry with Intra-cellular Cytokine Staining (ICS)

ICS was performed on fresh PBMC for REVOLVE (Chapter 3), and RESOLVE (Chapter 4), PRISM (Chapter 5), and on cryopreserved PBMC for EBL07 (Chapter 6). 1.5×10^6 PBMCs were resuspended into 1 mL of R10 media within polypropylene FACS tubes with 1 $\mu\text{g}/\text{mL}$ of anti-human CD28 and CD49d and 1 μL of CD107a PE-Cy5 (eBioscience). Samples were stimulated with either a positive control (*S. enterotoxin B* at 1 $\mu\text{g}/\text{mL}$, Sigma Aldrich), a mega pool of EBOV GP and/or SUDV multimers at a final concentration of 2 $\mu\text{g}/\text{mL}$. A negative control of unstimulated cells (R10 alone) was included for every sample. Cells were incubated at 37 °C with 5% CO₂ for 16 to 20 hours, brefeldin A (3 $\mu\text{g}/\text{mL}$) and monensin (2 mM) (eBioscience) were added after 2 hours.

At the end of the incubation, cells were washed with PBS containing 0.1% bovine serum albumin and 0.01% NaN₃ (FACS buffer). A surface staining cocktail was first added containing Aqua Live/Dead stain (Thermo Fisher Scientific). Cells were incubated in the dark for 20 minutes and washed with FACS buffer. Then, cells were permeabilized with 250 µl of CytoFix/CytoPerm solution (BD Biosciences) and incubated for 20 minutes at RT. Cells were then washed with Perm/Wash buffer. Samples were stained in the dark at RT for 30 min with appropriate antibodies (Table 2.4). Cells were washed with Perm/Wash buffer before resuspension in 100 µl of 1% paraformaldehyde. Samples were acquired using an LSRII (BD Biosciences) and FACS Diva software v8.02 (BD Biosciences). Sample analysis was performed with FlowJo™ v10.7.2 software. A hierarchical gating strategy was applied for sample analysis as is available in the supplementary (Figure S 8, Figure S 9). Cytokine responses were background subtracted and a QC process was applied to remove samples with fewer than 100,000 events in the live CD3+ gate and samples with <1% any of three cytokine response to the positive control, S. enterotoxin B (CD4+ or CD8+ expressing any combination of IFN-γ, IL-2 or TNF). In all cases, cells were stimulated with a single peptide megapool spanning GP1 and GP2. Sequences are detailed in Table S 3 and Table S 5.

The lower limit of detection was set as the reciprocal of the mean CD4+ and CD8+ counts for each data set.

Table 2.4: Intracellular and extracellular stains for the ICS panel.

Marker	Fluorophore	Supplier	Catalogue Number	Volume in test (µL) in 50 µL
IFN-γ	FITC	eBioscience UK	11-7319-82	0.2
IL-2	PE	eBioscience UK	12-7029-82	1
CD107a*	PE-Cy5	eBioscience UK	15-1079-42	0.05
TNF	PE-Cy7	eBioscience UK	25-7349-82	0.05
CD14	eFluor 450	eBioscience UK	48-0149-42	0.5
CD19	eFluor 450	eBioscience UK	48-0199-42	0.5
Viability	AmCyan (for Aqua)	ThermoFisher Scientific	L34957	0.025
CD4	APC	eBioscience UK	17-0049-42	2
CD3	Alexa Fluor 700	eBioscience UK	56-0038-82	1
CD8a	APC-eFluor 780	eBioscience UK	47-0088-42	5
CD45RA [§]	BV605	Biolegend	304133	0.05
CCR7 [§]	BV711	Biolegend	353227	1

*Staining for CD107a was conducted during the stimulation step due to the nature of its early and transient surface expression. [§]These fluorophores were not included in the panel used for EBL07 (biEBOV) samples (Chapter 6) where a 9-colour panel was used.

Molecular Biology

Endonuclease Restriction Digests

Restriction digests were performed with a range of high-fidelity restriction enzymes according to the manufacturer's instructions. Briefly, 20 units of enzyme (1 μ L) was added to 1 μ g pcDNA, reactions were incubated with CutSmart buffer then made up to the required volume with nuclease-free water. The reactions were incubated at 37 °C for 5 to 15 minutes.

Agarose Gel Electrophoresis

For visualisation and for gel extraction, DNA reaction products were separated by 1% agarose gel electrophoresis (100 V, 30-50 minutes) in 1x Tris-acetate-EDTA (TAE), stained with 1X Sybr Safe DNA stain, and visualised on a Dark Reader Transilluminator (Clare Chemical Company). Size estimates of DNA bands were calculated by comparing against 1 kb GeneRuler ladder.

Agarose Gel Extraction

DNA digest fragment or PCR products were excised from agarose gels and purified using a gel extraction kit (New England Biolabs) according to the manufacturer's instructions. Briefly, 400 μ L of gel dissolving buffer was added for every 100 mg of gel in a 1.5 mL Eppendorf tube and the sample incubated at 50 °C for 10 minutes.

Following the dissolution of the agarose the sample was transferred to a column and washed before being eluted with \geq 6 μ L DNA Elution Buffer, also from the New England Biolabs kit.

DNA ligation

Ligations were performed on ice with T4 DNA ligase with a 1:3 molar ratio of vector to insert (New England Biolabs) according to the following generalised protocol in a 20 μL total volume reaction mixture:

2 μL T4 DNA ligase

1 μL 10X T4 DNA ligase buffer

X μL for 50 ng (0.020 pmol) of vector DNA

Y μL for 37.5 ng (0.060 pmol) of insert DNA

Z μL of H_2O for a total reaction volume of 20 μL

Reactions were incubated for 10 minutes at RT and then heat inactivated at 65 $^{\circ}\text{C}$ for 10 minutes. All ligations were carried out on DNA digests with cohesive (sticky) ends.

DNA concentration quantification

Quantification of DNA concentrations were performed by A_{260} spectroscopy using a NanoDrop One (ThermoFisher Scientific). A_{260}/A_{280} ratios were recorded.

Bacterial Transformation

Competent DH5 α *Escherichia coli* cells (New England Biolabs) were transformed for plasmid following ligation reactions. Transformations were carried out according to the manufacturer's instructions. Cells were then plated onto 20 mL Lysogeny broth (LB) agar containing selective antibiotics at 50 $\mu\text{g}/\text{mL}$. Bacteria were grown overnight at 37 $^{\circ}\text{C}$ and stored at 4 $^{\circ}\text{C}$.

Plasmid DNA preparations

Single colonies of transformed bacteria were cultured individually in 3 mL LB medium supplemented with selection antibiotics. Following overnight culture, plasmid constructs were purified by Qiagen Miniprep Kits according to the manufacturer's instructions and screened using restriction digests. Bacteria containing the correctly ligated or recombined plasmid were further amplified in 50 mL of LB culture medium with selection antibiotics. After overnight incubation, plasmid DNA was purified using Qiagen Plasmid Plus Midiprep kits as per the manufacturer's instructions. DNA was stored at -20 °C.

Plasmid Sequencing

Following cloning, plasmid sequences were confirmed via Nanopore sequencing performed by Source BioScience. DNA was provided to Source BioScience at a concentration of 30 ng/μL in nuclease-free water to a volume of 30 μL.

Production of Lentiviral Pseudotypes

Pseudotyped viruses were produced in HEK293T/17 cells. HEK293T/17 producer cells were sub-cultured in 6-well Delta Nunc cell culture plates (Thermo Fisher Scientific) at 3×10^5 cells per well and transfected at 60% confluence with 250 ng of the p8.91 lentiviral packaging plasmid, 375 ng of the pCSFLW firefly luciferase reporter plasmid and 50 ng, 100 ng or 200 ng of SUDV GP pcDNA per well in Opti-MEM media (ThermoFisher Scientific) with FuGENE-HD transfection reagent (Promega). Following incubation for 72

hours at 37 °C with 5% CO₂, the cell supernatant was filtered through a 0.45 µm cellulose acetate membrane. Viruses were stored in single-use aliquots at -80 °C.

Titration of Lentiviral Pseudotypes

HEK293T/17 target cells were sub-cultured in T25 flasks. 2-fold serial dilutions of 100 µL of pseudotype-containing cell supernatant were prepared in complete DMEM in white 96-well Nunclon Delta-Treated flat-bottom 96-well plates. Target cells were detached and 1.5×10^4 cells in 50 µL complete DMEM were added per well to the diluted viruses. Cell and virus mix was incubated at 37 °C in 5% CO₂ for 48 hours. Bright-Glo™ reagent (Promega) and Dulbecco's Phosphate Buffered Saline were mixed at a 1:1 ratio and 30 µL added to each well to lyse cells; luciferase reporter gene activity was measured after a 5-minute incubation at RT using CLARIOstar Plus plate reader (BMG LABTECH).

Pseudovirus (PV) titres are reported in RLU/ mL. Titres above 1×10^8 RLU / mL are considered feasible to use in assay set-up.

Western Blotting

Following the harvesting of pseudoviruses bearing SUDV GP from HEK293T/17 producer cells, cells were washed twice with 1 mL of dPBS on ice. Total protein was extracted from HEK293T/17 cells by incubating with 200 µL of radioimmunoprecipitation assay (RIPA) Lysis Buffer supplemented with 1 X protease inhibitor cocktail for 5 minutes on ice. Cells and lysate were mechanically harvested with a sterile P1000 pipette tip and transferred to a microcentrifuge tube. The harvested lysate sample was centrifuged at $14,000 \times g$ for 15 minutes. Supernatant containing cell lysate was collected and protein concentration determined using the NanoDrop One. Cell lysates and SUDV GP trimeric antigen as a positive control were denatured in 6 × sodium dodecyl sulfate polyacrylamide gel

electrophoresis (SDS-PAGE) loading buffer, separated by SDS-PAGE at 200V for 30 minutes, and electro-transferred to a nitrocellulose membrane using a Trans-Blot turbo for 7 minutes (Bio-Rad). The immunoblots were probed with 1 µg mouse anti - Sudan Ebola virus glycoprotein for one hour followed by incubation with Goat Anti-Mouse IgG conjugated with horseradish peroxidase at a 1:1000 dilution for 1 h. Antibody binding, blocking and washing was carried out using an iBind Flex (ThermoFisher Scientific) according to the manufacturer's instructions. Protein bands were visualized using horseradish peroxidase (HRP) substrate in a ChemiDoc MP gel imager (Bio-Rad).

DNA extraction from PBMC

DNA was extracted from cryopreserved PBMC. PBMCs were incubated with 100 µL ATL buffer (Qiagen) and 20 µL Proteinase K (Qiagen) at 56 °C for 1 hour 30 minutes until the cells were lysed. 130 µL AL buffer was added, and DNA was extracted automatically using a QIAasymphony SP 2.0 instrument with the QIAasymphony DSP DNA Midi Kit (Qiagen) following the manufacturer's instructions. DNA concentration was measured using a NanoDrop One (ThermoFisher).

HLA typing

High resolution class I (HLA-A/B/C) and class II (DRB1/DQB1) human leukocyte antigen (HLA) typing was performed by Timothy Rostron at The University of Oxford by amplifying Exons 2 and 3 and Exon 2 respectively for each locus from DNA extracted from previously cryopreserved PBMC using in-house sequence-specific primers. Sequencing was conducted on an Applied Biosystems AB3730 instrument (ThermoFisher).

Image creation

Infographics and other image-based flowcharts were created for this thesis with BioRender.com

Statistics

Data were tested for normality by D'Agostina-Pearson omnibus normality test, and parametric or non-parametric tests were then used as appropriate. For non-parametric data, geometric means with 95% confidence intervals are presented. Where appropriate, differences between two groups were tested using Mann-Whitney analysis and differences between multiple groups were tested using Kruskal- Wallis with Dunn's multiple comparisons post-test. Wilcoxon matched-pairs analysis and Friedman's test were used to compare paired data. Spearman's rank was calculated for correlations. Where other tests are used, details are given in the appropriate results sections. Statistically significant differences were determined at a significance level of $p \leq 0.05$ and tests were two tailed. Graphs were generated, and statistical analyses were conducted using GraphPad Prism v10.0.3 for MacOS unless stated otherwise in figure captions.

3. Durability of the immune response to three cAd3-EBO Z prime-boost regimens and the administration of an Ad26.ZEBOV boost in UK volunteers.

Introduction

The cAd3-EBO Z vaccine has been shown to provide 100% sterile protection of cynomolgus macaques against an intramuscular challenge with 1000 PFU of highly virulent Ebola virus when the challenge was given 5 weeks after a single 1×10^{10} - 1×10^{11} vp dose of the vaccine. When a separate group of NHPs were challenged 10 months after vaccination with the single 1×10^{11} vp dose, 50% remained fully protected while adding an MVA boost vaccination at 2 months after priming with the 1×10^{10} vp dose was sufficient to confer 100% protection at 10 months [123]. This study provided good evidence for boosting cAd3-EBO Z vaccine recipients if the view was to induce durable protection against EVD.

Between 2014 and 2016, as part of the international response to the Ebola virus epidemic, several candidate vaccines were trialled at The Jenner Institute, University of Oxford [124]. These trials included the evaluation of the cAd3-EBO Z vaccine in combination with either the multivalent MVA-BN-Filo (EBL01 clinical trial; NCT02240875), the monovalent MVA-EBO Z (EBL04 clinical trial; NCT02485912) or Ad26.ZEBOV (EBL05 clinical trial). All three trials were open label, phase I studies and recruited healthy UK adults between 18 – 55 years of age and have now been completed. As expected, they show that boosting cAd3-EBOZ with heterologous viral

vectored vaccine boosts the humoral and cellular response. Full results for EBL01 [71] and EBL04 [96] are published and available, the manuscript for EBL05 is currently being prepared for publication (Katie Ewer, personal communication). As with all phase I trials, these studies focused on safety data as their primary output. Following the completion of these studies, no data were available on the durability of the vaccine induced immune responses beyond six months after prime vaccination for all three trials. It was also unknown whether the primary regimen had established immune memory that could be rapidly reactivated upon antigen re-exposure. Although these three regimens are not currently approved for use against ebola virus, some components (the MVA-BN-Filo and Ad26.ZEBOV) have been licensed as Zabdeno and Mvabea and, as previously discussed, the cAd3-EBOZ/MVA-EBO Z has been particularly promising in NHP studies. Data on their durability will contribute to the wider field of immunology by providing data on the durability of viral vectors. Therefore, it is important that the durability be assessed as well as the response to a booster vaccination. If safe and immunogenic, boosting volunteers during outbreaks would be a viable strategy to control the transmission of Ebola virus.

Study-Specific Methods

REVOLVE clinical trial design.

Healthy adult volunteers who were previously enrolled in the EBL01, EBL04 or EBL05 clinical trial were approached for recruitment into the REVOLVE (Re-evaluating Optimal Vaccine Schedules against Ebola) clinical trial and enrolled at two UK sites: Centre for Clinical Vaccinology & Tropical Medicine, University of Oxford or Imperial Clinical

Research Facility Hammersmith Hospital, London. Participants were offered a dose of Ad26.ZEBOV but the acceptance of this was not a prerequisite for taking part. Those that opted out of the Ad26.ZEBOV vaccination were enrolled in an 'unboosted' group to evaluate the durability of vaccines administered in EBL01, EBL04 and EBL05.

The primary objective of the trial was to assess the persistence of humoral and cellular immunity against Ebola virus glycoprotein with or without a booster dose of Ad26.ZEBOV administered 2 to 5 years after adenoviral and MVA vectored Ebola vaccine schedules. In those that opted for a booster, Ad26.ZEBOV was administered as an intramuscular injection of 5×10^{10} vp into the anterolateral deltoid muscle. The vaccine was supplied in a single-use 2 mL glass vial with an extractable volume of 0.5 mL liquid suspension at a concentration of 1×10^{11} vp/mL, formulated in the final formulation buffer. The Ad26.ZEBOV drug substance and drug product were produced by or under the responsibility of Janssen Vaccines & Prevention B.V., Leiden, the Netherlands.

Blood samples were taken from the boosted cohort at four time points: day of boost, then 7, 28 and 364 days later. Blood samples were taken from the volunteers who declined a boost at two timepoints, one at enrolment and another 364 days later.

The clinical trial design is summarised in Figure 3.1.

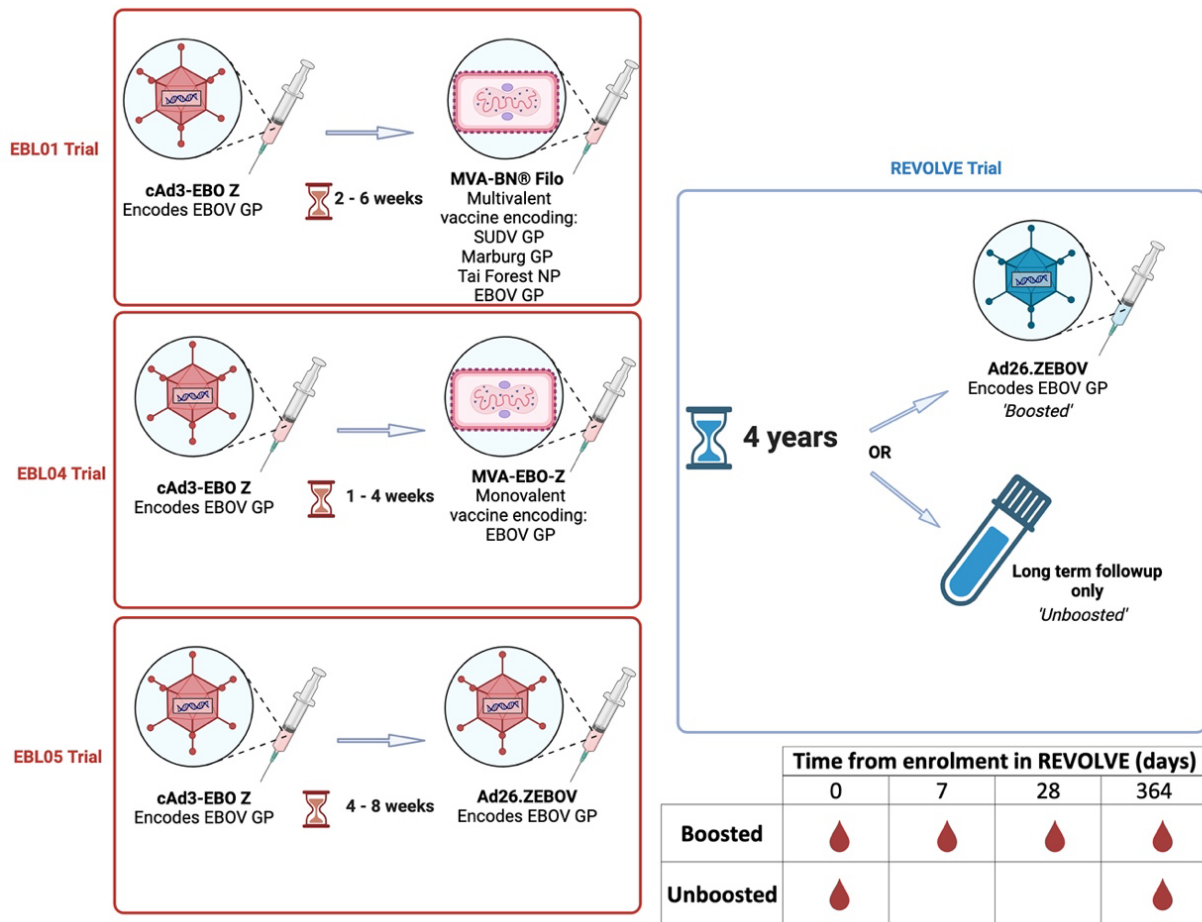


Figure 3.1: Schematic showing the outline and vaccination schedule for the EBL01, EBL04 and EBL05 parent trials and the REVOLVE clinical trial. Blood draws for the boosted and unboosted groups are depicted as red droplets in a time course table.

Objectives

1. To evaluate the longevity of the immune response to EBOV in volunteers vaccinated with cAd3- EBO Z and boosted with either MVA-BN-Filo, MVA-EBO Z or Ad26.ZEBOV as administered in the EBL01, EBL04 and EBL05 parent clinical trials
2. To evaluate the cellular and humoral response to an Ad26.ZEBOV boost administered between a median of 51 to 60 months post original vaccination.

Results

Recruitment

A total of 47 participants, representing 30% of the combined EBL01, EBL04 and EBL05 cohorts (47/156), were recruited into the REVOLVE study. Of the 47 participants, 25 volunteers were previously enrolled in EBL01, 17 volunteers from EBL04 and 5 volunteers from EBL05. Volunteers returned for their first visit and blood draw for immunological analysis, or booster vaccine if opted in, in REVOLVE between 43 – 62 months from their original priming vaccination. A total of 28 recruited volunteers opted to receive a booster vaccination of Ad26.ZEBOV.

Demographic information is detailed in Table 3.1.

Table 3.1: Volunteer demographics in the REVOLVE clinical trial. Age on the date first clinical trial visit for REVOLVE is shown.

Parent Trial	EBL01		EBL04		EBL05	
Boost?	Yes	No	Yes	No	Yes	No
n=	16	9	11	6	1	4
Sex						
Male	11 (69%)	2 (22%)	6 (55%)	3 (50%)	1 (100%)	4 (100%)
Female	5 (31%)	7 (78%)	5 (45%)	3 (50%)	0 (0%)	0 (0%)
Age						
Range						
(median)	28-53 (39)	29-53 (39)	27-53 (41)	29-52 (38)	N/A (30)	25-54 (31)
Ethnicity*						
White	15 (94%)	9 (100%)	10 (91%)	6 (100%)	1 (100%)	4 (100%)
Other	1 (6%)					
Mixed			1 (9%)			
Time from prime vaccination (months)						
Range						
(median)	43-62 (60)		48-52 (51)		46-48 (47)	

*ethnicity was self-reported.

Humoral Immunology

At the first sampling time point, in house standardised ELISA was conducted to enumerate the durability of antigen specific IgG. Some responses were detectable in all regimens with GMT of 114.1 [95% CI 50.03-260], 66.84 [95% CI 26.61-167.9] and 229.1 [95% CI 80.97-648.2] for EBL01 (cAd3-EBO Z/MVA-BN-Filo), EBL04 (cAd3-EBOZ/MVA-EBO Z) and EBL05 (cAd3-EBOZ/Ad26.ZEBOV) respectively. 24 - 60% were seropositive depending on regimen (Figure 3.2A).

As only one volunteer from EBL05 (cAd3-EBO Z/ Ad26.ZEBOV) was boosted, data is not presented or discussed for the boosting of cAd3-EBO Z/ Ad26.ZEBOV with Ad26.ZEBOV alongside the summary data discussed here. The ELISA result for this volunteer can be found in the supplementary data (Table S 6).

Anti-EBOV GP total IgG (tIgG) titres were assessed using a standardised in-house ELISA on the day of the Ad26.ZEBOV boost, and at 7, 28, and 365 days after the boost.

Following the administration of Ad26.ZEBOV, a 129 and 239-fold increase in GMTs was observed for EBL01 and EBL04 volunteers, respectively. Geometric mean titres (GMTs) rose as early as day 7 and peaked at 16871 [95% CI 9637-27822] aEU for EBL01 and 19716 [95% CI 1034-4001] for EBL04 on day 28. This elevation above baseline was sustained up to 365 days post-boost, where GMTs were 2034 [95% CI 1034-4001] and 3038 [95% CI 1629-5668] aEU, significantly higher than pre-boost titres (Wilcoxon matched-pairs signed rank test, $P < 0.0001$ for EBL01, $P = 0.0039$ for EBL04) (Figure 3.2B).

Volunteers who had not received a boost had stable titres across the 12-month time period. When data from EBL01 and EBL04 volunteers was combined, 100% of the volunteers who had opted to receive a boost were seropositive and had significantly higher titres than those that declined a boost at the final time point (Mann Whitney, $P < 0.0001$) Figure 3.1 Figure 3.2C)

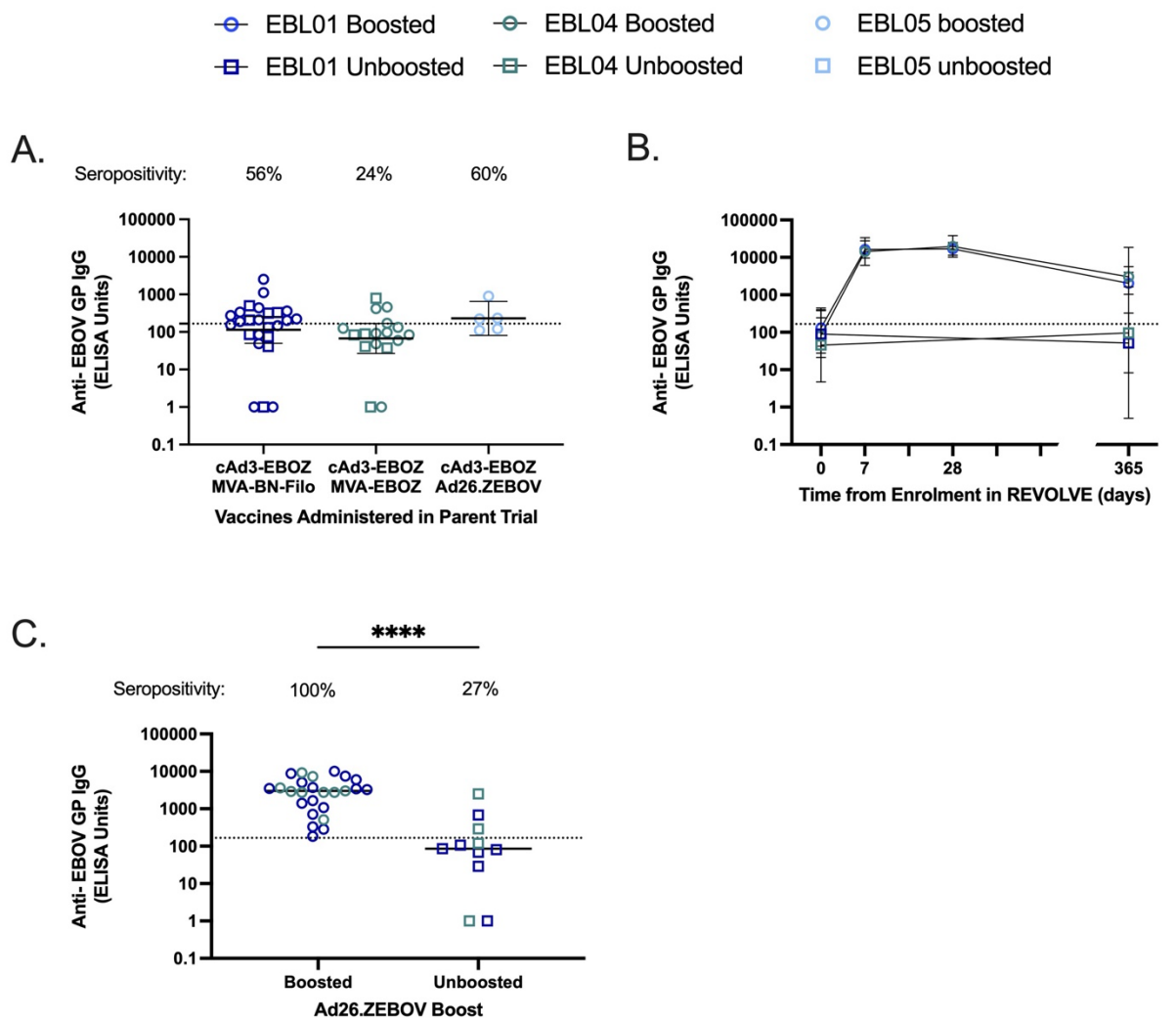


Figure 3.2: anti-EBOV GP IgG as measured by in house standardised ELISA. Circles denote volunteers who received an Ad26.ZEBOV boost in the REVOLVE trial, squares denote volunteers who opted out of an Ad26.ZEBOV boost and are 'unboosted'. Dark blue shapes represent volunteers recruited from EBL01, green shapes represent volunteers recruited from EBL04 and light blue shapes represent volunteers recruited from EBL05. In all cases lines represent geometric means and bars show 95% confidence intervals. A) Durability of ELISA titres and rates of seropositivity at the first time point in all volunteers by original trial. B) ELISA units over time in boosted and unboosted EBL01 and EBL04 volunteers. In boosted volunteers, Ad26.ZEBOV was administered at D0. Shapes show geometric means C) ELISA units at the final time point (365 days after enrolment in REVOLVE) in EBL01 and EBL04 volunteers who did and did not receive an Ad26.ZEBOV boost. Asterisks show statistical significance with Mann Whitney test. **** P<0.0001.

As the assay was conducted using the same standard operating procedure (SOP) within the same laboratory for the parent trials, results for the EBL01 and EBL04 boosted volunteers across the parent trials and REVOLVE are combined to give a time course from baseline and across the three vaccinations. The Ad26.ZEBOV boost delivered in the REVOLVE trial boosted tIgG titres 5.8-fold and 4.0-fold higher than the peak measured in the original trial for EBL01 (MVA-BN-Filo + 28 days) and EBL04 (MVA-EBO Z + 28 days) volunteers respectively (Figure 3.3)

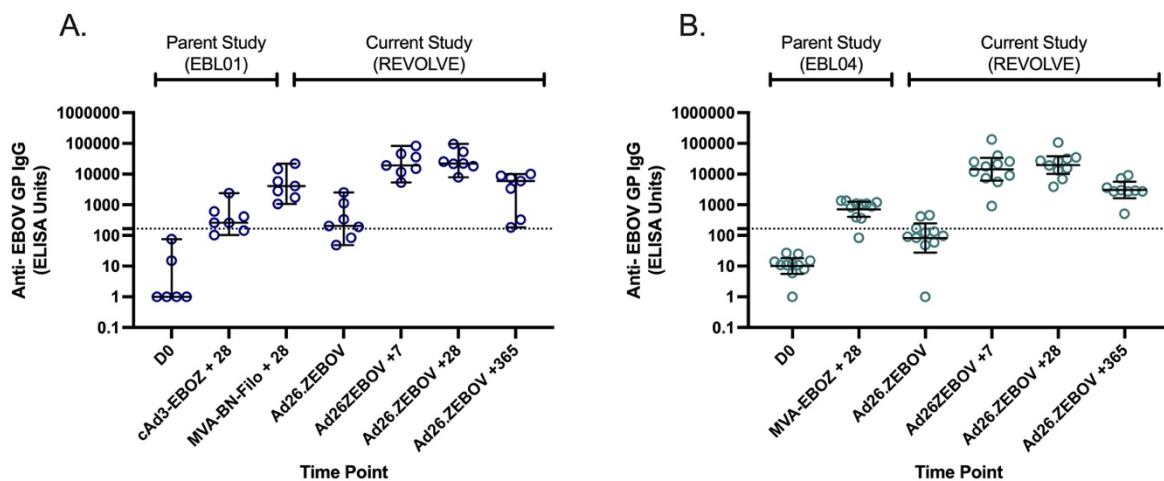


Figure 3.3: anti-EBOV GP IgG as measured by in house standardised ELISA measured over the three vaccinations in the parent and current study. A. EBL01 volunteers (vaccine schedule: cAd3-EBOZ, MVA-BN-Filo, Ad26.ZEBOV) B. EBL04 volunteers (vaccine schedule cAd3-EBOZ, MVA-BN-Filo, Ad26.ZEBOV).

The avidity of IgG antibodies to EBOV trimeric GP was assessed in boosted volunteers from EBL01 and EBL04 using a displacement ELISA with NaSCN as a chaotropic agent on both the day of, and 365 days after, Ad26.ZEBOV vaccination. Samples from volunteers showing seropositivity for anti-EBOV GP IgG, as defined by a titre above the assay cut-off of 166 aEUs (as described in Materials and Methods: Anti-EBOV GP and anti-SUDV GP total IgG ELISA) at both time points were exclusively chosen to allow for

paired analyses, pending sample availability (n=12). The antigen specific IgG induced by cAd3-EBO Z/MVA-BN-Filo and cAd3/MVA-BN-Filo vaccination measured prior to the Ad26.ZEBOV boost have a median IC50 of 1.906 after Ad26.ZEBOV administration the median IC50 of IgG antibodies had significantly increased to 2.058 (Wilcoxon matched pairs test, P=0.0452). All individual volunteers except for one had an increase in IC50. (Figure 3.4)

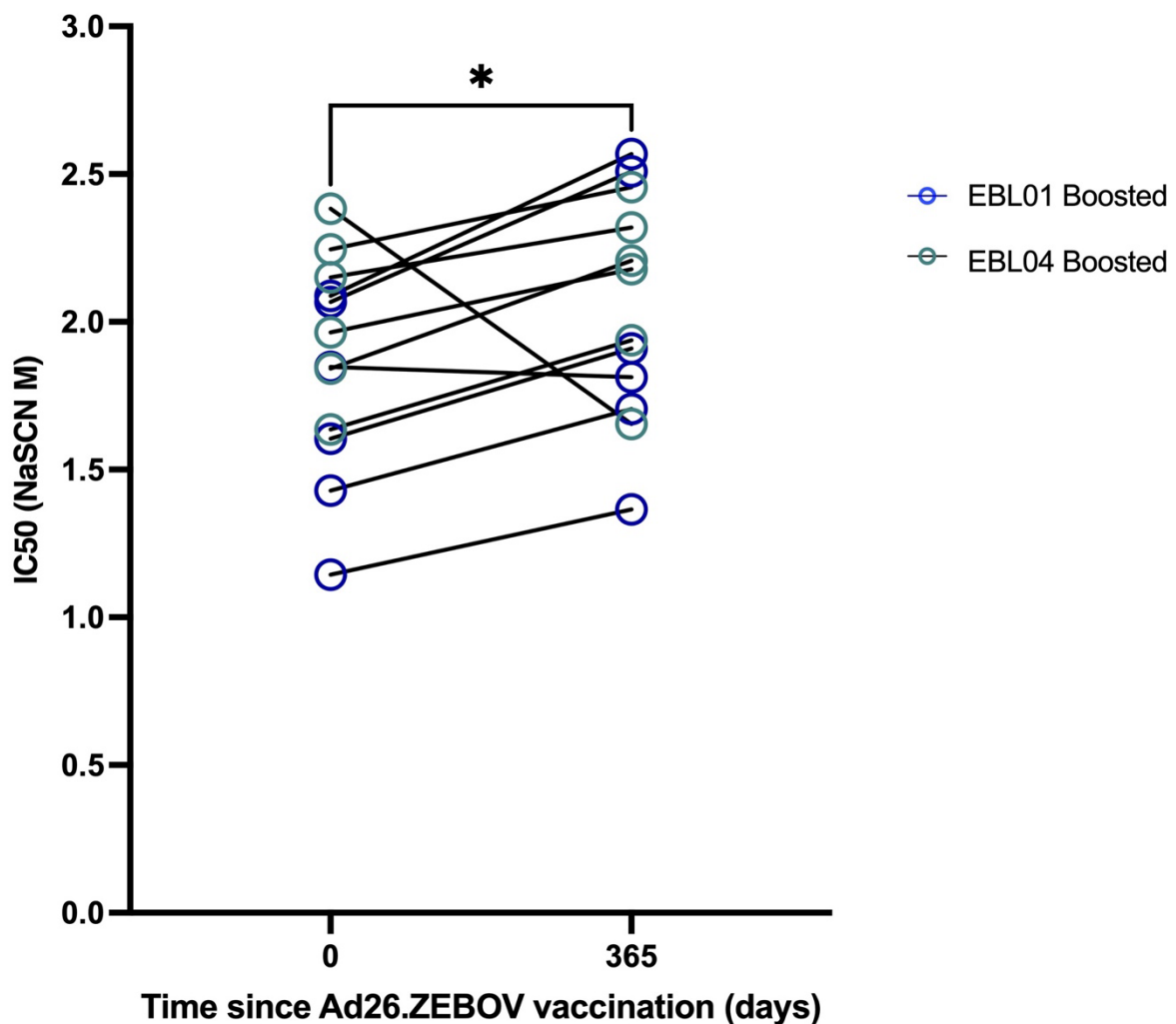


Figure 3.4: Avidity of IgG antibodies to EBOV-GP. Individual data points were expressed as an IC50 and shown here as scatter dot plots. Asterisk shows significant difference as determined by two-tailed Wilcoxon paired test *, P=0.0425.

Due to the time and reagent-intensive nature of the assay, the assessment of neutralising antibodies was conducted using samples from boosted EBL01 and EBL04 volunteers by pseudoneutralisation of lentiviruses bearing the EBOV GP at baseline, to assess the durability of the regimens, and at 7-days after Ad26.ZEBOV boost to assess the utility of the Ad26.ZEBOV boost, only. These two time points provide a good ‘snapshot’ of functionality of the humoral response at key timepoints. At baseline, there was a wide range of neutralising capacity between volunteers. However, the administration of the Ad26.ZEBOV boost significantly increased the neutralising capacity of plasma EBOV GP bearing pseudotypes (Wilcoxon matched pairs signed rank test, $P=0.005$) (Figure 3.5A). All but one volunteer showed an increase in neutralising capacity; the volunteer with a decrease in IC50 also displayed a decrease in IgG avidity (Figure 3.4). There was a strong positive correlation between IC50 and titres of anti-EBOV GP IgG as quantified with the standardised in-house ELISA (Spearman’s $r=0.705$, $P<0.0001$) (Figure 3.5B)

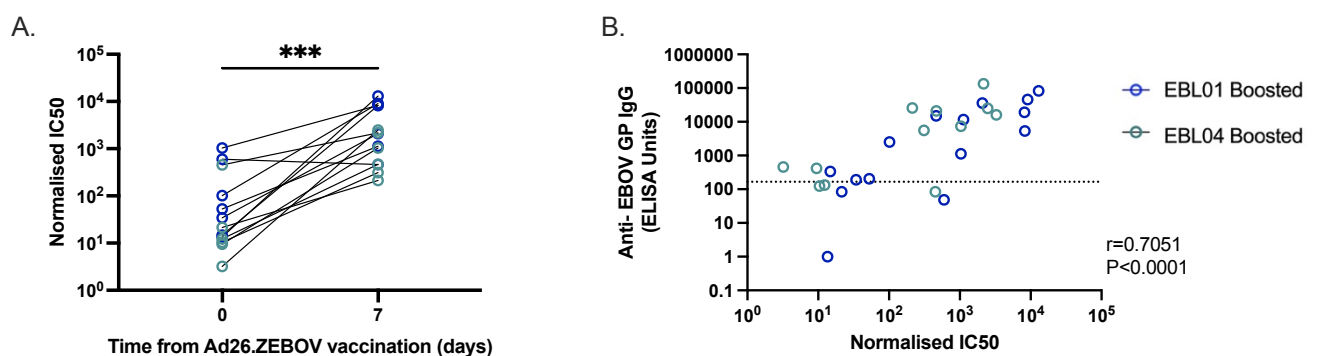


Figure 3.5: Pseudoneutralisation of EBOV GP-bearing lentiviral pseudotypes at day of, and 7 days post-boost. Shapes represent neutralisation IC50 with lines showing median. A) IC50 in EBL01 and EBL04 boosted volunteers at long term follow-up/time of Ad26.ZEBOV vaccination and 7 days post boost Asterisks show statistical significant as measured by Wilcoxon signed rank test * $P=0.005$. B)**

Correlation between pseudoneutralisation IC50 and antigen specific binding IgG with aggregated data from day of boost and 7 days post boost.

T cell immunology

At the first time point, IFN- γ ELISpot assays were conducted to measure the durability of the T cell response. T cell responses to the EBOV GP were detectable, with a geometric mean of 104.6 [95% CI 83.57-236.5] SFC/10⁶ PBMC, 189.2 [95% CI 114.1-313.6] SFC/10⁶ PBMC and 432.9 [145.5-1288] SFC/10⁶ PBMC for volunteers recruited from EBL01 (cAd3-EBO Z/MVA-BN-Filo), EBL04 (cAd3-EBOZ/MVA-EBO Z) and EBL05 (cAd3-EBOZ/Ad26.ZEBOV) respectively (Figure 3.6A).

Following the Ad26.ZEBOV boost, responses significantly increased by 18-fold to peak at 1983 [95% CI 1065-3693] SFC/10⁶ PBMC in EBL01 volunteers, and 18-fold to peak at 2582 [95% CI 1745-3821] SFC/10⁶ PBMC in EBL04 volunteers at 7 days after boost. 365 days after the Ad26.ZEBOV booster vaccination, responses contracted to 827 [95% CI 405 – 1685] SFC/10⁶ PBMC in EBL01 volunteers and 535 [95% CI 274-1044] SFC/10⁶ PBMC in EBL04 volunteers. These T cell responses at 1-year post-boost were significantly higher than those measured at baseline, pre-boost (Kruskal Wallis, P=0.0002 for EBL01 and P=0.0091 for EBL04) (Figure 3.6B)

When comparing those participants who received a booster vaccination with those who did not receive a booster vaccination at the final time point, T cell responses were significantly higher in those who were boosted than in those who opted out (Mann-Whitney, P=0.0006) (Figure 3.6C)

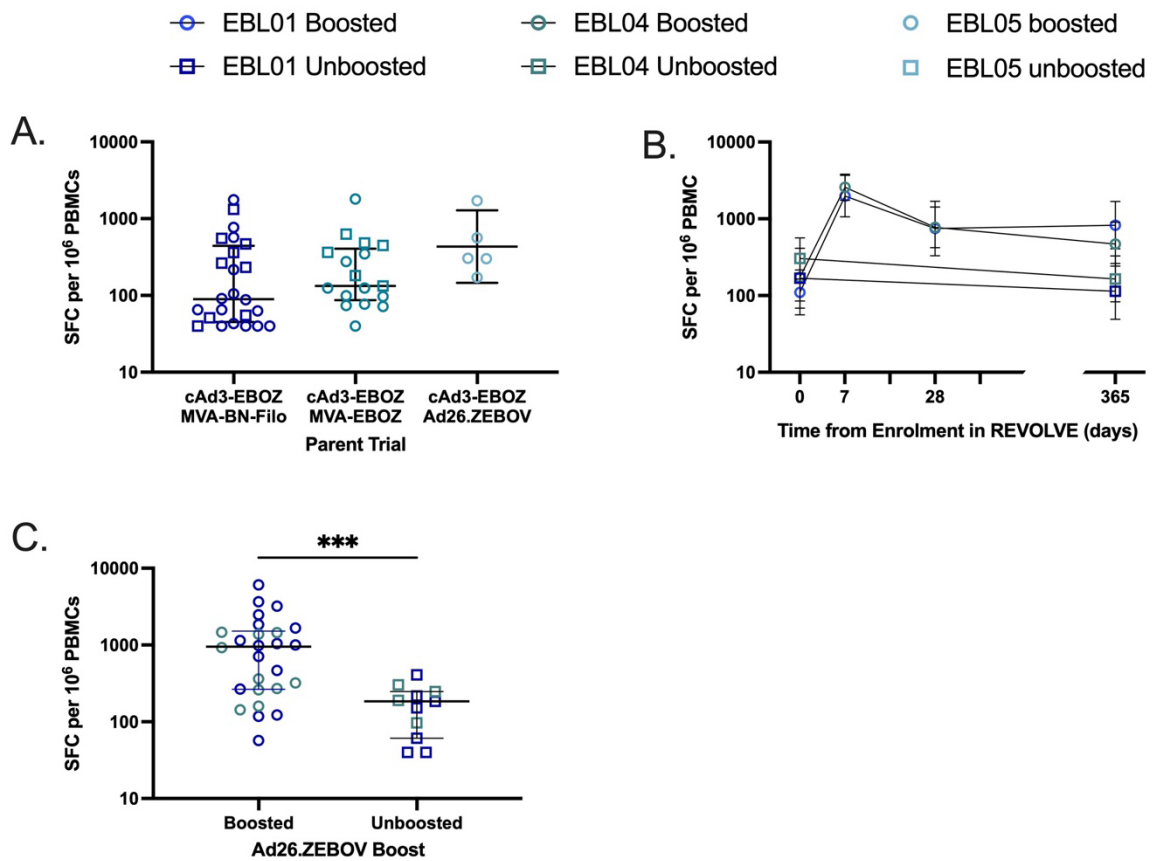


Figure 3.6: EBOV GP-specific IFN-γ T cell responses as measured in PBMC by IFN-γ ELISpot. Circles denote volunteers who received an Ad26.ZEBOV boost in the REVOLVE trial, squares denote volunteers who opted out of an Ad26.ZEBOV boost and are 'unboosted'. Dark blue shapes represent volunteers recruited from EBL01, green shapes represent volunteers recruited from EBL04 and light blue shapes represent volunteers recruited from EBL05. In all cases lines represent geometric means and bars show 95% confidence intervals. A) Durability of the T cell response at the first time point in all volunteers by original trial. B) T cell response over time in boosted and unboosted EBL01 and EBL04 volunteers. In boosted volunteers, Ad26.ZEBOV was administered at D0. Shapes show geometric means C) T cell response at the final time point (365 days after enrolment in REVOLVE) in EBL01 and EBL04 volunteers who did and did not receive an Ad26.ZEBOV boost. Asterisks show statistical significance with Mann Whitney test. * $P= 0.0006$**

As the ELISpot assay was conducted using the same SOP within the same laboratory for the parent trials, results for the EBL01 and EBL04 boosted volunteers across the parent

trials and REVOLVE are combined to give a time course from baseline and across the three vaccinations. The Ad26.ZEBOV boost delivered in the REVOLVE trial boosted T cell titres 1.6-fold and 1.4-fold higher than the peak measured in their original trial (MVA-BN-Filo+7) for EBL01 and EBL04 volunteers respectively (Figure 3.7).

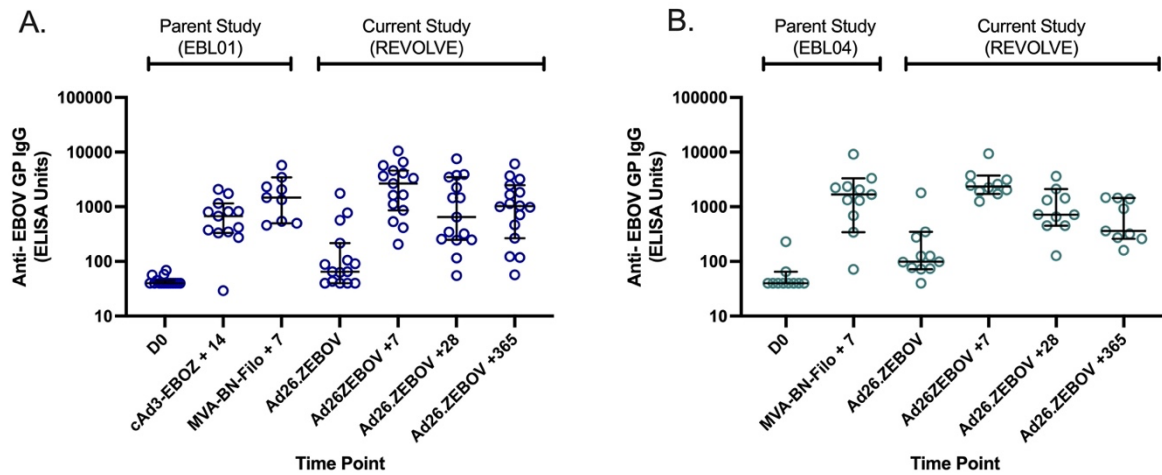


Figure 3.7: EBOV GP-specific IFN- γ T cell responses as measured in PBMC by IFN- γ ELISpot over the three vaccinations in the parent and current study. A. EBL01 volunteers (vaccine schedule: cAd3-EBOZ, MVA-BN-Filo, Ad26.ZEBOV) B. EBL04 volunteers (vaccine schedule cAd3-EBOZ, MVA-BN-Filo, Ad26.ZEBOV).

Pool analysis in the boosted cohort at 7 days post-Ad26.ZEBOV boost revealed detectable T cell responses to all peptide pools spanning both GP₁ and GP₂ of the glycoprotein in at least one volunteer indicative of the recognition of multiple epitopes across the glycoprotein. Responses to the individual pools were comparable regardless of the parent trial. When data from the three groups is combined, the highest average response observed to the peptide pool spanning amino acids 103-180 within GP₁ with a geometric mean of 320.5 [95% CI 167.6-612.6] SFC/10⁶ PBMC. Although still immunogenic, the lowest responses were observed to the peptides in the pool spanning amino acids 305-389, also in GP₁, which had a geometric mean response of 24.0 [95%

CI 9.8-58.6] SFC/ 10^6 PBMC. The measured responses to peptides following Ad26.ZEBOV administration also followed a similar pattern of recognition to those seen at the peak response generated from cAd3-EBOZ/ MVA-EBO Z vaccination in the original regimen although the response to most pools was higher upon the third vaccination (Ad26.ZEBOV +7), boosting was particularly evident in the pool spanning amino acids 103 to 180 (Figure 3.8).

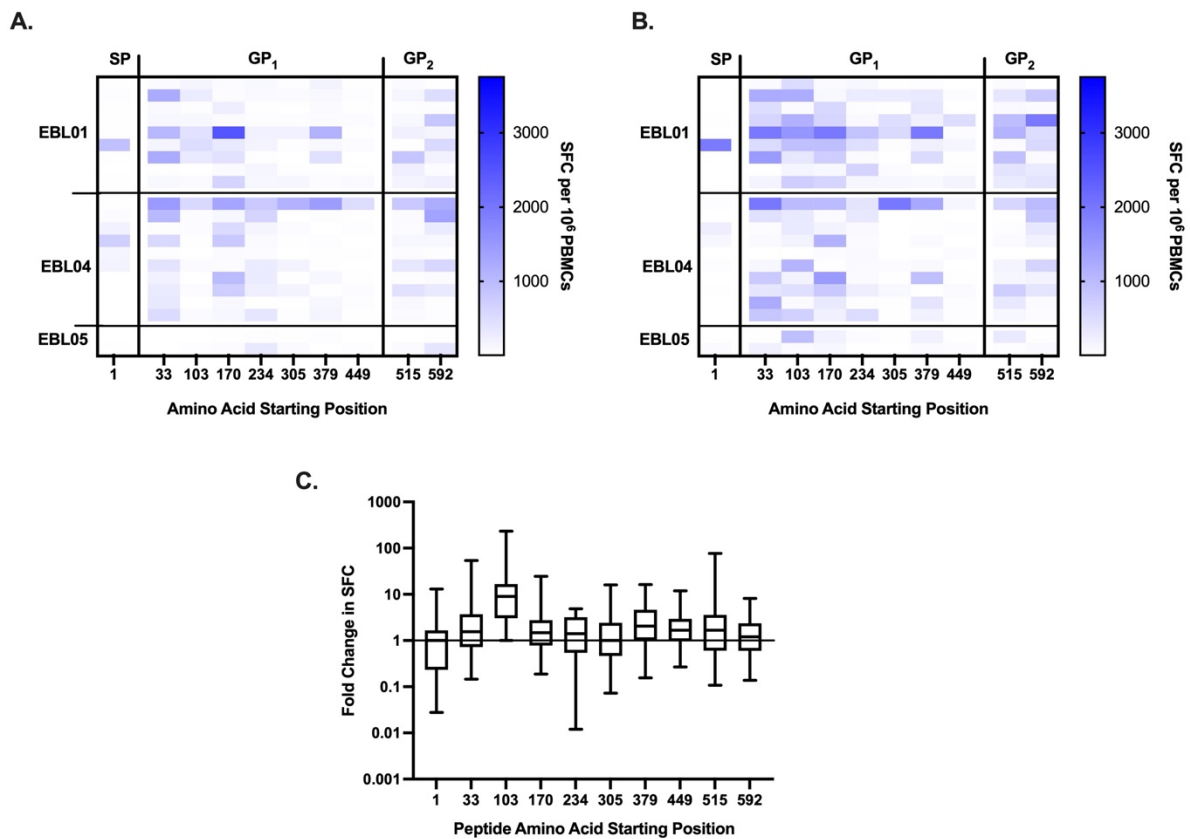


Figure 3.8: Heat map of responses to individual peptide pools spanning the EBOV GP at: A. 7 days after cAd3-EBOZ/MVA-BN-Filo (EBL01) cAd3-EBO Z/ MVA-EBO Z (EBL04), or cAd3-EBOZ/Ad26.ZEBOV (EBL05) vaccination or **B.** 7 days after Ad26.ZEBOV vaccination (REVOLVE clinical trial). Panel C shows fold change in SFC between responses 7 days after MVA boost in the EBL01, EBL04 and EBL05 trials and 7 days after Ad26.ZEBOV vaccination in the REVOLVE trial. Lines show median with whiskers showing range.

Flow cytometry with ICS was performed 28 days post-Ad26.ZEBOV boost. Analysis of polyfunctionality via Boolean gating indicated that the pattern of cytokine secretion was similar for both EBL01 and EBL04 volunteers. Double positive cells expressing IFN- γ and TNF are the most frequent proportions of CD8+ cells. Polyfunctional T-cells expressing IFN- γ , IL-2, and TNF constituted the largest subgroup in the CD4+ T-cell response (Figure 3.9A). At the same time point, a median of 0.08% [IQR 0.0193% – 0.4850%] of prior EBL01 vaccinees and 0.15% [IQR 0.07600% – 0.2240%] of prior EBL04 vaccinees CD8+ T cells expressed CD107a (LAMP-1), a marker indicating the capacity for cytotoxic degranulation (Figure 3.9B)

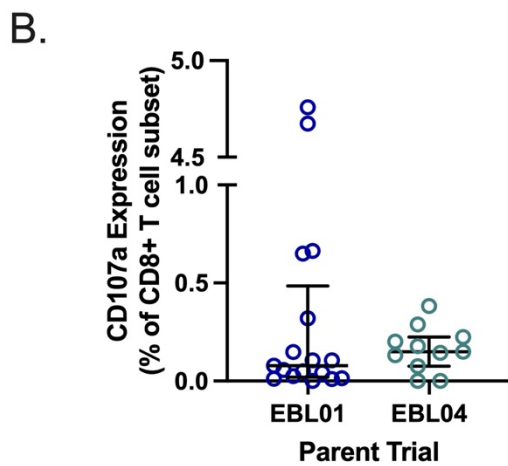
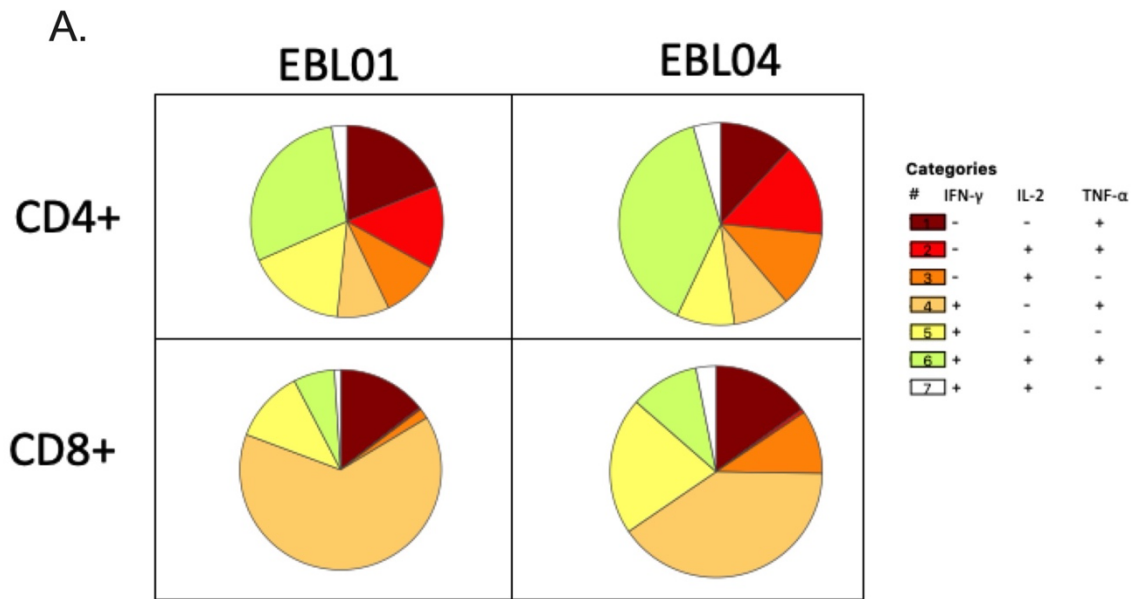


Figure 3.9: ICS analysis in EBL01 and EBL04 boosted volunteers, 28 days after Ad26.ZEBOV vaccination. A. The proportions of CD4+ and CD8+ T cells that secreted any combination of interferon- γ , interleukin-2, and TNF in EBL01 or EBL04 volunteers 28 days after boosting with Ad26.ZEBOV. B. The proportion of CD8+ cells secreting CD107a (LAMP1).

Discussion

This study is the first to evaluate the longevity of the cAd3-EBOZ vaccine when administered with MVA-BN-Filo, MVA-EBO Z or Ad26.ZEBOV and the only study to administer a third Ebola virus vaccine to individuals who had previously been vaccinated with these regimens.

These vaccine immunogenicity results can be interpreted through the two arms of humoral immune memory: the maintenance of long-term antibodies and the induction of B cell memory. Up to 60 months (approximately 5 years) after receiving the primary regimen, 24-60% of volunteers still had EBOV GP- specific IgG antibodies in circulation and were considered responders prior to booster administration, depending on the original vaccine regimen in the trial they were recruited from. This indicates that the primary regimen can induce long lasting vaccine-specific antibody responses in a proportion of healthy UK adults. The Ad26.ZEBOV boost induced a strong anamnestic response, as evidenced by a rapid increase in Ebola virus glycoprotein-specific binding antibody titres, detected at the earliest post-boost sampling time point (7 days post-boost) which were 4 and 5.8-fold higher than those measured during the original regimen. This is indicative of robust B cell memory established during the cAd3-EBO Z/ MVA-BN-Filo and cAd3/EBOZ regimen.

At long-term follow-up, functional analysis of the serological response in prior EBL01 and EBL04 participants found that plasma was able to neutralise pseudotyped lentiviruses bearing the EBOV GP at low levels. When these volunteers received a booster dose, neutralising activity as measured by normalised IC50 was significantly

increased 7 days after Ad26.ZEBOV administration. At the long-term follow-up time point, this neutralising response is most likely to be driven by IgG antibodies; however, 7 days after the Ad26.ZEBOV boost, neutralising activity may also be mediated by antigen specific immunoglobins from the IgM subclass, as is observed in recipients of the rVSV-ZEBOV [125], as well as the IgG subclass. The Ad26.ZEBOV vaccination also induced a small but significant long-term increase of the avidity of the antigen specific IgG one year after the Ad26.ZEBOV boost. Increased antibody binding strength is often considered to be important for immunoglobulin viral neutralisation [126-128].

Observationally, the only volunteer who did not exhibit an increase in avidity also did not have a boosting effect on neutralising antibody titres. In a study of the RTS,S/AS01 vaccine against malaria, higher avidity of vaccine-induced antibodies was positively associated with protection against *Plasmodium falciparum* infection [129]. It is often thought that this is likely to apply across other diseases and vaccines, however, a recently published study showed that Ebola virus GP antigen specific avidity did increase with multiple doses of protein-subunit vaccine, but NH4SCN IC50 values only weakly correlated between study week eight and survival day [130]. However, as with many NHP studies due to ethical concerns, this research had a limited sample size. Nevertheless, these results shown here in humans are at least indicative of antibody avidity maturation caused by the repeated exposure to EBOV GP antigen as delivered a third time by the Ad26.ZEBOV vector. Regarding the cellular response, an increase in IFN- γ secreting T cells were measured and reached titres higher than those seen in the original regimen, but they were not boosted to the same level that IgG binding antibodies were.

There were several limitations to this study. As the premise of the study necessitated reapproaching volunteers who had participated in completed clinical trials, and multiple years had passed since they participated in their parent study, there is a reduction in number of participants than was seen in the parent studies with only 30% of the total cohort enrolling onto the trial. While the exact reason for the reduced recruitment rate is unknown, factors may include participants relocating out of the geographical area and changing life circumstances. For example, the administration of the Ad26.ZEBOV boost required the use of an effective method of contraception up to three months after vaccination which may no longer align with the participant's lifestyles. Unfortunately, this sample size was smaller than predicted for the trial and was particularly impactful for participants who had previously received cAd3-EBOZ and Ad26.ZEBOV vaccines as part of the EBL05 trial. Only five volunteers from this cohort were recruited into REVOLVE, and only one opted to receive an Ad26.ZEBOV boost limiting the ability to calculate summary data and conduct a meaningful analysis on the boosting of this regimen. Had the sample size for this group been larger, it would have provided an interesting opportunity to look the impact of homologous boosting (as the Ad26.ZEBOV boost was given in REVOLVE as well as in EBL05) vs heterologous boosting (as the EBL01, EBL04 volunteers has not received Ad26.ZEBOV vaccine in their original trial) on antigen specific responses as an exploratory analysis. Meta-analysis from studies conducted during the COVID-19 booster vaccination efforts in adults suggest that when multiple doses are given, heterologous regimens have a higher protection against symptomatic or severe disease when compared to homologous booster doses [131, 132]. Strong anti-vector immunity has previously been observed in other Ad26 vectored vaccinees targeting SARS-CoV-2 [133] and HIV-1 [133, 134] although Ad26

virus neutralising titres did not correlate with reduced immunogenicity in both cases and anti-vector neutralising antibodies have been shown to persist in human sera as long as 9 months after vaccination [133]. This study would have allowed for the comparison of titres to Ad26 naïve volunteers at very long-term follow-up with volunteers who received cAd3-EBO Z boosted with non-adenovirus viral vectored vaccines (boosting was with the pox virus MVA) in their original trials as a control group (EBL01, EBL04).

The long-term follow-up was carried out up to 1 year after boost. Given that antigen specific T cell responses and IgG both remain above elevated at the final timepoint, and significantly higher than the responses of volunteers who opted out of a boost. It would be valuable to follow up to beyond a year assess the durability of the booster dose. Such work would be informative for decision makers when analysing if, or how often, booster vaccines may need to be administered in outbreak scenarios. However, this was beyond the scope of the current trial.

Lastly, the study was conducted in a predominantly white British UK population and may not be reflective of populations most at risk of EBOV. This limitation is partially addressed in the next chapter, where the durability, and boosting, of the cAd3-EBOZ/MVA-EBO Z vaccine is assessed in a Senegalese population (Chapter 4).

Conclusions

Overall, good longevity of antigen-specific IgG and T cell responses was observed to cAd3-EBOZ boosted with MVA-BN-Filo, MVA-EBO Z or Ad26.ZEBOV. A single dose of

Ad26.ZEBOV given to a cohort of the study participants was amnestic with a marked increase in antigen specific binding IgG, pseudoneutralising antibodies and T cell responses 7 days post boost. Those that received a boost remained 100% seropositive and had significantly higher binding IgG and T cell responses one year later than those who opted out of a booster vaccine. A subset of this data (cAd3/EBOZ/ MVA-EBO Z vaccinees) will be compared to a Senegalese cohort matched for vaccine administration in the following chapter to evaluate the vaccine in a different population.

4. Durability of cAd3-EBO Z/MVA-EBO Z and the administration of a delayed Ad26.ZEBOV boost in Senegalese adults.

Introduction

Human Cytomegalovirus

Human Cytomegalovirus (CMV) is a ubiquitous beta human herpesvirus type 5 which typically causes a mild or asymptomatic acute infection in immunocompetent individuals, followed by the establishment of lifelong latency [135]. Following primary infection, the host seroconverts, leading to lifelong CMV-specific immunoglobulin G (IgG) alongside cellular immune responses. However, in certain subsets of the population, such as those with compromised or immature immune systems (e.g. organ transplant recipients, patients with AIDS, and neonates) primary CMV infection or reactivation from latency can lead to symptomatic outcomes and morbidity [136, 137].

The control of CMV infection leads to a substantial increase in CMV-specific T cells over time, comprising approximately 5–30% of peripheral CD8+ T cells [138, 139]. The increased expansion of terminally differentiated and senescent T cells may come at the expense of the naïve T cell pool [139-141]. This effect on the T cell repertoire, resulting from virus-specific cells undergoing major expansions, has been linked to the concept of “memory inflation” described for the murine model of MCMV [142]. This immune senescent phenotype may have far-reaching immunological

consequences, including affecting responses to vaccination in adult populations, although evidence is conflicting [143].

EBL06 Clinical Trial

In the EBL06 clinical trial, 40 healthy Senegalese adults (aged 18 -50 years) were recruited for a phase Ib safety and immunogenicity trial of heterologous prime-boost immunisation with cAd3-EBO Z and MVA-EBO Z (EBL06, NCT02485912). The trial has ended, and results have been published [96]. All volunteers received a priming vaccination of 3.6×10^{10} viral particles (vp) (range: 2.5×10^{10} - 3.7×10^{10} vp) of cAd3-EBO Z followed by a boost of 1.0×10^8 PFU of MVA-EBO Z seven days later. The one-week prime-boost interval was selected for its suitability in an outbreak scenario. The site of MVA-EBO Z administration differed between two groups: one group received the MVA-EBO Z vaccine in the same (ipsilateral) arm as the cAd3-EBO Z vaccine and the other received the MVA-EBO Z vaccine in the opposite (contralateral) arm.

Results from the study showed that this regimen was safe, immunogenic and elicited both humoral and cellular responses to EBOV GP. However, interestingly, both Senegalese groups had significantly lower EBOV-specific IgG titres at both one week and six months post-MVA vaccination compared to a vaccine regime-matched group from a UK cohort [96]. This reduction in immunogenicity correlated with CMV carriage. When volunteers were serotyped, CMV seropositivity was found to be ubiquitous in the Senegalese cohort and 50% in the UK group. Among CMV-seropositive (CMV+) individuals, there were increased proportions of effector

memory and TEMRA CD4+ and CD8+ T cells, as well as an expansion of phenotypically senescent CD4+ and CD8+ T cells expressing CD57 and killer cell lectin-like receptor G1 (KLRG1), which was negatively correlated with vaccine responses in both cohorts [144].

Following the completion of this trial, no data were available on the durability of the vaccine induced immune response in Senegalese adults beyond one year. It was also unknown whether the primary regimen had established immune memory that could be rapidly reactivated upon antigen re-exposure. Therefore, it is important to assess the longevity of these regimens in Senegalese volunteers as well as assess the response to a booster. If safe and immunogenic, boosting volunteers during outbreaks would be a viable strategy to control the spread of Ebola virus.

Given that a successful vaccine targeting Ebola virus will need to be effective in West and Central African populations, it is also important to assess whether the differences in immunogenicity between the UK and the Senegalese cohort persist beyond those previously observed up to 6 months post-MVA vaccination and if the correlation between CMV serostatus and immunogenicity impacts the immune memory from the cAd3-EBO Z/ MVA-EBO Z regimen.

Objectives:

1. To evaluate the longevity of the immune response to cAd3-EBO Z and MVA-EBO Z regimen as administered in the EBL06 clinical trial.

2. To evaluate the cellular and humoral response to an Ad26.ZEBOV boost administered a median of 4.25 years after the original regimen.
3. To compare the immunogenicity in Senegalese volunteers to a UK cohort who received the same vaccination schedule.
4. To investigate if CMV serostatus correlates with immunogenicity.

Study-Specific Methods

RESOLVE clinical trial design.

Healthy adult volunteers who were previously enrolled in the EBL06 clinical trial were approached for recruitment into the RESOLVE (Re-evaluating in Senegal Optimal Vaccine Schedules against Ebola) clinical trial at the Institut de Recherche en Santé, de Surveillance Epidémiologique et de Formation (IRESSEF) in Dakar, Senegal (ISRCTN15434137). The primary objective of the trial was to assess humoral and cellular immunity against the Ebola virus glycoprotein one year after receiving a booster dose of Ad26.ZEBOV, administered as an intramuscular injection of 5×10^{10} vp into the anterolateral deltoid muscle. The vaccine was supplied in a single-use 2 mL glass vial with an extractable volume of 0.5 mL liquid suspension at a concentration of 1×10^{11} vp/mL, formulated in the final formulation buffer. This booster dose was administered approximately 4.25 years after receiving the initial heterologous prime/boost vaccination regimen of cAd3-EBO Z /MVA-EBO Z, with a 7-day interval. Blood samples were taken from the boosted volunteers at day of boost, then 7, 28 and 364 days later.

The Ad26.ZEBOV drug substance and drug product were produced by or under the responsibility of Janssen Vaccines & Prevention B.V., Leiden, the Netherlands. The clinical trial design is summarised in Figure 4.1.

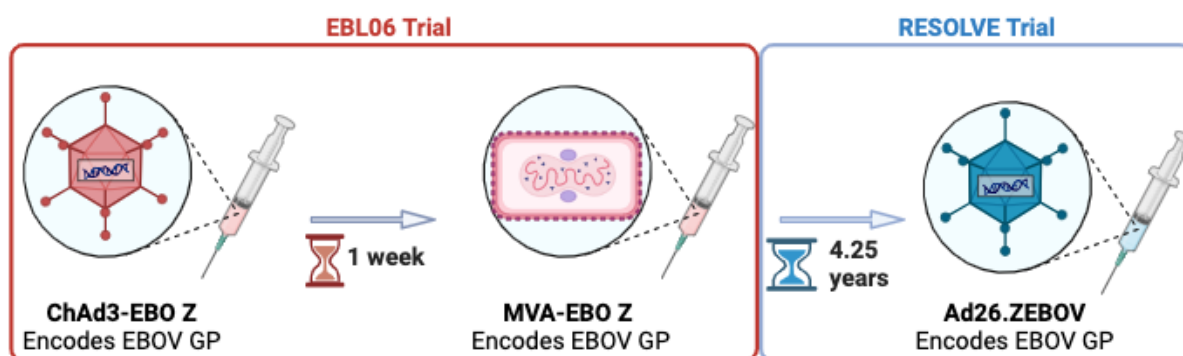


Figure 4.1: Schematic showing the outline and vaccination schedule for the EBL06 (parent trial) and RESOLVE clinical trials.

REVOLVE clinical trial design

A subset of primary data generated from the REVOLVE clinical study and data from ad-hoc CMV ELISAs completed on plasma samples from REVOLVE volunteers are used in this chapter. The clinical trial design and methodology of the REVOLVE study has been summarised in Chapter 3, REVOLVE clinical trial design.

Results

Recruitment

A total of 28 participants, representing 70% of the original EBL06 cohort (28/40), were recruited into the RESOLVE study. All recruited volunteers opted to receive a booster vaccination of Ad26.ZEBOV, delivered with a median interval of 4.25 years after

receiving dose one of their primary series of vaccinations. Demographic information is detailed in Table 4.1.

Table 4.1: Volunteer demographics for the RESOLVE clinical trial. Age on the date of the first clinical trial visit for RESOLVE.

Senegal	
n=	28
Sex	
Male	24 (86%)
Female	4 (14%)
Ethnicity*	
Black African	28 (100%)
Age	
Range (median)	31-34 (33)

*ethnicity was self-reported.

Humoral Immunology

Binding IgG Antibodies

Anti-EBOV GP total IgG (tIgG) titres were assessed using a standardised in-house ELISA on the day of the Ad26.ZEBOV boost, and at 7, 28, and 365 days after the boost. In the original regimen (EBL06) anti-EBOV GP ELISAs were also carried out at baseline (D0), on the day of, and 4 weeks after, MVA-EBO Z vaccination. As responses were measured according to the same SOP within the same laboratory, results for the same volunteers across the two trials are combined. Data generated in the EBL06 trial from volunteers who were not recruited into RESOLVE were excluded (n=12).

Therefore, absolute numbers from the summary data from the parent study presented here will differ from the published results of EBL06 although trends remain the same.

Prior to the booster vaccination, the GMT of Ebola GP-specific IgG was 278 [95% CI 201-384] arbitrary ELISA units (aEU). Following the administration of Ad26.ZEBOV, a 113-fold increase in GMTs was observed, with GMT peaking at 31460 [95% CI 26279-37662] aEU on day 28. This peak after Ad26.ZEBOV boosting was 76-fold higher than the peak response as measured 28 days after cAd3-EBO Z vaccination during the original regimen. This elevation above baseline was sustained up to 365 days post-boost, where GMTs were 1529 [95% CI 1206-1938] aEU, significantly higher than pre-boost titres (Kruskal-Wallis with Dunn's multiple comparisons, $P=0.0057$) (Figure 4.2)

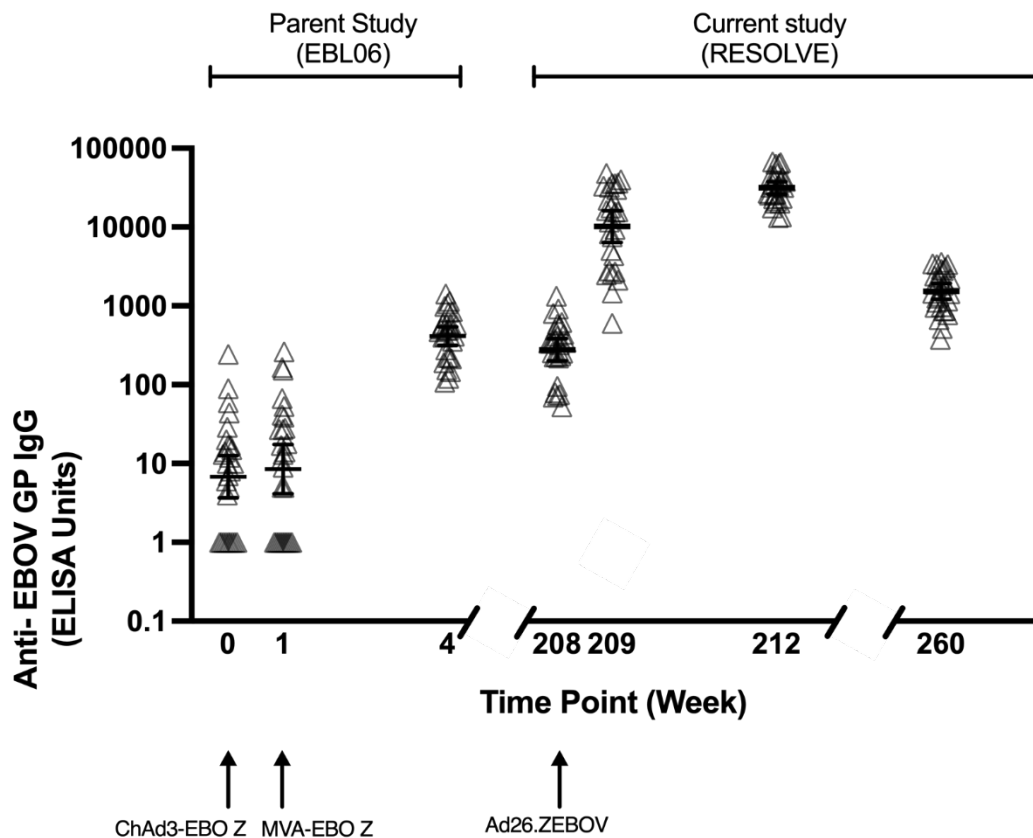


Figure 4.2: anti-EBOV GP IgG as measured by in house standardised ELISA. Triangles represent individual data points; lines show geometric means with bars showing 95% confidence intervals. Arrows indicate time points where a vaccination was administered. Dotted line shows the seropositive cut-off.

The avidity of IgG antibodies to EBOV trimeric GP was assessed using a displacement ELISA with NaSCN as a chaotropic agent on both the day of, and 365 days after, Ad26.ZEBOV vaccination. Samples from volunteers showing seropositivity for anti-EBOV GP IgG, as defined by a titre above the assay cut-off of 166 aEUs (described in Materials and Methods, Anti-EBOV GP and anti-SUDV GP total IgG ELISA), at both time points were exclusively chosen to allow for paired analyses (n=22). The antigen specific IgG induced by cAd3-EBO Z and MVA-BN-Filo vaccination measured prior to the Ad26.ZEBOV boost have a median IC_{50} of 2.083 4.25 years later. 365 days after Ad26.ZEBOV administration the median IC_{50} of IgG antibodies was 2.154. All

volunteers except for three had an increase in IC_{50} . The small rise in average IC_{50} was not statistically significant (Wilcoxon matched pairs test, $P=0.0634$) (Figure 4.3).

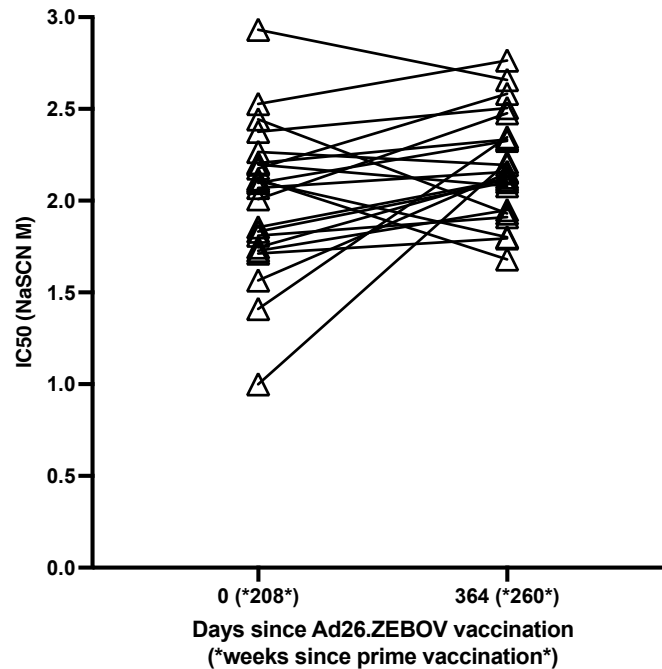


Figure 4.3: Avidity of IgG antibodies to EBOV-GP. Individual data points were expressed as an IC_{50} and shown here as scatter dot plots. Significant difference was determined by two-tailed Wilcoxon test ($P=0.0634$).

T cell immunology

T cell responses were measured by interferon- γ (IFN- γ) ELISpot prior to the Ad26.ZEBOV boost to assess the longevity of response to the original cAd3-EBO Z and MVA-EBOV Z vaccination regimen, and at 7, 28, and 365 days after administration of the Ad26.ZEBOV boost. In the original regimen (EBL06) IFN- γ ELISpot assays were also carried out at baseline (D0) and 7 days-post MVA-EBOV Z boost (D14). As with the total IgG data, responses were measured using the SOP within the same laboratory so results for the same volunteers across the two trials were combined. Data generated in the EBL06 trial from volunteers who were not

recruited into RESOLVE were excluded (n=12); therefore, summary data presented here will differ from the published results of EBL06.

T cell responses to the EBOV GP were detectable prior to Ad26.ZEBOV booster, with a geometric mean of 381.8 [95% CI 141.2-1032] SFC/10⁶ PBMC observed at 4.25 years after cAd3-EBO Z / MVA-EBOV Z vaccination. Following the Ad26.ZEBOV boost, responses significantly increased by 5.2-fold to 1995 [95% CI 1448-2748] SFC/10⁶ PBMC, at 7 days after boost (P=0.0063). Responses contracted to 523.5 [95% CI 297 – 924.0] SFC/10⁶ PBMC at 365 days post-boost, representing no significant difference from pre-boost titres (Kruskal-Wallis with Dunn's multiple comparisons, P>0.9999) (Figure 4.4).

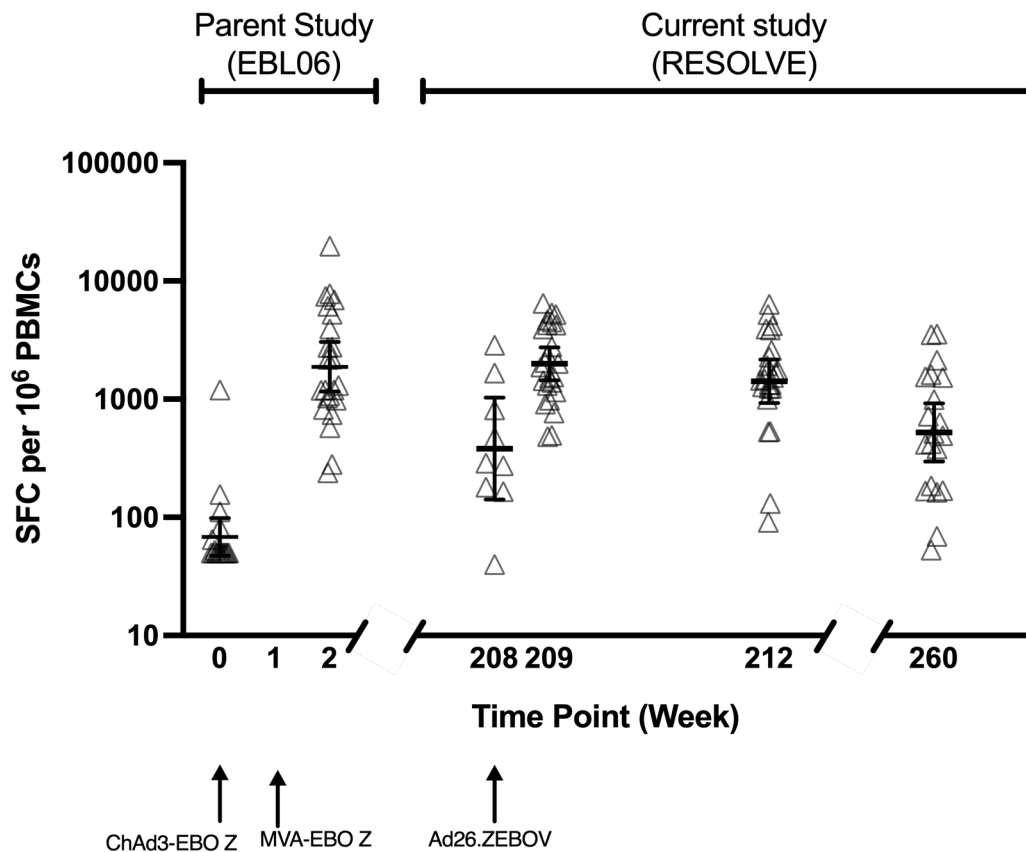


Figure 4.4: EBOV GP-specific IFN- γ T cell responses as measured in PBMC by ELISpot. Triangles represent individual data points; lines show geometric mean with bars representing 95% confidence intervals. Arrows indicate time points where a vaccination was administered.

Pool analysis at 7 days post-Ad26.ZEBOV boost revealed detectable T cell responses to all peptide pools spanning both GP₁ and GP₂ of the glycoprotein in at least one volunteer, with the highest average response observed to the peptide pool spanning amino acids 234-315 within GP₁ with a geometric mean of 295.7 [95% CI 135-775] SFC/10⁶ PBMC. Although still immunogenic, the lowest responses were observed to the peptides in the pool spanning amino acids 379-459, also in GP₁, which had a geometric mean response of 37.4 [95% CI 4-113] SFC/10⁶ PBMC. The measured responses to peptides following Ad26.ZEBOV administration followed a similar pattern of recognition to those seen at the peak response generated from cAd3-

EBOZ/ MVA-EBO Z vaccination in the original regimen with little fold-change difference in pool specific responses (Figure 4.5).

Flow cytometry with ICS was performed 28 days post-Ad26.ZEBOV boost. Analysis of polyfunctionality via Boolean gating indicated that cells positive only for IFN- γ were the largest subgroup in the CD8+ T-cell response, with cells double positive for IFN- γ and TNF the second most frequent. Polyfunctional T-cells expressing IFN- γ , IL-2, and TNF constituted the largest subgroup in the CD4+ T-cell response. At the same time point, a median of 0.07% of CD8+ T cells expressed CD107a (LAMP-1), a marker indicating the capacity for cytotoxic degranulation (Figure 4.6).

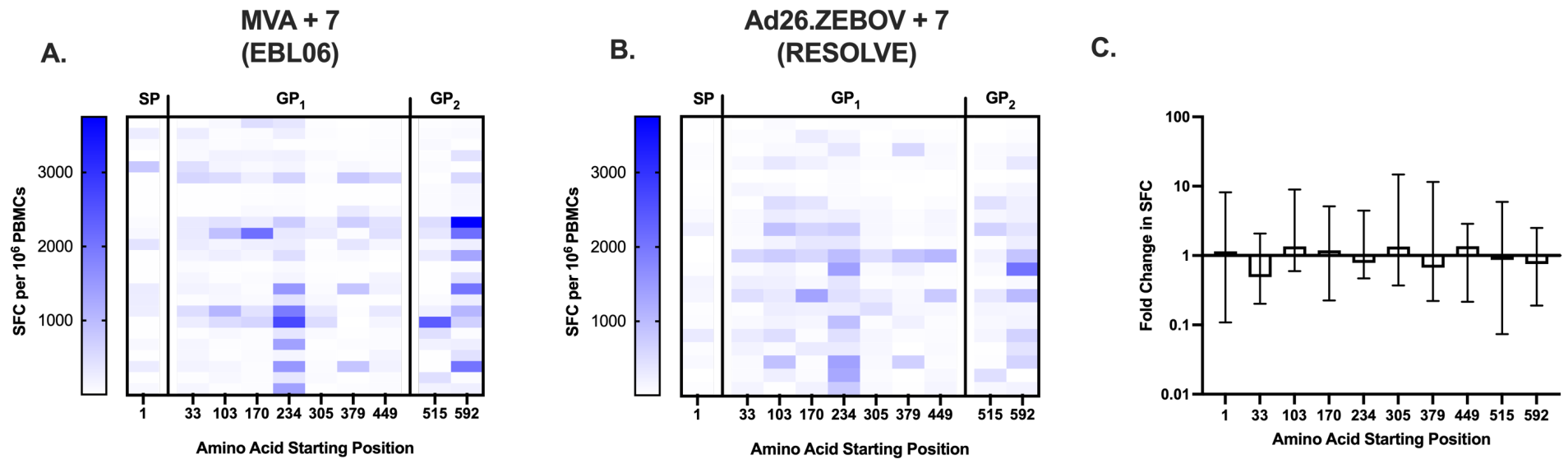


Figure 4.5: Heat map of responses to individual peptide pools spanning the EBOV GP at: A. 7 days after cAd3-EBO Z/ MVA-EBO Z vaccination (EBL06 trial) or B. 7 days after Ad26.ZEBOV vaccination (RESOLVE clinical trial). Panel C shows fold change in SFC between responses 7 days after MVA boost in the EBL06 trial and 7 days after Ad26.ZEBOV vaccination in the RESOLVE trial. Lines show median with whiskers showing range.

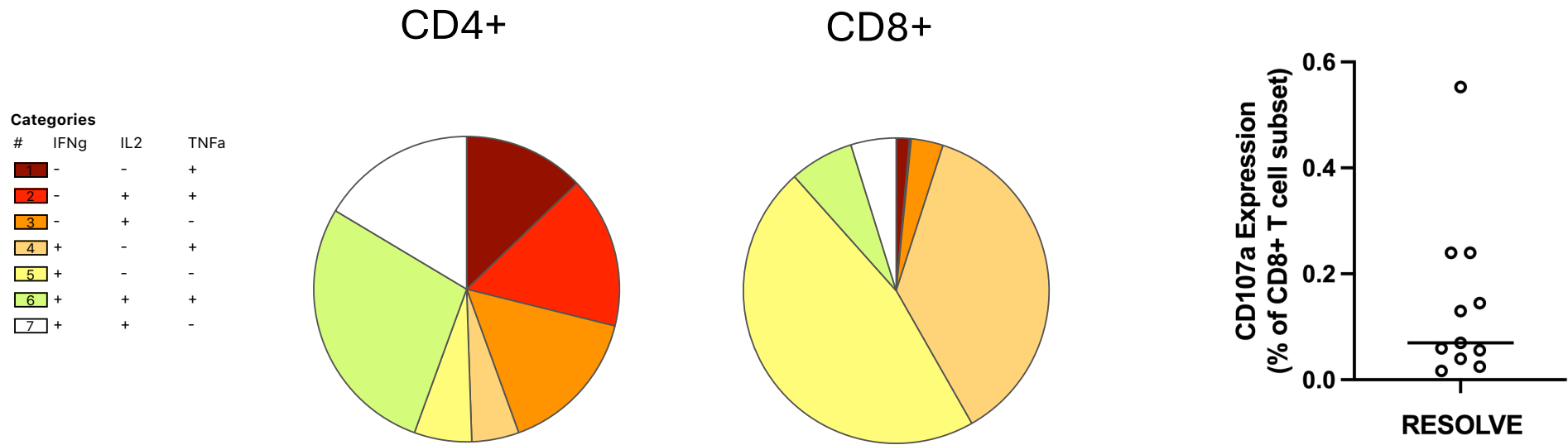


Figure 4.6: Results from flow cytometry with ICS. A. The proportions of CD4+ and CD8+ T cells that secreted any combination of interferon- γ , interleukin-2, and TNF 28 days after boosting with Ad26.ZEBOV. B. CD107a expression as a percentage of CD8+ T cells at 28 days after boosting with Ad26.ZEBOV.

Responses in Senegalese volunteers compared to UK volunteers.

A comparison of responses in the Senegalese volunteers to those in a UK cohort who received the same vaccination regimen was conducted. Despite differences in IgG titres being observed in their original regimen [96], the Ad26.ZEBOV vaccination performed similarly between the UK and Senegalese cohort and there were no significant differences in the primary measured immunological outcomes including peak antigen-specific T cell response and IgG titre (

Figure 4.7).

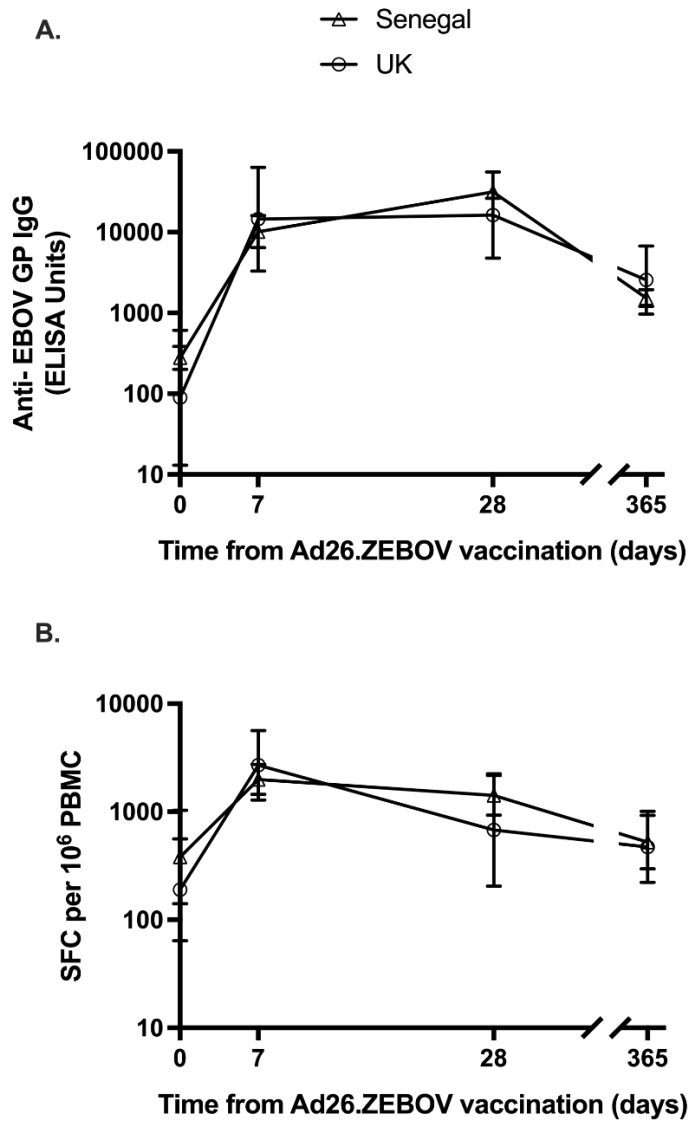


Figure 4.7: Comparison between the primary immunology outcomes A. tIgG ELISA and B. IFN- γ ELISpot) between the UK and Senegalese cohorts receiving Ad26.ZEBOV boost as part of the REVOLVE and RESOLVE clinical trials. Lines show geometric means with bars showing 95% CI. Time on the x-axis represents time from Ad26.ZEBOV boost in days.

CMV and vaccination response

Volunteers had previously been serotyped for CMV during the EBL06 clinical trial. At the point of recruitment into the RESOLVE and REVOLVE clinical trials, all volunteers were screened again for CMV IgG using a commercially available anti-CMV ELISA

coated with CMV lysate. Additionally, any volunteers who had not previously been serotyped in the original study were also tested on the CMV ELISA kit. The demographic information stratified by CMV serostatus is detailed in Table 4.2. At the time of Ad26.ZEBOV boost, 100% (28/28) of Senegalese volunteers remained seropositive for CMV, whilst 50% (22/44) of UK volunteers were seropositive for CMV (Table 4.3). This represents an 18.5% seroconversion rate over 4.25 years, with an annual rate of 4.4% among UK volunteers.

Table 4.2: Volunteer demographics in the RESOLVE and REVOLVE clinical trials. Age on the date first clinical trial visit for RESOLVE or REVOLVE is shown.

	Senegal (CMV+)	UK CMV+	UK CMV-
n=	28	22	22
Sex			
Male	24 (86%)	12 (55%)	9 (41%)
Female	4 (14%)	10 (45%)	13(59%)
Age			
Range (median)	23-48 (34)	24-54 (45)	19-55 (39)
Ethnicity*			
White	-	21 (95%)	22 (100%)
Black African	28 (100%)	-	-
Asian or Asian British - Other	-	1 (4.5%)	-

Table 4.3: CMV serostatus data at the time of enrolment into parent study and at the time of administration of Ad26.ZEBOV boost (time of enrolment into the REVOLVE or RESOLVE clinical trials) stratified by country of recruitment.

Country of sampling	UK	Senegal
Sample size (N=)	44	28
Seropositivity at recruitment into parent study n/N (%)	17/44 (39)	28/28 (100)
Seropositivity at time of Ad26.ZEBOV boost n/N (%)	22/44 (50)	28/28 (100)

The ages of volunteers in the UK CMV-, UK CMV+ and Senegalese cohorts were comparable and did not correlate with CMV IgG titre (UK cohort: $r=-0.07$, $P=0.61$; Senegalese cohort: $r=0.29$, $P=0.13$) (Table 4.2, Figure 4.8).

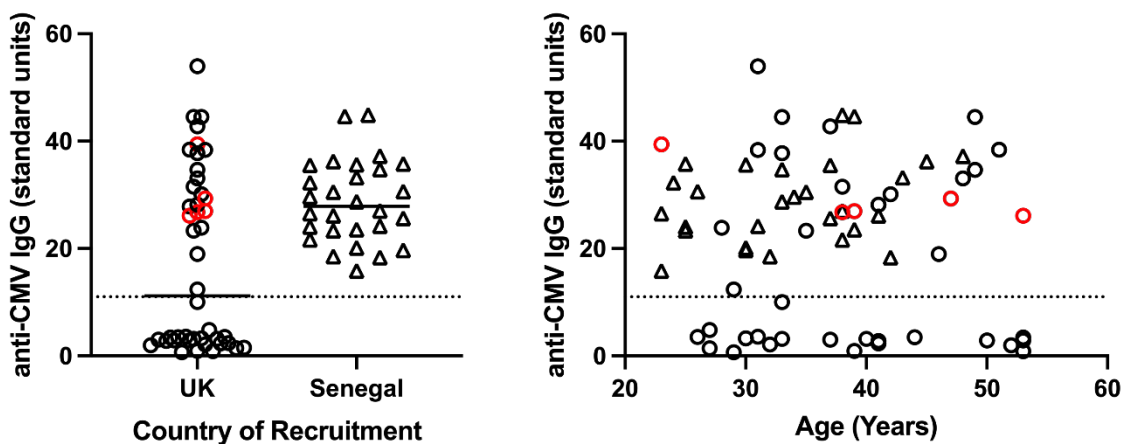


Figure 4.8: anti-CMV IgG units at the time of enrolment into the RESOLVE and REVOLVE studies as generated by ELISA. Dashed lines indicate the seropositive threshold set as 11 standard units as defined by the ELISA manufacturer’s instructions. Red shapes represent volunteers that have seroconverted in the 4.25 years since they were last serotyped A. anti-CMV IgG titres stratified by country of recruitment. B. Relationship between CMV IgG titre and age in each population, triangles represent Senegalese volunteers, circles represent UK volunteers. No correlation was

found between age and anti-CMV IgG (Spearman's rank analysis, all UK volunteers $r:-0.07$, $P=0.61$, Senegal $r:0.29$, $P=0.13$).

To examine the impact of CMV seropositivity on the T cell repertoire, surface expression of CCR7 and CD45RA were quantified on CD4+ and CD8+ T cells by flow cytometry using PBMC (Figure 4.9). Four main subsets of CD4+ and CD8+ T cells (naive [T_N]: CD45RA⁺CCR7⁺, central memory [T_{CM}]: CD45RA⁻CCR7⁺, effector memory [T_{EM}]: CD45RA⁻CCR7⁻, effector memory re-expressing CD45RA [T_{EMRA}]: CD45RA⁺CCR7⁻) were characterised. The percentage of CD4+ and CD8+ T cells were not significantly different between the three groups (Figure 4.9A, Figure 4.9B) and the median CD4:CD8 ratio was 1.770 in Senegalese volunteers, 1.760 in UK CMV+ and 2.240 in the UK CMV- group (Figure 4.9C). Three individuals were found to have an inverted CD4: CD8 ratio and all were CMV+ (UK CMV+ $n=2$, Senegalese $n=1$).

CD4+ T cell populations were comparable between the three groups (Figure 9D).

Conversely, in the UK cohort, CMV seropositivity was associated with a significantly increased proportion of T_{EM} CD8+ T cells ($P=0.0130$), and a trend in a decrease in T_N (CD45RA⁺CCR7⁺) CD8+ T cells. This significantly increased proportion of T_{EM} T cells was also evident in the Senegalese cohort where CMV seropositivity was ubiquitous ($P=0.0230$) (Figure 4.9E).

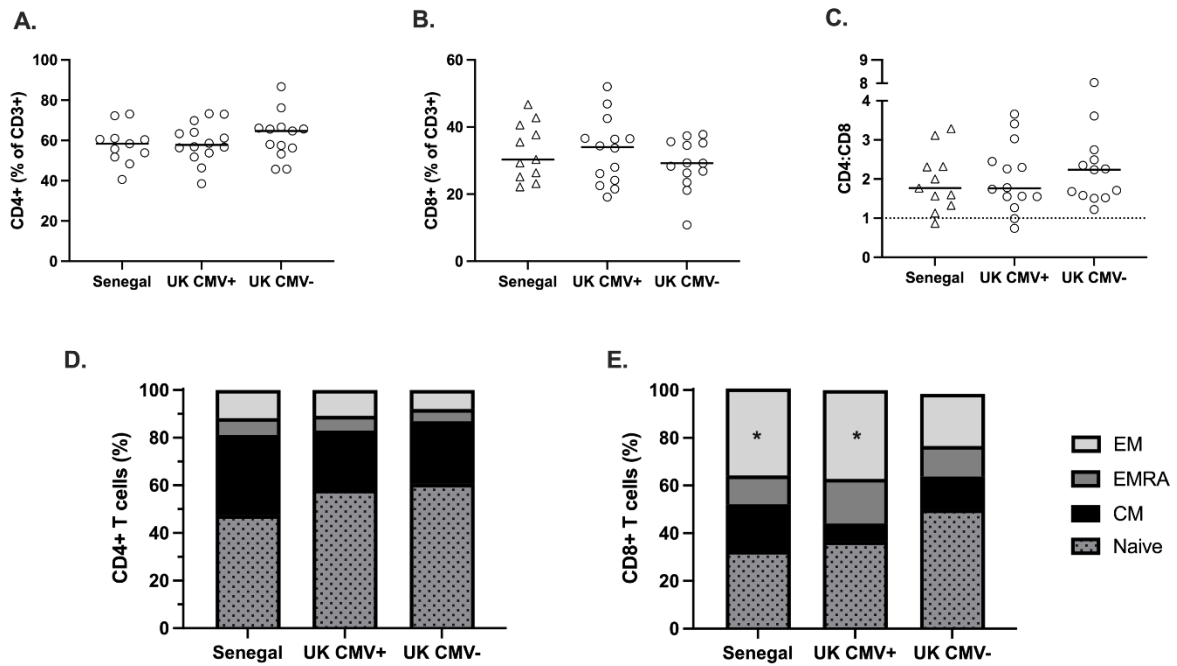


Figure 4.9: Effect of CMV serostatus on the peripheral T cell repertoire. T cell populations from isolated PBMC were assessed by flow cytometry in UK CMV-seropositive (CMV+) and CMV-seronegative (CMV-) individuals as well as in Senegalese volunteers who were all CMV+. A. CD4+ as a percentage of CD3+ T cells B) CD8+ as a percentage of CD3+ T cells C) CD4:CD8 ratio. Volunteers below the dotted line have an inverted ratio. D) The mean relative prevalence of CD4+ T cell subsets by cohort and CMV serostatus. E) The mean relative prevalence of CD8+ T cell subsets by cohort and CMV serostatus. Associations between groups and T cell subsets were assessed by Kruskal-Wallis with Dunn's multiple comparisons post-hoc. *p < 0.05.

Despite these phenotypic differences in the T cell repertoire, when stratified by CMV serostatus, there were no significant differences in T cell IFN- γ or in anti-EBOV GP IgG titres or avidity at long-term follow up to the cAd3- EBO Z / MVA-EBO Z regimen. There was also no difference in the primary immunological outputs (T cell IFN- γ or in anti-EBOV GP IgG titres) (Figure 4.10) or avidity (supplementary Figure S 12) after boosting with Ad26.ZEBOV.

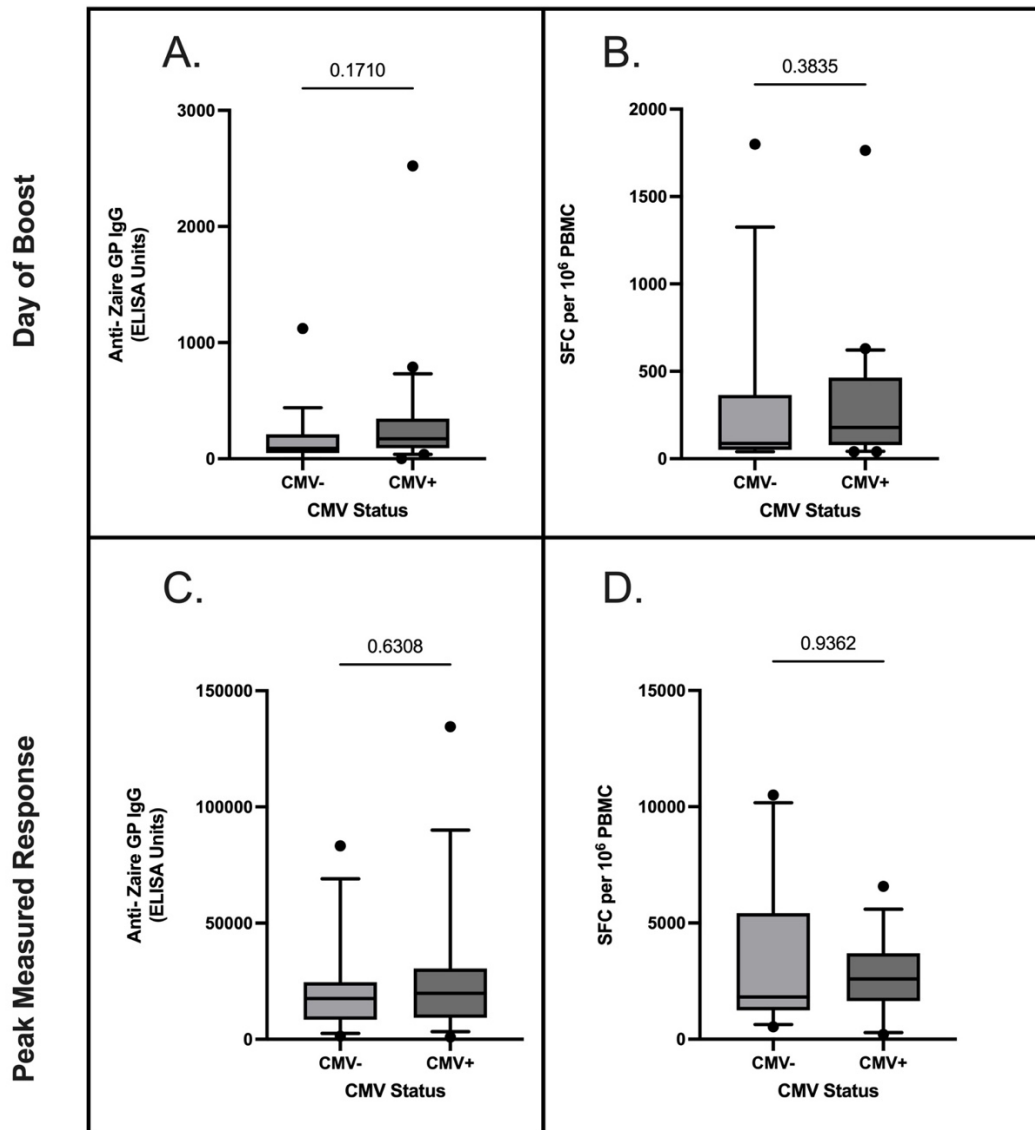


Figure 4.10: Immune responses stratified by CMV serotype in UK volunteers at day of Ad26.ZEBOV boost (cAd3-EBO Z / MVA-EBO Z long term follow-up) or at the peak measured response A. IgG titres at long term follow-up B. ELISpot responses at long term follow-up C. IgG titres at 7 days post boost D. ELISpot responses at 7-days post-boost. P numbers are shown above the plots as determined by Mann Whitney U test.

Discussion

This study is the first to assess the longevity of the cAd3-EBO Z / MVA-EBO Z regimen, the only study to administer a third Ebola virus vaccine to individuals who had received this regimen and the first to assess an Ad26.ZEBOV boost on any vaccine

regimen in Senegalese volunteers. Despite being conducted over 4 years from the original trial, 70% of volunteers were enrolled in this long-term follow-up trial and all accepted a dose of Ad26.ZEBOV as a booster vaccination.

These vaccine immunogenicity results can be interpreted through the two arms of humoral immune memory: the maintenance of long-term antibodies and the induction of B cell memory. At approximately 4.25 years after receiving the primary regimen, 78% of volunteers still had EBOV GP- specific IgG antibodies in circulation and were considered responders prior to booster administration. This indicates that the primary regimen can induce long lasting vaccine-specific antibody responses in adults. The Ad26.ZEBOV boost induced a strong anamnestic response, as evidenced by a rapid increase in Ebola virus glycoprotein-specific binding antibody concentrations, detected at the earliest sampling time point (7 days post-boost) which were higher than those measured during the original regimen. This is indicative of B cell memory established during the cAd3-EBO Z/ MVA-BN-Filo regimen.

Since this study, several others have trialled using Ad26.ZEBOV as a boost in volunteers who have been previously vaccinated with Ad26.ZEBOV/MVA-BN-Filo. The humoral findings reported in this thesis complement results shown from healthy adults in the Democratic Republic of the Congo (DRC) where a boost of Ad26.ZEBOV administered 1 or 2 years after their original Ad26.ZEBOV/MVA-BN-Filo regimen was also amnestic, producing an antibody response at 7 days post-boost which was 39 times higher than before booster vaccination [145]. The much higher fold increase in antibodies (113-fold higher than pre-boost) is likely to be reflective of several factors.

Firstly, the difference in the original regimen which, in the case of this thesis did not include homologous boosting with the Ad26 vector. Secondly, the longer interval between the parent study and the Ad26.ZEBOV boost (4.25 years in this study compared to 1 or 2 years in the DRC study). The latter is supported by a study in Human Immunodeficiency Virus positive (HIV+) Kenyan and Ugandan adults with well controlled infection where a boost of Ad26.ZEBOV administered 4.5 years after their original Ad26.ZEBOV/MVA-BN-Filo regimen, a similar interval to that in this thesis study, boosted antibodies 172 times higher than pre-boost titres [146].

This study is the first to present cellular immunogenicity to a booster dose of Ad26.ZEBOV with all previous studies focussing on humoral responses only [145-149]. The results show that T cells are boosted, although have contracted a year after boost to titres similar to those measured pre-boost. In contrast to the antigen specific IgG, T cell titres reach a level comparable to, but not higher than, those measured during the original vaccine regimen. T cell responses measured by IFN- γ ELISpot recognise multiple peptides spanning the whole glycoprotein and heterologous boosting with Ad26.ZEBOV has no effect on the pattern of peptide pool recognition by the T cells suggesting minimal role of the vector in peptide recognition. The IFN- γ and TNF double-positive CD8⁺ T cell population, which has previously been demonstrated to correlate with long-term protection in cAd3 vaccinated primates [123], is also represented following Ad26.ZEBOV boost in response to restimulation with the glycoprotein.

As this study was not conducted during an Ebola outbreak it is not known whether the immune responses measured here at long-term follow-up from cAd3-EBO Z/ MVA-EBO Z vaccination and to the Ad26.ZEBOV boost would be sufficient to confer protection against disease. However, previously hypothesised correlates of protection, including EBOV GP-binding IgG and neutralising antibodies [99, 150] as well as CD8+ T cell activation [102, 123] are all observed following Ad26.ZEBOV boost.

Comparisons between the UK and Senegalese Volunteers

It is increasingly recognised that some vaccines induce variable responses in populations living in different geographical areas or of different socioeconomic status [151]. Vaccines, typically developed and tested in high-income Western regions, can exhibit lower efficacy or immunogenicity when used in different settings. This phenomenon has been highlighted with the Bacillus Calmette–Guérin (BCG) vaccine [152] and has since been observed for vaccines against rotavirus [153], malaria [154] and yellow fever [155]. Various biological factors are likely to underlie these differences, including genetic variations such as human leucocyte antigen type [156, 157], pre-existing immunity to cross-reactive antigens [129, 158], pathogen exposure [159-161], gut microbiota composition [162, 163] and immune exhaustion [164].

Despite the Senegalese cohort presented in this chapter exhibiting lower immunogenicity than the UK cohort in their original vaccination regimen [96], when

the Ad26.ZEBOV vaccine is administered to the same volunteers in this study, T cells and antibodies are boosted comparably in both Senegalese and UK volunteers.

CMV positivity and Immunogenicity to ebola vaccination

The association between CMV serostatus and vaccine immunogenicity is a field of active research with the literature primarily consisting of small cohort studies which present conflicting findings. Some research on influenza vaccine responses have demonstrated a poor humoral or cellular response to vaccination in CMV-positive individuals [165-167]. Conversely, other studies have found no association between CMV seropositivity and the immune response to vaccinations against SARS-CoV-2 [168, 169], pneumococcus [170] or polio [171]. Interestingly, one study demonstrated a positive association between CMV infection and immune response to influenza vaccination in young adults [172].

The annual CMV seroconversion rate of 4.4% reported for UK volunteers here is high for a UK population [173], but does fall within previously reported ranges for European populations [174] and may be affected by many risk factors such as occupation [175] or socioeconomic status [176] for which data were not collected. When considering total seropositivity, 50% of the UK volunteers were seropositive at enrolment into the REVOLVE study which is in line with previously reported estimates for the UK adult population [173]. CMV carriage is known to increase with age in higher income countries [177-181] but interestingly in this study the average age of

CMV+ and CMV- UK cohorts were similar and anti-CMV IgG titre not correlate with age in either the UK CMV+ or the Senegalese group.

Whilst the vaccine elicited responses from the volunteers presented in this chapter had previously exhibited an association with CMV serostatus [144], the data presented in this thesis suggest that CMV seropositivity, despite still being associated with significant modifications in peripheral blood CD8+ T cell phenotype, does not negatively impact the durability of vaccine-elicited IgG or T cell responses.

Furthermore, CMV serostatus does not correlate with differences in the peak responses generated after the Ad26.ZEBOV boost. In summary, these findings show that antigen specific T cell IFN- γ and antibody production at long term follow-up or following the Ad26.ZEBOV boost is not affected by CMV serostatus. These results are reassuring given the extremely high rates of CMV seropositivity in West and Central African countries, where Ebola outbreaks have historically occurred, with some studies reporting up to 95% seroprevalence [182, 183]. The data have additional implications beyond Ebola vaccination; it demonstrates that it is possible for measured differences observed in immunogenicity between CMV serostatus to be mitigated within the same population. Although the mechanism is unclear, either the establishment of immunological memory, the number of boosters delivered, or the choice of vaccine vector play a role in this change.

There are several limitations to the work presented in this chapter. Due to limited PBMC sample availability, it was not possible to analyse samples further for markers and phenotypes known to be associated with CMV-specific CD8+ T cell responses

such as the downregulation of the activation markers CD28 and CD27 and increased expression of CD57 and KLRG1 [184]. The seroconversion of an additional 5 volunteers may skew the response as the seroconversion may have occurred any time within the 4.25 years since the volunteers were last serotyped. Longitudinal work with more sampling time points would be needed to evaluate any association between time since an individual's CMV primary infection or seroconversion and T cell phenotypes or vaccine response which this study was not designed for. Additionally, the Senegalese and UK cohort were not matched for sex with the former having a higher percentage of male volunteers, reflecting the differences in recruitment seen in the parent trial. The serostatus for 19 other pathogens was determined in the original trial, and some including herpes simplex virus (HSV-1) and Epstein-Barr Virus (EBV) Human polyomavirus 1 (BK virus) and Helicobacter pylori were highly seroprevalent in the Senegalese group. These pathogens were not re-screened for at long term follow-up in this study so the interplay of these pathogens or other infections which were not screened for in either trial, such as helminths, or adenoviruses, which may also cause anti-vector responses cannot be ruled out. Finally, the nature of Phase I vaccine trials means that the sample size in each population was relatively small and therefore this study was not appropriately powered to allow for multivariate analyses. Future research examining the impact of chronic infections on vaccine responses would benefit from larger cohorts and should consider any potential combined effects or interactions among multiple infections.

Conclusions

In conclusion, this chapter adds to a growing body of literature, and supporting data from the previous chapter in UK volunteers, providing strong evidence to support the use of Ad26.ZEBOV for prophylactic vaccination against Ebola virus disease in at-risk populations. Indeed, the European Medicines Agency (EMA) now recommends a booster dose to be given to populations who received the primary regimen Ad26.ZEBOV MVA-BN-Filo regimen more than four months earlier if they are at imminent risk of exposure to Ebola virus, such as during an outbreak [185].

5. Durability of the Immune Response to Ad26.ZEBOV /MVA-BN-Filo up to 46 months post-prime

Introduction

EVOLVE Study

The “Evaluating Optimal Vaccine Schedules against Ebola” (EVOLVE) study (NCT02416453) is a randomised, observer-blind, placebo-controlled, Phase II trial designed to assess the safety, tolerability and immunogenicity of three prime-boost regimens of the candidate Ebola virus vaccines Ad26.ZEBOV and MVA-BN-Filo EBOV in healthy adults. Participants received an intramuscular injection of Ad26.ZEBOV, followed by intramuscular injection of MVA-BN-Filo at either 28 days, 56 days, or 84 days post-prime vaccination.

Volunteers were recruited at seven hospitals in France (Creteil, Lyon, Paris, Rennes, Saint-Etienne, Strasbourg, and Tours) and two research centres in the UK (London and Oxford). The trial has ended and results have been published [68]. 21 Days after receiving the MVA-BN-Filo vaccine, geometric mean concentrations of Ebola virus glycoprotein-binding antibodies were 4627 ELISA units (EU)/mL [95% CI 3649–5867] in the 28-day interval group, 10131 EU/mL [95% CI 8554–11999] in the 56-day interval group, and 11312 EU/mL [95% CI 9072–14106] in the 84-day interval group. CD4+ and CD8+ T-cell responses were low post-Ad26.ZEBOV vaccination but observed in significant proportions after the MVA-BN-Filo vaccination. CD4+ T-cell responses were detected in 43% of participants in the 28-day interval group, 37% of the 56-day interval group, and 58% of the 84-day interval group; CD8+ T-cell responses were detected in 67%, 55%, and 61% in these respective groups [68].

This study assessed the immunological response up to 364 days post-vaccination. Since the completion of the study, the vaccine has gained European Medicines Agency (EMA) approval and licensure with a 56-day prime-boost interval [185]. Therefore, further evaluation of the immune response longevity beyond one year is necessary, particularly for the 56-day interval regimen. Additionally, it is important to assess whether the prime-boost interval influences the durability of the immune response and to determine if this vaccination regimen can elicit an immune response against Sudan virus.

Objectives

1. To evaluate whether the length of the interval between an Ad26.ZEBOV priming vaccination and an MVA-BN-Filo boosting vaccination impacts durability of humoral or cellular responses to EBOV GP.
2. To measure if a detectable antigen specific response is generated to SUDV GP as encoded in the MVA-BN-Filo boost at long term follow-up with any prime-boost interval.

Study Specific Methods

PRISM clinical trial design

Healthy adult volunteers who were previously enrolled in the EVOLVE study at the Oxford site were approached for recruitment into cohort 3 of the “Persistence of the Immune Response After Immunisation with Ebola Virus Vaccines” (PRISM) clinical trial (NCT03140774). Participants were deemed ineligible to partake in this follow-on study if they had suffered malignancy or undergone immunosuppressive therapy since their immunisation with an Ebola vaccine, received an adenovirus or MVA virus-vectored vaccine, or travelled to an Ebola endemic area. The primary objective of the trial was to measure the presence of IgG against the Ebola virus GP by ELISA up to 60 months following primary vaccination with Ad26.ZEBOV/MVA-BN-Filo.

This non-interventional trial involved collecting heparinised blood samples taken on two occasions, 6 months apart, to evaluate the durability of the immune response (Figure 5.1).

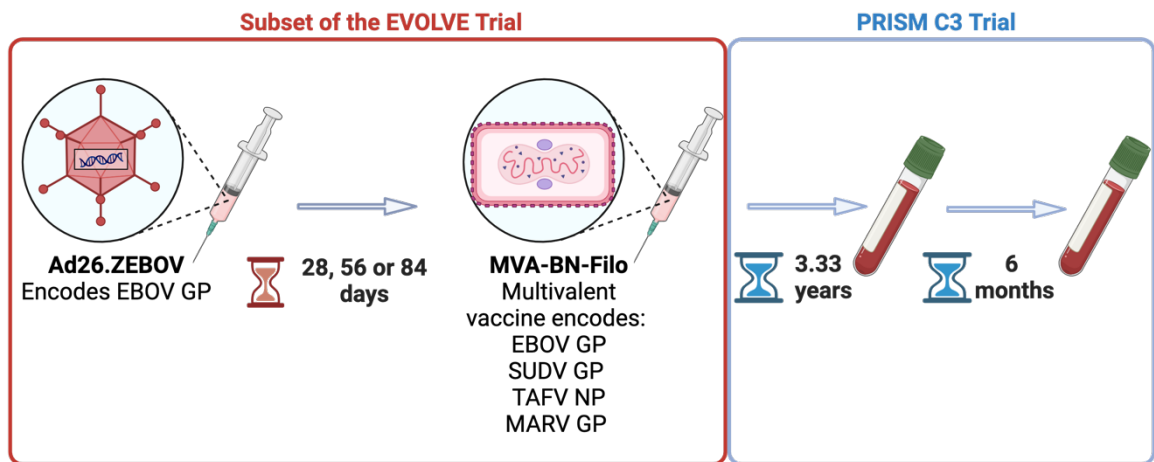


Figure 5.1: Schematic showing the outline and vaccination schedule for the subset of the EVOLVE (parent trial) and PRISM clinical trial groups presented in this chapter. EBOV = Ebola virus, SUDV = Sudan virus, TAFV = Tai Forest virus, MARV = Marburg virus. GP = glycoprotein, NP = nucleoprotein.

Results

Recruitment

A total of 74 volunteers, representing 47% of the vaccine recipients (74/158), were recruited into cohort 3 of the PRISM study. 20 of these volunteers were originally in the 28 day prime-boost interval group, 27 in the 56 day and 27 in the 84 day. None of the placebo group participants were recruited. When averaged across all three groups, the first sample in the PRISM study was collected at a median of 40 months after Ad26.ZEBOV priming vaccination. Demographic information is provided in Table 5.1.

Table 5.1: Volunteer Demographics at time of first PRISM visit by subgroup. Age is recorded at the time of enrolment into the PRISM study. Prime and boost vaccinations were administered as part of the EVOLVE clinical trial.

Prime-Boost Interval	28 days	56 days	84 days
n=	20	27	27
Sex			
Male	10 (50%)	10 (37%)	15 (56%)
Female	10 (50%)	17 (63%)	12 (44%)
Age			
Range (median)	28-68 (53)	23-68 (55)	21-67 (55)
Ethnicity*			
White British	16 (80%)	24 (89%)	19 (70%)
White Irish	-	-	1 (4%)
White (Other)	4 (20%)	2 (7%)	3 (11%)
Asian or Asian British - Chinese	-	-	1 (4%)
Black African	-	-	1 (4%)
Other	-	1 (4%)	1 (4%)
Mixed	-	-	1 (4%)
Time from Ad26.ZEBOV vaccination (months)			
Range (median)	38-46 (41)	36-44 (40)	37-42 (40)

*Ethnicity was self-reported

Durability to EBOV

Humoral Immunogenicity

Anti-EBOV GP total IgG (tIgG) titres were assessed using a standardised in-house ELISA at 40 and 46 months post-primary vaccination. At 40 months, GMTs were 299.1 [95% CI 183.7 – 487.1] aEUs, 264.2 [95% CI 166.6 – 418.9] aEUs, 273 [95% CI 182.7-408.8] aEUs for the 28-, 56- and 84-day prime-boost interval groups respectively. Six months later, responses persisted with GMTs of 317.7 [95% CI 204.0 - 494.8] aEUs,

292.2 [95% CI 187.9 - 454.6] aEUs and 277.7 [95% CI 176.2 - 437.8] aEUs. No significant differences in tIgG titre were observed between the three prime-boost groups at either the first (Kruskal-Wallis, $P=0.8711$) or second time point (Kruskal-Wallis, $P=0.8987$) (Figure 5.2).

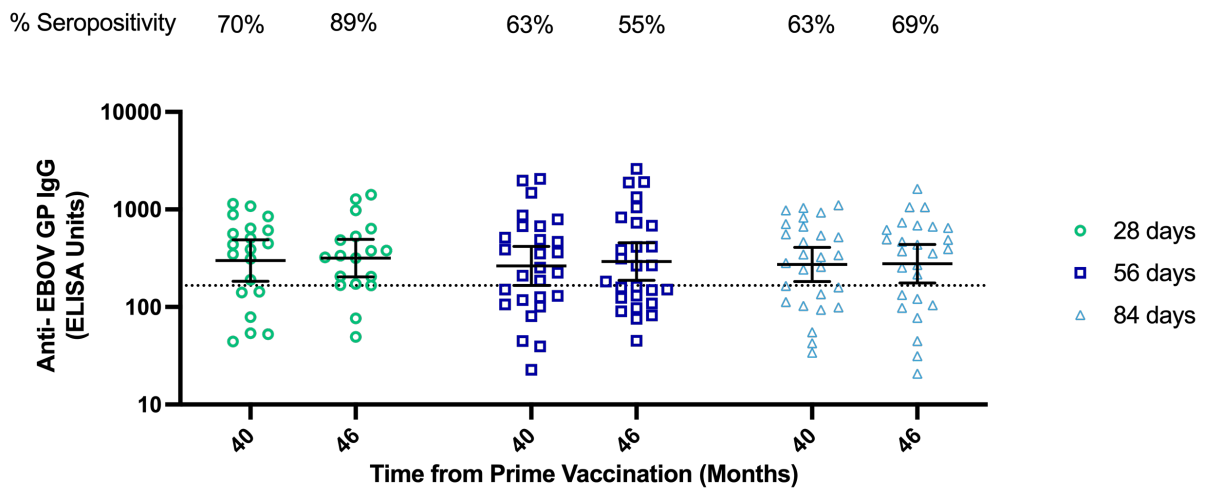


Figure 5.2: anti-EBOV GP IgG as measured by in house standardised ELISA. Shapes represent individual data points; circles, squares and triangles represent volunteers who originally received a 28, 56 and 84-day interval between their Ad26.ZEBOV prime and MVA-BN-Filo boost respectively. Lines show geometric means with bars showing 95% confidence intervals. The dotted line shows the seropositive cut-off (166 ELISA Units).

A pseudovirus neutralisation assay was carried out at the first long term follow-up time point to assess functional antibody responses to EBOV. A single time point was chosen to give a snapshot of the neutralisation capacity of the plasma due to the time intensive nature of the assay. Low levels of neutralisation were observed in all three groups. There was a strong positive correlation between IC50 and titres of anti-EBOV GP IgG as quantified with the standardised in-house ELISA (Spearman's correlation coefficient $r=0.8131$, $P<0.0001$) (Figure 5.3).

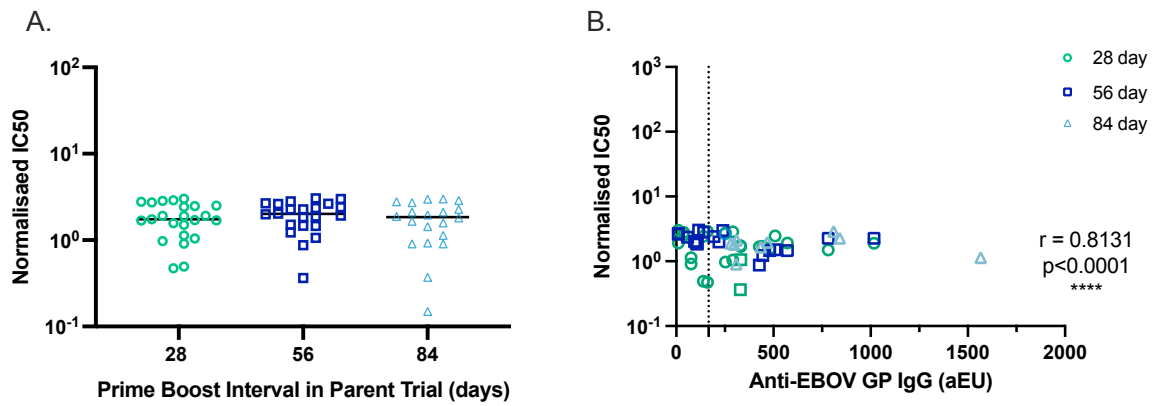


Figure 5.3: Pseudoneutralisation of EBOV GP-bearing lentiviral pseudotypes. Shapes represent neutralisation IC50 with lines showing median. A) IC50 by prime-boost interval at 40 months post vaccination. B) Correlation between pseudoneutralisation IC50 and antigen specific binding IgG.

Memory B cells

Antigen specific peripheral blood memory B cells (BMEM) were quantified using an IgG BMEM ELISpot at both time points in the PRISM study for a subset of volunteers who had the assay performed in their original regimen (manuscript in preparation) (28-day interval: n=6, 56-day interval: n=6, 84-day interval: n=6). Titres plateaued between the two long term follow-up timepoints (Figure 5.4) and are significantly higher than those measured at baseline at 40 and 46 months ($p < 0.0001$, Friedman's test with Dunn's multiple comparisons) (Figure 5.4B)

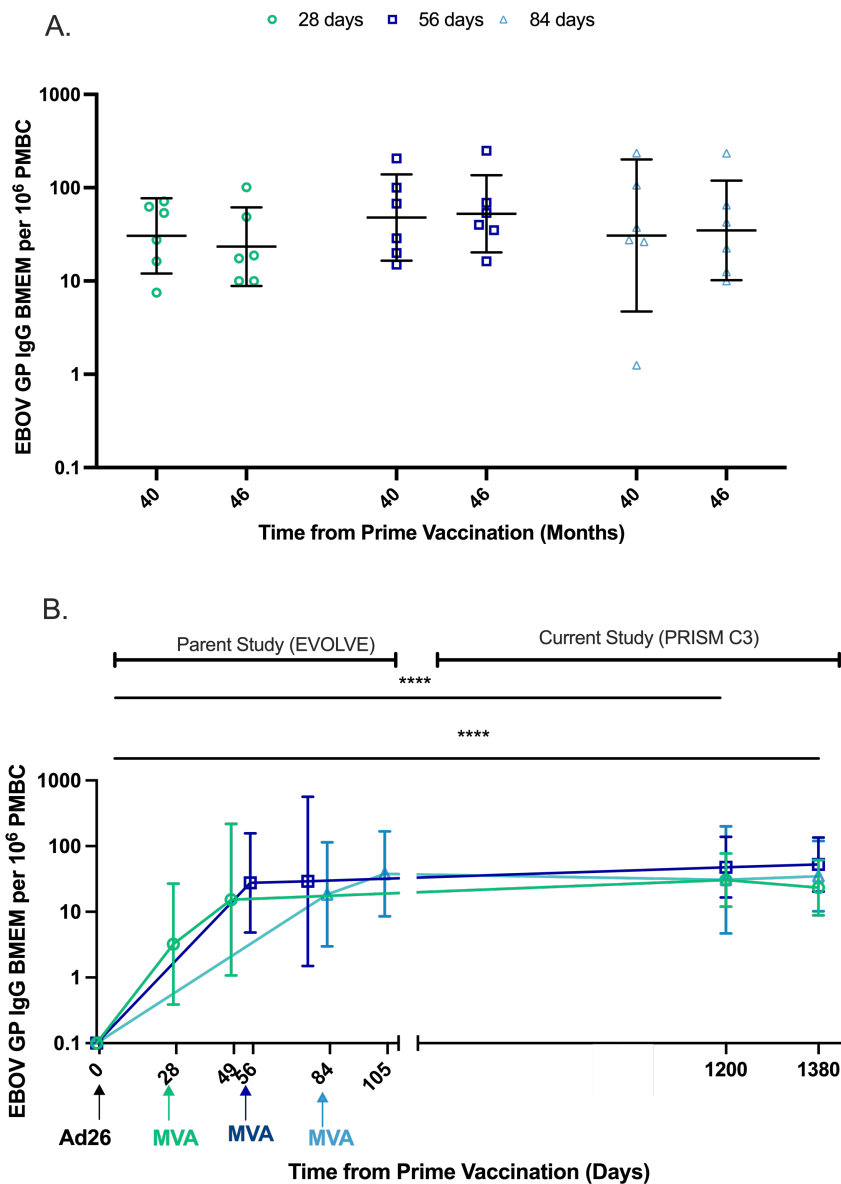


Figure 5.4: EBOV-GP specific IgG-BMEM response A. BMEM response at the two time points by prime-boost interval. Lines show median with bars showing interquartile range B. Time course from EVOLVE trial to PRISM cohort 3 trial for a subset of 18 volunteers for whom memory B cell ELISpots were carried out in the parent study. Shapes show medians with lines showing interquartile range. Asterisks indicate statistically significant differences determined by Friedman’s test with Dunn’s multiple comparisons post hoc *** $p < 0.0001$

Durability of T Cell Responses

As with the other immunological assays previously discussed in this chapter, T cell responses were measured by IFN- γ ELISpot at two timepoints approximately 40 and 46 months post-priming vaccination. At 40 months, T cell responses persisted with

geometric means of 378.0 [95% CI 206.3-692.8], 354.3 [95% CI 119.7-662.5] and 269.1 [95% CI 187.2-386.9] SFC/10⁶ PBMC for the 28-day, 56-day and 84-day intervals respectively. Six months later, there was minimal decline, with geometric means of 363.7 [95% CI 199.7-662.5], 316.1 [95% CI 217.8-458.8] and 234.4 [95% CI 162.2-338.8] SFC/10⁶ PBMC for the 28-day, 56-day and 84-day intervals respectively. No significant differences in the T cell responses were observed between the three prime-boost intervals at either 40 months (Kruskal-Wallis, P=0.5497) or 46 months (Kruskal-Wallis, P=0.3748) (Figure 5.5A). For a subset of volunteers (n=24), ELISpots were conducted using freshly isolated PBMC in the original clinical trial following the same standard operating procedure in the same laboratory (data unpublished). For these volunteers a complete time course is available from pre-vaccination (day 0) and peak responses in the EVOLVE clinical trial through to long-term follow-up in the PRISM trial is available. Responses in this subset remain elevated above those observed at baseline, pre-vaccination (Figure 5.5B).

Pool analysis at 40 months post-Ad26.ZEBOV boost revealed detectable T cell responses to all peptide pools spanning both GP₁ and GP₂ of the glycoprotein in at least one volunteer. The highest average response was observed for the peptide pool spanning amino acids 103-180 within GP₁ with a geometric mean of 41.86 [95% CI 32.0-54.54] SFC/10⁶ PBMC. The lowest responses were observed for the pool spanning amino acids 305-389, also in GP₁, with a geometric mean of 7.15 [95% CI 5.82-8.77] SFC/10⁶ PBMC (Figure 5.5C).

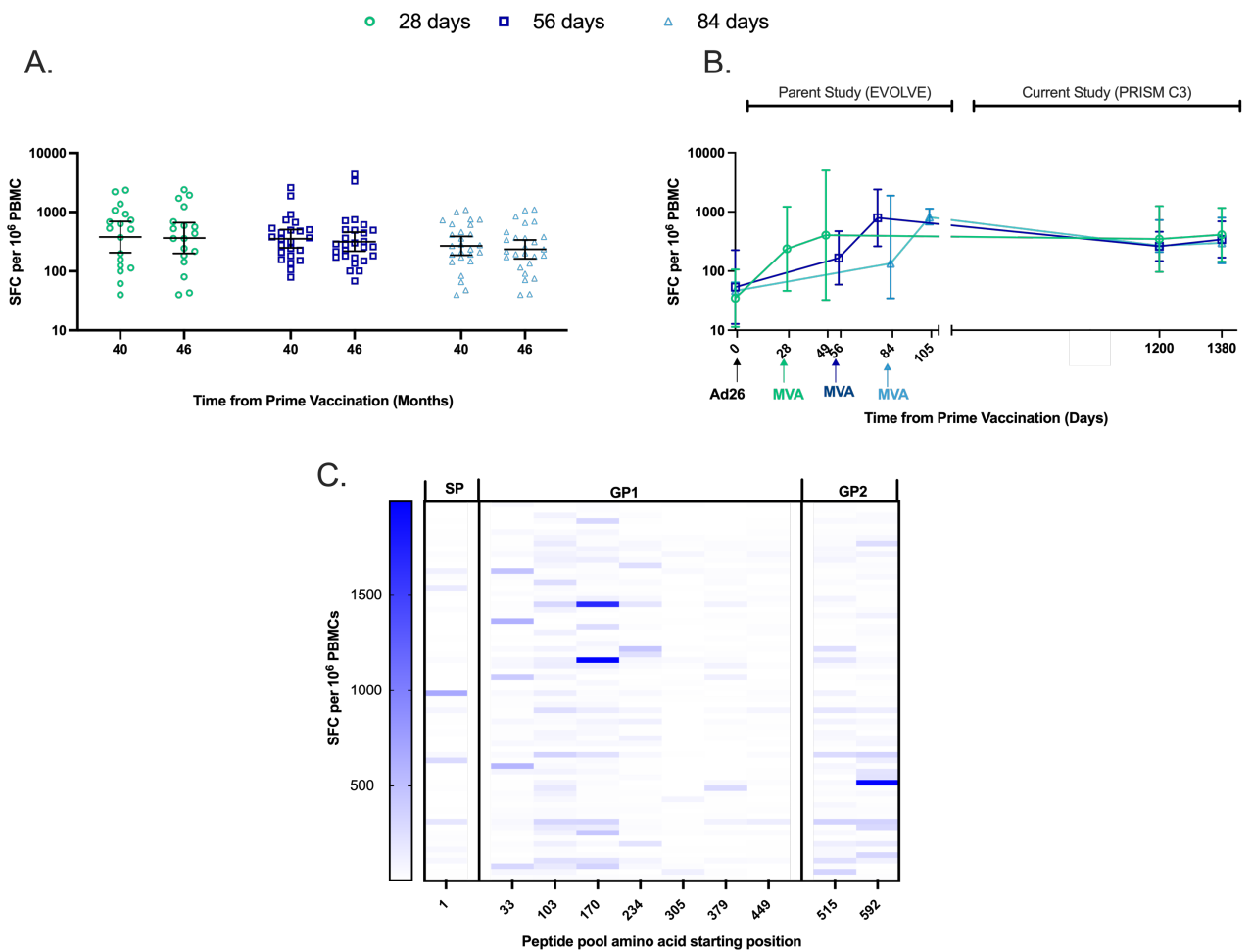


Figure 5.5: T cell responses measured by IFN- γ ELISpot assay to peptides spanning the EBOV GP.

Circles, squares and triangles represent volunteers who originally received a 28, 56 and 84-day interval between their Ad26.ZEBOV prime and MVA-BN-Filo boost respectively. A) Primary data generated from the PRISM C3 trial B) A time course from EVOLVE trial to PRISM cohort 3 trial for a subset of 24 volunteers for whom ELISpots were carried out on the same SOP for the original regimen. C) Heat map of responses to individual peptide pools in all volunteers spanning the EBOV GP at 40 months post-prime.

Flow cytometry with ICS was performed at the first time point (40 months) with results presented as percentage of CD4+ or CD8+ T cells expressing any combination of IFN- γ , IL-2, or TNF. A trend towards an augmented CD8+ response was observed (Figure 5.6A). The frequency of CD8+ T cells expressing the degranulation marker CD107a (LAMP1), an indicator of cytotoxic function, was also measured showing modest expression across all three regimens (Figure 5.6B).

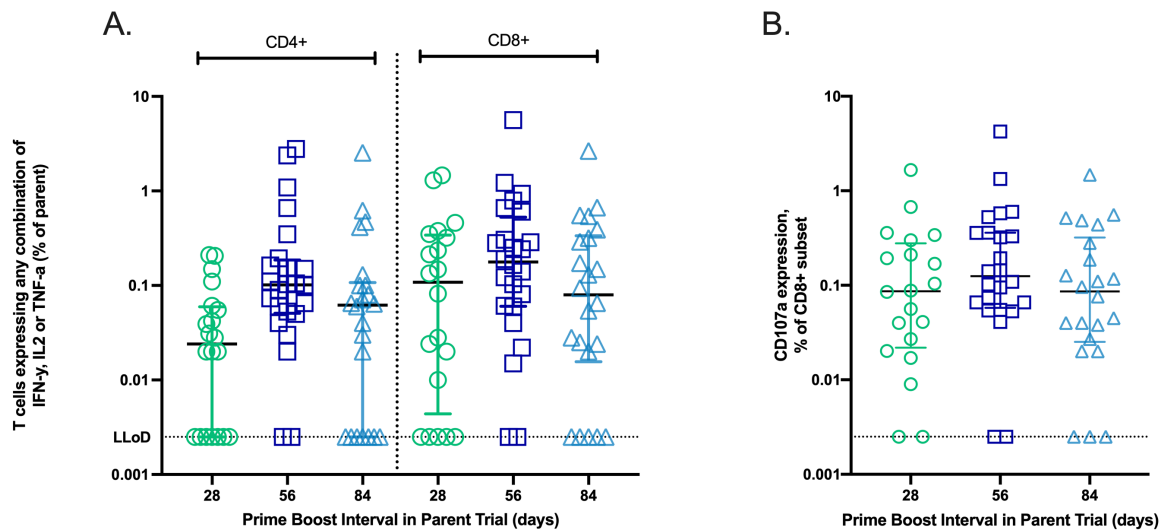


Figure 5.6: T cell responses to EBOV GP as measured by flow cytometry with ICS at the first time point (40 months). Lines show geometric mean with bars showing 95% confidence intervals. The dotted line shows the assay's LLoD. A) Percentage of CD4+ or CD8+ T cells producing any combination of IFN- γ , IL-2, or TNF in response to stimulation with peptides spanning the EBOV glycoprotein at the first time point by parent trial prime-boost interval dose. B) CD107a expression as % of CD8+ T cells by prime-boost interval.

Durability of immune responses to SUDV

Following the completion of the PRISM clinical trial, an ad-hoc analysis was conducted to evaluate the durability of the immune response to SUDV. While the Ad26.ZEBOV/MVA-BN-Filo regimen is approved for use against EBOV, the MVA-BN-Filo boost is multivalent and encodes antigens for multiple filoviruses, including the Sudan virus GP. Samples were selected for analysis against the SUDV GP antigen if sufficient plasma and PBMC samples were available at both time points and if volunteers had consented to future testing (n=64). As these assays were not performed during the original regimen (EVOLVE), and no samples are available from that time to do so, plasma and PBMC samples from volunteers matched for geographical region and date of blood draw who had never received a filovirus vaccine were accessed through the Oxford Vaccine Centre Biobank and used as controls.

Humoral Responses

Anti-SUDV IgG was detectable at low levels and in a smaller percentage of volunteers compared to anti-EBOV IgG. Since titres were similar across prime-boost intervals (Figure 5.7A), groups were collapsed into a single ‘vaccinee group’ at both time points. In this combined group, 28% of all volunteers were seropositive for anti-SUDV GP IgG with GMT of 33.2 [95% CI 22.3-49.5] aEUs at 40 months. At 46 months, 29% of volunteers were seropositive with a GMT of 25.5 [95% CI 16.2-40.2] aEUs. In the control group no volunteers were seropositive for anti-SUDV IgG with a GMT response of 6.4 [95% CI 2.1-19.5] aEUs. Responses in the vaccinated group were significantly higher at 40 months than the unvaccinated controls (Kruskal-Wallis with Dunn’s multiple comparisons, $P=0.0221$) but not at 46 months (Kruskal-Wallis with Dunn’s multiple comparisons, $P=0.0502$) (Figure 5.7B).

A weak positive correlation between anti-SUDV GP IgG and anti-EBOV GP IgG was observed at the first time point (Spearman’s correlation coefficient, $r=0.2717$ $P=0.0358$,) (Figure 5.7C).

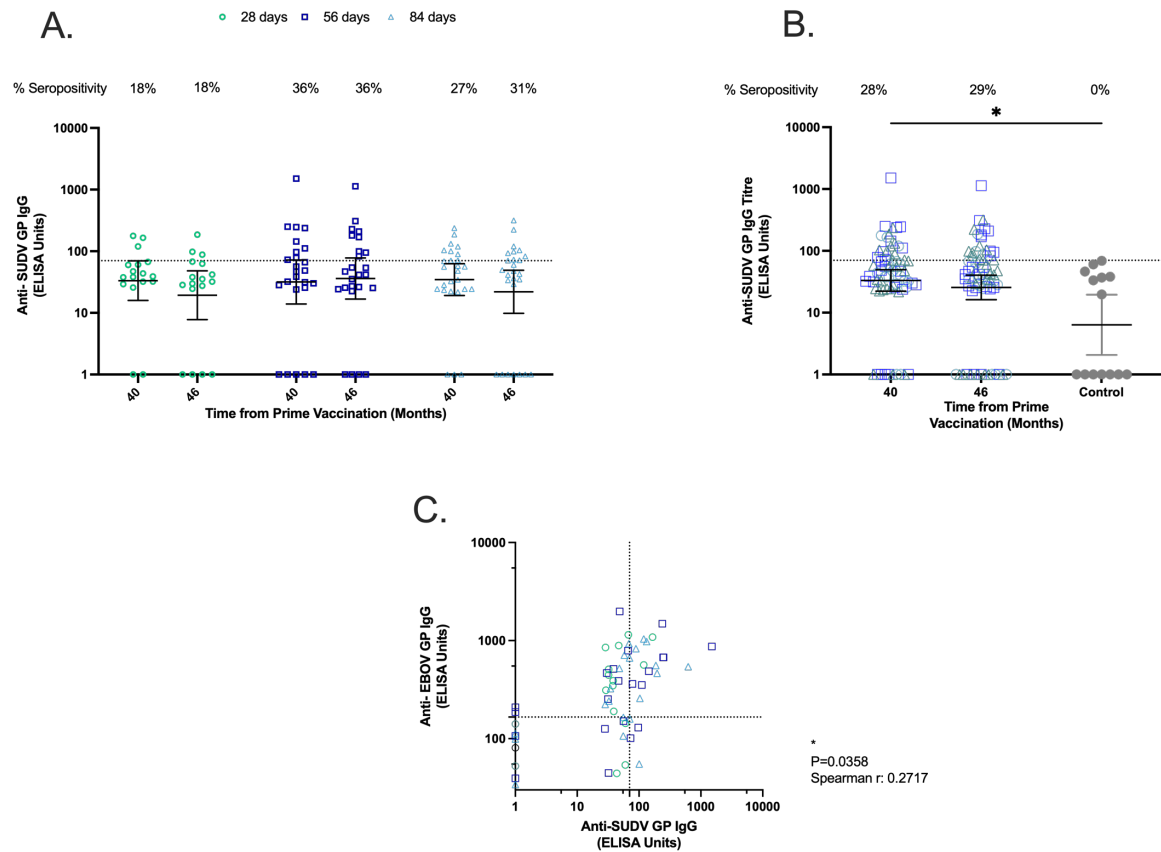


Figure 5.7: anti-SUDV GP IgG measured by in house standardised ELISA. Shapes represent individual data points; circles, squares and triangles represent volunteers who originally received a 28, 56 and 84-day interval between their Ad26.ZEBOV prime and MVA-BN-Filo boost respectively. Lines show geometric means with bars showing 95% confidence intervals. The dotted line shows the seropositive cut-off (72 ELISA units). A) Responses at the two long term follow-up time points by prime-boost interval. B) Data from all groups combined at both time points and responses from orthoebolavirus naïve volunteers used as control samples. Asterisk indicates a statistically significant difference determined by Kruskal-Wallis with Dunn's multiple comparisons post hoc * P=0.0221 C) Anti-SUDV GP and anti-EBOV GP IgG at the first long term follow-up time point. Significant correlation was determined by Spearman's correlation test.

T cell responses

Modest T cell responses were detectable following restimulation with peptides spanning the SUDV GP. As with the ELISA data, all three prime-boost intervals elicited comparable responses at both timepoints (Figure 5.8A) and were subsequently

collapsed into a single 'vaccinee' group. SUDV GP specific IFN- γ responses were low but detectable and significantly higher than unvaccinated controls up to 46 months from vaccination (Kruskal-Wallis with Dunns multiple comparisons, $P=0.0002$ at 40 months, $p<0.0001$ at 46 months). (Figure 5.8B). The geometric mean responses for the combined groups at 40 months were 64.5 [95% CI 50.8-80.8] SFC/ 10^6 PBMC which were maintained to a geometric mean of 69.4 [95% CI 54.2-88.9] SFC/ 10^6 PBMC at 46 months. Control PBMCs had a geometric mean response of 23.4 [95% CI 17.3-31.7] SFC/ 10^6 PBMC.

Deconvolution of total ELISpot responses to the constituent peptide pools at the first time point (40 months post-vaccination) showed that although responses are detectable to both GP₁ and GP₂, they are not evenly distributed across the GP. The peptides in the pool spanning amino acids 33-200 of GP₁ are immunodominant, eliciting the highest responses, with a median response of 23 SFC and a response above the cut-off in 43.5% of volunteers at the first timepoint. In contrast, the pool spanning amino acids 315-525 was the least recognised, eliciting a median response of 7 SFC above the cut-off in only 19.4% of volunteers. There was little response detectable to peptide pools in the control PBMC (Figure 5.8C).

Direct comparisons of the absolute numbers for the responses to EBOV and SUDV peptides are not possible as the EBOV ELISpot assays were carried out using freshly isolated PBMCs and, due to the ad hoc nature of the analysis, SUDV assays were performed using cryopreserved PBMCs. Evidence suggests that cryopreservation can affect lymphocyte phenotype [186] and measurable assay responses [187]. A difference in fresh and frozen responses has been previously observed when using this validated ELISpot assay to enumerate responses to different antigens in other projects. However, there is a significant moderate correlation between ELISpot responses enumerated with SUDV and EBOV peptides (Spearman's correlation coefficient, $r=0.4418$, $P=0.0007$) (Figure 5.8D).

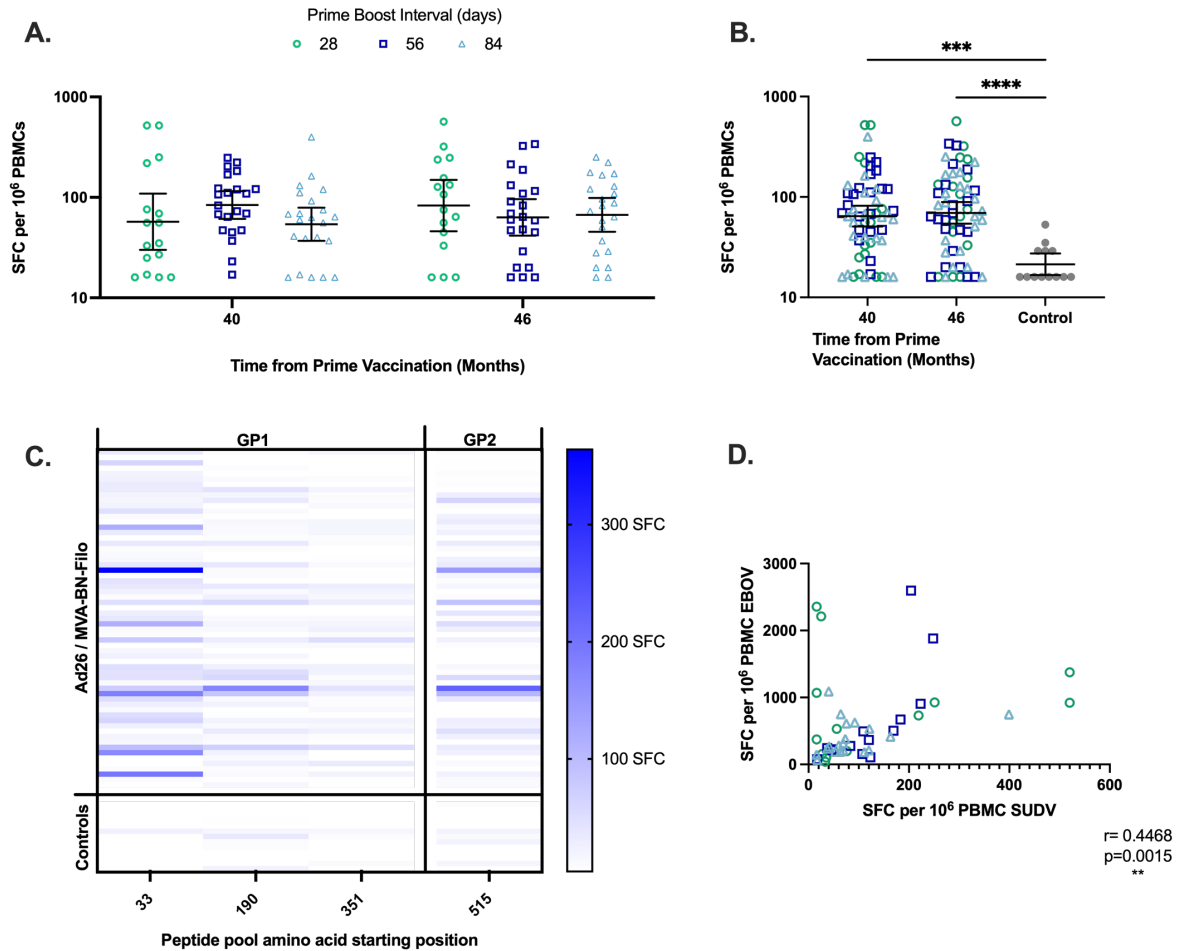


Figure 5.8: T cell responses measured by IFN- γ ELISpot assay to peptides spanning the SUDV GP.

Circles, squares and triangles represent volunteers who originally received a 28, 56 and 84-day interval between their Ad26.ZEBOV prime and MVA-BN-Filo boost respectively. A) Responses at the two long term follow-up time points by prime-boost interval. B) Data from all groups combined at both time points and responses from orthoebolavirus naïve volunteers used as control samples. Asterisks indicate statistically significant differences determined by Kruskal-Wallis with Dunn's multiple comparisons post hoc *** $P=0.0002$ **** $p<0.0001$. C) Heat map of responses to individual peptide pools spanning the SUDV GP in the ELISpot assay for all volunteers at 40 months post-prime. D) T cell responses to the SUDV GP and EBOV GP at 40 months post prime. Significant correlation was determined by Spearman's correlation test ** $P=0.0015$.

Peptide Mapping of the T cell response to the SUDV GP

Although several studies have sought to identify T cell epitopes for EBOV in both human vaccine recipients and survivors of EVD [188-191], a search of the literature and the Immune Epitope Database (IEDB) revealed that no studies have experimentally mapped epitopes to SUDV *in vitro* [192]. Given that T cell responses were detected in some Ad26.ZEBOV / MVA-BN-Filo vaccine recipients following re-stimulation with peptides spanning the SUDV GP via ELISpot assay (Figure 5.8), this presented an opportunity to “map” individual peptides within the GP that elicit a response addressing this knowledge gap. Due to the low responses, the peptides in the mega pool spanning amino acids 315-525 were not studied further. Samples from participants with the highest peak responses against the remaining three peptide pools were selected, based on sample availability, and tested by ELISpot against the individual constituent peptides of these respective pools (41 – 46 peptides per pool) to identify immunodominant peptides. Based on these criteria, between 2 and 5 participants were chosen per pool.

A response to an individual multimeric peptide was considered positive if it was higher than three standard deviations above the mean of the negative control wells after background subtraction. In total, 24 individual peptides were recognised by at least one volunteer (Figure 5.9, Figure 5.10). These positive peptides spanned multiple regions of both GP₁ and GP₂, with a notable cluster in the receptor binding region of GP₁ (Figure 5.9). Of these 24 peptides, a high degree of intra-species conservation was observed with GP sequences from other SUDV strains taken from previous outbreaks. Notably, all positive peptides have 100% amino acid sequence identity with the sequence of the SUDV strain responsible for the most recent outbreak in Uganda (NCBI: WEY06140) [193]. In terms of inter-species conservation, 29.1% (n=7) of the peptides exhibit 100% homology with at least one other member of the *Orthoebolavirus* genus (TAFV, RESTV, EBOV, BOMV or BDBV). Additionally, one peptide, LRQLANETTQALQLF, is conserved across all known *Orthoebolavirus* species as illustrated in the UpSet Plot [194] (Figure 5.10).

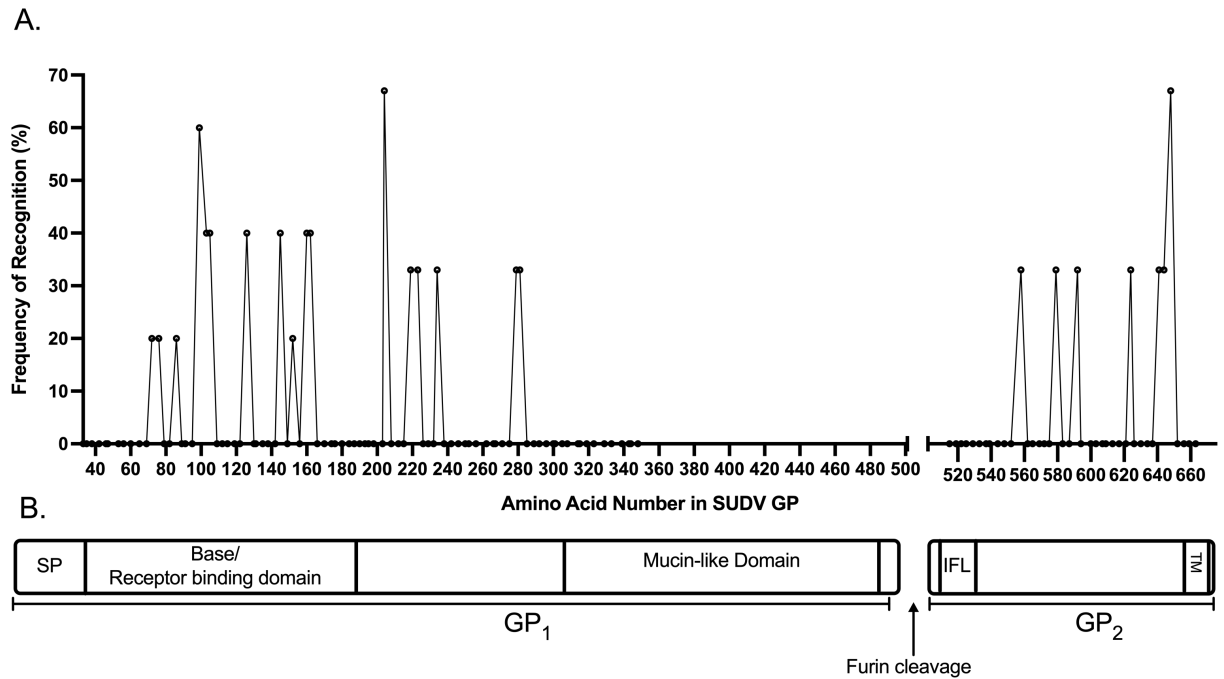


Figure 5.9: Immunodominant regions of T cell recognition in the Sudan virus glycoprotein (SUDV Gulu). (A) The frequency of responders was calculated as the percentage of volunteers assayed for a peptide with an ELISpot response above the cut off (mean + 3 standard deviations of the negative controls of the sample set). The x-axis label indicates the position in the glycoprotein of the first amino acid in the peptide. Peptides spanning amino acids 351 - 514 were not tested at the individual multimer level as no responders were found to the mega pool. (B) 2D representation of the key domain organizations of the SUDV GP. SP = signal peptide, IFL= internal fusion loop TM= transmembrane domain.

A.

Sequence	Starting amino Acid Position	# of donors positive	# of donors tested	Frequency of response (%)	Intra-Species Conservation						Inter-Species Conservation						
					1976 Nzara-Boniface	1976 Nzara-Maridi	1979 Maleo	2004 Yambio	2012 Kibaale	2012 Luwero	2011 Nakisamata	2022 Mubende	EBOV	BDBV	TAFV	RESTV	BOMV
GSGVSTDIPSATKRW	72	1	5	20	100	100	100	100	100	100	100	100	80	73.3	73.3	73.3	73.3
STDIPSATRWGFR	76	1	5	20	100	100	100	100	100	100	100	100	85.7	78.6	78.6	85.7	85.7
WGFRRSGVPPKWSY	86	1	5	20	100	100	100	100	100	100	100	100	92.9	85.7	85.7	100	85.7
YEAGEWAENCYNLEI	99	3	5	60	100	100	100	100	100	100	100	100	100	93.3	93.3	100	100
EWAENCYNLEIKK	103	2	5	40	100	100	100	100	100	100	100	100	100	92.3	92.3	100	100
AENCYNLEIKKPDGS	105	2	5	40	100	100	100	100	100	100	100	100	100	86.7	86.7	93.3	100
PDGVRGFPRCRVYHK	126	2	5	40	100	100	100	100	100	100	100	100	93.3	93.3	86.7	100	86.7
GPCPGDYAFHKDGAF	145	2	5	40	100	100	100	100	100	100	100	100	80	80	80	86.7	60
AFHKDGAFFLYDRLA	152	1	5	20	100	100	100	100	100	100	100	100	93.3	93.3	93.3	93.3	93.3
FLYDRLASTVIYR	160	2	5	40	100	100	100	100	100	100	100	100	100	92.3	92.3	100	92.3
YDRLASTVIYRGNF	162	2	5	40	100	100	100	100	100	100	100	100	86.7	73.3	80	86.7	80
NYTENTSSYATSYL	204	2	3	67	100	100	100	100	100	100	100	100	40	53.3	46.7	46.7	40
EYEIENFGAQHSTTL	219	1	3	33	100	100	100	100	100	93.3	100	100	40	53.3	46.7	46.7	40
ENFGAQHSTTLFKI	223	1	3	33	100	100	100	100	100	92.9	100	100	35.7	35.7	35.7	57.1	35.7
FKIDNNTFVRLDRPH	234	1	3	33	86.7	86.7	86.7	86.7	100	100	100	100	40	33.3	33.3	73.3	53.3
ANINADIGEWAFWF	279	1	3	33	100	100	100	100	100	100	100	100	61.5	46.2	46.2	61.5	53.5
INADICEWAFWENKK	281	1	3	33	100	100	100	100	100	100	100	100	73.3	66.7	66.7	73.3	73.3
LRQLANETQALQLF	558	1	3	33	100	100	100	100	100	100	100	100	100	100	100	100	100
LRTYILNRKAIDFL	579	1	3	33	100	100	100	100	100	100	100	100	86.7	86.7	86.7	86.7	86.7
FLLRRRWGGTCRIL	592	1	3	33	100	100	100	100	100	100	100	100	84.6	84.6	84.6	92.3	92.3
NQIHDFIDNPL	624	1	3	33	100	100	100	100	100	100	100	100	66.7	83.3	75	91.7	75
DDNNWWTGWQRWIPA	641	1	3	33	100	100	100	100	100	100	100	100	92.9	85.7	71.4	85.7	92.9
WWTGWQRWIPAGIGI	644	1	3	33	100	100	100	100	100	100	100	100	93.3	93.3	86.7	93.3	93.3
WRQWIPAGITGII	648	2	3	67	100	100	100	100	100	100	100	100	86.7	86.7	80	86.7	90

B.

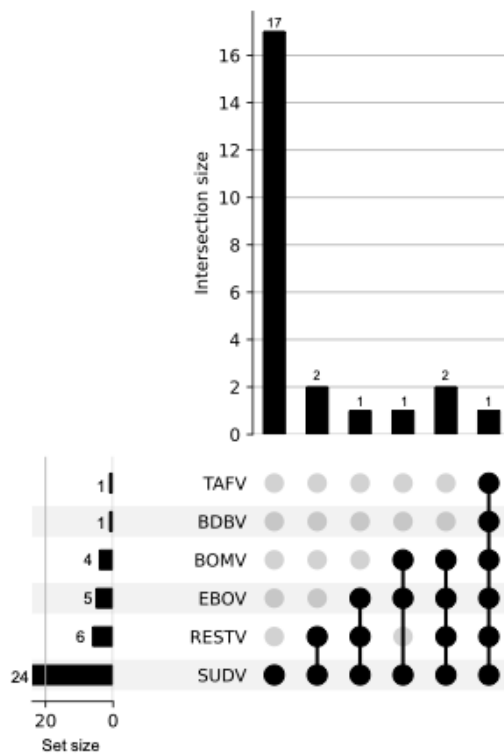


Figure 5.10: Details of positive peptides identified in this work. A) Table detailing peptides and their percentage amino acid identity with other sequenced SUDV strains, and the other five orthoebolaviruses to show intra or inter-species conservation. The accession and sequence data for SUDV sequences used for analysis of intra-species conservation are: 1976 Nzara-Boniface: MH121162, 1976 Nzara-Maridi: MK952150, 1979 Maleo: KC242783, 2004 Yambio: MH121169, 2012 Kibaale: KC545389-91, 2012 Luwero: KC589025, 2011 Nakisamata: JN638998 and 2022 Mubende: WEY06140. Orthoebolavirus sequences for inter-species analysis are: EBOV: Q05320, BDBV: B8XCN0, TAFV: Q66810, RESTV: Q66799 and BOMV: A0A4D5SG72. B) UpSet plot to visualise the inter-species data from (A) all putative epitopes identified in peptides showing their conservation across the six members of the Genus Orthoebolavirus. On the x-axis, each column represents a different combination of species (rows), showing which peptides are part of a given combination (displayed by filled circles in the combination matrix). The bar height corresponds to the number of peptides identified to be 100% conserved with the given species combination. Each combination is mutually exclusive. The total number of peptides to be 100% conserved with each individual antigen is indicated as a horizontal bar at the bottom left of each subpanel. Plot was created with Python 3.13.

As T cell epitope recognition is driven by HLA expression, high resolution HLA typing was performed for all the donors who had been selected for the single peptide analysis for the following class I and class II loci: HLA-A, HLA-B, HLA-C, DRB1, and DQB1. There were 46 unique alleles among the 90 sequenced. The most frequent alleles observed per locus were HLA-A*02:01 (33.3%), HLA-B*07:02 (27.8%) and HLA-C*07:01 (27.8%) for class I. For class II, the most frequent alleles were HLA-DQB1*06:04(22.2%)/*03:01 (22.2%) and HLA-DRB1*13:02 (22.2%). These alleles corresponded to well-documented common alleles. The full HLA frequency distribution is presented in Figure 5.11.

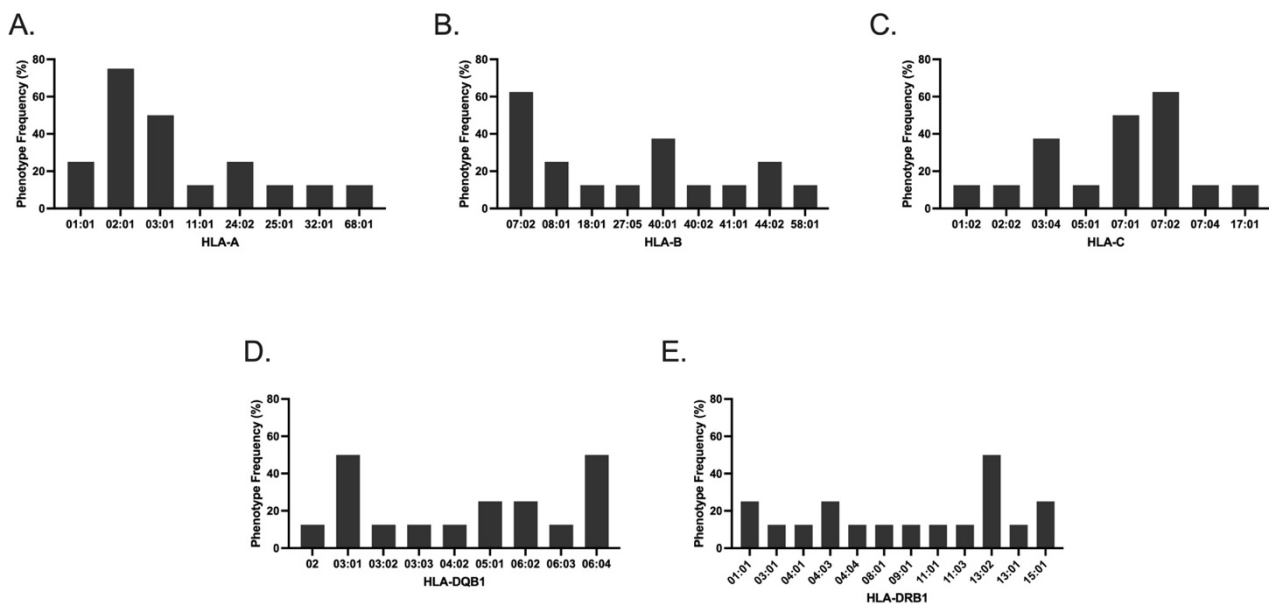


Figure 5.11: HLA allele frequency in the participants chosen for single peptide analysis (N=9) HLA class I frequency for A, B and C loci are shown in panels (A), (B) and (C), respectively. HLA class II frequency for DQ and DRB1 loci are shown in panels (D), (E) respectively.

Using the MHC class I and class II binding prediction tools from NetMHCpan-4.1 and NetMHCIIpan-4.1 [195-197] the HLA profile of each volunteer and the amino acid sequences of the peptides that elicited a positive response on the ELISpot assay were inputted to predict likely epitopes and their major histocompatibility complex (MHC) restriction. All putative epitope sequences with a rank of the predicted binding score

<2% for class I and <5% for class II are detailed in supplementary Table S 8 to Table S 13 alongside their core sequences and HLA allele. At least one restriction element was identified for all but one peptide and volunteer combination. In this particular volunteer-peptide combination, the sequence with the lowest predicted binding affinity was a class I allele and had a predicted rank binding score of 4%.

Discussion

Durability to EBOV

This data presented in this thesis demonstrate the durability of the Ad26.ZEBOV/MVA-BN-Filo regimen against EBOV up to 46 months post-vaccination. While clinical safety data is available up to five years post-vaccination [89], the data presented in this chapter represent the longest-term immunogenicity follow-up of Ad26.ZEBOV/MVA-BN-Filo vaccine recipients at the time of writing. Volunteers maintained antigen-specific binding IgG, memory B cells and T cell responses at 40 months, which remained stable six months later, indicating a sustained and plateaued immune response.

In other trials of the same vaccine, including the parent study for this trial, longer dosing intervals have trended towards higher peak antibody responses [198-201]. However, in the data presented here, no statistically significant differences were found between the three prime-boost intervals (28, 56 or 84 days) for any of the measured immunogenicity outcomes, including antigen-specific total IgG titres at long term follow-up. This suggests that if the goal is the maintenance of long-term immunogenicity- such as for vaccinating healthcare workers- any of the three prime-boost intervals could be used allowing for a level of flexibility and convenience. Nonetheless, further clinical trials with larger sample sizes and long-term NHP challenge studies would be needed to confirm these findings.

The 56-day interval, which was chosen for licensure by the EMA, has been the focus of several other durability studies and similarly well-maintained IgG binding antibody titres have been observed. Specifically, a similar follow-up duration was used in paediatric populations, where 77 - 96% of children remained seropositive three years after their

priming vaccination [148]. Comparable adult data is not available at a similar duration, but the closest duration comes from a study of healthcare workers vaccinated in Sierra Leone, in which 50% - 68% were seropositive for anti-EBOV GP IgG approximately two years after priming vaccination [147]. Data from all other durability studies is mostly available 1 year-post Ad26.ZEBOV dose and is summarised in the supplementary Table S 7. Finally, modelling studies which have been partially validated with data from the parent study of this trial corroborate these experimental findings. The model estimates the half-life of IgG antibodies to be 27.6 days for women and 19.6 days for men and half-life of long-lived antigen secreting cells is projected to be around 15 years [202].

Durability to SUDV

As the vaccine has been approved for EBOV only there is a paucity of publicly available data on its immunogenicity to SUDV. Consistent with the findings for EBOV, the prime-boost interval has no significant effect on responses to SUDV. The data show that low levels of anti-SUDV IgG and T cell responses are detectable in vaccinated individuals, and these responses are significantly higher than those measured in Ebola vaccine naïve control volunteers sampled at the same time in the same geographical region. However, fewer volunteers were seropositive for anti-SUDV GP IgG at both time points compared to EBOV (18%-36% vs 55%-89%).

As the vaccine was primarily marketed for protection for EBOV, the SUDV GP is encoded only in the MVA boost. Original exposure to EBOV GP during the prime may have limit the breadth and potency of immune responses towards SUDV GP via immune imprinting leading to a preferential recall of pre-existing memory B cells given that some EBOV GP-binding memory B cells may also recognise SUDV GP. In this case, delivering a dose of SUDV at prime and at boost would be likely to increase anti-SUDV titres, if both the prime and the boost were a multivalent vaccine this may circumvent potential for immune imprinting on either species.

Given that the GPs of EBOV (Mayinga strain) and SUDV (Boniface strain) share approximately 56% amino acid sequence identity, it is possible that the antibodies enumerated with the anti-SUDV GP IgG ELISA could arise from anti-EBOV GP IgG cross-

reacting and binding with SUDV GP rather than from a specific response generated from the SUDV GP insert encoded in the MVA-BN-Filo vaccine. To better understand the specificity of these responses, B cell linear epitope mapping or mAb isolation and subsequent characterisation using samples from these volunteers would shed light onto which areas of the SUDV GP are the target of cross-reactive responses and which are the target of species-specific responses. While linear epitope mapping would be easier and cheaper to conduct, it would be likely to overlook the conformational epitopes that could be identified through mAb isolation and characterisation. If the anti-SUDV GP ELISA were to be run on plasma in monovalent EBOV vaccinees at a similar long term follow-up interval, such as those from the EBL04 arm of the REVOLVE trial, further information could be gained on the expected frequency of cross-reactive IgG.

SUDV T cell peptide mapping

Defining a set of durable epitope specificities against the Sudan virus glycoprotein is important for several reasons. Firstly, it allows for the determination of whether certain regions are immunodominant within the SUDV GP. This will be important for vaccine design to ensure that future vaccine constructs targeting SUDV include not only the regions of the glycoprotein targeted by binding and neutralising immunoglobulins, but also include regions capable of delivering sufficient T cell help and are suitable targets of CD4⁺ T cell activity, as well as mediating CD8⁺ T cell responses. Secondly, a set of epitopes will help to define the breadth of responses in terms of the average number of peptides generally recognised by an individual. This data will be useful to monitor for potential viral escape from T cell immune recognition, to track if the sequences of the glycoprotein which are recognised following vaccination are significantly mutated in future outbreaks.

24 multimeric peptides from the SUDV GP elicited a positive response in the peptide mapping work, these peptides were present in both GP₁ and GP₂. A very high level of intra-species conservation was observed (86.7% to 100% across sequences from the 8 previous outbreaks). SUDV has an inter-outbreak mutation rate of 6.5705×10^{-5} substitutions/site/year with mutations being mostly silent and amino acid differences in the GP occurring mainly in the glycan cap and mucin-like domain [193]. This suggests

that the Ad26.ZEBOV/MVA-BN-Filo vaccine induced T cell response is likely to recognise strains of SUDV in future outbreaks making the vaccine elicited T cell response fairly robust against viral mutation.

Five peptides were found to have 100% homology with EBOV Mayinga, four of which have previously been identified as class I epitopes in CAd3-EBO Z/ MVA-BN-Filo UK vaccine recipients by Powlson et al [189]. Twelve additional peptides, though not 100% homologous with EBOV, were located in the same amino acid positions within the GP as EBOV epitopes identified by Powlson et al with one (DQIIHDFVDKTL) also identified in the same amino acid positions in survivors of EVD [190] except with different sequences as per the SUDV amino acid sequence, highlighting the potential of these regions of GP₁ as a T cell target. Aside from experimental studies, the peptide conserved across all orthoebolaviruses (LRQLANETTQALQLF) has been previously identified *in silico* as a CD4⁺ epitope and the smaller core nonamer sequences LANETTQAL and NETTQALQL have been predicted to be CD8⁺ epitopes [203]. Furthermore, the nonamer FLYDRLAST, predicted to be a core sequence within the positive peptide FLYDRLASTVIYR, identified in this chapter, had also been identified *in silico* by multiple studies [203, 204] highlighting the utility of bioinformatic approaches to epitope predictions.

No peptides between amino acids 295 and 501 of the C-terminus of GP1 were identified to give a positive response in the volunteers studied in this chapter. This result may be biased due to the peptides spanning residues 315-525 not being investigated at the single peptide level due to the low magnitude and frequency of responses to the mega pool. The low response could be attributed to this pool being the least conserved between EBOV and SUDV, potentially reducing cross-reactive T cell responses generated from the EBOV GP insert used in both the Ad26.ZEBOV prime and the MVA-BN-Filo boost. When searching the literature, data on T cell recognition of SUDV GP is sparse. However, similar observations have been made in studies of EBOV survivors or vaccinees, where these regions are also underrepresented in T cell responses. Specifically, in survivors of the 2014 EBOV outbreak little response was measured via IFN- γ ELISpot to peptides spanning amino acids 305–389 [190]. In the epitope mapping

study of UK recipients of the cAd3-EBO Z/ MVA-BN-Filo vaccine, peptides in the pool spanning amino-acids 305-389 and 449-515 were under-represented in the ELISpot, and although there was a detectable response to the mega-pool for peptides 379-459, when deconvoluted to the individual peptides no epitopes were found in this region [189]. This result recurs for EBOV vaccinees across the other chapters of this thesis where the peptide pool spanning amino acid residues 305 -389 was the least represented in UK vaccine recipients following a monovalent Ad26.ZEBOV boost (Chapter 3, Figure 3.8) the pool spanning amino residues 379-459 was the lowest responding pool in Senegalese vaccine recipients also following a monovalent Ad26.ZEBOV boost (Chapter 4, Figure 4.5). It is, of course, possible for all aforementioned studies that T cell responses or epitopes would have been detected if an assay with higher sensitivity was used such as a “cultured” ELISpot which uses an *in vitro* expansion step and increases the detection of low frequency antigen-specific responses [205]. Nevertheless, the region clearly shows a lower magnitude of T cell responses when compared to the rest of the glycoprotein and when considered with the data from these EBOV studies it is very likely that these regions of the GP are not particularly immunogenic.

The poorly represented pool mostly covers the C-terminal of GP₁ and much of the mucin domain of the glycoprotein, which is heavily glycosylated and spans amino acid residues 305 - 485. There are two hypotheses for this finding: (i) reduced immunogenicity may be due to steric shielding with O- and N- linked glycans blocking proteolytic sites from proteasome digestion, HLA anchor residues or TCR binding residues or, (ii) epitope residues modified by glycosylation could be loaded onto HLA class I or class II and recognized by the T cell receptor *in vivo*, but would not be recognised in the ELISpot assay which re-stimulates PBMC with synthetic peptides, which do not carry any post-translational modifications and are therefore not glycosylated. Further work is required across multiple antigens to analyse the effect of glycosylation on T cell recognition as this has implications for viral immune escape from T cell recognition or potentially in immunoassay design.

A major disadvantage of this study is that these epitopes were identified in a small number of UK volunteers where the HLA frequencies differ from those where SUDV outbreaks have historically occurred, such as in Ugandan or South Sudanese populations. For example, HLA-A*11:01 is under-represented or near absent while HLA-A*02:01, C*07:01 and C*02:02 are all frequent in Ugandan populations (defined as >10% frequency in at least one existing dataset as determined via allelefrequencies.net [206, 207], published frequencies by Kijak et al [208] and Alexander Mentzer, personal communication). Although it is possible that the pattern of recognition would be similar, given that some T cell epitopes can be promiscuous across multiple alleles of a supertype [209, 210], further experiments mapping of immunodominant regions in populations at risk of exposure to Sudan virus be required to investigate the epitope coverage across different ethnicities.

Although this work experimentally details regions of the glycoprotein which are the target of durable T cell recognition, likely MHC binding was only investigated using *in silico* methods. Future studies could validate these predictions using peptide-HLA tetramers to confirm epitope binding and presentation as has been done previously with other antigens [211-213].

Conclusions

This study shows the Ad26.ZEBOV/MVA-BN-Filo regimen elicits long-lasting cellular and humoral immunity to EBOV up to 46 months post-prime. Anti-SUDV GP immune responses were also detected but with lower rates of IgG seropositivity. For both species, it is not possible to know whether the observed immune responses will be sufficient to protect from disease, but it is promising for both for the possibility of deploying Ad26.ZEBOV / MVA-BN-Filo prophylactically against EBOV and for the ability of viral vectors to lay down robust and long-lasting immunological memory.

6. First-in-human immunogenicity data against a bivalent orthoebolavirus vaccine targeting both Ebola virus and Sudan virus (ChAdOx1 biEBOV)

Introduction

Several vaccines have been successfully developed and deployed against EBOV, since 2020, two have been approved for use (including WHO pre-qualification) on the basis of either clinical efficacy data or efficacy in non-human primate studies [214]. Currently, no vaccines have been approved for use against SUDV and a pre-clinical study indicates there may be limited cross-protection between the two species: NHPs vaccinated with VSV-EBOV and challenged with EBOV were not protected from a SUDV challenge delivered 1 year later, despite developing cross-reactive humoral responses [215]. This highlights the need to develop and test novel vaccines to specifically target SUDV. Given the unpredictability of outbreaks, a bi- or multivalent filovirus vaccine targeting both SUDV and EBOV would be preferable from a public health perspective. Such a vaccine would simplify deployment, potentially negating the need for multiple clinic visits. It would be well suited for the active immunisation of healthcare and frontline workers who are more likely to be at risk of exposure to multiple species of filovirus. In fact, such vaccines are the current preferred target product of the WHO for prophylactic vaccination [216]. There are two approaches to this when using viral vectored vaccines: (i) expressing multiple antigens within a single vector or (ii) delivering a cocktail of monovalent vaccines formulated in a single injection. The former approach would reduce manufacturing complexity.

To address this, ChAdOx1 biEBOV was developed. ChAdOx1 biEBOV uses the replication-deficient ChAdOx1 vector platform which is derived from a wildtype simian adenovirus Y25 with deletions in the E1 and E4 gene regions. The SUDV glycoprotein is expressed under the control of a tetracycline-repressor regulated CMV short promoter

at the E1 locus and the EBOV glycoprotein expressed under the control of a tetracycline-repressor regulated short CMV promoter at the E4/ITR locus.

Preclinical assessment of ChAdOx1 biEBOV in a small animal model showed that type I interferon receptor knockout (IFNAR^{-/-}) mice vaccinated with a single dose of the vaccine elicited strong cellular and humoral immunity and mice were completely protected against lethal challenges from either SUDV or EBOV [217]. As such, the vaccine progressed to human clinical trials. In 2022, based on favourable safety data as well as the early stage immunogenicity data which is presented in this chapter, ChAdOx1 biEBOV was one of three vaccines chosen by the WHO to be tested in a ring vaccination trial to evaluate potentially efficacious candidate vaccines [218].

This chapter presents the immunogenicity results from a Phase I, first-in-human dose escalation trial of ChAdOx1 biEBOV in UK volunteers.

Methods

EBL07 Trial Study Design

EBL07 (NCT05079750) study is a first-in-human, open-label, non-randomised, dose-escalation clinical trial of the ChAdOx1 biEBOV vaccine (Figure 6.1).

Healthy participants aged 18-55, with no prior exposure to adenovirus vaccines were recruited at a single site (Oxford, UK) and non-randomly enrolled to one of three dose groups: 5×10^9 viral particles (vp), 2.5×10^{10} vp or 5×10^{10} vp. A sub-group from the 5×10^{10} vp group received a booster dose of 5×10^{10} vp ChAdOx1 biEBOV 12 weeks later. Blood samples were taken from the single dose groups at baseline, pre-ChAdOx1 biEBOV vaccination, and then at the following timepoints: days 7, 14, 28, 56, 182 and 364. Participants receiving a second dose were samples at baseline and days 7, 14, 28, 56 and 84 days post prime and 7, 14-, 28-, 182- and 280-days post boost. The primary outcome measures were the assessment of adverse events, which are not presented here. The secondary outcome measures, and the focus of this chapter, were the assessment of humoral and cellular responses to both EBOV and SUDV. The

methodology used to assess these humoral and cellular responses is fully described in the Materials and Methods chapter.

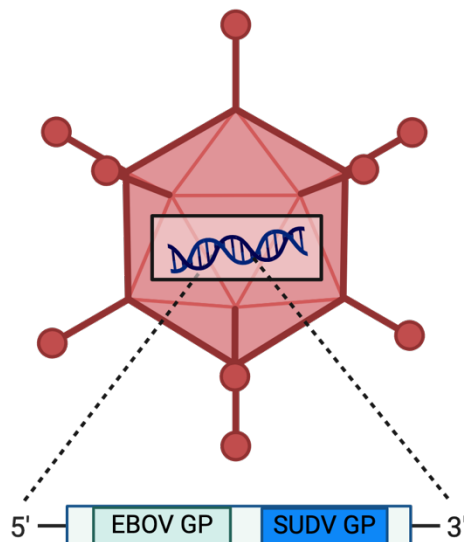


Figure 6.1: Infographic representation of ChAdOx1 biEBOV vaccine.

Objectives

1. Assess the humoral responses to both EBOV and SUDV elicited by single dose-escalation and multiple doses of ChAdOx1 biEBOV.
2. Assess the cellular responses to both EBOV and SUDV elicited by single dose-escalation and multiple doses of ChAdOx1 biEBOV.

Results

Recruitment

A total of 26 volunteers were recruited into the trial. 6 participants were enrolled into the low dose group (5×10^9 vp), 6 into the medium dose group (2.5×10^{10} vp) and 14 into the higher dose (5×10^{10} vp) group. All participants were initially recruited to receive a single

dose of vaccine. Following the approval of a substantial amendment permitting the administration of a second dose of vaccine in the high dose group, 7 out of 14 participants in this group consented to and received a second dose of vaccine. Demographic information for each group is detailed in Table 6.1.

Table 6.1: Demographic information for the EBL07 clinical trial. Data is presented as n (%) or range (median).

* ethnicity was self-reported.

Dose Group	5x10 ⁹ vp	5x10 ¹⁰ vp	2.5x10 ¹⁰ vp	2.5x10 ¹⁰ vp
			Single dose	Two doses
n=	6	6	7	7
Sex				
Male	2 (33%)	3 (50%)	2 (29%)	3 (43%)
Female	4 (67%)	3 (50%)	5 (71%)	4 (57%)
Age				
Range (median)	19-31 (24)	22-32 (26)	19-28 (20)	28-33 (30)
Ethnicity*				
White	6 (100%)	4 (67%)	4 (57%)	7 (100%)
Asian or Asian British	-	-	2 (29%)	-
Mixed White and Black Caribbean	-	1 (17%)	-	-
Other Asian background	-	1 (17%)	1 (14%)	-

Humoral Immunogenicity to biEBOV

A single dose of the ChAdOx1 vaccine elicited anti-EBOV glycoprotein IgG (Figure 6.2). Among the participants, 1 (16.6%) from the 5x10⁹ vp cohort, 3 (50%) from the 2.5x10¹⁰ vp cohort, and 14 (100%) individuals from the 5x10¹⁰ vp cohort were seropositive at one

or more time points following vaccination. Of the time points measured, the observed peak antibody response occurred 28 days post-vaccination across all single-dose groups. Geometric mean titres were 63.3 ELISA units [95% CI 7.2–555.0] for the 5×10^9 vp dose group, 164.2 ELISA units [95% CI 88.9–303.1] for the 2.5×10^{10} vp dose group and 260.1 ELISA units [95% CI 132.9–509.1] for the for the 5×10^{10} vp dose group (Figure 6.2A). In those that received a second dose, the titres increased to 1169.7 ELISA units [95% CI 719.8–1902.5] 28 days after the boost (D112), representing a 4.1-fold increase from pre-boost (D84) titres. All 7 (100%) volunteers were seropositive on day 28 after the second immunisation (Figure 6.2B). After 182 days, titres plateaued at 38.7 [95% CI 5.7-234.0], 119.0 [95% CI 58.8-240.9] and 183.6 [95% CI 75.8-444.9] for the 5×10^9 vp, 2.5×10^{10} vp and 5×10^{10} vp dose groups respectively. In those receiving a second dose, geometric mean titres were maintained at 242.3 ELISA units [95% CI 105.3-557.5] at day 364 (Figure 6.2B).

A single dose of the ChAdOx1 vaccine also elicited anti-SUDV glycoprotein IgG at the two higher doses that were evaluated. Among the participants, 0 (0%) from the 5×10^9 vp cohort, 5 (83.3%) from the 2.5×10^{10} vp cohort, and 12 (85.7%) individuals from the 5×10^{10} vp cohort were seropositive at one or more time point following vaccination. As with titres to EBOV, the observed peak antibody response to SUDV occurred 28 days post-vaccination across all single-dose groups, with geometric mean titres measured at 27.0 ELISA units [95% CI 4.9–148.5] for the 5×10^9 vp dose group, 101.7 ELISA units [48.4–213.8] 2.5×10^{10} vp dose group and 111.5 ELISA units [95% CI 48.2–256.6] in the 5×10^{10} vp dose group (Figure 6.2C). In those that received a second dose, the titres increased to 568.0 ELISA units [95% CI 296.4–1088] 28 days after the boost (D112) representing a 5.1-fold increase from pre-boost (D84) titres with all 7 (100%) volunteers seropositive 28 days after the second immunisation (Figure 6.2D). After 112 days, geometric mean titres measured at 19.4 [95% CI 4.1-92.9], 76.8 [95% CI 36.7-160.8] and 62.7 [95% CI 29.1-134.8] for the 5×10^9 vp, 2.5×10^{10} vp and 5×10^{10} vp dose groups respectively. In the group receiving a second dose, geometric mean titres measured at 116.6 [95% CI 43.5-312.8] at day 364 (Figure 6.2D).

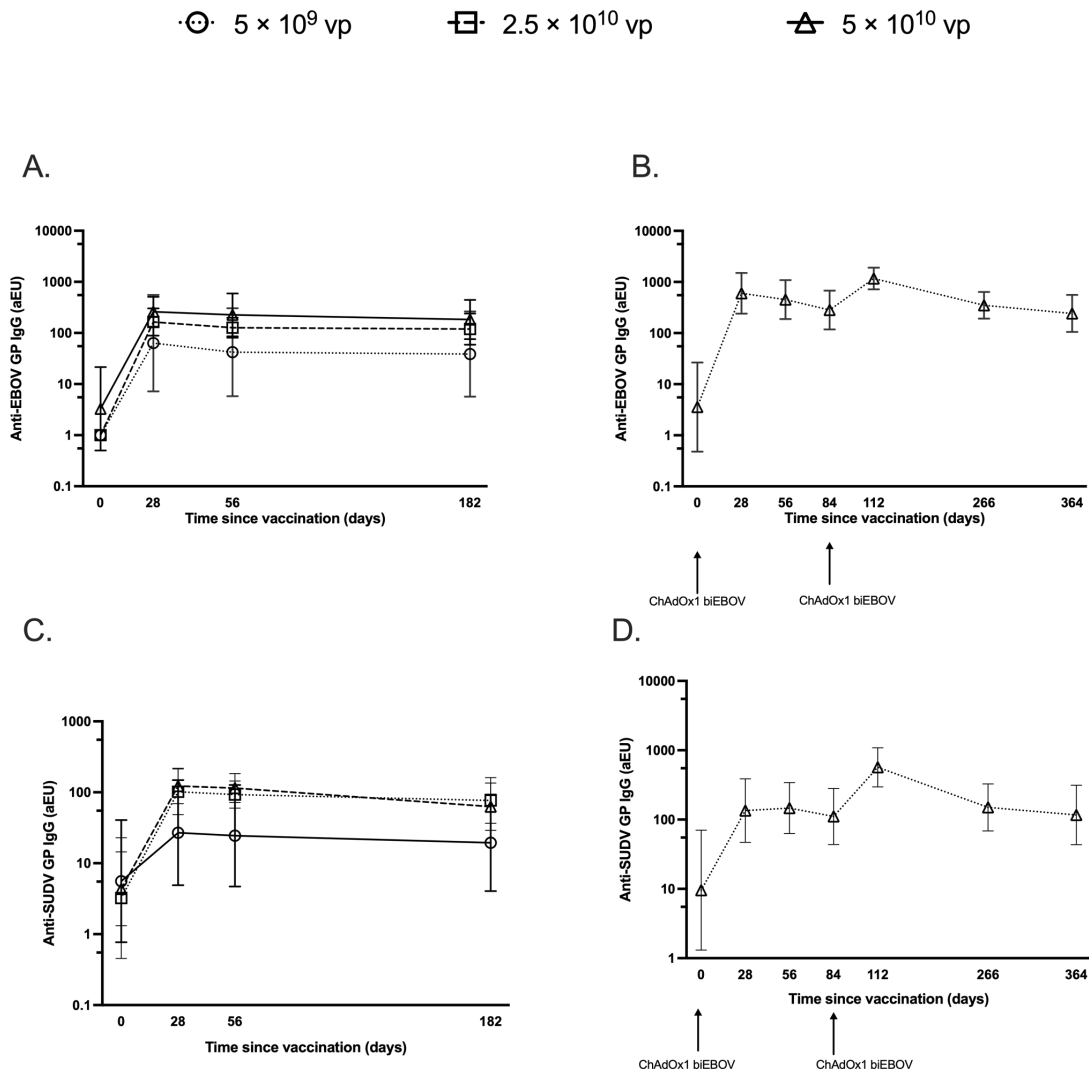


Figure 6.2: Anti-filovirus IgG as measured by in-house standardised enzyme-linked immunosorbent assay (ELISA). Shapes represent geometric means with error bars showing 95% confidence intervals. Arrows indicate vaccination time points. A. Anti-EBOV GP IgG following one dose of biEBOV B. Anti-EBOV GP IgG following two doses of biEBOV administered at D0 and D84 C. Anti-SUDV GP IgG following one dose of biEBOV D. Anti-SUDV GP IgG following two doses of biEBOV administered at D0 and D84.

A pseudovirus neutralisation assay was carried out at baseline (D0), 28 days-post prime (D28) and 28 days post-boost (V2+28) in the two dose group to assess functional antibody responses to EBOV and SUDV. An increase in neutralisation of EBOV GP bearing lentiviral pseudotypes was observed following a single dose. Although low levels of background neutralisation were observed in pre-vaccination samples, there was a mean increase in IC₅₀ of 1.97 [95% CI 0.18-3.76], 2.6 [95% CI 0.28-4.92] and 1.44

[95% CI 1.01-1.86] -fold between D0 and D28 samples for the low, medium and high groups respectively (Figure 6.3). In the two-dose group, this increased to a 4.73 [95% CI -0.90-10.38] -fold increase after a second dose. There was no detectable increase in neutralisation of SUDV GP bearing lentiviral pseudotypes in any group at any timepoint (Figure 6.3).

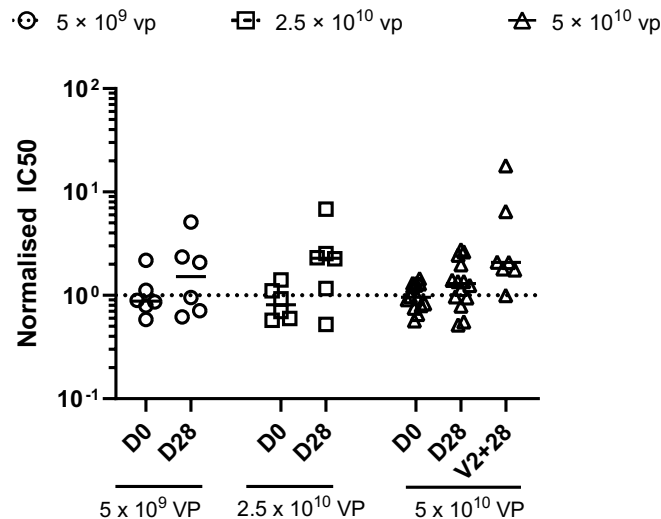


Figure 6.3: Pseudoneutralisation of EBOV GP-bearing lentiviral pseudotypes. Pseudoneutralisation of EBOV GP-bearing lentiviral pseudotypes as measured by in-house neutralisation assay. Shapes represent neutralisation IC50 with lines showing median.

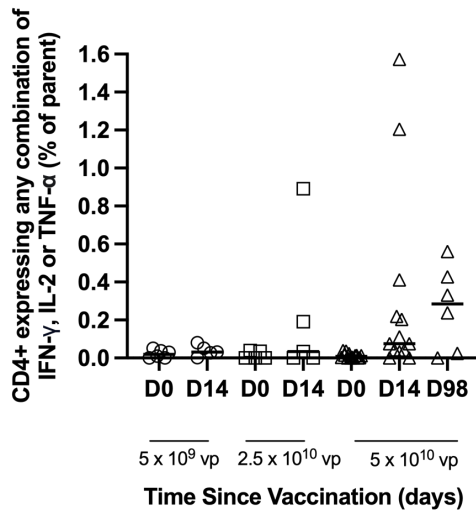
T Cell Immunogenicity to biEBOV

Intracellular cytokine staining (ICS) by flow cytometry was carried out at baseline (D0), 14 days-post prime (D14) and 14 days post-boost (D98) in the high dose group to assess vaccine-specific T cells responses induced by biEBOV. PBMC were stimulated with pools of multimeric synthetic peptides covering the glycoprotein of SUDV and EBOV, and analysed for production of either IFN- γ , TNF or IL-2. Five data points were excluded from analysis due to lack of PBMC sample availability or failure to meet the QC parameters. 14 days after vaccination, the median frequency of CD4+ T cells secreting interferon- γ , interleukin-2, or tumour necrosis factor- α to EBOV or SUDV (% of parent cells) were 0.0320 [IQR 0.0150 – 0.0665] and 0.0620 [IQR, 0.0560 to 0.0975] in the 5x10⁹ vp cohort, 0.0340 [IQR 0.000 – 0.5415] and 0.0860 [IQR, 0.0055 to 0.1510] in the

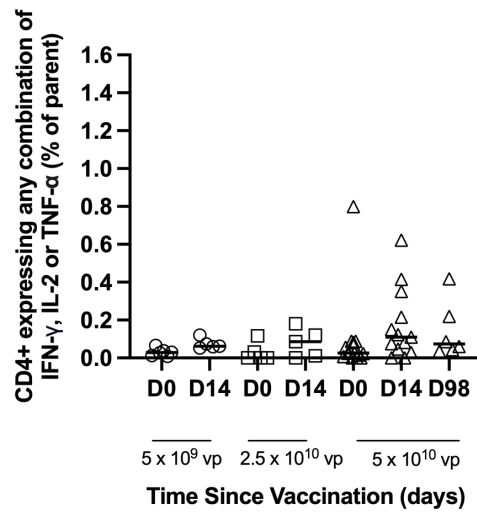
2.5x10¹⁰ vp cohort, and 0.0760 [IQR 0.0375 to 0.3160] and 0.1100 [IQR 0.0380 – 0.2835] in the 5x10¹⁰ vp cohort (Figure 6.4A, Figure 6.4B). Following administration of a second dose of 5 x 10¹⁰ vp the median frequency of CD4+ T cells expressing was 0.2845 [IQR 0.0188- 0.4613] to EBOV and 0.0735 [IQR 0.0420- 0.2695] for SUDV 14 days post-boost.

14 days after vaccination, the median frequency of antigen specific CD8+ T cells to EBOV and SUDV were 0.0300 [IQR 0.0090- 0.0395] and 0.0320 [IQR 0.0150– 0.0665] in the 5x10⁹ vp cohort, 0.0000 [IQR 0.0000 – 0.6945] and 0.0340 [IQR 0.0000 to 0.5415] in the 2.5x10¹⁰ vp cohort, and 0.08500 [IQR 0.0010– 0.2075] and 0.1120 [IQR 0.0425 to 0.3495] in the 5 x 10¹⁰ vp cohort. Following administration of a second dose of 5x10¹⁰ vp the median frequency of CD8+ T cells expressing was 0.1190 [IQR 0.0000- 0.3553] for EBOV and 0.0485 [IQR 0.0188– 0.4538] for SUDV (Figure 6.4C and D) 14 days post-boost.

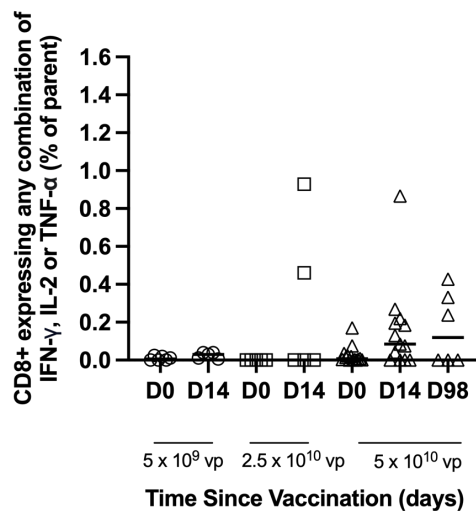
A. CD4+ EBOV



B. CD4+ SUDV



C. CD8+ EBOV



D. CD8+ SUDV

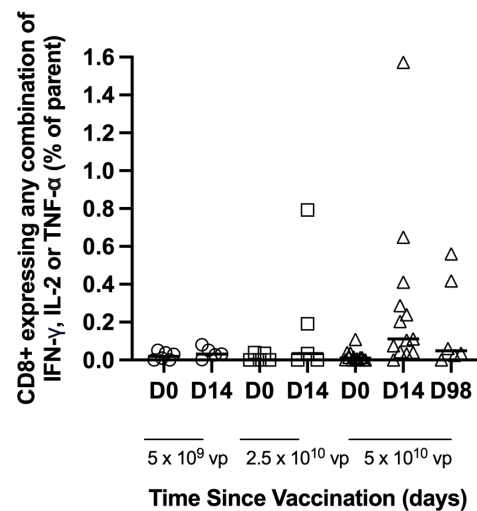


Figure 6.4: T cell responses to SUDV and EBOV GP as measured by flow cytometry with ICS. Lines show median. Percentage of T cells producing any of IFN- γ , IL-2, or TNF- α in response to stimulation with peptides spanning either the EBOV and SUDV glycoprotein at baseline (D0) and at 2 weeks post-vaccination (D14) and at two weeks post boost (D98) by dose. A) CD4+ T cell responses to EBOV GP peptides. B) CD4+ T cell responses to SUDV GP peptides. C) CD8+ T cell responses to EBOV GP peptides. D) CD8+ T cell responses to SUDV GP peptides.

Discussion

The data presented in this chapter show that a single dose of ChAdOx1 biEBOV induces both humoral and cell-mediated immune responses against both the EBOV and SUDV glycoproteins.

There are two main uses for vaccines targeting orthoebolaviruses: Reactive use i.e. the emergency deployment of vaccines during an outbreak and the targeting of high-risk groups (such as healthcare workers in endemic countries) in non-outbreak settings. For reactive use, vaccines that induce rapid immunity - ideally after a single dose- are preferable. In contrast, for non-outbreak settings, longer-term protection is a higher priority than speed of immune response. Considering these different uses, ChAdOx1 biEBOV was evaluated as both a single dose and as a two -dose regimen to assess the feasibility of use in both scenarios. A second dose of ChAdOx1 biEBOV, given at 12 weeks, boosted antibody responses (showing an increase of approximately 4-5 fold). An equivalent proportion of activated CD4+ and CD8+ T cells was measured post vaccination which is in contrast to recently published data demonstrating preferential CD4 activation following cAd3-EBO S immunisation [112]. This may reflect differences in cell entry target cells for cAd3 and ChAdOx1, differences in methodology or sampling timepoints and/or differences in the kinetics of vectored vaccines inducing immunity.

As a platform, the ChAdOx1 vector has several advantageous characteristics for use against outbreak pathogens, including its stability at refrigeration temperatures and its ability to generate strong a immune response after a single dose with the possibility to administer multiple doses with concomitant increase in immunogenicity [219]. During the COVID-19 pandemic, manufacturing processes for ChAdOx1-vectored vaccines were optimised, and this expertise was leveraged in 2022 when the Serum Institute of India rapidly manufactured and shipped 40,000 cGMP doses of ChAdOx1 biEBOV vaccine to Uganda in less than 80 days of the SUDV outbreak being declared by WHO [220]. Although not yet tested with this particular insert, the vector as used in the AstraZeneca ChAdOx1 nCoV-19 vaccine (AZD1222 or Vaxzevria) has demonstrated a good safety profile in at-risk cohorts including people living with HIV [221, 222],

pregnant women [223], and children aged 6 -17 [224]. These factors are all critical to consider given the geographical locations and outbreak scenarios in which filovirus vaccines are likely to be deployed. The rare but serious adverse reaction of vaccine-induced thrombosis with thrombocytopenia associated with adenoviral vectored SARS-CoV-2 vaccines warrants careful consideration, although the incidence following ChAdOx1 nCoV-19 vaccination shows wide geographical variation with very few cases reported outside of European and North American countries [225].

There are concerns that the prior use of low seroprevalence viral-vectored vaccines may result in the induction of anti-vector responses, potentially reducing the effectiveness of a homologous boost or of subsequent vaccines using the same vector [226, 227].

Specifically, for ChAdOx1, there are concerns that the widespread use of the AstraZeneca ChAdOx1 nCoV-19 vaccine might diminish antibody or T cell responses to a future vaccine using the same vector. Although the volunteers recruited in EBL07 had no prior exposure to adenovirus-based vaccines, precluding the possibility of drawing conclusions about ChAdOx1 with a different antigen, the homologous boost in the high-dose group did boost antigen specific IgG and T cell responses. Additionally, clinical studies of the ChAdOx1 nCoV-19 vaccine have shown no statistical relation between the level of adenoviral neutralisation titres following the first immunisation and the resultant antibody or T cell response following a further immunisation with the same vaccine [228, 229]. In studies of the ChAdOx1-HBV immunotherapeutic, volunteers who had received the ChAdOx1 nCoV-19 vaccine up to 18 weeks prior had significantly lower T cell responses to HBV antigens than ChAdOx1 naïve volunteers, who had instead received an mRNA covid-19 vaccine [230]. Conversely, in clinical testing of the ChAdOx1 nCoV-19 vaccine, it was shown that administration of a ChAdOx1 vaccine with an unrelated transgene (either the meningococcal capsular group B surface antigen or the Middle East respiratory syndrome spike protein) over one year prior had no effect on the antibody response to ChAdOx1 nCoV-19 [231]. Considering these data, it is possible that in order to circumvent reductions in immunogenicity associated with repeated vector use, an interval of over 4 months between ChAdOx1 vaccination with heterologous antigens may be required. Studies with a larger number of participants

with a wide range of intervals between ChAdOx1 vaccination with heterologous antigens would address this.

Small animal studies have demonstrated that the ChAdOx1 biEBOV vaccine provides protection against both EBOV and SUDV. Specifically, IFNRA knockout mice vaccinated with a single dose of the vaccine were completely protected against challenges from either SUDV or EBOV [217]. However, in a recently completed NHP study, ChAdOx1 biEBOV provided no protection against a stringent SUDV challenge [232]. Following vaccination, cynomolgus macaques formed a serological response to both SUDV and EBOV, including the induction of neutralising antibodies but minimal to no IFN- γ producing T cells. This contrasts with the human data presented here, where no SUDV GP neutralising antibodies were detected but a T cell response was observed, particularly in the medium and high dose groups, by ICS in response to restimulation with peptides spanning SUDV and EBOV GP. The efficacy of the biEBOV vaccine against EBOV has not been tested in the NHP model. Three other multivalent filovirus vaccines have demonstrated some level of protection against SUDV in NHP challenge models. Full protection was conferred by quadrivalent and trivalent vaccines which were both mixes of VSV vectored vaccines expressing the GPs of SUDV, EBOV, MARV or TAFV and, in the case of the quadrivalent vaccine, Lassa virus [233, 234]. Two doses of trivalent Ad26.Filo vaccine provided partial protection (75%) [87]. These vaccines, however, were all 'cocktails' of monovalent vaccines delivered in a single injection, unlike the biEBOV vaccine, which expresses both antigens within a single vector. One of the primary differences is likely to be that when two antigens are delivered as a monovalent mixture and not in the same vector, they may infect and be produced by different cells, whereas when expressed the same vector, they will be produced by the same cells. While NHP challenge studies are recognised as important models of Ebola virus infection, they differ from naturally occurring human exposure in some key respects. Primarily, the NHP model is uniformly lethal, with infection introduced intramuscularly, whereas human infection has CFRs below 100% and infection occurs mainly through mucosal membranes, percutaneously or sexually through direct contact with bodily fluids or fomites [235]. Nevertheless, these results should be carefully considered, and they support the optimisation of the ChAdOx1 biEBOV vaccine. Further strategies that could

be considered to enhance the immunogenicity of the vaccine against SUDV include optimisation of the vector design, antigen expression cassettes, or dose. These approaches have been used previously with other multivalent filovirus vaccines to optimise immunogenicity [234, 236]. Future studies evaluating the ChAdOx1 biEBOV vaccine should examine glycoprotein expression in tissues or cell lines. This research should compare the expression levels of both trimers and investigate the potential expression of either GP as monomers, homodimers, or heterotrimers composed of SUDV and EBOV monomeric GPs. Since the same cells will be expressing these glycoproteins, it is theoretically possible that monomeric glycoproteins from both species could bind via disulfide bonds to form a heterotrimer, though this would require experimental validation. Such a formation could potentially lead to an 'off-target' antibody response.

There are several limitations of this early phase study. The lack of accepted thresholds of protection and standardised assays limits the ability of immune responses from different vaccines to be compared with each other. The small number of participants within the trial precludes formal analysis of comparisons between dose groups and, for pragmatic reasons, no placebo arm was used in this trial. Furthermore, the trial population consisted exclusively of participants recruited in the UK which may not be representative of populations at risk of EBOD. Experimentally, the lack of a detectable neutralising antibody response towards lentiviruses bearing the SUDV GP may be hindered by missing antibodies which have previously been identified to not block cell entry but inhibiting binding to NPC1 [52], which would prevent viral replication but may not be detected in this assay.

A phase 1b trial of ChAdOx1 biEBOV is currently ongoing in Tanzania to further investigate the safety and immunogenicity of the vaccine (NCT05301504). This study will provide safety and immunogenicity data in a different geographical population and will have a larger sample size than that used in this phase I first-in-human study.

Conclusion

This early phase study showed detectable antigen specific IgG antibodies to both EBOV and SUDV GP following vaccination with ChAdOx1 biEBOV. CD4 and CD8 cell responses to EBOV and SUDV GP were also detectable by ICS, particularly in the high dose group from day 14. However, the lack of a SUDV pseudovirus neutralising antibody response shown in this trial in addition to the emerging NHP SUDV efficacy data supports optimising the vaccine approach.

7. Summary of Findings, Implications and Future Directions

This thesis addresses two key themes for viral vectored vaccines targeting orthoebolaviruses in order to answer longstanding questions in the field. Primarily it assesses the durability of viral vectored vaccines against ebola virus (discussed in Chapter 3, Chapter 4 and Chapter 5). It also tests the immunogenicity of two multivalent vaccines to both EBOV GP and SUDV GP: i) MVA-BN-Filo as given in prime-boost combination with Ad26.ZEBOV as an ad hoc analysis of the durability non-interventional trial (discussed in Chapter 5) and ii) the novel ChAdOx1 biEBOV in a dose escalation first-in-human clinical trial (discussed in Chapter 6).

Durability

This thesis presents data on the durability of immune responses induced by four key prime-boost *orthoebolavirus* vaccines: cAd3-EBO Z/MVA-EBO Z, cAd3-EBO Z/MVA-BN-Filo, cAd3-EBO Z/Ad26.ZEBOV and Ad26.ZEBOV/MVA-BN-Filo. Understanding the persistence of immune responses to vaccination against any pathogen, including both humoral (antibody-mediated) and cellular (T cell mediated) immunity, is essential for modelling vaccine effectiveness over time, especially for monitoring potential waning immunity in high-risk populations. Vaccines that induce long-lasting immunity reduce the need for frequent booster doses, lowering healthcare costs and simplifying vaccination schedules. Current licensed vaccines vary widely in the durability of protection they provide against infection and disease [237]. Some vaccines can provide long lived, or even lifelong immunogenicity or protection such as those targeting measles [238] (delivered as part of the measles-mumps-rubella [MMR-II]) and small pox [239, 240], while others, although still useful public health measures, are hampered by rapidly declining immunity, provide only limited protection and may require multiple boosters such as vaccines targeting typhoid fever [241]. Despite its importance, durability testing is often not prioritised in clinical trials due to practical and logistical constraints. In the early regulatory approval phases, vaccine trials are often short in

length, between six to twelve months, as they are typically designed to demonstrate safety and immunogenicity or efficacy in the short term.

Why some vaccines demonstrate superior durability to others remains unclear and a persistent issue in the field of vaccinology is the limited understanding of how to engineer long-lasting immune responses in target populations. For a durable response to be induced, a vigorous germinal centre reaction must be induced along with the generation of long-lasting plasma cells (LLPCs), memory B and T cells [242].

Current strategies to combat filovirus infection are currently either prophylactic vaccination or reactive use during outbreaks. The former would be beneficial to populations deemed at higher occupational risk, such as healthcare workers, and will likely be administered on a large scale to many individuals. Prophylactic vaccines targeting Ebola virus should ideally provide long-term protection by inducing both robust effector responses and long-lasting memory recall responses that can be rapidly reactivated upon antigen exposure. With the aim of prophylactic vaccination in mind, the longevity of the licensed Ad26.ZEBOV/MVA-BN-Filo was assessed up to 46 months. 55% of volunteers who had received the 56-day prime-boost interval, as licensed by the EMA, were found to be seropositive. The volunteers receiving the 28- or 84-day interval exhibited 89% and 69% seropositivity respectively. Average titres of binding IgG were similar across the three groups.

Furthermore, the three experimental candidates cAd3-EBO Z/MVA-BN-Filo, cAd3-EBO Z/MVA-EBO Z, and cAd3-EBO Z/Ad26.ZEBOV were also assessed for durability and showed varying seropositivity at 60, 46/48 and 47 months post-prime as summarised in Table 7.1. T cell responses at long-term follow-up are summarised in Table 7.2. In cAd3-EBOZ/MVA-BN-Filo vaccine recipients from a UK cohort and cAd3-EBOZ/MVA-EBO Z volunteers from both a UK and a Senegalese cohort, immunological memory is shown to be maintained to at least 4 years post-prime. It can be activated within 7 days by a booster immunization with Ad26.ZEBOV with IgG boosted to levels greater than those observed after the complete primary vaccine regime in both UK and Senegalese volunteers. T cells were also boosted above those achieved in the primary regimen in

UK volunteers. Given the high titres measured, it is very likely that the rise in antibodies and T cells occurs earlier than 7 days post-vaccination, but this has not been confirmed experimentally.

Table 7.1: A summary of the EBOV GP IgG seropositivity rate in vaccine regimens as measured across multiple chapters of this thesis.

Vaccine Regime	Population	Time Point (median)	% anti-EBOV GP seropositivity
cAd3- EBOZ/Ad26.ZEBOV	UK healthy adults	47 months post dose 1	60%
cAd3-EBOZ/MVA- BN-Filo	UK healthy adults	60 months post dose 1	56%
cAd3-EBOZ/MVA- EBO Z	UK healthy adults	51 months post dose 1	24%
cAd3-EBOZ/MVA- EBO Z	Senegalese healthy adults	47 months post dose 1	78%
Ad26.ZEBOV/MVA- BN-Filo	UK healthy adults	46 months post dose 1	55-89%*

*seropositivity differs depending on the interval between Ad26.ZEBOV prime and MVA-BN-Filo boost.

Table 7.2: A summary of the T cell response to peptides spanning EBOV GP as measured by ELISpot using freshly isolated PBMC.

Vaccine Regime	Population	Time Point (median)	T Cell Response (SFC per 10⁶ PBMC)
cAd3- EBOZ/Ad26.ZEBOV	UK healthy adults	47 months post dose 1	433
cAd3-EBOZ/MVA- BN-Filo	UK healthy adults	60 months post dose 1	105
cAd3-EBOZ/MVA- EBO Z	UK healthy adults	51 months post dose 1	189
cAd3-EBOZ/MVA- EBO Z	Senegalese healthy adults	47 months post dose 1	382
Ad26.ZEBOV/MVA- BN-Filo	UK healthy adults	46 months post dose 1	234 – 364*

* differs depending on the interval between Ad26.ZEBOV prime and MVA-BN-Filo boost.

There is no universally agreed upon correlate of protection against EBOV for any of the vaccines investigated in this thesis. In fact, no human vaccine efficacy data are available for any of the four investigated vaccines. For Ad26.ZEBOV/MVA-BN-Filo, immunobridging has been used to infer the likelihood of protection in humans from NHPs [66, 86]. Unfortunately, the current immunobridging model is based solely on circulating binding antibodies at 21 days post-boost, thus it does not provide information on how the persistence of the vaccine-induced immune response may associate with durability of protection in humans. In the absence of long-term follow-up studies, a new model has not yet been developed [243] therefore, candidate vaccines should aim to induce both a humoral and a cellular immune response. Although previously hypothesised correlates of protection such as, EBOV GP-binding IgG [99, 123], neutralising immunoglobulins [101] and CD8+ T cell responses [102] in vaccine

recipients are detected at long term follow-up in this thesis, it is not possible to know whether these would be sufficient to provide protection against disease. These immunological readouts are also boosted in the volunteers that received an Ad26.ZEBOV vaccine. Polyfunctionality of T cells was assessed 28-days after boosting and the polyfunctional CD8+ T cells expressing a combination of the Th1-type cytokines TNF and IFN- γ were well represented. Specifically, they formed the most commonly measured CD8+ response in the UK volunteers (REVOLVE) and the second most frequent CD8+ response in the Senegalese volunteers (RESOLVE). These polyfunctional T cells have been associated with improved NHP survival in an EBOV challenge study [123]. EBOV-specific IgG antibodies and robust, polyfunctional EBOV-specific memory T-cell responses have also been detected in survivors of EVD up to two years after discharge from treatment centres [244]. When considered together with the literature, the above results do therefore indicate the possible protective effect of these immune responses against EBOV infection and these data may be of further use to be re-considered in the future should a correlate of protection be discovered and agreed upon.

Future directions for durability work

The work represents a comprehensive analysis of binding IgG and T cell responses and focused on these aspects as they have previously been hypothesised to correlate with protection in animal studies. However, a drawback of the vaccine longevity work is that it has all been conducted and analysed using samples isolated from peripheral blood, namely plasma and PBMC. While this does provide initial insights into the induction of antigen-specific cells following vaccination, analyses of other tissues such as bone marrow and lymphoid tissue would be additionally important to investigate durable vaccine-induced B and T cell populations [245]. In both cases sophisticated tools and sampling methods are now available. Bone marrow aspirates as used in other vaccine studies [246-250] would give insights into ebola virus glycoprotein specificity in LLPCs, a mechanism for maintaining circulating antibodies [251] in particular, CD19⁻ CD38^{hi} CD138⁺ LLPCs have been found to be the cellular basis of durable humoral responses [246]. These samples could also be used to track B cell clones and somatic hypermutation. Fine needle aspirate (FNA) samples from a secondary lymph node

would provide insight into germinal centre and central memory activity, and this sampling technique is increasingly being employed in other vaccine studies [252-254]. Future long term follow-up studies of candidate ebola vaccines should consider collecting such samples. The analysis and phenotyping for EBOV specific populations could then be conducted using a variety of techniques such as single cell sequencing or spectral flow cytometry which would supplement the work carried out in this thesis. It is worth noting, however, that there are barriers to using these techniques as they are more invasive and costly than intravenous blood sampling, require specialist personnel and often yield highly variable cell numbers adding complexity to study design and analysis [245].

Multivalent vaccines

Multivalent vaccines are designed to incorporate multiple antigens, which may include either distinct strains of the same species or antigens derived from different pathogens. The antigenic components are combined into a single vaccine formulation, allowing for the simultaneous induction of an immune response against multiple species or strains. A multivalent filovirus vaccine is currently part of the WHO preferred target product profile for the next generation of prophylactic vaccines [216]. Historically, multivalent vaccines have been formulated by the combination of multiple monovalent vaccines, such as the measles-mumps-rubella (MMR). This is also the approach several multivalent filovirus vaccines have taken [87, 233]. However, each component has to be manufactured separately, and the method of combination can be complex [255]. With advancements in viral vectored vaccines, it has become possible to combine two or more putatively protective antigens into a single viral vector, particularly if leveraging the larger viral vectors such as adenoviruses (as is the case for ChAdOx1 biEBOV) and pox viruses (such as MVA-BN-Filo). When developing multivalent vaccines, it is important to consider the interaction of the various components with each other; potential interactions include antigenic competition [256] and/or epitope suppression, resulting in an inappropriate immune response [257-259].

The work presented in this thesis is the first to show that the MVA-BN-Filo elicits an antigen specific immune response to SUDV at long term follow-up. T cell epitope mapping revealed multiple putative epitopes spanning the SUDV GP across almost all domains except the mucin-like-domain. The majority of recognised peptides were conserved across other SUDV strains isolated from previous outbreaks. A smaller number of peptides were also conserved across multiple orthoebolaviruses, with some showing lower cross-reactivity indicating some SUDV exclusive recognition. Anti-SUDV GP binding IgG were also enumerated but at much lower levels to those measured against EBOV GP.

Finally, the assessment of the novel biEBOV vaccine in a phase I trial showed a T cell and binding antibody response to both EBOV and SUDV GP. T cell responses as measured by ICS were comparable across the two antigens. However, neutralising responses were detected towards pseudoviruses bearing the GP from EBOV, but not to SUDV.

Future directions for multivalent vaccine work

The work presented for biEBOV presents a coherent account of first-in-human data. As the vaccine was not protective in the NHP model [232], future work should include optimising the approach. There are many different experimental approaches, but the optimisation of promoters and the expression cassette should be trialled pre-clinically. The re-testing of a monovalent SUDV vaccine, head-to-head with the bivalent in humans would shed light on whether antigenic competition from encoding the two glycoproteins was hampering efficacy.

8.3. Final remarks

I believe that the work presented here adds an important body of knowledge to the study of candidate ebola vaccines in clinical trial settings. Despite more than 300,000 doses of rVSV-ZEBOV or Ad26.ZEBOV/MVA-BN-Filo having been administered during various ebola virus outbreaks from 2018 onwards, publicly available data on their durability is lacking. The data here aims to fill this void and also shows the potential for viral vectored vaccines to exhibit good durability, which could be leveraged using the

same adenovirus or pox-virus vectors to target other diseases. Furthermore, first-in-human data on the bivalent orthoebolavirus vaccine biEBOV is an important step forward for a vaccine against SUDV, for which none are currently licensed. Alongside the SUDV specific data from Ad26.ZEBOV/MVA-BN-Filo vaccine recipients, it confirms that bi- or multivalent filovirus vaccines encoded in a single vector can induce an immune response to multiple glycoproteins although, in the case of biEBOV, it was not sufficient to protect NHPs in a challenge model. Finally, the work presented in this thesis also represents the first time anti-SUDV GP binding antibodies have been measured on a standardised assay in either the Jenner Institute or the Oxford Vaccine Group laboratories. The ELISA assay was set up and partially validated as part of this thesis to ensure that it was fit-for-purpose as the immunology readout for the EBL07 trial. The anti-SUDV GP pseudovirus neutralisation assay was also set-up to facilitate evaluation of the biEBOV vaccine. It is hoped that this work will allow for the continued evaluation of vaccines targeting SUDV in clinical trials within the research group. Continued research into vaccines targeting SUDV is essential so that a licensed vaccine can be made available to combat this devastating disease.

8. Supplementary Chapter

Set-up and Qualification of an ELISA to measure anti-SUDV

IgG

Introduction

The measurement of total immunoglobulin G (IgG) antibodies that bind to a target antigen by enzyme linked immunosorbent assay (ELISA) is one of the primary immunological readouts for assessing the humoral response of many novel vaccine candidates. ELISAs are often preferred for their simplicity, ease of use and relative cost-effectiveness compared with other methods of antibody enumeration such as multiplexed assays (mesoscale discovery or Luminex).

Anti-SUDV GP IgG had not been measured using a standardised assay in either the Jenner Institute or Oxford Vaccine Group laboratories and since anti-SUDV GP IgG had been deemed to be important prior to the commencement of the EBL07 clinical trial and to the work presented in this thesis, the development of a new methodology was necessary.

This supplementary chapter details the development, and partial validation of an in-house standardised indirect anti-SUDV GP IgG ELISA for use testing human plasma samples in clinical trials and exploratory immunology studies. The core methodology, including all reagents (except for the antigen and standard pool) and incubation times, followed the same approach as has been previously optimised and used with multiple antigens in the Jenner Institute laboratory [117, 260-263]. Following the set-up and qualification of this assay the ELISA was used to measure anti-SUDV-IgG as the immunological output for the EBL07 trial (Chapter 6), and as exploratory measures for the PRISM clinical trial (Chapter 5).

Materials and Methods

Anti-SUDV GP IgG ELISA procedure

The standardised ELISA was performed as described in materials and methods section 1.2.1.5 'Anti-EBOV GP and anti-SUDV GP total IgG ELISA'.

Antigen

The antigen used in this assay is recombinant Sudan ebolavirus glycoprotein (amino acids 32-649), expressed in HEK293 cells with a C-terminal His₆-tag and a heterologous signal peptide to drive secretion. The trimeric fraction was purified using size exclusion chromatography. This antigen was custom-made for this project by the Native Antigen Company. It is stored in single-use aliquots at -20 °C until use.

Standard Pool & Positive Control

The standard curve on each assay plate was prepared from a pool of SUDV-GP positive plasma samples from previously vaccinated humans. To avoid multiple freeze-thaw cycles of the stock standard pool, small aliquots enough to prepare standard dilutions for four ELISA plates were prepared at a 1:100 dilution in casein and stored at -80 °C. For the assay, the aliquots were serially diluted two-fold in duplicate to create the standard curve and plated in triplicate as the internal control at a 1:1600 dilution.

Test Samples

The assay was optimised, and validation experiments were conducted using post-vaccination plasma or serum samples as international reference standards were not available at the time of development. Samples were used from vaccinated volunteers enrolled in the EBL01 (NCT02240875) and EBL07 (NCT05079750) clinical trials. Samples from the COV002 trial (NCT04400838), as well as pre-vaccination (D0) samples from the EBL07 clinical trial, were used as naïve plasma to calculate for the assay seropositivity cut-off. The sample set used differs between parameters and were chosen based following an assessment of the remaining volume of sample and type of sample of sample required.

Parameter definitions

Table S 1: A list of parameters assessed for the assay and the criteria for deciding fit-for-purpose.

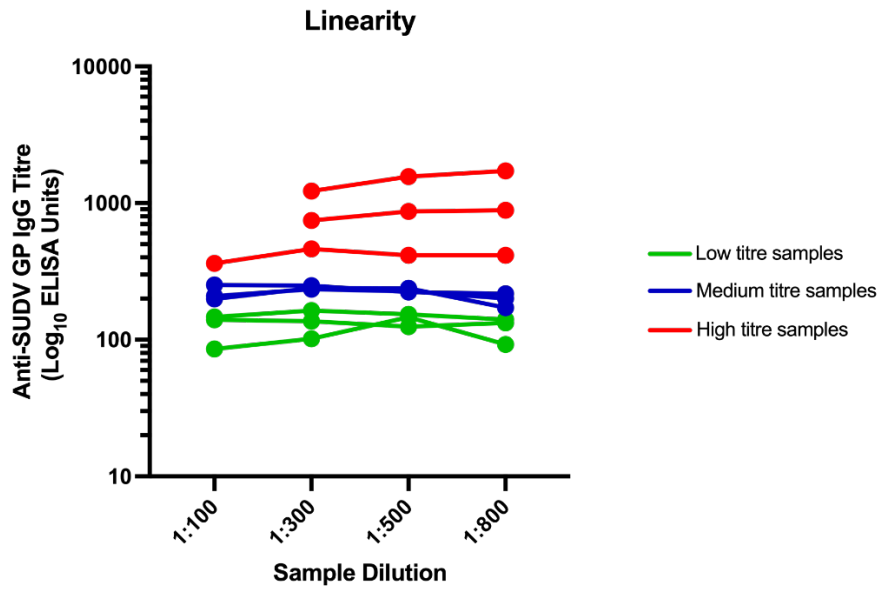
Target criteria were set prior to the commencement of the partial validation.

	Parameter	Means of assessment	Target for demonstrating fit-for-purpose
1	Linearity/ Parallelism	Dilution of antigen-specific IgG positive plasma	R>0.8 with significant positive correlation.
2	Precision	a) Determination of %CV for triplicates for single operators b) Determination of %CV for assay results performed simultaneously by 3 operators	a) % CV of the ELISA units less than 20% between replicates b) % CV of the ELISA units less than 20% between operators
3	Robustness	a) 7 sample freeze-thaw cycles b) Comparability of plasma and serum	No effect on magnitude of response. P>0.5 for matched-pair analysis of samples tested under different conditions
4	Detection limit (Cut-off)	Testing of responses in a naive population.	Mean + 3 standard deviations of responses at D0 in target population using a dilution of serum or plasma that gives the greatest discrimination of pre- and post-vaccination samples. With 100 naive samples, 3SD should be sufficient to give a cut-off with a high degree of confidence (>99%).
5	Selectivity	Testing of samples in the presence of other <i>orthoebolavirus</i> antibodies	Assay performed on SUDV vaccine and infection naive volunteers who are known to be seropositive for EBOV 28-

			days after vaccination with a monovalent EBOV vaccine.
--	--	--	--

Linearity

Linearity provides information about the precision of results for samples tested at various dilution levels, which is important for accurate measurement of analyte concentration across the dynamic range of the assay. 9 samples were selected with a varying known titres of anti-SUDV IgG antibodies (3 low responders, 3 medium responders, 3 high responders) and assessed at 4 different dilutions (1:100, 1:300, 1:500, 1:800). Figure S 1 shows the linearity of the assay at the 4 different working dilutions for the nine samples. At the 1:100 dilution high titre samples 2 and 3 were too concentrated and returned OD₄₀₅ that were above the linear range of the curve and were therefore non-quantifiable at 1:100 according to the protocol. These results were not able to be converted into an ELISA unit and therefore only 3 dilutions are presented for these samples. A plot of the OD measurements against dilutions showed significant positive correlation with an $r > 0.98$ (Spearman's rank correlation coefficient) for all samples tested (Figure S 2).



	Mean	Number of dilutions in linear range	CV	Range
Low 1	106.5	4	27.1	85.7 - 146.3
Low 2	151.2	4	7.7	140.5 - 163.7
Low 3	133.5	4	4.5	124.8 - 139.7
Medium 1	217.5	4	8.1	200.7 - 234.4
Medium 2	212.1	4	18.3	171.7 - 239.4
Medium 3	235.4	4	7.0	217.5 - 251.8
High 1	413.4	4	6.7	362.5 - 462.2
High 2	833.8	3	9.0	747.8 - 885.4
High 3	1502.8	3	16.7	1227 - 1717.4

Figure S 1 : Linearity of the ELISA units from 4 different plasma dilutions of nine samples. Each point represents the mean of 3 triplicate values on one plate. Descriptive statistics are tabulated.

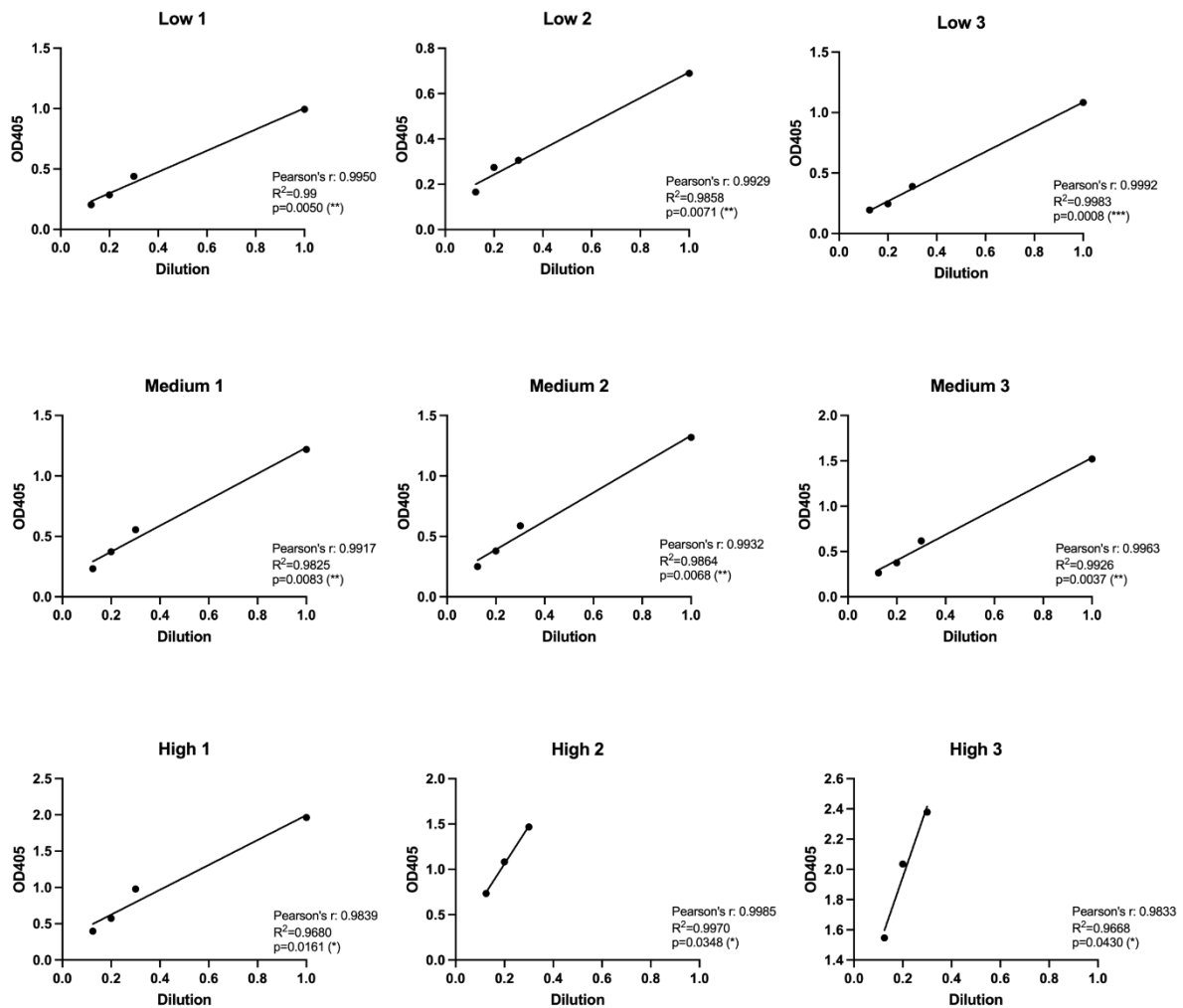


Figure S 2: Correlation of dilution and OD₄₀₅ for the nine samples.

Precision

Precision was defined as the closeness of agreement between independent test results obtained under stipulated conditions. Precision was assessed at two levels: (i) repeatability, also known as ‘within-run precision’, where the same samples were assessed under the same conditions on the same day and (ii) intermediate precision, also known as ‘within laboratory precision’ where the same plasma samples were assayed by three different operators in the same laboratory on the same day. CVs for both within-run precision, tabulated at % CV between triplicates for each operator, and within laboratory precision, tabulated as % CV between operators, met the acceptance criteria of <20% and are detailed in Table S 2.

Table S 2: Repeatability and intermediate precision measured using 10 samples covering a range of titres. Assay performed on the same day by 3 independent analysts trained in the protocol.

Sample ID	No. of observations	Mean ELISA units	% CV	% CV	% CV	% CV
			between triplicates (Operator A)	between triplicates (Operator B)	between triplicates (Operator C)	between operators
1	9	1.0	0.0	0.0	0.0	0.0
2	9	290.3	5.8	4.1	12.1	11.8
3	9	283.8	2.8	3.1	13.5	15.3
4	9	373.4	4.4	4.6	5.8	9.2
5	9	458.3	7.8	7.2	5.5	9.2
6	9	748.0	6.7	6.4	6.8	4.0
7	9	428.6	8.0	8.3	14.4	8.1
8	9	2958.6	6.3	5.7	16.1	0.8
9	9	638.6	7.2	6.9	8.2	1.9
10	9	2512.6	3.5	2.5	16.1	18.8

Robustness

Comparability of matched plasma and serum

Some clinical trials may collect only plasma or only serum for their serological analysis, depending on the blood draw volume and if cellular analysis is specified in the protocol. Therefore, the levels of agreement in measured IgG titres between matched plasma and serum samples at a pre-determined single dilution (1:100 or 1:500 chosen so that the OD₄₀₅ would fall within the linear range of the curve) were used to evaluate the effectiveness and reliability of the assay against both sample types. Samples were chosen to cover a range of antigen specific IgG titres, including three negative samples. There was no significant difference between titres measured using either plasma or serum (p=0.1953) (Figure S 3). Both plasma and serum can be used on the assay interchangeably and results compared between the two.

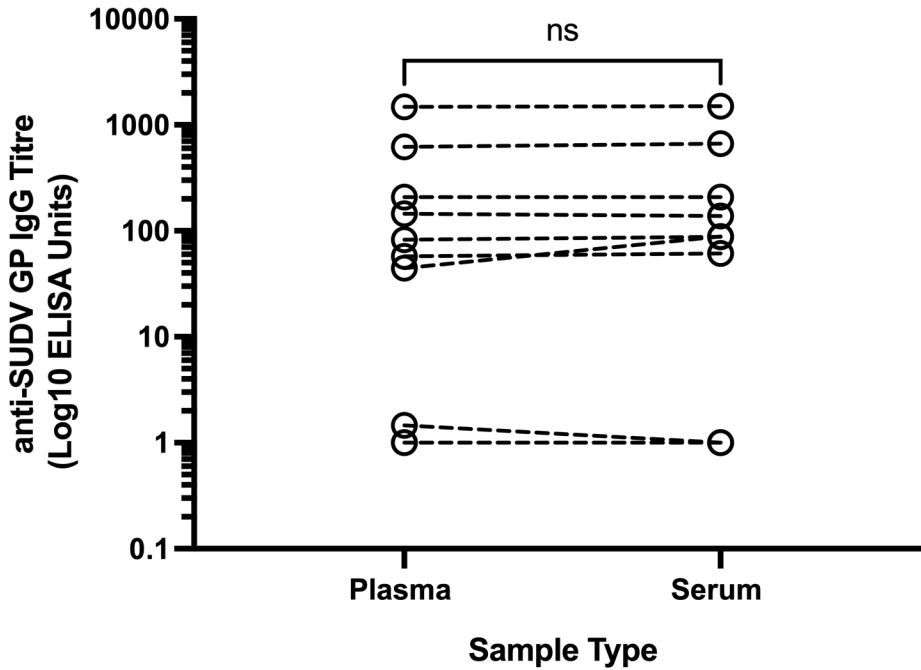


Figure S 3: Comparison of matched plasma and serum samples. Significant difference was determined using Wilcoxon matched pair signed rank test, $p=0.1953$.

Sample stability from repeated freeze-thaw cycles

The stability of the control samples over multiple freeze-thaw cycles from storage at -80°C was also evaluated using single use aliquots of the antigen. The samples were thawed for 1h at RT prior to their dilution and analysis as per the protocol. Titres from the measurement of the control samples with 1 freeze thaw cycle were compared with those obtained from the analysis of the same samples for up to seven freeze-thaw cycles. The repeated freeze-thaw cycle tested was aimed at mimicking the sample handling conditions likely to be used during normal sample analysis. There were no significant differences in IgG titres between the baseline and the titres from the repeated freeze-thaw cycles (Friedman's test, $p=0.7534$). This data demonstrates that if repeated analysis of the same samples is required, up to seven freeze-thaw cycles are validated as acceptable (Figure S 4)

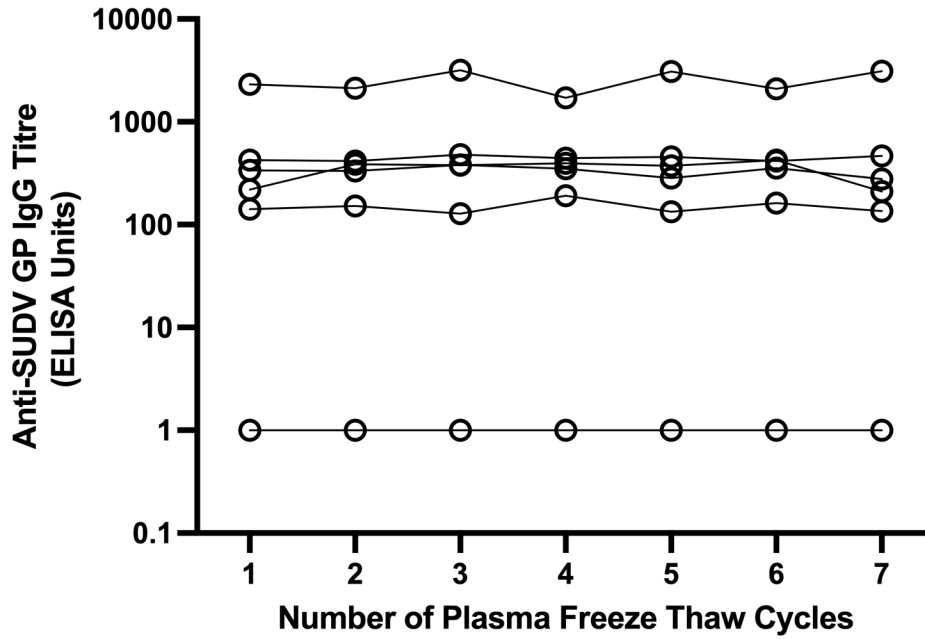


Figure S 4: Effect of multiple freeze-thaw cycles on plasma stability.

Assay cut-off

A total of 137 plasma samples were assayed on the anti-SUDV GP IgG ELISA from filovirus vaccine naïve healthy adults (18-55 years old, n=91) and older adults (over 55 years old, n=46) (Figure S 5). The assay seropositive cut-off was derived mathematically using the resulting EUs. The cut-off is set as the mean of the responses + 3 standard deviations. This corresponds to the analytical sensitivity of the assay.

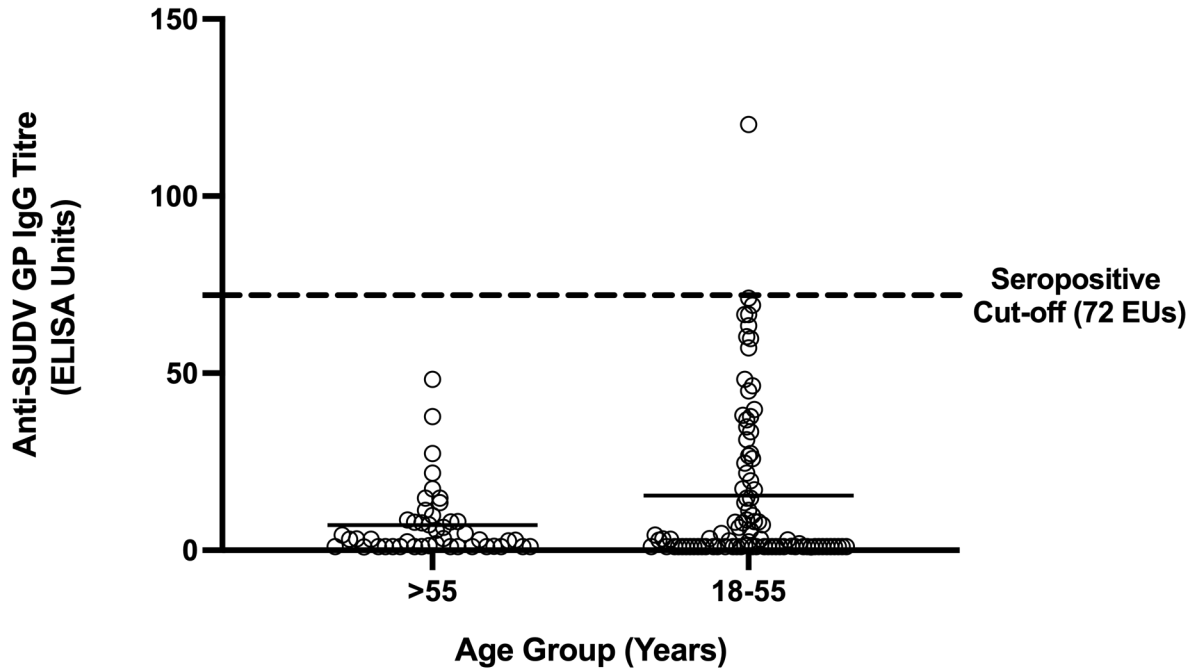


Figure S 5: Assay seropositive cut-off. IgG titres of the 138 orthoebolavirus infection or vaccination naïve samples used for calculation of the assay seropositive cut-off (mean plus three standard deviations of the EUs). The dotted line represents the ELISA seropositive cut-off). 18- 55 years old, n=91; >55 years old, n=46.

Selectivity was analysed by assaying plasma samples from 32 volunteers vaccinated with any monovalent vaccine against Ebola virus (EBOV) which were known to be seropositive for anti-EBOV GP IgG at D28 as measured by in-house standardised anti-EBOV GP IgG ELISA.

Prior to vaccination with an EBOV vaccine, all samples were seronegative for SUDV, 28-days after EBOV vaccination 4 samples (12.5%) were above the seropositivity threshold. This data suggests the assay can cross react with some EBOV IgG and would not be suitable for diagnostically distinguishing between the two species of *orthoebolavirus* with high levels of certainty (Figure S 6)

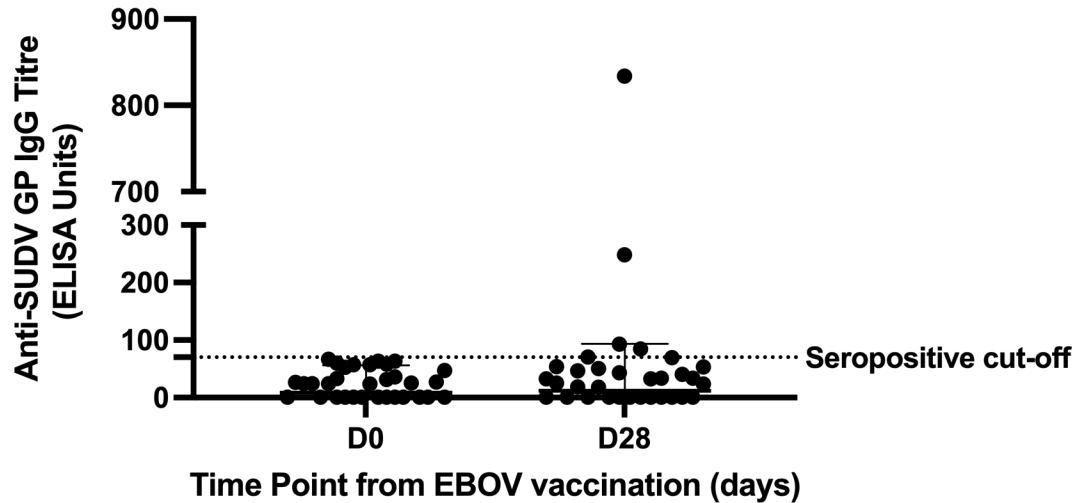


Figure S 6: Selectivity of the assay as evaluated by the testing of plasma samples before and after receiving a monovalent EBOV vaccine. All samples were known to be seropositive for EBOV at D28.

Ongoing Assay Monitoring

The experiments in the validation were performed within a the time frame of a few months and therefore the results represent a snapshot of the assay’s performance. To ascertain that the quality does not degrade over time, the performance of its standard curve as quantified by the parameters of the four-parameter hyperbolic curve equation, A, B, C, D and R^2 were monitored over time in all ELISA plates assayed between May 2022 and August 2023. All plates included in the longitudinal analysis were conducted by the same operator in the same laboratory. No trend in changes to the values have been observed over time (Figure S 7). The ELISA units for the internal control were also monitored over time and were found to exhibit a CV of 15% across the same range of dates.

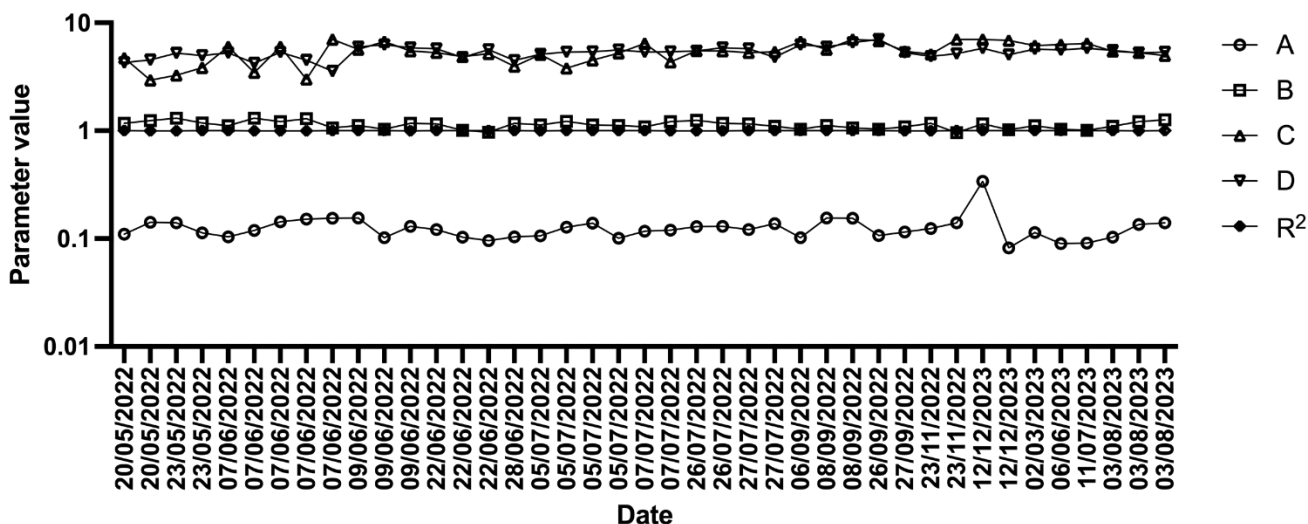


Figure S 7: the value of the 4 parameters of the standard curve, and R² as measured in 41 ELISA plates assayed from May 2022 to August 2023.

Discussion

The data reported in this chapter cover the key performance characteristics relevant to the intended use of the assay as defined by the ICH [264]. The assay meets the pre-determined fit-for-use criteria for linearity, precision and robustness (**Error! Reference source not found.**). Many of these parameters are also evaluated in the same way for serological assessments used for other novel vaccines [265].

The assay detects some cross-reactive responses arising from anti-EBOV GP IgG in the 32 samples used to validate the assay. This finding is consistent with observations from other ELISA assays using polyclonal serum or mAbs derived from vaccinees or survivors, where cross-reactive responses between different members of the *orthoebolavirus* genus can be detected [266-270]. Since the assay's intended use is not to diagnostically distinguish between members of the genus, and this cross-reactivity is likely to represent what happens *in vivo*, this is deemed acceptable. Nevertheless, it would be beneficial to record any history of EBOV vaccination or infection during clinical trials for SUDV vaccines as they may influence the humoral results. If an anti-SUDV GP IgG assay with higher specificity for SUDV is required, a new ELISA may need to be developed. Using linear epitopes from the least conserved regions of the GP could

be a viable strategy to improve specificity for this purpose although this would be unlikely to be reflective of the full spectrum of the antibody response seen *in vivo* as thus may influence the assay's accuracy.

The assay is not currently validated for any changes in parameters not evaluated in the robustness section of this report such as changes to the antigen coating times, sample incubation time or blocking time. For these experimental steps, the time frames specified in the protocol must be adhered to. Should this assay be used for clinical trials for vaccines beyond phase I, a full validation should be performed as per the ICH guidelines. Specifically, it would be beneficial to validate the assay for several other parameters which were not possible at this current time. Future validation experiments should assess assay's accuracy and inter-laboratory precision once an international standard and an alternative laboratory are available, respectively. If validation of the inter-laboratory precision was acceptable it would allow for a multi-site trial to carry out immunological outputs independently which would be key for comparing titres in early phase UK trials to those in later stage trials in a different geographical location.

References

1. Le Guenno, B., et al., *Isolation and partial characterisation of a new strain of Ebola virus*. Lancet, 1995. **345**(8960): p. 1271-4.
2. Cantoni, D., et al., *Risks Posed by Reston, the Forgotten Ebolavirus*. mSphere, 2016. **1**(6).
3. Marsh, G.A., et al., *Ebola Reston virus infection of pigs: clinical significance and transmission potential*. J Infect Dis, 2011. **204** Suppl 3: p. S804-9.
4. Centers for Disease Control and Prevention, *Update: filovirus infection in animal handlers*. MMWR Morb Mortal Wkly Rep, 1990. **39**(13): p. 221.
5. Forbes, K.M., et al., *Bombali Virus in Mops condylurus Bat, Kenya*. Emerg Infect Dis, 2019. **25**(5): p. 955-957.
6. Goldstein, T., et al., *The discovery of Bombali virus adds further support for bats as hosts of ebolaviruses*. Nat Microbiol, 2018. **3**(10): p. 1084-1089.
7. Judson, S.D. and V.J. Munster, *The Multiple Origins of Ebola Disease Outbreaks*. J Infect Dis, 2023. **228**(Suppl 7): p. S465-s473.
8. Leroy, E.M., et al., *Fruit bats as reservoirs of Ebola virus*. Nature, 2005. **438**(7068): p. 575-6.
9. Leroy, E.M., et al., *Human Ebola outbreak resulting from direct exposure to fruit bats in Luebo, Democratic Republic of Congo, 2007*. Vector Borne Zoonotic Dis, 2009. **9**(6): p. 723-8.
10. Baize, S., et al., *Emergence of Zaire Ebola virus disease in Guinea*. N Engl J Med, 2014. **371**(15): p. 1418-25.
11. Vetter, P., et al., *Ebola Virus Shedding and Transmission: Review of Current Evidence*. J Infect Dis, 2016. **214**(suppl 3): p. S177-s184.
12. World Health Organisation, *Health worker Ebola infections in Guinea, Liberia and Sierra Leone: a preliminary report 2015*.
13. World Health Organization, *Ebola Disease caused by Sudan virus - Uganda*, in *Disease Outbreak News*. 2022. p. <https://www.who.int/emergencies/disease-outbreak-news/item/2022-DON410>.
14. Tsou, T.P., *Sudan virus disease - A quick review*. J Formos Med Assoc, 2024. **123**(1): p. 16-22.
15. Malvy, D., et al., *Ebola virus disease*. Lancet, 2019. **393**(10174): p. 936-948.
16. de La Vega, M.A., et al., *Ebola viral load at diagnosis associates with patient outcome and outbreak evolution*. J Clin Invest, 2015. **125**(12): p. 4421-8.
17. Vetter, P., et al., *Sequelae of Ebola virus disease: the emergency within the emergency*. Lancet Infect Dis, 2016. **16**(6): p. e82-e91.
18. Deen, G.F., et al., *Ebola RNA Persistence in Semen of Ebola Virus Disease Survivors - Final Report*. N Engl J Med, 2017. **377**(15): p. 1428-1437.
19. Thorson, A.E., et al., *Persistence of Ebola virus in semen among Ebola virus disease survivors in Sierra Leone: A cohort study of frequency, duration, and risk factors*. PLoS Med, 2021. **18**(2): p. e1003273.
20. Mate, S.E., et al., *Molecular Evidence of Sexual Transmission of Ebola Virus*. N Engl J Med, 2015. **373**(25): p. 2448-54.

21. Diallo, B., et al., *Resurgence of Ebola Virus Disease in Guinea Linked to a Survivor With Virus Persistence in Seminal Fluid for More Than 500 Days*. *Clinical Infectious Diseases*, 2016. **63**(10): p. 1353-1356.
22. Schindell, B.G., et al., *Stigmatization of Ebola virus disease survivors in 2022: A cross-sectional study of survivors in Sierra Leone*. *J Infect Public Health*, 2024. **17**(1): p. 35-43.
23. Overholt, L., et al., *Stigma and Ebola survivorship in Liberia: Results from a longitudinal cohort study*. *PLoS One*, 2018. **13**(11): p. e0206595.
24. Zalwango, G.M., et al., *Stigma among Ebola Disease Survivors in Mubende and Kassanda districts, Central Uganda, 2022*. medRxiv, 2024: p. 2024.05.07.24307005.
25. Izudi, J. and F. Bajunirwe, *Case fatality rate for Ebola disease, 1976-2022: A meta-analysis of global data*. *J Infect Public Health*, 2024. **17**(1): p. 25-34.
26. Centers for Disease Control and Prevention. *Ebola Disease Distribution Map: Cases of Ebola Disease in Africa Since 1976*. 2023 March 24, 2023 March 20, 2024]; Available from: <https://www.cdc.gov/vhf/ebola/history/distribution-map.html>.
27. Mühlberger, E., *Filovirus replication and transcription*. *Future Virol*, 2007. **2**(2): p. 205-215.
28. Volchkov, V.E., et al., *Characterization of the L gene and 5' trailer region of Ebola virus*. *J Gen Virol*, 1999. **80** (Pt 2): p. 355-362.
29. Kiley, M.P., et al., *Conservation of the 3' terminal nucleotide sequences of Ebola and Marburg virus*. *Virology*, 1986. **149**(2): p. 251-4.
30. Sanchez, A. and P.E. Rollin, *Complete genome sequence of an Ebola virus (Sudan species) responsible for a 2000 outbreak of human disease in Uganda*. *Virus Res*, 2005. **113**(1): p. 16-25.
31. Pappalardo, M., et al., *Conserved differences in protein sequence determine the human pathogenicity of Ebolaviruses*. *Sci Rep*, 2016. **6**: p. 23743.
32. Majid, M.U., et al., *Nature and History of Ebola Virus: An Overview*. *Arch Neurosci*, 2016. **3**(3): p. e35027.
33. Sanchez, A., et al., *The virion glycoproteins of Ebola viruses are encoded in two reading frames and are expressed through transcriptional editing*. *Proceedings of the National Academy of Sciences*, 1996. **93**(8): p. 3602-3607.
34. Mehedi, M., et al., *A new Ebola virus nonstructural glycoprotein expressed through RNA editing*. *J Virol*, 2011. **85**(11): p. 5406-14.
35. Volchkov, V.E., et al., *GP mRNA of Ebola virus is edited by the Ebola virus polymerase and by T7 and vaccinia virus polymerases*. *Virology*, 1995. **214**(2): p. 421-30.
36. Volchkova, V.A., H.D. Klenk, and V.E. Volchkov, *Delta-peptide is the carboxy-terminal cleavage fragment of the nonstructural small glycoprotein sGP of Ebola virus*. *Virology*, 1999. **265**(1): p. 164-71.
37. Volchkova, V.A., et al., *The nonstructural small glycoprotein sGP of Ebola virus is secreted as an antiparallel-orientated homodimer*. *Virology*, 1998. **250**(2): p. 408-14.
38. Volchkov, V.E., et al., *Processing of the Ebola virus glycoprotein by the proprotein convertase furin*. *Proc Natl Acad Sci U S A*, 1998. **95**(10): p. 5762-7.
39. Lee, J.E. and E.O. Saphire, *Ebolavirus glycoprotein structure and mechanism of entry*. *Future virology*, 2009. **4**(6): p. 621-635.
40. Volchkova, V.A., et al., *Genomic RNA editing and its impact on Ebola virus adaptation during serial passages in cell culture and infection of guinea pigs*. *J Infect Dis*, 2011. **204** Suppl 3: p. S941-6.

41. Escudero-Pérez, B., et al., *Shed GP of Ebola virus triggers immune activation and increased vascular permeability*. PLoS Pathog, 2014. **10**(11): p. e1004509.
42. Mohan, G.S., et al., *Antigenic subversion: a novel mechanism of host immune evasion by Ebola virus*. PLoS Pathog, 2012. **8**(12): p. e1003065.
43. Saphire, E.O., et al., *Systematic Analysis of Monoclonal Antibodies against Ebola Virus GP Defines Features that Contribute to Protection*. Cell, 2018. **174**(4): p. 938-952.e13.
44. Gunn, B.M., et al., *Antibodies against the Ebola virus soluble glycoprotein are associated with long-term vaccine-mediated protection of non-human primates*. Cell Rep, 2023. **42**(4): p. 112402.
45. Zhu, W., et al., *The Roles of Ebola Virus Soluble Glycoprotein in Replication, Pathogenesis, and Countermeasure Development*. Viruses, 2019. **11**(11).
46. Takada, A., *Filovirus tropism: cellular molecules for viral entry*. Front Microbiol, 2012. **3**: p. 34.
47. Nanbo, A., et al., *Ebolavirus is internalized into host cells via macropinocytosis in a viral glycoprotein-dependent manner*. PLoS Pathog, 2010. **6**(9): p. e1001121.
48. Alvarez, C.P., et al., *C-type lectins DC-SIGN and L-SIGN mediate cellular entry by Ebola virus in cis and in trans*. J Virol, 2002. **76**(13): p. 6841-4.
49. Takada, A., et al., *Downregulation of beta1 integrins by Ebola virus glycoprotein: implication for virus entry*. Virology, 2000. **278**(1): p. 20-6.
50. Kondratowicz, A.S., et al., *T-cell immunoglobulin and mucin domain 1 (TIM-1) is a receptor for Zaire Ebolavirus and Lake Victoria Marburgvirus*. Proc Natl Acad Sci U S A, 2011. **108**(20): p. 8426-31.
51. Bhattacharyya, S. and T.J. Hope, *Cellular factors implicated in filovirus entry*. Adv Virol, 2013. **2013**: p. 487585.
52. Bornholdt, Z.A., et al., *Host-Primed Ebola Virus GP Exposes a Hydrophobic NPC1 Receptor-Binding Pocket, Revealing a Target for Broadly Neutralizing Antibodies*. mBio, 2016. **7**(1): p. e02154-15.
53. Carette, J.E., et al., *Ebola virus entry requires the cholesterol transporter Niemann-Pick C1*. Nature, 2011. **477**(7364): p. 340-3.
54. Côté, M., et al., *Small molecule inhibitors reveal Niemann-Pick C1 is essential for Ebola virus infection*. Nature, 2011. **477**(7364): p. 344-8.
55. Salata, C., et al., *Ebola Virus Entry: From Molecular Characterization to Drug Discovery*. Viruses, 2019. **11**(3).
56. Lamontagne, F., et al., *Evidence-based guidelines for supportive care of patients with Ebola virus disease*. Lancet, 2018. **391**(10121): p. 700-708.
57. World Health Organization, *Therapeutics for Ebola virus disease, 19 August 2022*. 2022, World Health Organization.
58. Mulangu, S., et al., *A Randomized, Controlled Trial of Ebola Virus Disease Therapeutics*. N Engl J Med, 2019. **381**(24): p. 2293-2303.
59. Gaudinski, M.R., et al., *Safety, tolerability, pharmacokinetics, and immunogenicity of the therapeutic monoclonal antibody mAb114 targeting Ebola virus glycoprotein (VRC 608): an open-label phase 1 study*. Lancet, 2019. **393**(10174): p. 889-898.
60. Tshiani Mbaya, O., P. Mukumbayi, and S. Mulangu, *Review: Insights on Current FDA-Approved Monoclonal Antibodies Against Ebola Virus Infection*. Front Immunol, 2021. **12**: p. 721328.
61. Sivapalasingam, S., et al., *Safety, pharmacokinetics, and immunogenicity of a co-formulated cocktail of three human monoclonal antibodies targeting Ebola virus*

- glycoprotein in healthy adults: a randomised, first-in-human phase 1 study.* Lancet Infect Dis, 2018. **18**(8): p. 884-893.
62. Almeida-Pinto, F., R. Pinto, and J. Rocha, *Navigating the Complex Landscape of Ebola Infection Treatment: A Review of Emerging Pharmacological Approaches.* Infect Dis Ther, 2024. **13**(1): p. 21-55.
 63. Feldmann, H., F. Feldmann, and A. Marzi, *Ebola: Lessons on Vaccine Development.* Annu Rev Microbiol, 2018. **72**: p. 423-446.
 64. Henao-Restrepo, A.M., et al., *Efficacy and effectiveness of an rVSV-vectored vaccine in preventing Ebola virus disease: final results from the Guinea ring vaccination, open-label, cluster-randomised trial (Ebola Ça Suffit!).* The Lancet, 2017. **389**(10068): p. 505-518.
 65. *New drug and biological drug products; evidence needed to demonstrate effectiveness of new drugs when human efficacy studies are not ethical or feasible. Final rule.* Fed Regist, 2002. **67**(105): p. 37988-98.
 66. Roozendaal, R., et al., *Nonhuman primate to human immunobridging to infer the protective effect of an Ebola virus vaccine candidate.* NPJ Vaccines, 2020. **5**(1): p. 112.
 67. Barry, H., et al., *Safety and immunogenicity of 2-dose heterologous Ad26. ZEBOV, MVA-BN-Filo Ebola vaccination in healthy and HIV-infected adults: A randomised, placebo-controlled Phase II clinical trial in Africa.* PLoS medicine, 2021. **18**(10): p. e1003813.
 68. Pollard, A.J., et al., *Safety and immunogenicity of a two-dose heterologous Ad26. ZEBOV and MVA-BN-Filo Ebola vaccine regimen in adults in Europe (EBOVAC2): a randomised, observer-blind, participant-blind, placebo-controlled, phase 2 trial.* The Lancet Infectious Diseases, 2021. **21**(4): p. 493-506.
 69. Dolzhikova, I.V., et al., *Safety and immunogenicity of GamEvac-Combi, a heterologous VSV- and Ad5-vectored Ebola vaccine: An open phase I/II trial in healthy adults in Russia.* Hum Vaccin Immunother, 2017. **13**(3): p. 613-620.
 70. Zhu, F.C., et al., *Safety and immunogenicity of a recombinant adenovirus type-5 vector-based Ebola vaccine in healthy adults in Sierra Leone: a single-centre, randomised, double-blind, placebo-controlled, phase 2 trial.* Lancet, 2017. **389**(10069): p. 621-628.
 71. Ewer, K., et al., *A monovalent chimpanzee adenovirus Ebola vaccine boosted with MVA.* New England Journal of Medicine, 2016. **374**(17): p. 1635-1646.
 72. Martin, J.E., et al., *A DNA vaccine for Ebola virus is safe and immunogenic in a phase I clinical trial.* Clin Vaccine Immunol, 2006. **13**(11): p. 1267-77.
 73. Bockstal, V., et al., *First-in-human study to evaluate safety, tolerability, and immunogenicity of heterologous regimens using the multivalent filovirus vaccines Ad26.Filo and MVA-BN-Filo administered in different sequences and schedules: A randomized, controlled study.* PLoS One, 2022. **17**(10): p. e0274906.
 74. Clarke, D.K., et al., *Safety and immunogenicity of a highly attenuated rVSVN4CT1-EBOVGP1 Ebola virus vaccine: a randomised, double-blind, placebo-controlled, phase 1 clinical trial.* Lancet Infect Dis, 2020. **20**(4): p. 455-466.
 75. Fries, L., et al., *Randomized, Blinded, Dose-Ranging Trial of an Ebola Virus Glycoprotein Nanoparticle Vaccine With Matrix-M Adjuvant in Healthy Adults.* J Infect Dis, 2020. **222**(4): p. 572-582.

76. Tebas, P., et al., *Intradermal SynCon® Ebola GP DNA Vaccine Is Temperature Stable and Safely Demonstrates Cellular and Humoral Immunogenicity Advantages in Healthy Volunteers*. *J Infect Dis*, 2019. **220**(3): p. 400-410.
77. Wong, G., et al., *Immunization with vesicular stomatitis virus vaccine expressing the Ebola glycoprotein provides sustained long-term protection in rodents*. *Vaccine*, 2014. **32**(43): p. 5722-9.
78. Jones, S.M., et al., *Assessment of a vesicular stomatitis virus-based vaccine by use of the mouse model of Ebola virus hemorrhagic fever*. *J Infect Dis*, 2007. **196 Suppl 2**: p. S404-12.
79. Marzi, A., et al., *EBOLA VACCINE. VSV-EBOV rapidly protects macaques against infection with the 2014/15 Ebola virus outbreak strain*. *Science*, 2015. **349**(6249): p. 739-42.
80. Jones, S.M., et al., *Live attenuated recombinant vaccine protects nonhuman primates against Ebola and Marburg viruses*. *Nat Med*, 2005. **11**(7): p. 786-90.
81. Geisbert, T.W., et al., *Vesicular stomatitis virus-based ebola vaccine is well-tolerated and protects immunocompromised nonhuman primates*. *PLoS Pathog*, 2008. **4**(11): p. e1000225.
82. Feldmann, H., et al., *Effective post-exposure treatment of Ebola infection*. *PLoS Pathog*, 2007. **3**(1): p. e2.
83. Henao-Restrepo, A.M., et al., *Efficacy and effectiveness of an rVSV-vectored vaccine expressing Ebola surface glycoprotein: interim results from the Guinea ring vaccination cluster-randomised trial*. *Lancet*, 2015. **386**(9996): p. 857-66.
84. Meakin, S., et al., *Effectiveness of rVSV-ZEBOV vaccination during the 2018-20 Ebola virus disease epidemic in the Democratic Republic of the Congo: a retrospective test-negative study*. *Lancet Infect Dis*, 2024.
85. Huttner, A., et al., *Determinants of antibody persistence across doses and continents after single-dose rVSV-ZEBOV vaccination for Ebola virus disease: an observational cohort study*. *Lancet Infect Dis*, 2018. **18**(7): p. 738-748.
86. Bockstal, V., et al., *Non-human primate to human immunobridging demonstrates a protective effect of Ad26.ZEBOV, MVA-BN-Filo vaccine against Ebola*. *NPJ Vaccines*, 2022. **7**(1): p. 156.
87. Callendret, B., et al., *A prophylactic multivalent vaccine against different filovirus species is immunogenic and provides protection from lethal infections with Ebolavirus and Marburgvirus species in non-human primates*. *PloS one*, 2018. **13**(2): p. e0192312.
88. Struyf, F., et al., *Thrombosis with thrombocytopenia syndrome: A database review of clinical trial and post-marketing experience with Ad26.COVS.2*. *Vaccine*, 2023. **41**(37): p. 5351-5359.
89. Puri, A., et al., *Long-Term Clinical Safety of the Ad26.ZEBOV and MVA-BN-Filo Ebola Vaccines: A Prospective, Multi-Country, Observational Study*. *Vaccines (Basel)*, 2024. **12**(2).
90. Milligan, I.D., et al., *Safety and immunogenicity of novel adenovirus type 26–and modified vaccinia ankara–vectored ebola vaccines: a randomized clinical trial*. *Jama*, 2016. **315**(15): p. 1610-1623.
91. Nyombayire, J., et al., *Monitoring of Adverse Events in Recipients of the 2-Dose Ebola Vaccine Regimen of Ad26.ZEBOV Followed by MVA-BN-Filo in the UMURINZI Ebola Vaccination Campaign*. *J Infect Dis*, 2023. **227**(2): p. 268-277.

92. De Santis, O., et al., *Safety and immunogenicity of a chimpanzee adenovirus-vectored Ebola vaccine in healthy adults: a randomised, double-blind, placebo-controlled, dose-finding, phase 1/2a study*. *The Lancet infectious diseases*, 2016. **16**(3): p. 311-320.
93. Stanley, D.A., et al., *Chimpanzee adenovirus vaccine generates acute and durable protective immunity against ebolavirus challenge*. *Nat Med*, 2014. **20**(10): p. 1126-9.
94. Tapia, M.D., et al., *Safety, reactogenicity, and immunogenicity of a chimpanzee adenovirus vectored Ebola vaccine in children in Africa: a randomised, observer-blind, placebo-controlled, phase 2 trial*. *Lancet Infect Dis*, 2020. **20**(6): p. 719-730.
95. Tapia, M.D., et al., *Safety, reactogenicity, and immunogenicity of a chimpanzee adenovirus vectored Ebola vaccine in adults in Africa: a randomised, observer-blind, placebo-controlled, phase 2 trial*. *Lancet Infect Dis*, 2020. **20**(6): p. 707-718.
96. Venkatraman, N., et al., *Safety and immunogenicity of a heterologous prime-boost Ebola virus vaccine regimen in healthy adults in the United Kingdom and Senegal*. *The Journal of infectious diseases*, 2019. **219**(8): p. 1187-1197.
97. Plotkin, S.A. and P.B. Gilbert, *Nomenclature for immune correlates of protection after vaccination*. *Clin Infect Dis*, 2012. **54**(11): p. 1615-7.
98. Meyer, M., D.C. Malherbe, and A. Bukreyev, *Can Ebola Virus Vaccines Have Universal Immune Correlates of protection?* *Trends Microbiol*, 2019. **27**(1): p. 8-16.
99. Marzi, A., et al., *Antibodies are necessary for rVSV/ZEBOV-GP-mediated protection against lethal Ebola virus challenge in nonhuman primates*. *Proc Natl Acad Sci U S A*, 2013. **110**(5): p. 1893-8.
100. Menicucci, A.R., et al., *Transcriptomic analysis reveals a previously unknown role for CD8(+) T-cells in rVSV-EBOV mediated protection*. *Sci Rep*, 2017. **7**(1): p. 919.
101. Grais, R.F., et al., *Estimation of the correlates of protection of the rVSVΔG-ZEBOV-GP Zaire ebolavirus vaccine: a post-hoc analysis of data from phase 2/3 clinical trials*. *Lancet Microbe*, 2021. **2**(2): p. e70-e78.
102. Sullivan, N.J., et al., *CD8+ cellular immunity mediates rAd5 vaccine protection against Ebola virus infection of nonhuman primates*. *Nature medicine*, 2011. **17**(9): p. 1128-1131.
103. Zhao, X., et al., *Immunization-Elicited Broadly Protective Antibody Reveals Ebolavirus Fusion Loop as a Site of Vulnerability*. *Cell*, 2017. **169**(5): p. 891-904.e15.
104. Qiu, X., et al., *Reversion of advanced Ebola virus disease in nonhuman primates with ZMapp*. *Nature*, 2014. **514**(7520): p. 47-53.
105. Kozlov, M., *Ebola outbreak in Uganda: how worried are researchers?* *Nature*, 2022.
106. Iversen, P.L., et al., *Recent successes in therapeutics for Ebola virus disease: no time for complacency*. *Lancet Infect Dis*, 2020. **20**(9): p. e231-e237.
107. World Health Organisation *Sudan Ebolavirus – Experts deliberations Candidate treatments prioritization and trial design discussions*. 2022.
108. Kuang, E., et al., *Reversion of Ebolavirus Disease from a Single Intramuscular Injection of a Pan-Ebolavirus Immunotherapeutic*. *Pathogens*, 2022. **11**(6).
109. Bornholdt, Z.A., et al., *A Two-Antibody Pan-Ebolavirus Cocktail Confers Broad Therapeutic Protection in Ferrets and Nonhuman Primates*. *Cell Host Microbe*, 2019. **25**(1): p. 49-58.e5.
110. Cross, R.W., et al., *Combination therapy with remdesivir and monoclonal antibodies protects nonhuman primates against advanced Sudan virus disease*. *JCI Insight*, 2022. **7**(10).

111. Wailagala, A., et al., *Sudan Virus Disease among Health Care Workers, Uganda, 2022*. N Engl J Med, 2024. **391**(3): p. 285-287.
112. Mwesigwa, B., et al., *Safety, tolerability, and immunogenicity of the Ebola Sudan chimpanzee adenovirus vector vaccine (cAd3-EBO S) in healthy Ugandan adults: a phase 1, open-label, dose-escalation clinical trial*. Lancet Infect Dis, 2023. **23**(12): p. 1408-1417.
113. Tiemessen, M.M., et al., *Protection against Marburg Virus and Sudan Virus in NHP by an Adenovector-Based Trivalent Vaccine Regimen Is Correlated to Humoral Immune Response Levels*. Vaccines (Basel), 2022. **10**(8).
114. Bosaeed, M., et al., *Safety and immunogenicity of ChAdOx1 MERS vaccine candidate in healthy Middle Eastern adults (MERS002): an open-label, non-randomised, dose-escalation, phase 1b trial*. Lancet Microbe, 2022. **3**(1): p. e11-e20.
115. Antrobus, R.D., et al., *Clinical assessment of a novel recombinant simian adenovirus ChAdOx1 as a vectored vaccine expressing conserved Influenza A antigens*. Mol Ther, 2014. **22**(3): p. 668-674.
116. Stylianou, E., et al., *Improvement of BCG protective efficacy with a novel chimpanzee adenovirus and a modified vaccinia Ankara virus both expressing Ag85A*. Vaccine, 2015. **33**(48): p. 6800-8.
117. Folegatti, P.M., et al., *A single dose of ChAdOx1 Chik vaccine induces neutralizing antibodies against four chikungunya virus lineages in a phase 1 clinical trial*. Nature Communications, 2021. **12**(1): p. 4636.
118. Jenkin, D., et al., *Safety and immunogenicity of a ChAdOx1 vaccine against Rift Valley fever in UK adults: an open-label, non-randomised, first-in-human phase 1 clinical trial*. Lancet Infect Dis, 2023. **23**(8): p. 956-964.
119. Cargill, T., et al., *HBV001: Phase I study evaluating the safety and immunogenicity of the therapeutic vaccine ChAdOx1-HBV*. JHEP Rep, 2023. **5**(11): p. 100885.
120. Voysey, M., et al., *Safety and efficacy of the ChAdOx1 nCoV-19 vaccine (AZD1222) against SARS-CoV-2: an interim analysis of four randomised controlled trials in Brazil, South Africa, and the UK*. The Lancet, 2021. **397**(10269): p. 99-111.
121. World Health Organisation, *Update with the development of Ebola vaccines and implications of emerging evidence to inform future policy recommendations. Background paper for SAGE deliberations*.
122. Bausch, D.G., *The need for a new strategy for Ebola vaccination*. Nature Medicine, 2021. **27**(4): p. 580-581.
123. Stanley, D.A., et al., *Chimpanzee adenovirus vaccine generates acute and durable protective immunity against ebolavirus challenge*. Nature medicine, 2014. **20**(10): p. 1126-1129.
124. Ewer, K., *EBOLA Outbreak: Four vaccines assessed in Oxford in six months*. 2016: Jenner Institute Newsletter - Autumn 2016. p. <https://www.jenner.ac.uk/about/newsletter/jenner-institute-newsletter-autumn-2016/ebola-outbreak-four-vaccines-assessed-in-oxford-in-six-months>.
125. Khurana, S., et al., *Human antibody repertoire after VSV-Ebola vaccination identifies novel targets and virus-neutralizing IgM antibodies*. Nat Med, 2016. **22**(12): p. 1439-1447.
126. Tsuji, I., et al., *Development of a Novel Assay to Assess the Avidity of Dengue Virus-Specific Antibodies Elicited in Response to a Tetravalent Dengue Vaccine*. J Infect Dis, 2022. **225**(9): p. 1533-1544.

127. Bauer, G., *The potential significance of high avidity immunoglobulin G (IgG) for protective immunity towards SARS-CoV-2*. *Int J Infect Dis*, 2021. **106**: p. 61-64.
128. Bachmann, M.F., et al., *The role of antibody concentration and avidity in antiviral protection*. *Science*, 1997. **276**(5321): p. 2024-7.
129. Dobaño, C., et al., *Concentration and avidity of antibodies to different circumsporozoite epitopes correlate with RTS,S/AS01E malaria vaccine efficacy*. *Nat Commun*, 2019. **10**(1): p. 2174.
130. Williams, C.A., et al., *High-Avidity Anti-Filovirus IgG Elicited Using Protein Subunit Vaccines Does Not Correlate with Protection*. *Immuno*, 2023. **3**(4): p. 358-374.
131. Cheng, H., et al., *Immunogenicity and Safety of Homologous and Heterologous Prime-Boost Immunization with COVID-19 Vaccine: Systematic Review and Meta-Analysis*. *Vaccines (Basel)*, 2022. **10**(5).
132. Deng, J., et al., *Comparison of the Effectiveness and Safety of Heterologous Booster Doses with Homologous Booster Doses for SARS-CoV-2 Vaccines: A Systematic Review and Meta-Analysis*. *Int J Environ Res Public Health*, 2022. **19**(17).
133. Byazrova, M.G., et al., *Anti-Ad26 humoral immunity does not compromise SARS-COV-2 neutralizing antibody responses following Gam-COVID-Vac booster vaccination*. *NPI Vaccines*, 2022. **7**(1): p. 145.
134. Baden, L.R., et al., *First-in-human evaluation of the safety and immunogenicity of a recombinant adenovirus serotype 26 HIV-1 Env vaccine (IPCAVD 001)*. *J Infect Dis*, 2013. **207**(2): p. 240-7.
135. Crough, T. and R. Khanna, *Immunobiology of human cytomegalovirus: from bench to bedside*. *Clin Microbiol Rev*, 2009. **22**(1): p. 76-98, Table of Contents.
136. Adler, S.P., G. Nigro, and L. Pereira, *Recent advances in the prevention and treatment of congenital cytomegalovirus infections*. *Semin Perinatol*, 2007. **31**(1): p. 10-8.
137. Rowshani, A.T., et al., *Clinical and immunologic aspects of cytomegalovirus infection in solid organ transplant recipients*. *Transplantation*, 2005. **79**(4): p. 381-6.
138. Khan, N., et al., *Herpesvirus-specific CD8 T cell immunity in old age: cytomegalovirus impairs the response to a coresident EBV infection*. *J Immunol*, 2004. **173**(12): p. 7481-9.
139. Sylwester, A.W., et al., *Broadly targeted human cytomegalovirus-specific CD4+ and CD8+ T cells dominate the memory compartments of exposed subjects*. *J Exp Med*, 2005. **202**(5): p. 673-85.
140. Koch, S., et al., *Cytomegalovirus infection: a driving force in human T cell immunosenescence*. *Ann N Y Acad Sci*, 2007. **1114**: p. 23-35.
141. Chidrawar, S., et al., *Cytomegalovirus-seropositivity has a profound influence on the magnitude of major lymphoid subsets within healthy individuals*. *Clin Exp Immunol*, 2009. **155**(3): p. 423-32.
142. Karrer, U., et al., *Memory inflation: continuous accumulation of antiviral CD8+ T cells over time*. *J Immunol*, 2003. **170**(4): p. 2022-9.
143. Crooke, S.N., et al., *Immunosenescence and human vaccine immune responses*. *Immun Ageing*, 2019. **16**: p. 25.
144. Bowyer, G., et al., *Reduced Ebola vaccine responses in CMV+ young adults is associated with expansion of CD57+KLRG1+ T cells*. *J Exp Med*, 2020. **217**(7).
145. Larivière, Y., et al., *Ad26.ZEBOV, MVA-BN-Filo Ebola virus disease vaccine regimen plus Ad26.ZEBOV booster at 1 year versus 2 years in health-care and front-line*

- workers in the Democratic Republic of the Congo: secondary and exploratory outcomes of an open-label, randomised, phase 2 trial. *Lancet Infect Dis*, 2024.
146. Man-Lik Choi, E., et al., *Safety and immunogenicity of an Ad26.ZEBOV booster vaccine in Human Immunodeficiency Virus positive (HIV+) adults previously vaccinated with the Ad26.ZEBOV, MVA-BN-Filo vaccine regimen against Ebola: A single-arm, open-label Phase II clinical trial in Kenya and Uganda*. *Vaccine*, 2023. **41**(50): p. 7573-7580.
 147. Ishola, D., et al., *Safety and long-term immunogenicity of the two-dose heterologous Ad26.ZEBOV and MVA-BN-Filo Ebola vaccine regimen in adults in Sierra Leone: a combined open-label, non-randomised stage 1, and a randomised, double-blind, controlled stage 2 trial*. *Lancet Infect Dis*, 2022. **22**(1): p. 97-109.
 148. Manno, D., et al., *Safety and immunogenicity of an Ad26.ZEBOV booster dose in children previously vaccinated with the two-dose heterologous Ad26.ZEBOV and MVA-BN-Filo Ebola vaccine regimen: an open-label, non-randomised, phase 2 trial*. *Lancet Infect Dis*, 2023. **23**(3): p. 352-360.
 149. Goldstein, N., et al., *Lot-to-lot consistency, immunogenicity, and safety of the Ad26.ZEBOV, MVA-BN-Filo Ebola virus vaccine regimen: A phase 3, randomized, double-blind, placebo-controlled trial*. *Hum Vaccin Immunother*, 2024. **20**(1): p. 2327747.
 150. Wong, G., et al., *Immune parameters correlate with protection against ebola virus infection in rodents and nonhuman primates*. *Sci Transl Med*, 2012. **4**(158): p. 158ra146.
 151. van Dorst, M.M.A.R., et al., *Immunological factors linked to geographical variation in vaccine responses*. *Nature Reviews Immunology*, 2024. **24**(4): p. 250-263.
 152. Fine, P.E., *Variation in protection by BCG: implications of and for heterologous immunity*. *Lancet*, 1995. **346**(8986): p. 1339-45.
 153. Jiang, V., et al., *Performance of rotavirus vaccines in developed and developing countries*. *Hum Vaccin*, 2010. **6**(7): p. 532-42.
 154. Jongo, S.A., et al., *Safety, Immunogenicity, and Protective Efficacy against Controlled Human Malaria Infection of Plasmodium falciparum Sporozoite Vaccine in Tanzanian Adults*. *Am J Trop Med Hyg*, 2018. **99**(2): p. 338-349.
 155. Muyanja, E., et al., *Immune activation alters cellular and humoral responses to yellow fever 17D vaccine*. *J Clin Invest*, 2014. **124**(7): p. 3147-58.
 156. Mentzer, A.J., et al., *Human leukocyte antigen alleles associate with COVID-19 vaccine immunogenicity and risk of breakthrough infection*. *Nature Medicine*, 2023. **29**(1): p. 147-157.
 157. Mentzer, A.J., et al., *High-resolution African HLA resource uncovers HLA-DRB1 expression effects underlying vaccine response*. *Nat Med*, 2024. **30**(5): p. 1384-1394.
 158. Barreto, M.L., et al., *Causes of variation in BCG vaccine efficacy: examining evidence from the BCG REVAC cluster randomized trial to explore the masking and the blocking hypotheses*. *Vaccine*, 2014. **32**(30): p. 3759-64.
 159. Morter, R., et al., *Impact of exposure to malaria and nutritional status on responses to the experimental malaria vaccine ChAd63 MVA ME-TRAP in 5-17 month-old children in Burkina Faso*. *Front Immunol*, 2022. **13**: p. 1058227.
 160. Nookala, S., et al., *Impairment of tetanus-specific cellular and humoral responses following tetanus vaccination in human lymphatic filariasis*. *Infect Immun*, 2004. **72**(5): p. 2598-604.

161. Malhotra, I., et al., *Helminth- and Bacillus Calmette-Guérin-induced immunity in children sensitized in utero to filariasis and schistosomiasis*. J Immunol, 1999. **162**(11): p. 6843-8.
162. Harris, V.C., et al., *Significant Correlation Between the Infant Gut Microbiome and Rotavirus Vaccine Response in Rural Ghana*. J Infect Dis, 2017. **215**(1): p. 34-41.
163. Ng, S.C., et al., *Gut microbiota composition is associated with SARS-CoV-2 vaccine immunogenicity and adverse events*. Gut, 2022. **71**(6): p. 1106-1116.
164. Moorman, J.P., et al., *Impaired hepatitis B vaccine responses during chronic hepatitis C infection: involvement of the PD-1 pathway in regulating CD4(+) T cell responses*. Vaccine, 2011. **29**(17): p. 3169-76.
165. Frasca, D., et al., *Cytomegalovirus (CMV) seropositivity decreases B cell responses to the influenza vaccine*. Vaccine, 2015. **33**(12): p. 1433-9.
166. Derhovanessian, E., et al., *Cytomegalovirus-associated accumulation of late-differentiated CD4 T-cells correlates with poor humoral response to influenza vaccination*. Vaccine, 2013. **31**(4): p. 685-90.
167. Nielsen, C.M., et al., *Impaired NK Cell Responses to Pertussis and H1N1 Influenza Vaccine Antigens in Human Cytomegalovirus-Infected Individuals*. J Immunol, 2015. **194**(10): p. 4657-67.
168. Sharpe, H.R., et al., *CMV-associated T cell and NK cell terminal differentiation does not affect immunogenicity of ChAdOx1 vaccination*. JCI Insight, 2022. **7**(6).
169. Breznik, J.A., et al., *Cytomegalovirus Seropositivity in Older Adults Changes the T Cell Repertoire but Does Not Prevent Antibody or Cellular Responses to SARS-CoV-2 Vaccination*. J Immunol, 2022. **209**(10): p. 1892-1905.
170. O'Connor, D., et al., *The effect of chronic cytomegalovirus infection on pneumococcal vaccine responses*. J Infect Dis, 2014. **209**(10): p. 1635-41.
171. Church, J.A., et al., *Immune responses to oral poliovirus vaccine in HIV-exposed uninfected Zimbabwean infants*. Hum Vaccin Immunother, 2017. **13**(11): p. 2543-2547.
172. Furman, D., et al., *Cytomegalovirus infection enhances the immune response to influenza*. Sci Transl Med, 2015. **7**(281): p. 281ra43.
173. Department of Health and Social Care, *Report of the Cytomegalovirus Steering Group*, D.o.H.a.S. Care, Editor. 2012, The Advisory Committee on the Safety of Blood, Tissues and Organs.
174. Hyde, T.B., D.S. Schmid, and M.J. Cannon, *Cytomegalovirus seroconversion rates and risk factors: implications for congenital CMV*. Rev Med Virol, 2010. **20**(5): p. 311-26.
175. Balegamire, S.J., et al., *Prevalence, incidence, and risk factors associated with cytomegalovirus infection in healthcare and childcare worker: a systematic review and meta-analysis*. Syst Rev, 2022. **11**(1): p. 131.
176. Dowd, J.B., A.E. Aiello, and D.E. Alley, *Socioeconomic disparities in the seroprevalence of cytomegalovirus infection in the US population: NHANES III*. Epidemiol Infect, 2009. **137**(1): p. 58-65.
177. Winter, J.R., et al., *Factors associated with cytomegalovirus serostatus in young people in England: a cross-sectional study*. BMC Infect Dis, 2020. **20**(1): p. 875.
178. Staras, S.A., et al., *Seroprevalence of cytomegalovirus infection in the United States, 1988-1994*. Clin Infect Dis, 2006. **43**(9): p. 1143-51.
179. Lachmann, R., et al., *Cytomegalovirus (CMV) seroprevalence in the adult population of Germany*. PLoS One, 2018. **13**(7): p. e0200267.

180. Furui, Y., et al., *Cytomegalovirus (CMV) seroprevalence in Japanese blood donors and high detection frequency of CMV DNA in elderly donors*. *Transfusion*, 2013. **53**(10): p. 2190-7.
181. Vyse, A.J., L.M. Hesketh, and R.G. Pebody, *The burden of infection with cytomegalovirus in England and Wales: how many women are infected in pregnancy?* *Epidemiol Infect*, 2009. **137**(4): p. 526-33.
182. Bates, M. and A.B. Brantsaeter, *Human cytomegalovirus (CMV) in Africa: a neglected but important pathogen*. *J Virus Erad*, 2016. **2**(3): p. 136-42.
183. Zuhair, M., et al., *Estimation of the worldwide seroprevalence of cytomegalovirus: A systematic review and meta-analysis*. *Rev Med Virol*, 2019. **29**(3): p. e2034.
184. Appay, V., et al., *Memory CD8+ T cells vary in differentiation phenotype in different persistent virus infections*. *Nat Med*, 2002. **8**(4): p. 379-85.
185. European Medicines Agency, *New vaccine for prevention of Ebola virus disease recommended for approval in the European Union*, E.p. office, Editor. 2020. p. 1.
186. Costantini, A., et al., *Effects of cryopreservation on lymphocyte immunophenotype and function*. *J Immunol Methods*, 2003. **278**(1-2): p. 145-55.
187. Ford, T., et al., *Cryopreservation-related loss of antigen-specific IFN γ producing CD4(+) T-cells can skew immunogenicity data in vaccine trials: Lessons from a malaria vaccine trial substudy*. *Vaccine*, 2017. **35**(15): p. 1898-1906.
188. Sakabe, S., et al., *Analysis of CD8(+) T cell response during the 2013-2016 Ebola epidemic in West Africa*. *Proc Natl Acad Sci U S A*, 2018. **115**(32): p. E7578-e7586.
189. Powlson, J., et al., *Characterization of Antigenic MHC-Class-I-Restricted T Cell Epitopes in the Glycoprotein of Ebolavirus*. *Cell Rep*, 2019. **29**(9): p. 2537-2545.e3.
190. Tipton, T.R.W., et al., *Characterisation of the T-cell response to Ebola virus glycoprotein amongst survivors of the 2013-16 West Africa epidemic*. *Nat Commun*, 2021. **12**(1): p. 1153.
191. Jain, S. and M. Baranwal, *Conserved immunogenic peptides of Ebola glycoprotein elicit immune response in human peripheral blood mononuclear cells*. *Microbiol Immunol*, 2021. **65**(11): p. 505-511.
192. Vita, R., et al., *The Immune Epitope Database (IEDB): 2018 update*. *Nucleic Acids Res*, 2019. **47**(D1): p. D339-d343.
193. Balinandi, S., et al., *Molecular characterization of the 2022 Sudan virus disease outbreak in Uganda*. *J Virol*, 2023. **97**(10): p. e0059023.
194. Lex, A., et al., *UpSet: Visualization of Intersecting Sets*. *IEEE Trans Vis Comput Graph*, 2014. **20**(12): p. 1983-92.
195. Andreatta, M. and M. Nielsen, *Gapped sequence alignment using artificial neural networks: application to the MHC class I system*. *Bioinformatics*, 2016. **32**(4): p. 511-7.
196. Nielsen, M., et al., *Reliable prediction of T-cell epitopes using neural networks with novel sequence representations*. *Protein Sci*, 2003. **12**(5): p. 1007-17.
197. Reynisson, B., et al., *NetMHCpan-4.1 and NetMHCIIpan-4.0: improved predictions of MHC antigen presentation by concurrent motif deconvolution and integration of MS MHC eluted ligand data*. *Nucleic Acids Res*, 2020. **48**(W1): p. W449-w454.
198. Barry, H., et al., *Safety and immunogenicity of 2-dose heterologous Ad26.ZEBOV, MVA-BN-Filo Ebola vaccination in healthy and HIV-infected adults: A randomised, placebo-controlled Phase II clinical trial in Africa*. *PLoS Med*, 2021. **18**(10): p. e1003813.

199. Choi, E.M.-L., et al., *Immunogenicity of an Extended Dose Interval for the Ad26.ZEBOV, MVA-BN-Filo Ebola Vaccine Regimen in Adults and Children in the Democratic Republic of the Congo*. *Vaccines*, 2024. **12**(8): p. 828.
200. Pollard, A.J., et al., *Safety and immunogenicity of a two-dose heterologous Ad26.ZEBOV and MVA-BN-Filo Ebola vaccine regimen in adults in Europe (EBOVAC2): a randomised, observer-blind, participant-blind, placebo-controlled, phase 2 trial*. *Lancet Infect Dis*, 2021. **21**(4): p. 493-506.
201. Mutua, G., et al., *Safety and Immunogenicity of a 2-Dose Heterologous Vaccine Regimen With Ad26.ZEBOV and MVA-BN-Filo Ebola Vaccines: 12-Month Data From a Phase 1 Randomized Clinical Trial in Nairobi, Kenya*. *J Infect Dis*, 2019. **220**(1): p. 57-67.
202. Alexandre, M., et al., *Prediction of long-term humoral response induced by the two-dose heterologous Ad26.ZEBOV, MVA-BN-Filo vaccine against Ebola*. *NPJ Vaccines*, 2023. **8**(1): p. 174.
203. Yasmin, T. and A.H. Nabi, *B and T Cell Epitope-Based Peptides Predicted from Evolutionarily Conserved and Whole Protein Sequences of Ebola Virus as Vaccine Targets*. *Scand J Immunol*, 2016. **83**(5): p. 321-37.
204. Srivastava, P.N., et al., *Prediction of Epitope-Based Peptides for Vaccine Development from Coat Proteins GP2 and VP24 of Ebola Virus Using Immunoinformatics*. *International Journal of Peptide Research and Therapeutics*, 2016. **22**(1): p. 119-133.
205. Goonetilleke, N., et al., *Induction of multifunctional human immunodeficiency virus type 1 (HIV-1)-specific T cells capable of proliferation in healthy subjects by using a prime-boost regimen of DNA- and modified vaccinia virus Ankara-vectored vaccines expressing HIV-1 Gag coupled to CD8+ T-cell epitopes*. *J Virol*, 2006. **80**(10): p. 4717-28.
206. Gonzalez-Galarza, Faviel F., et al., *Allele frequency net database (AFND) 2020 update: gold-standard data classification, open access genotype data and new query tools*. *Nucleic Acids Research*, 2019. **48**(D1): p. D783-D788.
207. Cao, K., et al., *Differentiation between African populations is evidenced by the diversity of alleles and haplotypes of HLA class I loci*. *Tissue Antigens*, 2004. **63**(4): p. 293-325.
208. Kijak, G.H., et al., *HLA class I allele and haplotype diversity in Ugandans supports the presence of a major east African genetic cluster*. *Tissue Antigens*, 2009. **73**(3): p. 262-9.
209. Panina-Bordignon, P., et al., *Universally immunogenic T cell epitopes: promiscuous binding to human MHC class II and promiscuous recognition by T cells*. *Eur J Immunol*, 1989. **19**(12): p. 2237-42.
210. Gomez-Perosanz, M., et al., *Characterization of Conserved and Promiscuous Human Rhinovirus CD4 T Cell Epitopes*. *Cells*, 2021. **10**(9).
211. Stryhn, A., et al., *A Systematic, Unbiased Mapping of CD8(+) and CD4(+) T Cell Epitopes in Yellow Fever Vaccinees*. *Front Immunol*, 2020. **11**: p. 1836.
212. Hombrink, P., et al., *Discovery of T cell epitopes implementing HLA-peptidomics into a reverse immunology approach*. *J Immunol*, 2013. **190**(8): p. 3869-77.
213. Kuzushima, K., et al., *Tetramer-assisted identification and characterization of epitopes recognized by HLA A*2402-restricted Epstein-Barr virus-specific CD8+ T cells*. *Blood*, 2003. **101**(4): p. 1460-8.

214. Malik, S., et al., *Ebola Virus Disease Vaccines: Development, Current Perspectives & Challenges*. Vaccines (Basel), 2023. **11**(2).
215. Marzi, A., et al., *Species-specific immunogenicity and protective efficacy of a vesicular stomatitis virus-based Sudan virus vaccine: a challenge study in macaques*. Lancet Microbe, 2023. **4**(3): p. e171-e178.
216. World Health Organisation, *WHO Target Product Profile for multivalent filovirus vaccines: providing long-term protection to high-risk populations*. 2016.
217. Flaxman, A., et al., *Potent immunogenicity and protective efficacy of a multi-pathogen vaccination targeting Ebola, Sudan, Marburg and Lassa virus*. PLoS Pathog, 2024. **20**(6): p. e1012262.
218. Samarasekera, U., *Solidarity Against Ebola: an update*. Lancet Microbe, 2023. **4**(3): p. e139.
219. Flaxman, A., et al., *Reactogenicity and immunogenicity after a late second dose or a third dose of ChAdOx1 nCoV-19 in the UK: a substudy of two randomised controlled trials (COV001 and COV002)*. Lancet, 2021. **398**(10304): p. 981-990.
220. University of Oxford. *Oxford Ebola vaccine manufactured and shipped in record time by SII*. 2022 [cited 2024 20th September 2024]; Available from: <https://www.ox.ac.uk/news/2022-12-15-oxford-ebola-vaccine-manufactured-and-shipped-record-time-sii>.
221. Frater, J., et al., *Safety and immunogenicity of the ChAdOx1 nCoV-19 (AZD1222) vaccine against SARS-CoV-2 in HIV infection: a single-arm substudy of a phase 2/3 clinical trial*. Lancet HIV, 2021. **8**(8): p. e474-e485.
222. Madhi, S.A., et al., *Safety and immunogenicity of the ChAdOx1 nCoV-19 (AZD1222) vaccine against SARS-CoV-2 in people living with and without HIV in South Africa: an interim analysis of a randomised, double-blind, placebo-controlled, phase 1B/2A trial*. Lancet HIV, 2021. **8**(9): p. e568-e580.
223. Hillson, K., et al., *Fertility rates and birth outcomes after ChAdOx1 nCoV-19 (AZD1222) vaccination*. Lancet, 2021. **398**(10312): p. 1683-1684.
224. Li, G., et al., *Safety and immunogenicity of the ChAdOx1 nCoV-19 (AZD1222) vaccine in children aged 6-17 years: a preliminary report of COV006, a phase 2 single-blind, randomised, controlled trial*. Lancet, 2022. **399**(10342): p. 2212-2225.
225. Soboleva, K., et al., *Geographical distribution of TTS cases following AZD1222 (ChAdOx1 nCoV-19) vaccination*. The Lancet Global Health, 2022. **10**(1): p. e33-e34.
226. Cervantes-Torres, J., et al., *Caveats of chimpanzee ChAdOx1 adenovirus-vectored vaccines to boost anti-SARS-CoV-2 protective immunity in mice*. Appl Microbiol Biotechnol, 2024. **108**(1): p. 179.
227. Zamai, L. and M.B.L. Rocchi, *Hypothesis: Possible influence of antivector immunity and SARS-CoV-2 variants on efficacy of ChAdOx1 nCoV-19 vaccine*. Br J Pharmacol, 2022. **179**(2): p. 218-226.
228. Ramasamy, M.N., et al., *Safety and immunogenicity of ChAdOx1 nCoV-19 vaccine administered in a prime-boost regimen in young and old adults (COV002): a single-blind, randomised, controlled, phase 2/3 trial*. Lancet, 2021. **396**(10267): p. 1979-1993.
229. Barrett, J.R., et al., *Phase 1/2 trial of SARS-CoV-2 vaccine ChAdOx1 nCoV-19 with a booster dose induces multifunctional antibody responses*. Nat Med, 2021. **27**(2): p. 279-288.

230. Davis, C., et al., *Effect of Prior ChAdOx1 COVID-19 Immunisation on T-Cell Responses to ChAdOx1-HBV Vaccines* (Basel), 2024. **12**(6).
231. Emary, K.R.W., et al., *Efficacy of ChAdOx1 nCoV-19 (AZD1222) vaccine against SARS-CoV-2 variant of concern 202012/01 (B.1.1.7): an exploratory analysis of a randomised controlled trial*. *Lancet*, 2021. **397**(10282): p. 1351-1362.
232. van Tol, S., et al., *A Bivalent Adenovirus-Vectored Vaccine Induces a Robust Humoral Response, but Does Not Protect Cynomolgus Macaques Against a Lethal Challenge With Sudan Virus*. *The Journal of Infectious Diseases*, 2024.
233. Cross, R.W., et al., *Quadrivalent VesiculoVax vaccine protects nonhuman primates from viral-induced hemorrhagic fever and death*. *J Clin Invest*, 2020. **130**(1): p. 539-551.
234. Geisbert, T.W., et al., *Single-injection vaccine protects nonhuman primates against infection with marburg virus and three species of ebola virus*. *J Virol*, 2009. **83**(14): p. 7296-304.
235. Tsung-Pei, T., *Sudan virus disease – A quick review*. *Journal of the Formosan Medical Association*, 2024. **123**(1): p. 16-22.
236. Matassov, D., et al., *Single-Dose Trivalent VesiculoVax Vaccine Protects Macaques from Lethal Ebolavirus and Marburgvirus Challenge*. *J Virol*, 2018. **92**(3).
237. Vashishtha, V.M. and P. Kumar, *The durability of vaccine-induced protection: an overview*. *Expert Rev Vaccines*, 2024. **23**(1): p. 389-408.
238. Markowitz, L.E., et al., *Duration of live measles vaccine-induced immunity*. *Pediatr Infect Dis J*, 1990. **9**(2): p. 101-10.
239. Taub, D.D., et al., *Immunity from smallpox vaccine persists for decades: a longitudinal study*. *Am J Med*, 2008. **121**(12): p. 1058-64.
240. Hammarlund, E., et al., *Duration of antiviral immunity after smallpox vaccination*. *Nature Medicine*, 2003. **9**(9): p. 1131-1137.
241. Milligan, R., et al., *Vaccines for preventing typhoid fever*. *Cochrane Database Syst Rev*, 2018. **5**(5): p. Cd001261.
242. Palin, A.C., et al., *The persistence of memory: defining, engineering, and measuring vaccine durability*. *Nat Immunol*, 2022. **23**(12): p. 1665-1668.
243. McLean, C., et al., *Persistence of immunological memory as a potential correlate of long-term, vaccine-induced protection against Ebola virus disease in humans*. *Front Immunol*, 2023. **14**: p. 1215302.
244. Wiedemann, A., et al., *Long-lasting severe immune dysfunction in Ebola virus disease survivors*. *Nat Commun*, 2020. **11**(1): p. 3730.
245. Kwiatkowska, K.M., C.G. Mkindi, and C.M. Nielsen, *Human lymphoid tissue sampling for vaccinology*. *Front Immunol*, 2022. **13**: p. 1045529.
246. Halliley, J.L., et al., *Long-Lived Plasma Cells Are Contained within the CD19(-)CD38(hi)CD138(+) Subset in Human Bone Marrow*. *Immunity*, 2015. **43**(1): p. 132-45.
247. Nguyen, D.C., et al., *SARS-CoV-2-specific plasma cells are not durably established in the bone marrow long-lived compartment after mRNA vaccination*. *Nat Med*, 2024.
248. Mei, H.E., et al., *A unique population of IgG-expressing plasma cells lacking CD19 is enriched in human bone marrow*. *Blood*, 2015. **125**(11): p. 1739-48.
249. Davis, C.W., et al., *Influenza vaccine-induced human bone marrow plasma cells decline within a year after vaccination*. *Science*, 2020. **370**(6513): p. 237-241.

250. Barrett, J.R., et al., *Analyses of human vaccine-specific circulating and bone marrow-resident B cell populations reveal benefit of delayed vaccine booster dosing with blood-stage malaria antigens*. *Front Immunol*, 2023. **14**: p. 1193079.
251. Slifka, M.K., et al., *Humoral immunity due to long-lived plasma cells*. *Immunity*, 1998. **8**(3): p. 363-72.
252. Kim, W., et al., *Germinal centre-driven maturation of B cell response to mRNA vaccination*. *Nature*, 2022. **604**(7904): p. 141-145.
253. Turner, J.S., et al., *Human germinal centres engage memory and naive B cells after influenza vaccination*. *Nature*, 2020. **586**(7827): p. 127-132.
254. Lederer, K., et al., *Germinal center responses to SARS-CoV-2 mRNA vaccines in healthy and immunocompromised individuals*. *Cell*, 2022. **185**(6): p. 1008-1024.e15.
255. Lauer, K.B., R. Borrow, and T.J. Blanchard, *Multivalent and Multipathogen Viral Vector Vaccines*. *Clin Vaccine Immunol*, 2017. **24**(1).
256. Taussig, M.J., *CHAPTER 5 - Antigenic Competition*, in *The Antigens*, M. Sela, Editor. 1977, Academic Press. p. 333-368.
257. Schwartzkoff, C.L., et al., *The effects of antigenic competition on the efficacy of multivalent footrot vaccines*. *Aust Vet J*, 1993. **70**(4): p. 123-6.
258. Kallas, E.G., et al., *Antigenic competition in CD4(+) T cell responses in a randomized, multicenter, double-blind clinical HIV vaccine trial*. *Sci Transl Med*, 2019. **11**(519).
259. Böckl, K., et al., *Altering an artificial Gagpolnef polyprotein and mode of ENV co-administration affects the immunogenicity of a clade C HIV DNA vaccine*. *PLoS One*, 2012. **7**(4): p. e34723.
260. Folegatti, P.M., et al., *Safety and immunogenicity of the ChAdOx1 nCoV-19 vaccine against SARS-CoV-2: a preliminary report of a phase 1/2, single-blind, randomised controlled trial*. *The Lancet*, 2020. **396**(10249): p. 467-478.
261. Datto, M.S., et al., *Efficacy and immunogenicity of R21/Matrix-M vaccine against clinical malaria after 2 years' follow-up in children in Burkina Faso: a phase 1/2b randomised controlled trial*. *Lancet Infect Dis*, 2022. **22**(12): p. 1728-1736.
262. Tiono, A.B., et al., *First field efficacy trial of the ChAd63 MVA ME-TRAP vectored malaria vaccine candidate in 5-17 months old infants and children*. *PLoS One*, 2018. **13**(12): p. e0208328.
263. Folegatti, P.M., et al., *Safety and immunogenicity of a candidate Middle East respiratory syndrome coronavirus viral-vectored vaccine: a dose-escalation, open-label, non-randomised, uncontrolled, phase 1 trial*. *Lancet Infect Dis*, 2020. **20**(7): p. 816-826.
264. European Medicines Agency. *ICH Q2(R2) Validation of analytical procedures - Scientific guideline*. 2024 [cited 2024 23rd September 2024]; Available from: <https://www.ema.europa.eu/en/ich-q2r2-validation-analytical-procedures-scientific-guideline>.
265. Rudge, T.L., Jr., et al., *Development, qualification, and validation of the Filovirus Animal Nonclinical Group anti-Ebola virus glycoprotein immunoglobulin G enzyme-linked immunosorbent assay for human serum samples*. *PLoS One*, 2019. **14**(4): p. e0215457.
266. Kainulainen, M.H., et al., *Recombinant Sudan virus and evaluation of humoral cross-reactivity between Ebola and Sudan virus glycoproteins after infection or rVSV-ΔG-ZEBOV-GP vaccination*. *Emerg Microbes Infect*, 2023. **12**(2): p. 2265660.

267. King, L.B., et al., *Achieving cross-reactivity with pan-ebolavirus antibodies*. *Curr Opin Virol*, 2019. **34**: p. 140-148.
268. Diallo, M.S.K., et al., *Temporal evolution of the humoral antibody response after Ebola virus disease in Guinea: a 60-month observational prospective cohort study*. *Lancet Microbe*, 2021. **2**(12): p. e676-e684.
269. Flyak, A.I., et al., *Cross-Reactive and Potent Neutralizing Antibody Responses in Human Survivors of Natural Ebolavirus Infection*. *Cell*, 2016. **164**(3): p. 392-405.
270. Macneil, A., Z. Reed, and P.E. Rollin, *Serologic cross-reactivity of human IgM and IgG antibodies to five species of Ebola virus*. *PLoS Negl Trop Dis*, 2011. **5**(6): p. e1175.

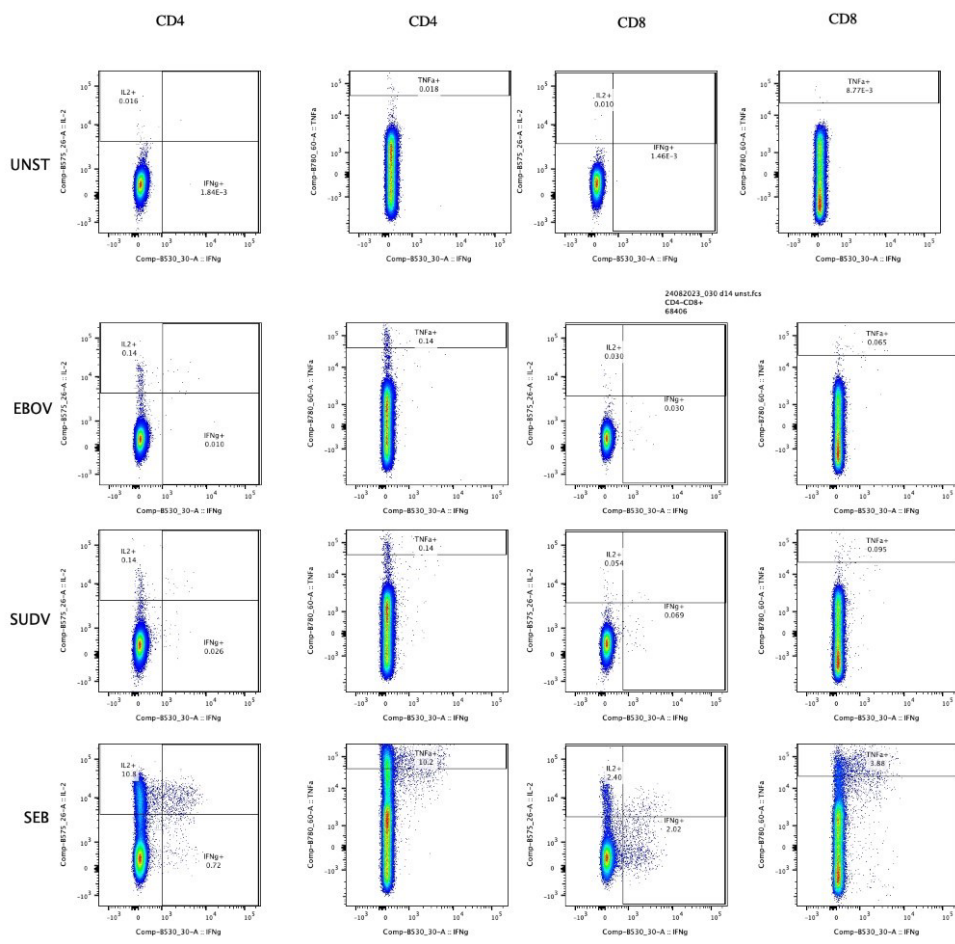
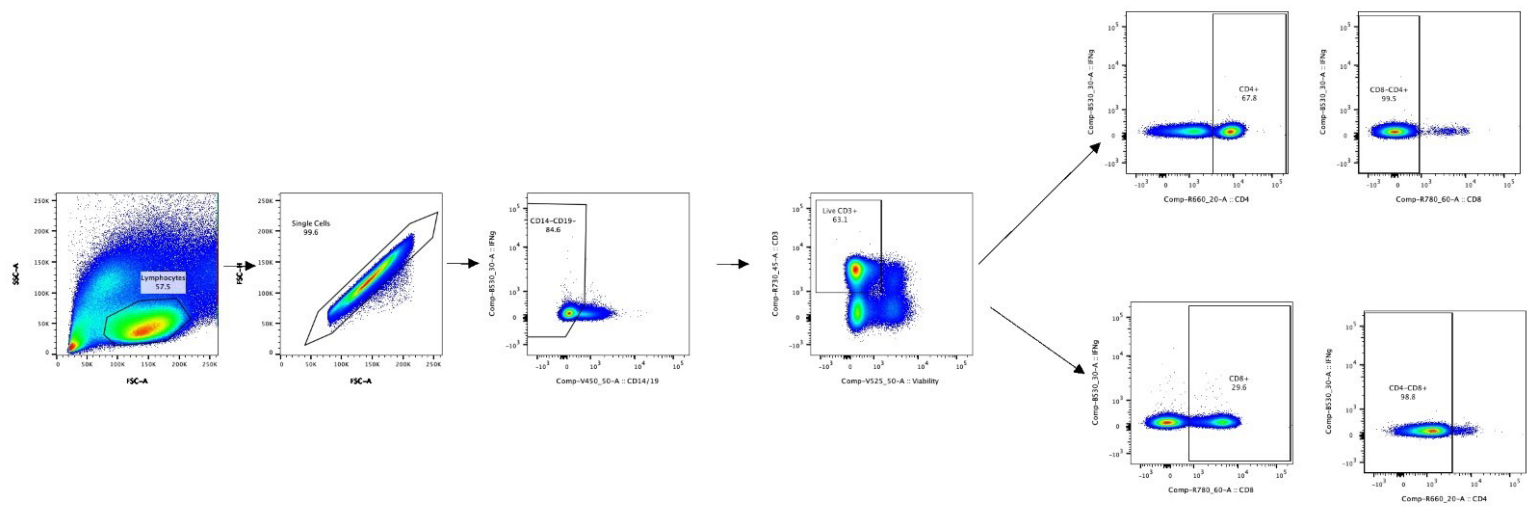


Figure S 8: Exemplar gating strategy for flow cytometry with intracellular cytokine staining from a single sample. SUDV was used in the EBL07 ICS only. A) Lineage gating: Cells were gated on single lymphocytes based on size. Dead cells, CD14+ and CD19+ cells were excluded, and T cells were identified by CD3 expression. T cell subsets were gated as CD4+ and CD8+ populations B) Cytokine gating for CD4+ or CD8+ T cells: cytokine expression was quantified by plotting pairs of cytokines against each other and gating positive populations. Note: stimulation with SUDV peptides was carried out for the EBL07 chapter only (Chapter 6).

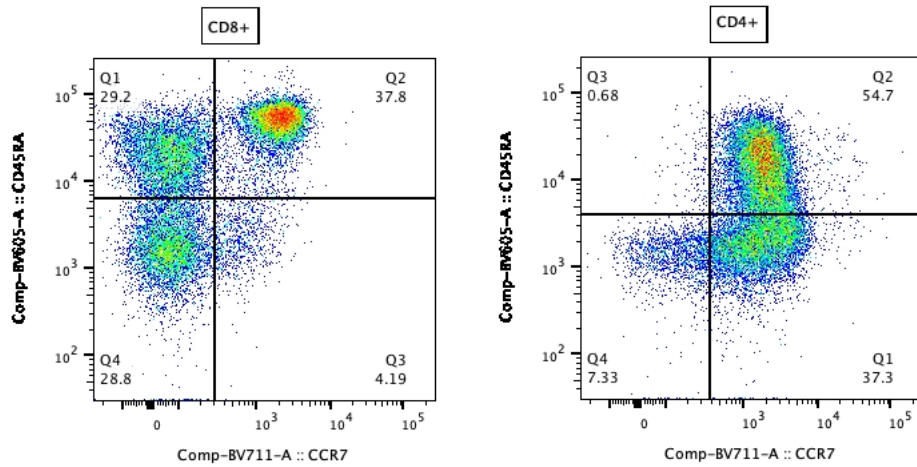


Figure S 9: Exemplar gating strategy for memory markers CCR7 and CD45RA. Lineage gating was carried out as per figure 8 before quadrant gating as shown in this figure.

Table S 3: Amino acid sequences of the peptides spanning either EBOV GP used to stimulate PBMC in ICS assays for the REVOLVE (Chapter 3), RESOLVE (Chapter 4) and PRISM (Chapter 5) clinical trials.

Sequence	Peptide name	ELISpot pools	No. peptides
MGVTGILQLPRDRFK	EB-GP-Z-1	SP	8
GILQLPRDRFKRTSF	EB-GP-Z-2		
LPRDRFKRTSFFLWV	EB-GP-Z-3		
RFKRTSFFLWVILF	EB-GP-Z-4		
TSFFLWVILFQRTF	EB-GP-Z-5		
LWVILFQRTFSIPL	EB-GP-Z-6		
ILFQRTFSIPLGVIH	EB-GP-Z-7		
RTFSIPLGVIHNSTL	EB-GP-Z-8		
IPLGVIHNSTLQV	EB-GP-Z-9	GP1-1	20
LGVIHNSTLQVSDV	EB-GP-Z-10		
IHNSTLQVSDVDKLV	EB-GP-Z-11		
TLQVSDVDKLVCRDK	EB-GP-Z-12		
SDVDKLVCRDKL	EB-GP-Z-13		
DVDKLVCRDKLSSTNQL	EB-GP-Z-14		
CRDKLSSTNQLRSV	EB-GP-Z-15		
KLSSTNQLRSVGLNL	EB-GP-Z-16		
TNQLRSVGLNLEGNGV	EB-GP-Z-17		

SVGLNLEGNVATDV	EB-GP-Z-18		
NLEGNVATDVPSA	EB-GP-Z-19		
GNGVATDVPSATKRW	EB-GP-Z-20		
ATDVPSATKRWGFR	EB-GP-Z-21		
VPSATKRWGFRSGV	EB-GP-Z-22		
ATKRWGFRSGVPPKV	EB-GP-Z-23		
WGFRSGVPPKVVNY	EB-GP-Z-24		
RSGVPPKVVNYEA	EB-GP-Z-25		
GVPPKVVNYEAGEWA	EB-GP-Z-26		
KVVNYEAGEWAENCY	EB-GP-Z-27		
YEAGEWAENCYNLEI	EB-GP-Z-28		
EWAENCYNLEIKK	EB-GP-Z-29		
AENCYNLEIKKPDGS	EB-GP-Z-30		
YNLEIKKPDGSECL	EB-GP-Z-31		
EIKKPDGSECLPAA	EB-GP-Z-32		
KPDGSECLPAAPDGI	EB-GP-Z-33		
SECLPAAPDGIRGF	EB-GP-Z-34		
LPAAPDGIRGFPRCR	EB-GP-Z-35		
PDGIRGFPRCRYVHK	EB-GP-Z-36		
RGFPRCRYVHKV	EB-GP-Z-37		
GFPRCRYVHKVSGTG	EB-GP-Z-38		
CRYVHKVSGTGPCA	EB-GP-Z-39	GP1-2	20
VHKVSGTGPCAGDFA	EB-GP-Z-40		
SGTGPCAGDFAFHK	EB-GP-Z-41		
GPCAGDFAFHKEGAF	EB-GP-Z-42		
GDFAFHKEGAFFLY	EB-GP-Z-43		
AFHKEGAFFLYDRLA	EB-GP-Z-44		
EGAFFLYDRLASTVI	EB-GP-Z-45		
FLYDRLASTVIYR	EB-GP-Z-46		
YDRLASTVIYRGTTF	EB-GP-Z-47		
ASTVIYRGTTFAEGV	EB-GP-Z-48		
IYRGTTFAEGVVAFL	EB-GP-Z-49		
TTFAEGVVAFLIL	EB-GP-Z-50		
FAEGVVAFLILPQAK	EB-GP-Z-51		
VVAFLILPQAKKDF	EB-GP-Z-52	GP1-3	20
LILPQAKKDFSSH	EB-GP-Z-53		
PQAKKDFSSHPLR	EB-GP-Z-54		
KKDFSSHPLREPV	EB-GP-Z-55		

FFSSHPLREPVNA	EB-GP-Z-56		
SSHPLREPVNATED	EB-GP-Z-57		
PLREPVNATEDPSSGY	EB-GP-Z-58		
VNATEDPSSGY	EB-GP-Z-59		
NATEDPSSGYSTTI	EB-GP-Z-60		
DPSSGYSTTIRYQA	EB-GP-Z-61		
GYSTTIRYQATGF	EB-GP-Z-62		
STTIRYQATGFGTNE	EB-GP-Z-63		
RYQATGFGTNETEYL	EB-GP-Z-64		
TGFGTNETEYLFEV	EB-GP-Z-65		
GTNETEYLFVDNL	EB-GP-Z-66		
ETEYLFVDNLTYV	EB-GP-Z-67		
YLFVDNLTYVQL	EB-GP-Z-68		
FEVDNLTYVQLESRF	EB-GP-Z-69	GP1-4	20
NLTYVQLESRFTPQF	EB-GP-Z-70		
VQLESRFTPQFLQL	EB-GP-Z-71		
SRFTPQFLQLNETI	EB-GP-Z-72		
PQFLQLNETIY	EB-GP-Z-73		
FLLQLNETIYTSQKR	EB-GP-Z-74		
LNETIYTSQKRSNTTGK	EB-GP-Z-75		
TSQKRSNTTGKLIWK	EB-GP-Z-76		
RSNTTGKLIWKV	EB-GP-Z-77		
SNTTGKLIWKVNPEI	EB-GP-Z-78		
GKLIWKVNPEIDTTI	EB-GP-Z-79		
WKVNPEIDTTIGEWA	EB-GP-Z-80		
PEIDTTIGEWAFW	EB-GP-Z-81		
IDTTIGEWAFWETKK	EB-GP-Z-82		
IGEWAFWETKKNLTR	EB-GP-Z-83		
AFWETKKNLTRKIR	EB-GP-Z-84		
ETKKNLTRKIRSEEL	EB-GP-Z-85		
NLTRKIRSEELSFTV	EB-GP-Z-86		
KIRSEELSFTVV	EB-GP-Z-87		
IRSEELSFTVVSNGA	EB-GP-Z-88		
ELSFTVVSNGAKNI	EB-GP-Z-89	GP1-5	20
FTVVSNGAKNISGQSPA	EB-GP-Z-90		
GAKNISGQSPAR	EB-GP-Z-91		
AKNISGQSPARTSSD	EB-GP-Z-92		
SGQSPARTSSDPGTN	EB-GP-Z-93		

PARTSSDPGTNTTTEDH	EB-GP-Z-94		
DPGTNTTTEDHKIMA	EB-GP-Z-95		
NTTTEDHKIMASENSSA	EB-GP-Z-96		
HKIMASENSSAMVQV	EB-GP-Z-97		
ASENSSAMVQVH	EB-GP-Z-98		
SENSSAMVQVHSQGR	EB-GP-Z-99		
SAMVQVHSQGREAAV	EB-GP-Z-100		
VQVHSQGREAAVSHL	EB-GP-Z-101		
SQGREAAVSHLTTLA	EB-GP-Z-102		
EAAVSHLTTLATI	EB-GP-Z-103		
AVSHLTTLATISTS	EB-GP-Z-104		
HLTTLATISTSPQSL	EB-GP-Z-105		
LATISTSPQSLTTK	EB-GP-Z-106		
ISTSPQSLTTKPGPD	EB-GP-Z-107		
PQSLTTKPGPDNSTH	EB-GP-Z-108		
TTKPGPDNSTHNTPV	EB-GP-Z-109	GP1-6	20
GPDNSTHNTPVYKL	EB-GP-Z-110		
NSTHNTPVYKLDI	EB-GP-Z-111		
THNTPVYKLDISEA	EB-GP-Z-112		
TPVYKLDISEATQV	EB-GP-Z-113		
YKLDISEATQVEQHH	EB-GP-Z-114		
ISEATQVEQHRR	EB-GP-Z-115		
EATQVEQHRRRDND	EB-GP-Z-116		
VEQHRRRDNDSTA	EB-GP-Z-117		
HRRRDNDSTASDTPSA	EB-GP-Z-118		
NDSTASDTPSATTA	EB-GP-Z-119		
ASDTPSATTAAGPPK	EB-GP-Z-120		
PSATTAAGPPKA	EB-GP-Z-121		
SATTAAGPPKAENTN	EB-GP-Z-122		
AAGPPKAENTNTSK	EB-GP-Z-123		
PPKAENTNTSKSTDF	EB-GP-Z-124		
ENTNTSKSTDFLDPA	EB-GP-Z-125		
TSKSTDFLDPATTS	EB-GP-Z-126		
TDFLDPATTTSPQNH	EB-GP-Z-127		
DPATTTSPQNHSETA	EB-GP-Z-128		
TTSPQNHSETAGNNNTH	EB-GP-Z-129	GP1-7	18
HSETAGNNNTHH	EB-GP-Z-130		
SETAGNNNTHHQDTG	EB-GP-Z-131		

GNNNTHHQDTGEESA	EB-GP-Z-132		
THHQDTGEESASSGK	EB-GP-Z-133		
DTGEESASSGKLGLI	EB-GP-Z-134		
ESASSGKLGLITNTI	EB-GP-Z-135		
SGKLGLITNTIAGVA	EB-GP-Z-136		
GLITNTIAGVAGLI	EB-GP-Z-137		
TNTIAGVAGLITGGR	EB-GP-Z-138		
AGVAGLITGGRTRRR	EB-GP-Z-139		
GLITGGRTRREAIV	EB-GP-Z-140		
GGRTRREAIVNA	EB-GP-Z-141		
RRTRREAIVNAQPK	EB-GP-Z-142		
RREAIVNAQPKCNP	EB-GP-Z-143		
VNAQPKCNP	EB-GP-Z-144		
AQPKCNP	EB-GP-Z-145		
PKCNP	EB-GP-Z-146		
LHYWTTQDEGAAIGL	EB-GP-Z-147		
TTQDEGAAIGLAWI	EB-GP-Z-148		
DEGAAIGLAWIPYF	EB-GP-Z-149		
AAIGLAWIPYFGPAA	EB-GP-Z-150		
LAWIPYFGPAAEGIY	EB-GP-Z-151		
PYFGPAAEGIYIEGL	EB-GP-Z-152		
PAAEGIYIEGLMH	EB-GP-Z-153		
AEGIYIEGLMHNQDGL	EB-GP-Z-154		
IEGLMHNQDGLICGL	EB-GP-Z-155		
MHNQDGLICGLRQLA	EB-GP-Z-156		
DGLICGLRQLANETTQA	EB-GP-Z-157		
LRQLANETTQALQLF	EB-GP-Z-158		
ANETTQALQLFLRA	EB-GP-Z-159		
TTQALQLFLRATTEL	EB-GP-Z-160		
LQLFLRATTELRTF	EB-GP-Z-161		
FLRATTELRTFSIL	EB-GP-Z-162		
ATTELRTFSILNRKA	EB-GP-Z-163		
LRTFSILNRKAIDFL	EB-GP-Z-164		
SILNRKAIDFLLQRW	EB-GP-Z-165		
RKAIDFLLQRWGGTCH	EB-GP-Z-166		
FLLQRWGGTCHIL	EB-GP-Z-167		
LQRWGGTCHILGPDCCI	EB-GP-Z-168	GP2-2	21
TCHILGPDCCIEPH	EB-GP-Z-169		

ILGPDCCIEPHDWTK	EB-GP-Z-170		
DCCIEPHDWTKNI	EB-GP-Z-171		
CIEPHDWTKNITDKI	EB-GP-Z-172		
HDWTKNITDKIDQII	EB-GP-Z-173		
KNITDKIDQIIHDFV	EB-GP-Z-174		
DKIDQIIHDFVDKTL	EB-GP-Z-175		
DQIIHDFVDKTL	EB-GP-Z-176		
IIHDFVDKTLPDQGD	EB-GP-Z-177		
FVDKTLPDQGDNDNW	EB-GP-Z-178		
TLPDQGDNDNWWTGW	EB-GP-Z-179		
DQGDNDNWWTGWRQW	EB-GP-Z-180		
NDNWWTGWRQWIPA	EB-GP-Z-181		
WWTGWRQWIPAGIGV	EB-GP-Z-182		
WRQWIPAGIGVTGVV	EB-GP-Z-183		
IPAGIGVTGVVIAVI	EB-GP-Z-184		
IGVTGVVIAVIALF	EB-GP-Z-185		
TGVVIAVIALFCICK	EB-GP-Z-186		
IAVIALFCICKFVF	EB-GP-Z-187		

R10	R10	R10	GP1-6	GP1-6	GP1-6	R10	R10	R10	GP1-6	GP1-6	GP1-6
R10	R10	R10	GP1-7	GP1-7	GP1-7	R10	R10	R10	GP1-7	GP1-7	GP1-7
SP	SP	SP	GP2-1	GP2-1	GP2-1	SP	SP	SP	GP2-1	GP2-1	GP2-1
GP1-1	GP1-1	GP1-1	GP2-2	GP2-2	GP2-2	GP1-1	GP1-1	GP1-1	GP2-2	GP2-2	GP2-2
GP1-2	GP1-2	GP1-2	Blank	Blank	Blank	GP1-2	GP1-2	GP1-2	Blank	Blank	Blank
GP1-3	GP1-3	GP1-3	Blank	Blank	Blank	GP1-3	GP1-3	GP1-3	Blank	Blank	Blank
GP1-4	GP1-4	GP1-4	Blank	Blank	Blank	GP1-4	GP1-4	GP1-4	Blank	Blank	Blank
GP1-5	GP1-5	GP1-5	PHA/SEB	PHA/SEB	PHA/SEB	GP1-5	GP1-5	GP1-5	PHA/SEB	PHA/SEB	PHA/SEB

Figure S 10: Layout of ELISpot plates as used to assay T cell responses against EBOV GP in the PRISM, REVOLVE and RESOLVE clinical trials. Two volunteers were assayed per plate, 6 negative controls (R10) and 3 positive control wells (PHA/SEB) were including alongside wells containing peptides as described in Table S3. Cells were not added to blank wells, and they were not included in analysis.

Table S 4: Amino acid sequences of the peptides spanning SUDV GP used to stimulate PBMC in ELISpot assays using samples isolated from the PRISM clinical trial (Chapter 5). Peptides were pooled into 4 pools as per Figure S11.

Sequence	Peptide name	ELISpot pools	No. peptides
MPLGVVTNSTLEV	35263_196	GP1-1	46
LGVVTNSTLEVTEI	35263_197		
VTNSTLEVTEIDQLV	35263_198		
TLEVTEIDQLVCKDH	35263_199		
TEIDQLVCKDHL	35263_200		
EIDQLVCKDHLASTDQL	35263_201		
CKDHLASTDQLKSV	35263_202		
HLASTDQLKSVGLNL	35263_203		
TDQLKSVGLNLEGSGV	35263_204		
SVGLNLEGSGVSTDI	35263_205		
NLEGSGVSTDIPSA	35263_206		
GSGVSTDIPSATKRW	35263_207		
STDIPSATKRWGFR	35263_208		
IPSATKRWGFRSGV	35263_209		
ATKRWGFRSGVPPKV	35650_002		
WGFRSGVPPKVVSYS	35650_003		
RSGVPPKVVSYSYA	35650_004		
GVPPKVVSYSYAGEWA	35650_005		
KVVSYSYAGEWAENCY	35650_006		
YEAGEWAENCYNLEI	35263_215		

EWAENCYNLEIKK	35263_216		
AENCYNLEIKKPDGS	35263_217		
YNLEIKKPDGSECL	35263_218		
EIKKPDGSECLPPP	35263_219		
KPDGSECLPPPPDGV	35263_220		
SECLPPPPDGVRGF	35263_221		
LPPPPDGVRGFPRCR	35263_222		
PDGVRGFPRCRYVHK	35263_223		
RGFPRCRYVHKA	35263_224		
GFPRCRYVHKAQGTG	35263_225		
CRYVHKAQGTGPCP	35263_226		
VHKAQGTGPCPGDYA	35263_227		
QGTGPCPGDYAFHK	35263_228		
GPCPGDYAFHKDGAF	35263_229		
GDYAFHKDGAFFLY	35263_230		
AFHKDGAFFLYDRLA	35263_231		
DGAFFLYDRLASTVI	35263_232		
FLYDRLASTVIYR	35263_233		
YDRLASTVIYRGNF	35263_234		
ASTVIYRGNFAEGV	35263_235		
IYRGNFAEGVIAFL	35263_236		
VNFAEGVIAFLIL	35263_237		
FAEGVIAFLILAKPK	35263_238		
VIAFLILAKPKETFL	35263_239		
LILAKPKETFLQSP	35263_240		
AKPKETFLQSPPIR	35263_241		
KETFLQSPPIREAV	35650_007	GP1-2	46
FLQSPPIREAVNY	35650_008		
QSPPIREAVNYTEN	35650_009		
PIREAVNYTENTSSYY	35650_010		
VNYTENTSSYYA	35650_011		
NYTENTSSYYATSYL	35263_247		
NTSSYYATSYLEYEI	35263_248		
YYATSYLEYEIEINF	35263_249		
TSYLEYEIEINFGAQH	35263_250		
EYEIEINFGAQHSTTL	35263_251		
ENFGAQHSTTLFKI	35263_252		
GAQHSTTLFKIDNN	35650_012		

HSTTLFKIDNNTFV	35650_013		
TLFKIDNNTFVRL	35650_014		
FKIDNNTFVRLDRPH	35650_015		
NNTFVRLDRPHTPQF	35650_016		
VRLDRPHTPQFLFQL	35650_017		
RPHTPQFLFQLNDTI	35263_259		
PQFLFQLNDTIH	35650_018		
FLFQLNDTIHLHQQ	35650_019		
LNDTIHLHQQLSNTTGR	35650_020		
LHQQLSNTTGRLIWT	35650_021		
LSNTTGRLIWTL	35650_022		
SNTTGRLIWTLDANI	35650_023		
GRLIWTLDANINADI	35650_024		
WTLDANINADIGEWA	35263_267		
ANINADIGEWAFW	35263_268		
INADIGEWAFWENKK	35263_269		
IGEWAFWENKKNLSE	35263_270		
AFWENKKNLSEQLR	35263_271		
ENKKNLSEQLRGEEL	35263_272		
NLSEQLRGEELSFEA	35650_025		
QLRGEELSFEAL	35650_026		
LRGEELSFEALSLNE	35650_027		
ELSLNEFEALSLNETED	35650_028		
FEALSLNETEDDDAASS	35650_029		
NETEDDDAASSR	35650_030		
ETEDDDAASSRITKG	35650_031		
DDAASSRITKGRISD	35650_032		
SSRITKGRISDRATRKY	35650_033		
GRISDRATRKYSDLV	35263_282		
DRATRKYSDLVPKNSPG	35650_034		
YSDLVPKNSPGMVPL	35650_035		
VPKNSPGMVPLH	35650_036		
PKNSPGMVPLHIPEG	35650_037		
PGMVPLHIPEGETTL	35650_038		
VPLHIPEGETTLPSQ	35650_039		
IPEGETTLPSQNSTE	35650_040		
ETTLPSQNSTEGR	35263_290		
TLPSQNSTEGRRVG	35650_041		
		GP1-3	46

SQNSTEGRRVGVNTQ	35650_042		
TEGRRVGVNTQETI	35650_043		
RRVGVNTQETITETA	35650_044		
VNTQETITETAATII	35650_045		
ETITETAATIIGTNG	35650_046		
ETAATIIGTNGNHM	35650_047		
ATIIGTNGNHMQI	35650_048		
IIGTNGNHMQISTI	35650_049		
TNGNHMQISTIGIR	35650_050		
NHMQISTIGIRPSSS	35650_051		
ISTIGIRPSSSQI	35650_052		
TIGIRPSSSQIPSSS	35650_053		
RPSSSQIPSSSPTT	35650_054		
SSQIPSSSPTTAPSPEA	35650_055		
SSPTTAPSPEAQTPT	35650_056		
TAPSPEAQPTTHTS	35650_057		
PEAQPTTHTSG	35650_058		
EAQPTTHTSGPSVM	35650_059		
PTTHTSGPSVMATE	35650_060		
HTSGPSVMATEEPTT	35650_061		
PSVMATEEPTTPPGS	35650_062		
ATEEPTTPPGSSPGP	35650_063		
PTTPPGSSPGPTTEA	35650_064		
PGSSPGPTTEAPTLT	35650_065		
PGPTTEAPTLTTPENIT	35650_066		
APTLTTPENITT	35263_317		
PTLTPENITTAVKT	35263_318		
TPENITTAVKTVLPQ	35650_067		
ITTAVKTVLPQUESTS	35650_068		
VKTVLPQUESTSNGLI	35650_069		
LPQUESTSNGLITSTV	35650_070		
STSNGLITSTVTGIL	35263_323		
GLITSTVTGILGSL	35263_324		
TSTVTGILGSLGLRK	35263_325		
TGILGSLGLRKRSRR	35263_326		
GSLGLRKRSRRQTNT	35650_071		
LRKRSRRQTNTKA	35650_072		
KRSRRQTNTKATGK	35650_073		

RRQTNTKATGKCNPNL	35650_074		
TKATGKCNPNLHYW	35650_075		
ATGKCNPNLHYW	35263_332		
GKCNPNLHYWTAQEQHN	35263_333		
LHYWTAQEQHNAAGI	35263_334		
TAQEQHNAAGIAWI	35263_335		
EQHNAAGIAWIPYF	35263_336		
NAAGIAWIPYFGPGA	35263_337		
IAWIPYFGPGAEGIY	35263_338		
PYFGPGAEGIYTEGL	35263_339		
PGAEGIYTEGLMH	35263_340		
AEGIYTEGLMHNQNAL	35263_341		
TEGLMHNQNALVCGL	35263_342		
MHNQNALVCGLRQLA	35263_343		
NALVCGLRQLANETTQA	35263_344		
LRQLANETTQALQLF	35263_345		
ANETTQALQLFLRA	35263_346		
TTQALQLFLRATTEL	35263_347		
LQLFLRATTELRTY	35263_348		
FLRATTELRTYIL	35263_349		
ATTELRTYILNRKA	35263_350		
LRTYILNRKAIDFL	35263_351	GP2	41
TILNRKAIDFLLRRW	35263_352		
RKAIDFLLRRWGGTCR	35263_353		
FLLRRWGGTCRIL	35263_354		
LRRWGGTCRILGPDCCI	35263_355		
TCRILGPDCCIEPH	35263_356		
ILGPDCCIEPHDWTK	35263_357		
DCCIEPHDWTKNI	35263_358		
CIEPHDWTKNITDKI	35263_359		
HDWTKNITDKINQII	35263_360		
KNITDKINQIIHDFI	35263_361		
DKINQIIHDFIDNPL	35263_362		
NQIIHDFIDNPL	35263_363		
IIHDFIDNPLPNQDN	35263_364		
FIDNPLPNQDNDDNW	35263_365		
PLPNQDNDDNWWTGW	35263_366		
NQDNDDNWWTGWWRQW	35263_367		

DDNWWTGWRQWIPA	35263_368		
WWTGWRQWIPAGIGI	35263_369		
WRQWIPAGIGITGII	35263_370		
IPAGIGITGIIIAII	35263_371		
IGITGIIIAIALL	35263_372		
TGIIIAIALLCVCK	CPD69133		
IAIALLCVCKLLC	35263_374		

R10	R10	R10	R10	R10	R10	R10	R10	R10	R10	R10	R10
GP1-1	GP1-1	GP1-1	GP1-1	GP1-1	GP1-1	GP1-1	GP1-1	GP1-1	GP1-1	GP1-1	GP1-1
GP1-2	GP1-2	GP1-2	GP1-2	GP1-2	GP1-2	GP1-2	GP1-2	GP1-2	GP1-2	GP1-2	GP1-2
GP1-3	GP1-3	GP1-3	GP1-3	GP1-3	GP1-3	GP1-3	GP1-3	GP1-3	GP1-3	GP1-3	GP1-3
GP2	GP2	GP2	GP2	GP2	GP2	GP2	GP2	GP2	GP2	GP2	GP2
Blank	Blank	Blank	Blank	Blank	Blank	Blank	Blank	Blank	Blank	Blank	Blank
Blank	Blank	Blank	Blank	Blank	Blank	Blank	Blank	Blank	Blank	Blank	Blank
anti-CD3	anti-CD3	anti-CD3	anti-CD3	anti-CD3	anti-CD3	anti-CD3	anti-CD3	anti-CD3	anti-CD3	anti-CD3	anti-CD3

Figure S 11: Layout of the ELISpot plates as used to assay T cell responses against SUDV GP using samples isolated from the PRISM clinical trial. Two volunteers were assayed per plate, 6 negative controls (R10) and 3 positive control wells (PHA/SEB) were including alongside wells containing peptides as described in table S4. Cells were not added to blank wells, and they were not included in analysis. Peptides spanning the SP were not used to stimulate cells in the ELISpot assay.

Table S 5: Amino acid sequences of the peptides spanning either EBOV GP or SUDV GP used to stimulate PBMC in ICS assays for the EBL07 clinical trial. Peptides were pooled into one megapool per species (one for EBOV GP and one for SUDV GP)

Sequence	Peptide no	Mega Pool (species)
MGVTGILQLPRDRFK	1.	EBOV GP
GILQLPRDRFKRTSF	2.	EBOV GP
LPRDRFKRTSFFLWV	3.	EBOV GP
RFKRTSFFLWVILF	4.	EBOV GP
TSFFLWVILFQRTF	5.	EBOV GP
LWVILFQRTFSIPL	6.	EBOV GP
ILFQRTFSIPLGVIH	7.	EBOV GP
RTFSIPLGVIHNSTL	8.	EBOV GP
IPLGVIHNSTLQV	9.	EBOV GP
LGVIHNSTLQVSDV	10.	EBOV GP
IHNSTLQVSDVDKLV	11.	EBOV GP

TLQVSDVDKLVCRDK	12.	EBOV GP
SDVDKLVCRDKL	13.	EBOV GP
DVDKLVCRDKLSSTNQL	14.	EBOV GP
CRDKLSSTNQLRSV	15.	EBOV GP
KLSSTNQLRSVGLNL	16.	EBOV GP
TNQLRSVGLNLEGNV	17.	EBOV GP
SVGLNLEGNVATDV	18.	EBOV GP
NLEGNVATDVPSA	19.	EBOV GP
GNGVATDVPSATKRW	20.	EBOV GP
ATDVPSATKRWGFR	21.	EBOV GP
VPSATKRWGFRSGV	22.	EBOV GP
ATKRWGFRSGVPPKV	23.	EBOV GP
WGFRSGVPPKVVNY	24.	EBOV GP
RSGVPPKVVNYEA	25.	EBOV GP
GVPPKVVNYEAGEWA	26.	EBOV GP
KVVNYEAGEWAENCY	27.	EBOV GP
YEAGEWAENCYNLEI	28.	EBOV GP
EWAENCYNLEIKK	29.	EBOV GP
AENCYNLEIKKPDGS	30.	EBOV GP
YNLEIKKPDGSECL	31.	EBOV GP
EIKKPDGSECLPAA	32.	EBOV GP
KPDGSECLPAAPDGI	33.	EBOV GP
SECLPAAPDGIRGF	34.	EBOV GP
LPAAPDGIRGFPRCR	35.	EBOV GP
PDGIRGFPRCRYVHK	36.	EBOV GP
RGFPRCRYVHKV	37.	EBOV GP
GFPRCRYVHKVSGTG	38.	EBOV GP
CRYVHKVSGTGPCA	39.	EBOV GP
VHKVSGTGPCAGDFA	40.	EBOV GP
SGTGPCAGDFAFHK	41.	EBOV GP
GPCAGDFAFHKEGAF	42.	EBOV GP
GDFAFHKEGAFFLY	43.	EBOV GP
AFHKEGAFFLYDRLA	44.	EBOV GP
EGAFFLYDRLASTVI	45.	EBOV GP
FLYDRLASTVIYR	46.	EBOV GP
YDRLASTVIYRGTTF	47.	EBOV GP
ASTVIYRGTTFAEGV	48.	EBOV GP
IYRGTTFAEGVVAFL	49.	EBOV GP
TTFAEGVVAFLIL	50.	EBOV GP
FAEGVVAFLILPQAK	51.	EBOV GP
VVAFLILPQAKKDF	52.	EBOV GP
LILPQAKKDFSSH	53.	EBOV GP

PQAKKDFSSHPLR	54.	EBOV GP
KKDFSSHPLREPV	55.	EBOV GP
FFSSHPLREPVNA	56.	EBOV GP
SSHPLREPVNATED	57.	EBOV GP
PLREPVNATEDPSSGY	58.	EBOV GP
VNATEDPSSGY	59.	EBOV GP
NATEDPSSGYSTTI	60.	EBOV GP
DPSSGYSTTIRYQA	61.	EBOV GP
GYSTTIRYQATGF	62.	EBOV GP
STTIRYQATGFGTNE	63.	EBOV GP
RYQATGFGTNETEYL	64.	EBOV GP
TGFGTNETEYLFV	65.	EBOV GP
GTNETEYLFVDNL	66.	EBOV GP
ETEYLFVDNLTYV	67.	EBOV GP
YLFVDNLTYVQL	68.	EBOV GP
FEVDNLTYVQLESRF	69.	EBOV GP
NLTYVQLESRFTPQF	70.	EBOV GP
VQLESRFTPQFLQL	71.	EBOV GP
SRFTPQFLQLNETI	72.	EBOV GP
PQFLQLNETIY	73.	EBOV GP
FLLQLNETIYASGKR	74.	EBOV GP
LNETIYASGKRSNTTGK	75.	EBOV GP
ASGKRSNTTGKLIWK	76.	EBOV GP
RSNTTGKLIWKV	77.	EBOV GP
SNTTGKLIWKVNPEI	78.	EBOV GP
GKLIWKVNPEIDTTI	79.	EBOV GP
WKVNPEIDTTIGEWA	80.	EBOV GP
PEIDTTIGEWAFW	81.	EBOV GP
IDTTIGEWAFWETKK	82.	EBOV GP
IGEWAFWETKKNLTR	83.	EBOV GP
AFWETKKNLTKIR	84.	EBOV GP
ETKKNLTKIRSEEL	85.	EBOV GP
NLTKIRSEELSFTA	86.	EBOV GP
KIRSEELSFTAV	87.	EBOV GP
IRSEELSFTAVSNGP	88.	EBOV GP
ELSFTAVSNGPKNI	89.	EBOV GP
FTAVSNGPKNISGQSPA	90.	EBOV GP
GPKNISGQSPAR	91.	EBOV GP
PKNISGQSPARTSSD	92.	EBOV GP
SGQSPARTSSDPETN	93.	EBOV GP
PARTSSDPETNTTNEHDH	94.	EBOV GP
DPETNTTNEHDHKIMA	95.	EBOV GP

NTTNEHDHKIMASENSSA	96.	EBOV GP
HKIMASENSSAMVQV	97.	EBOV GP
ASESSAMVQVH	98.	EBOV GP
SENSAMVQVHSQGR	99.	EBOV GP
SAMVQVHSQGRKAAV	100.	EBOV GP
VQVHSQGRKAAVSHL	101.	EBOV GP
SQGRKAAVSHLTTLA	102.	EBOV GP
KAAVSHLTTLATI	103.	EBOV GP
AVSHLTTLATISTS	104.	EBOV GP
HLTTLATISTSPQSL	105.	EBOV GP
LATISTSPQSLTTK	106.	EBOV GP
ISTSPQSLTTKPGPD	107.	EBOV GP
PQSLTTKPGPDNSTH	108.	EBOV GP
TTKPGPDNTHNTPV	109.	EBOV GP
GPDNTHNTPVYKL	110.	EBOV GP
NSTHNPVYKLDI	111.	EBOV GP
THNPVYKLDISEA	112.	EBOV GP
TPVYKLDISEATQV	113.	EBOV GP
YKLDISEATQVGQHH	114.	EBOV GP
ISEATQVGQHRR	115.	EBOV GP
EATQVGQHRRADND	116.	EBOV GP
VGQHRRADNDSTA	117.	EBOV GP
HHRRADNDSTASDTPPA	118.	EBOV GP
NDSTASDTPPATTA	119.	EBOV GP
ASDTPPATTAAGPLK	120.	EBOV GP
PPATTAAGPLKA	121.	EBOV GP
PATTAAGPLKAENTN	122.	EBOV GP
AAGPLKAENTNTSK	123.	EBOV GP
PLKAENTNTSKSADS	124.	EBOV GP
ENTNTSKSADSLDLA	125.	EBOV GP
TSKSADSLDLATTS	126.	EBOV GP
ADSLDLATTTSPQNY	127.	EBOV GP
DLATTTSPQNYSETA	128.	EBOV GP
TTSPQNYSETAGNNTH	129.	EBOV GP
YSETAGNNTHH	130.	EBOV GP
SETAGNNTHHQDTG	131.	EBOV GP
GNNTHHQDTGEESA	132.	EBOV GP
THHQDTGEESASSGK	133.	EBOV GP
DTGEESASSGKLGLI	134.	EBOV GP
ESASSGKLGLITNTI	135.	EBOV GP
SGKLGLITNTIAGVA	136.	EBOV GP
GLITNTIAGVAGLI	137.	EBOV GP

TNTIAGVAGLITGGR	138.	EBOV GP
AGVAGLITGRRTRR	139.	EBOV GP
GLITGRRTRREVIV	140.	EBOV GP
GRRTRREVIVNA	141.	EBOV GP
RRTRREVIVNAQPK	142.	EBOV GP
RREVIVNAQPKCNPNL	143.	EBOV GP
VNAQPKCNPNLHYW	144.	EBOV GP
AQPKCNPNLHYW	145.	EBOV GP
PKCNPNLHYWTTQDEGA	146.	EBOV GP
LHYWTTQDEGAAIGL	147.	EBOV GP
TTQDEGAAIGLAWI	148.	EBOV GP
DEGAAIGLAWIPYF	149.	EBOV GP
AAIGLAWIPYFGPAA	150.	EBOV GP
LAWIPYFGPAAEGIY	151.	EBOV GP
PYFGPAAEGIYTEGL	152.	EBOV GP
PAAEGIYTEGLMH	153.	EBOV GP
AEGIYTEGLMHNQDGL	154.	EBOV GP
TEGLMHNQDGLICGL	155.	EBOV GP
MHNQDGLICGLRQLA	156.	EBOV GP
DGLICGLRQLANETTQA	157.	EBOV GP
LRQLANETTQALQLF	158.	EBOV GP
ANETTQALQLFLRA	159.	EBOV GP
TTQALQLFLRATTEL	160.	EBOV GP
LQLFLRATTELRTF	161.	EBOV GP
FLRATTELRTFSIL	162.	EBOV GP
ATTELRTFSILNRKA	163.	EBOV GP
LRTFSILNRKAIDFL	164.	EBOV GP
SILNRKAIDFLLQRW	165.	EBOV GP
RKAIDFLLQRWGGTCH	166.	EBOV GP
FLLQRWGGTCHIL	167.	EBOV GP
LQRWGGTCHILGPDCCI	168.	EBOV GP
TCHILGPDCCIEPH	169.	EBOV GP
ILGPDCCIEPHDWTK	170.	EBOV GP
DCCIEPHDWTKNI	171.	EBOV GP
CIEPHDWTKNITDKI	172.	EBOV GP
HDWTKNITDKIDQII	173.	EBOV GP
KNITDKIDQIIHDFV	174.	EBOV GP
DKIDQIIHDFVDKTL	175.	EBOV GP
DQIIHDFVDKTL	176.	EBOV GP
IIHDFVDKTLPDQGD	177.	EBOV GP
FVDKTLPDQGDNDNW	178.	EBOV GP
TLPDQGDNDNWWTGW	179.	EBOV GP

DQGDNDNWWTGWRQW	180.	EBOV GP
NDNWWTGWRQWIPA	181.	EBOV GP
WWTGWRQWIPAGIGV	182.	EBOV GP
WRQWIPAGIGVTGVI	183.	EBOV GP
IPAGIGVTGVIIAVI	184.	EBOV GP
IGVTGVIIAVIALF	185.	EBOV GP
TGVIIAVIALFCICK	186.	EBOV GP
IAVIALFCICKFVF	187.	EBOV GP
MEGLSLLQLPRDKFR	188.	SUDV GP
SLLQLPRDKFRKSSF	189.	SUDV GP
LPRDKFRKSSFFVWV	190.	SUDV GP
KFRKSSFFVWVILF	191.	SUDV GP
SSFFVWVILFQKAF	192.	SUDV GP
VWVILFQKAFSAMPL	193.	SUDV GP
ILFQKAFSAMPLGVVT	194.	SUDV GP
KAFSAMPLGVVTNSTL	195.	SUDV GP
MPLGVVTNSTLEV	196.	SUDV GP
LGVVTNSTLEVTEI	197.	SUDV GP
VTNSTLEVTEIDQLV	198.	SUDV GP
TLEVTEIDQLVCKDH	199.	SUDV GP
TEIDQLVCKDHL	200.	SUDV GP
EIDQLVCKDHLASTDQL	201.	SUDV GP
CKDHLASTDQLKSV	202.	SUDV GP
HLASTDQLKSVGLNL	203.	SUDV GP
TDQLKSVGLNLEGSGV	204.	SUDV GP
SVGLNLEGSGVSTDI	205.	SUDV GP
NLEGSGVSTDIPSA	206.	SUDV GP
GSGVSTDIPSATKRW	207.	SUDV GP
STDIPSATKRWGFR	208.	SUDV GP
IPSATKRWGFRSGV	209.	SUDV GP
ATKRWGFRSGVPPQV	210.	SUDV GP
WGFRSGVPPQVVS	211.	SUDV GP
YEA	212.	SUDV GP
GVPPQVVS	213.	SUDV GP
QVVS	214.	SUDV GP
YEAG	215.	SUDV GP
EA	216.	SUDV GP
ANCYN	217.	SUDV GP
LEIK	218.	SUDV GP
PDGS	219.	SUDV GP
SECL	220.	SUDV GP
PPPD	221.	SUDV GP
GV		
RGF		

LPPPPDGVRGFPRCR	222.	SUDV GP
PDGVRGFPRCRYVHK	223.	SUDV GP
RGFPRCRYVHKA	224.	SUDV GP
GFPRCRYVHKAQGTG	225.	SUDV GP
CRYVHKAQGTGPCP	226.	SUDV GP
VHKAQGTGPCPGDYA	227.	SUDV GP
QGTGPCPGDYAFHK	228.	SUDV GP
GPCPGDYAFHKDGAF	229.	SUDV GP
GDYAFHKDGAFFLY	230.	SUDV GP
AFHKDGAFFLYDRLA	231.	SUDV GP
DGAFFLYDRLASTVI	232.	SUDV GP
FLYDRLASTVIYR	233.	SUDV GP
YDRLASTVIYRGVNF	234.	SUDV GP
ASTVIYRGVNFAEGV	235.	SUDV GP
IYRGVNFAEGVIAFL	236.	SUDV GP
VNFAEGVIAFLIL	237.	SUDV GP
FAEGVIAFLILAKPK	238.	SUDV GP
VIAFLILAKPKETFL	239.	SUDV GP
LILAKPKETFLQSP	240.	SUDV GP
AKPKETFLQSPPIR	241.	SUDV GP
KETFLQSPPIREAA	242.	SUDV GP
FLQSPPIREAAANY	243.	SUDV GP
QSPPIREAAANYTEN	244.	SUDV GP
PIREAAANYTENTSSYY	245.	SUDV GP
ANYTENTSSYYA	246.	SUDV GP
NYTENTSSYYATSYL	247.	SUDV GP
NTSSYYATSYLEYEI	248.	SUDV GP
YYATSYLEYEIENF	249.	SUDV GP
TSYLEYEIENFGAQH	250.	SUDV GP
EYEIENFGAQHSTTL	251.	SUDV GP
ENFGAQHSTTLFKI	252.	SUDV GP
GAQHSTTLFKINNN	253.	SUDV GP
HSTTLFKINNTFV	254.	SUDV GP
TLFKINNTFVLL	255.	SUDV GP
FKINNTFVLLDRPH	256.	SUDV GP
NNTFVLLDRPHTPQF	257.	SUDV GP
VLLDRPHTPQFLFQL	258.	SUDV GP
RPHTPQFLFQLNDTI	259.	SUDV GP
PQFLFQLNDTIQ	260.	SUDV GP
FLFQLNDTIQLHQQL	261.	SUDV GP
LNDTIQLHQQLSNTTGK	262.	SUDV GP
LHQQLSNTTGKLIWT	263.	SUDV GP

LSNTTGKLIWTL	264.	SUDV GP
SNTTGKLIWTLDANI	265.	SUDV GP
GKLIWTLDANINADI	266.	SUDV GP
WTLDANINADIGEWA	267.	SUDV GP
ANINADIGEWAFW	268.	SUDV GP
INADIGEWAFWENKK	269.	SUDV GP
IGEWAFWENKKNLSE	270.	SUDV GP
AFWENKKNLSEQLR	271.	SUDV GP
ENKKNLSEQLRGEEL	272.	SUDV GP
NLSEQLRGEELSFET	273.	SUDV GP
QLRGEELSFETL	274.	SUDV GP
LRGEELSFETLSLNE	275.	SUDV GP
ELSFETLSLNETED	276.	SUDV GP
FETLSLNETEDDDATSS	277.	SUDV GP
NETEDDDATSSR	278.	SUDV GP
ETEDDDATSSRRTTKG	279.	SUDV GP
DDATSSRRTTKGRISD	280.	SUDV GP
SSRRTTKGRISDRATRKY	281.	SUDV GP
GRISDRATRKYSDLV	282.	SUDV GP
DRATRKYSDLVPKDSPG	283.	SUDV GP
YSDLVPKDSPPGMVSL	284.	SUDV GP
VPKDSPPGMVSLH	285.	SUDV GP
PKDSPPGMVSLHVPEG	286.	SUDV GP
PGMVSLHVPEGETTL	287.	SUDV GP
VSLHVPEGETTLPSQ	288.	SUDV GP
VPEGETTLPSQNSTE	289.	SUDV GP
ETTLPSQNSTEGR	290.	SUDV GP
TLPSQNSTEGRRVD	291.	SUDV GP
SQNSTEGRRVDVNTQ	292.	SUDV GP
TEGRRVDVNTQETI	293.	SUDV GP
RRVDVNTQETITETT	294.	SUDV GP
VNTQETITETTATII	295.	SUDV GP
ETITETTATIIGTNG	296.	SUDV GP
ETTATIIGTNGNNM	297.	SUDV GP
ATIIGTNGNNMQI	298.	SUDV GP
IIGTNGNNMQISTI	299.	SUDV GP
TNGNNMQISTIGTG	300.	SUDV GP
NNMQISTIGTGLSSS	301.	SUDV GP
ISTIGTGLSSSQI	302.	SUDV GP
TIGTGLSSSQILSSS	303.	SUDV GP
GLSSSQILSSSPTM	304.	SUDV GP
SSQILSSSPTMAPSPET	305.	SUDV GP

SSPTMAPSPETQTST	306.	SUDV GP
MAPSPETQTSTTYTP	307.	SUDV GP
PETQTSTTYTPK	308.	SUDV GP
ETQTSTTYTPKLPVM	309.	SUDV GP
STTYTPKLPVMTTE	310.	SUDV GP
YTPKLPVMTTEESTT	311.	SUDV GP
LPVMTTEESTTPPRN	312.	SUDV GP
TTEESTTPPRNSPGS	313.	SUDV GP
STTPPRNSPGSTTEA	314.	SUDV GP
PRNSPGSTTEAPTLT	315.	SUDV GP
PGSTTEAPTLTTPENIT	316.	SUDV GP
APTLTTPENITT	317.	SUDV GP
PTLTTPENITTAVKT	318.	SUDV GP
TPENITTAVKTVWPQ	319.	SUDV GP
ITTAVKTVWPQUESTS	320.	SUDV GP
VKTVPQUESTSNGLI	321.	SUDV GP
WPQUESTSNGLITSTV	322.	SUDV GP
STSNGLITSTVTGIL	323.	SUDV GP
GLITSTVTGILGSL	324.	SUDV GP
TSTVTGILGSLGLRK	325.	SUDV GP
TGILGSLGLRKRARR	326.	SUDV GP
GSLGLRKRARRQVNT	327.	SUDV GP
LRKRARRQVNTRA	328.	SUDV GP
KRARRQVNTRATGK	329.	SUDV GP
RRQVNTRATGKCNPNL	330.	SUDV GP
TRATGKCNPNLHYW	331.	SUDV GP
ATGKCNPNLHYW	332.	SUDV GP
GKCNPNLHYWTAQEQHN	333.	SUDV GP
LHYWTAQEQHNAAGI	334.	SUDV GP
TAQEQHNAAGIAWI	335.	SUDV GP
EQHNAAGIAWIPYF	336.	SUDV GP
NAAGIAWIPYFGPGA	337.	SUDV GP
IAWIPYFGPGAEGIY	338.	SUDV GP
PYFGPGAEGIYTEGL	339.	SUDV GP
PGAEGIYTEGLMH	340.	SUDV GP
AEGIYTEGLMHNQNAL	341.	SUDV GP
TEGLMHNQNALVCGL	342.	SUDV GP
MHNQNALVCGLRQLA	343.	SUDV GP
NALVCGLRQLANETTQA	344.	SUDV GP
LRQLANETTQALQLF	345.	SUDV GP
ANETTQALQLFLRA	346.	SUDV GP
TTQALQLFLRATTEL	347.	SUDV GP

LQLFLRATTELRTY	348.	SUDV GP
FLRATTELRTYTIL	349.	SUDV GP
ATTELRTYTILNRKA	350.	SUDV GP
LRTYTILNRKAIDFL	351.	SUDV GP
TILNRKAIDFLLRRW	352.	SUDV GP
RKAIDFLLRRWGGTCR	353.	SUDV GP
FLLRRWGGTCRIL	354.	SUDV GP
LRRWGGTCRILGPDCCI	355.	SUDV GP
TCRILGPDCCIEPH	356.	SUDV GP
ILGPDCCIEPHDWTK	357.	SUDV GP
DCCIEPHDWTKNI	358.	SUDV GP
CIEPHDWTKNITDKI	359.	SUDV GP
HDWTKNITDKINQII	360.	SUDV GP
KNITDKINQIIHDFI	361.	SUDV GP
DKINQIIHDFIDNPL	362.	SUDV GP
NQIIHDFIDNPL	363.	SUDV GP
IIHDFIDNPLPNQDN	364.	SUDV GP
FIDNPLPNQDNDDNW	365.	SUDV GP
PLPNQDNDDNWWTGW	366.	SUDV GP
NQDNDDNWWTGWRQW	367.	SUDV GP
DDNWWTGWRQWIPA	368.	SUDV GP
WWTGWRQWIPAGIGI	369.	SUDV GP
WRQWIPAGIGITGII	370.	SUDV GP
IPAGIGITGIIIAII	371.	SUDV GP
IGITGIIIAIALL	372.	SUDV GP
TGIIIAIALLCVCK	373.	SUDV GP
IAIIALLCVCKLLC	374.	SUDV GP

Table S 6: Binding IgG and ELISpot response for the single volunteer recruited from EBL05 who opted for an Ad26.ZEBOV booster vaccination in the REVOLVE trial. No ELISpot data is available at week 187 as the assay failed to meet QC parameters.

Trial	EBL05				REVOLVE			
Time Point (week)	0	2	8	9	184	185	188	236
Vaccine	cAd3-EBOZ		Ad26.ZEBOV		Ad26.ZEBOV			
Binding IgG (aEU)	56	294	117	3132	121	4768	5275	267
ELISpot response (SFC/10 ⁶ PBMC)	102	535	82	1143	171	X	464	143

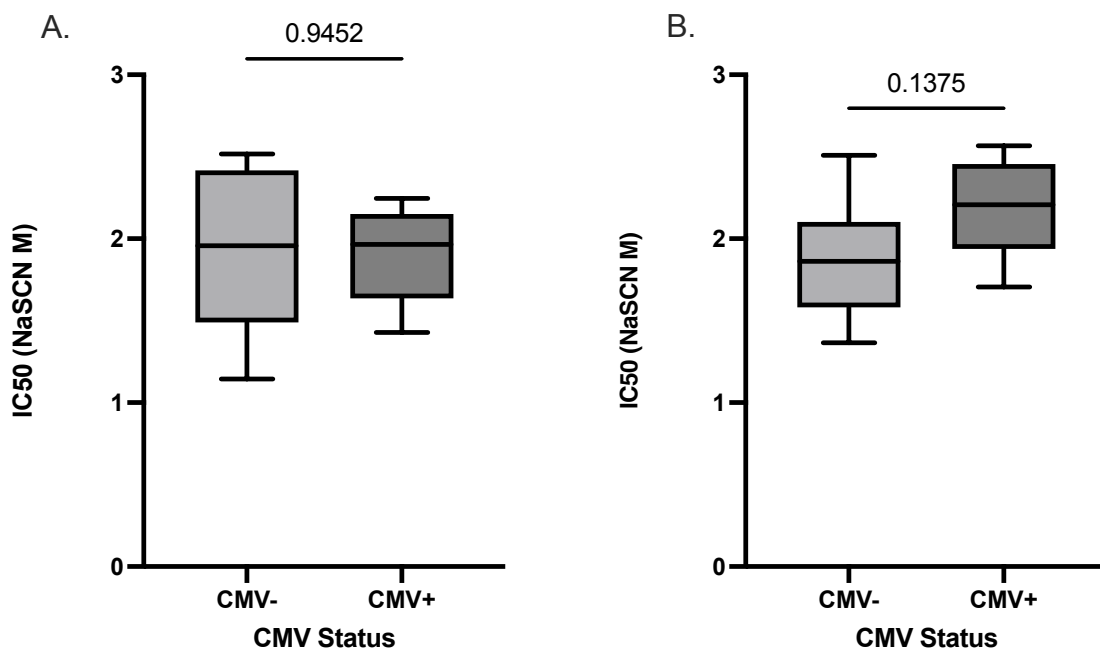


Figure S 12: Antigen-specific IgG avidity stratified by CMV serostatus. A. Avidity at 4.25 post-prime vaccination. B. Avidity 1 year after Ad26.ZEBOV boost.

Table S 7: Persistence of Ebola virus glycoprotein circulating binding antibody response in healthy adults, adolescents and children as measured by the Q2 solutions anti-EBOV GP ELISA assay. Table is adapted from source data [243].

Study	Location Population	Time Point	N	% Persisting Response
EBL2001	France, UK <i>Healthy adults</i>	1 year post-dose 1	50	100%
EBL2002	Burkina Faso, Cote d'Ivoire, Kenya, Uganda <i>Healthy adults</i>	1 year post-dose 1	133	78%
EBL2004	Guinea, Liberia, Mali, Sierra Leone <i>Healthy Adults</i>	1 year post-dose 1	254	80%
EBL3001	Sierra Leone <i>Healthy adults</i>	2 years post-dose 1	158	50-68%
EBL2002	Burkina Faso, Cote d'Ivoire, Kenya, Uganda 4-11 years	1 year post-dose 1	53	98%
EBL2002	Burkina Faso, Cote d'Ivoire, Kenya, Uganda 12–17 years	1 year post-dose 1	54	90%
EBL2004	Guinea, Liberia, Mali, Sierra Leone 1–4 years	1 year post-dose 1	105	100%
EBL2004	Guinea, Liberia, Mali, Sierra Leone 5–11 years	1 year post-dose 1	109	94%
EBL2004	Guinea, Liberia, Mali, Sierra Leone 12–17 years	1 year post-dose 1	127	77%
EBL2011	Sierra Leone 1-3 years	3.2 years post-dose 1	27	96%
EBL2011	Sierra Leone 4-11 years	3.2 years post-dose 1	23	77%

Table S 8: Predicted binding of epitopes to participant MHC class I alleles for each recognised peptide within the pool spanning amino acid positions 33-200. Core: The minimal 9 amino acid binding core directly in contact with the MHC. Rank score binding value: Rank of the predicted binding score compared to a set of random natural peptides.

Experimentally Determined Peptide	Predicted Peptide	Predicted Binding Core	Participant	Predicted Binding Allele	Rank Score Binding Value (%)
GSGVSTDIPSATKRW	GVSTDIPSA	GVSTDIPSA	110	HLA-A*02:01	1.937
	STDIPSATK	STDIPSATK	110	HLA-A*11:01	0.048
	STDIPSATKR	STIPSATKR	110	HLA-A*11:01	0.178
	GVSTDIPSATK	GVSTPSATK	110	HLA-A*11:01	0.202
	VSTDIPSATK	VSTDPSATK	110	HLA-A*11:01	0.284
	SGVSTDIPSATK	STDIPSATK	110	HLA-A*11:01	0.902
	GSGVSTDIPSATK	GTDIPSATK	110	HLA-A*11:01	1.902
STDIPSATKRWGFR	STDIPSATK	STDIPSATK	110	HLA-A*11:01	0.048
	STDIPSATKR	STIPSATKR	110	HLA-A*11:01	0.178
	IPSATKRWGF	IPSATKRGF	110	HLA-B*07:02	0.852
WGFRSGVPPKVVSY	GVPPKVVSY	GVPPKVVSY	130	HLA-A*01:01	0.681
	RSGVPPKVVSY	RSPPKVVSY	130	HLA-A*01:01	0.919
	SGVPPKVVSY	SVPPKVVSY	130	HLA-A*01:01	1.06
	FRSGVPPKVVSY	FVPPKVVSY	130	HLA-A*01:01	1.938
	FRSGVPPKV	FRSGVPPKV	130	HLA-C*07:01	0.034
	FRSGVPPKVVSY	FRPPKVVSY	130	HLA-C*07:01	0.174
	GVPPKVVSY	GVPPKVVSY	130	HLA-C*07:01	0.214
	FRSGVPPKVV	FRSGPPKVV	130	HLA-C*07:01	1.173
	SGVPPKVVSY	SVPPKVVSY	130	HLA-C*07:01	1.38
	VPPKVVSY	VP-PKVVSY	130	HLA-C*07:01	1.389
	RSGVPPKVVSY	RSPPKVVSY	130	HLA-C*07:01	1.745
	FRSGVPPKVVSY	FRPPKVVSY	130	HLA-C*07:02	0.097
	FRSGVPPKV	FRSGVPPKV	130	HLA-C*07:02	0.117

	GVPPKVVS	GVPPKVVS	130	HLA-C*07:02	0.168
	SGVPPKVVS	SVPPKVVS	130	HLA-C*07:02	1.009
	VPPKVVS	VP-PKVVS	130	HLA-C*07:02	1.363
	RSGVPPKVVS	RVPPKVVS	130	HLA-C*07:02	1.826
YEAGEWAENCYNLEI	GEWAENCYNL	GEWAENYNL	110	HLA-B*40:01	0.413
	AENCYNLEI	AENCYNLEI	110	HLA-B*40:01	0.559
	EWAENCYNL	EWAENCYN	0121	HLA-A*24:02	1.352
	GEWAENCYNL	GEWAENYNL	0121	HLA-B*40:01	0.412
	AENCYNLEI	AENCYNLEI	0121	HLA-B*40:01	0.559
	AENCYNLEI	AENCYNLEI	0121	HLA-B*44:02	0.492
	YEAGEWAENCY	YEAGEWAEY	0121	HLA-B*44:02	0.836
	GEWAENCY	GEWAE-NCY	0121	HLA-B*44:02	1.383
	GEWAENCYNL	GEWAENYNL	0121	HLA-B*44:02	1.923
	GEWAENYNL	GEWAENYNL	82	HLA-B*40:01	0.413
EWAENCYNLEIKK	AENCYNLEI	AENCYNLEI	82	HLA-B*40:01	0.559
	AENCYNLEI	AENCYNLEI	110	HLA-B*40:01	0.559
	GVRGFPRCRYVHK	GVRGFVHK	60	HLA-A*03:01	1.425
AENCYNLEIKKPDGS	AENCYNLEI	AENCYNLEI	82	HLA-B*40:01	0.559
PDGVRGFPRCRYVHK	RGFPRCRYVHK	RGFPRYVHK	60	HLA-A*03:01	1.51
	GVRGFPRCR	GVRGFPRCR	60	HLA-A*03:01	1.881
	VRGFPRCRY	VRGFPRCRY	60	HLA-C*07:02	0.732
	VRGFPRCRY	VRGFPRCRY	82	HLA-C*07:01	0.625
	RGFPRCRYV	RGFPRCRYV	82	HLA-C*07:01	1.056
GPCPGDYAFHKDGAF	GPCPGDYAF	GPCPGDYAF	60	HLA-C*07:02	0.94
	YAFHKDGAF	YAFHKDGAF	60	HLA-C*07:02	1.2
	YAFHKDGAF	YAFHKDGAF	82	HLA-B*08:01	1.141
	YAFHKDGAF	YAFHKDGAF	82	HLA-C*03:04	0.082
	YAFHKDGAF	YAFHKDGAF	82	HLA-C*07:01	1.27

AFHKDGAFFLYDRLA	HKDGAFFLY	HKDGAFFLY	82	HLA-A*01:01	0.808
	FHKDGAFFLY	FHKDGAFFLY	82	HLA-A*01:01	1.112
	AFHKDGAFFLY	FHKDGAFFLY	82	HLA-A*01:01	1.231
	FHKDGAFFL	FHKDGAFFL	82	HLA-C*07:01	0.093
	HKDGAFFLY	HKDGAFFLY	82	HLA-C*07:01	0.348
	FHKDGAFFLY	FHKDGAFLY	82	HLA-C*07:01	0.609
	FHKDGAFF	FHKDGAF-F	82	HLA-C*07:01	1.615
FLYDRLASTVIYR	FLYDRLAST	FLYDRLAST	60	HLA-A*02:01	0.032
	FLYDRLASTV	FLYDRLSTV	60	HLA-A*02:01	0.051
	FLYDRLASTVI	FLYDRLASI	60	HLA-A*02:01	0.441
	RLASTVIYR	RLASTVIYR	60	HLA-A*03:01	0.036
	DRLASTVIYR	RLASTVIYR	60	HLA-A*03:01	1.544
	DRLASTVIY	DRLASTVIY	60	HLA-C*07:02	0.468
	YDRLASTVIY	YRLASTVIY	60	HLA-C*07:02	0.53
	LYDRLASTV	LYDRLASTV	60	HLA-C*07:02	1.065
	FLYDRLAST	FLYDRLAST	60	HLA-C*07:02	1.863
	FLYDRLAST	FLYDRLAST	0121	HLA-A*02:01	0.032
	FLYDRLASTV	FLYDRLSTV	0121	HLA-A*02:01	0.051
	FLYDRLASTVI	FLYDRLASI	0121	HLA-A*02:01	0.441
	LYDRLASTV	LYDRLASTV	0121	HLA-A*24:02	0.886
	LYDRLASTV	LYDRLASTV	0121	HLA-C*05:01	1.025
	FLYDRLASTV	FLDRLASTV	0121	HLA-C*05:01	1.959
	YDRLASTVIYRGNF	RLASTVIYRGV	RLASTVIYV	60	HLA-A*02:01
RLASTVIYR		RLASTVIYR	60	HLA-A*03:01	0.036
RLASTVIYRG		RLASTVIYR	60	HLA-A*03:01	1.504
DRLASTVIYR		RLASTVIYR	60	HLA-A*03:01	1.544
DRLASTVIY		DRLASTVIY	60	HLA-C*07:02	0.468

	YDRLASTVIY	YRLASTVIY	60	HLA-C*07:02	0.53
	RLASTVIYRGV	RLASTVIYV	0121	HLA-A*02:01	0.496
	TVIYRGVNF	TVIYRGVNF	0121	HLA-A*24:02	1.978
	TVIYRGVNF	TVIYRGVNF	0121	HLA-C*03:04	1.104

Table S 9: Predicted binding of epitopes to participant MHC class I alleles for each recognised peptide within the pool spanning amino acid positions 190-362. Core: The minimal 9 amino acid binding core directly in contact with the MHC. Rank score binding value: Rank of the predicted binding score compared to a set of random natural peptides.

Experimentally Determined Peptide	Predicted Peptide	Predicted Binding Core	Participant	Predicted Binding Allele	Rank Score Binding Value (%)
NYTENTSSYYATSYL	TENTSSYY	TENTSSY-Y	0106	HLA-B*18:01	0.123
	TENTSSYYATSY	TENTSSTSY	0106	HLA-B*18:01	0.745
	NYTENTSSY	NYTENTSSY	0106	HLA-B*18:01	1.253
	TENTSSYYA	TENTSSYYA	0106	HLA-B*18:01	1.44
	NYTENTSSY	NYTENTSSY	0106	HLA-C*07:01	0.195
	YTENTSSYY	YTENTSSYY	0106	HLA-C*07:01	0.678
	SSYYATSYL	SSYYATSYL	0106	HLA-C*07:01	0.834
	TSSYYATSY	TSSYYATSY	0106	HLA-C*07:01	0.955
	SYYATSYL	SYY-ATSYL	0106	HLA-C*07:01	1.276
	NYTENTSSY	NYTENTSSY	0106	HLA-C*07:02	0.062
	SYYATSYL	SYY-ATSYL	0106	HLA-C*07:02	0.353
	NYTENTSSYY	NYTENTSSY	0106	HLA-C*07:02	0.796
	YTENTSSYY	YTENTSSYY	0106	HLA-C*07:02	1.175
	NYTENTSSY	NYTENTSSY	88	HLA-A*24:02	0.793

	SYATSYL	SY-ATSYL	88	HLA-A*24:02	0.964
	TENTSSYYA	TENTSSYYA	88	HLA-B*41:01	0.072
	YTENTSSYYA	YENTSSYYA	88	HLA-B*41:01	0.914
	TENTSSYYATSY	TENTSSTSY	88	HLA-B*44:02	0.389
	TENTSSYY	TEN-TSSYY	88	HLA-B*44:02	0.54
	TENTSSYYA	TENTSSYYA	88	HLA-B*44:02	1.663
	SYATSYL	SY-ATSYL	88	HLA-C*07:04	0.947
	NYTENTSSY	NYTENTSSY	88	HLA-C*07:04	0.951
	SSYATSYL	SSYATSYL	88	HLA-C*07:04	1.614
	SSYATSYL	SSYATSYL	66	HLA-C*17:01	0.13
EYEIENFGAQHSTTL	FGAQHSTTL	FGAQHSTTL	0106	HLA-B*07:02	1.326
	YEIENFGAQH	YEIEFGAQH	88	HLA-B*18:01	0.44
	YEIENFGAQ	YEIENFGAQ	88	HLA-B*18:01	0.804
	IENFGAQH	IEN-FGAQH	88	HLA-B*18:01	1.058
	YEIENFGA	YEIENF-GA	88	HLA-B*18:01	1.339
	FGAQHSTTL	FGAQHSTTL	66	HLA-C*07:01	0.652
	FGAQHSTTL	FGAQHSTTL	66	HLA-C*07:02	0.795
ENFGAQHSTTLFKI	AQHSTTLFK	AQHSTTLFK	0106	HLA-A*03:01	0.111
	GAQHSTTLFK	GQHSTTLFK	0106	HLA-A*03:01	0.538
	FGAQHSTTLFK	FQHSTTLFK	0106	HLA-A*03:01	1.906
	FGAQHSTTL	FGAQHSTTL	88	HLA-B*07:02	1.326
	AQHSTTLF	AQH-STTLF	88	HLA-B*18:01	1.936
	FGAQHSTTL	FGAQHSTTL	66	HLA-C*07:01	0.652
	FGAQHSTTL	FGAQHSTTL	66	HLA-C*07:02	0.795
FKIDNNTFVRLDRPH	KIDNNTFVR	KIDNNTFVR	106	HLA-A*03:01	1.103
	FKIDNNTFV	FKIDNNTFV	106	HLA-C*07:01	1.123

	FKIDNNTF	FKIDN-NTF	106	HLA-C*07:02	1.318
	FKIDNNTFV	FKIDNNTFV	66	HLA-C*07:02	1.32
ANINADIGEWAFFW	NINADIGEWF	NINADIGEWF	88	HLA-A*25:01	0.148
	NADIGEWAFFW	NAIGEWAFFW	88	HLA-A*25:01	1.2
	NADIGEWAFFW	NAIGEWAFFW	88	HLA-B*58:01	0.717
	INADIGEWAFFW	INADIGEWF	88	HLA-B*58:01	0.739
	NINADIGEWF	NINADIGEWF	88	HLA-B*58:01	1.238
	ANINADIGEWF	AINADIGEWF	88	HLA-B*58:01	1.396
	INADIGEWF	INADIGE-W	88	HLA-B*58:01	1.788
	ADIGEWAFFW	ADIGEWAFFW	88	HLA-B*58:01	1.808
	NADIGEWAFF	NADIGEWAFF	88	HLA-C*02:02	1.887
INADIGEWAFFWENKK	NADIGEWAFFW	NAIGEWAFFW	88	HLA-A*25:01	1.2
	NADIGEWAFFW	NAIGEWAFFW	88	HLA-B*58:01	0.717
	INADIGEWAFFW	INADIGEWF	88	HLA-B*58:01	0.739
	INADIGEWF	INADIGE-W	88	HLA-B*58:01	1.788
	ADIGEWAFFW	ADIGEWAFFW	88	HLA-B*58:01	1.808
	NADIGEWAFF	NADIGEWAFF	88	HLA-C*02:02	1.887

Table S 10: Predicted binding of epitopes to participant MHC class I alleles for each recognised peptide within the pool spanning amino acid positions 515-676. Core: The minimal 9 amino acid binding core directly in contact with the MHC. Rank score binding value: Rank of the predicted binding score compared to a set of random natural peptides.

Experimentally Determined Peptide	Predicted Peptide	Predicted Binding Core	Participant	Predicted Binding Allele	Rank Score Binding Value (%)
LRQLANETTQALQLF	ETTQALQLF	ETTQALQLF	88	HLA-A*25:01	0.015
	NETTQALQLF	NTTQALQLF	88	HLA-A*25:01	1.479
	LANETTQAL	LANETTQAL	88	HLA-A*25:01	1.668
	NETTQALQL	NETTQALQL	88	HLA-B*40:02	0.214
	ANETTQALQL	AETTQALQL	88	HLA-B*40:02	0.485
	ETTQALQLF	ETTQALQLF	88	HLA-B*58:01	0.825
	ANETTQALQLF	ATTQALQLF	88	HLA-B*58:01	1.153
	LANETTQAL	LANETTQAL	88	HLA-C*07:01	0.749
	LANETTQAL	LANETTQAL	88	HLA-C*02:02	0.04
	ETTQALQLF	ETTQALQLF	88	HLA-C*02:02	1.436
LRTYTILNRKAIDFL	YTILNRKAI	YTILNRKAI	88	HLA-A*25:01	1.658
	ILNRKAIDF	ILNRKAIDF	88	HLA-A*32:01	0.94
	RTYTILNRK	RTYTILNRK	88	HLA-A*32:01	1.565
	RTYTILNRKAI	RTYTILNAI	88	HLA-A*32:01	1.765
	YTILNRKAI	YTILNRKAI	88	HLA-C*02:02	1.196
FLLRRWGGTCRIL	RRWGGTCRI	RRWGGTCRI	88	HLA-C*07:01	0.222
	RRWGGTCRIL	RRWGGTRIL	88	HLA-C*07:01	0.276
NQIIHDFIDNPL	HDFIDNPL	HDF-IDNPL	88	HLA-B*40:02	1.111
WWTGWRQWIPAGIGI	WRQWIPAGI	WRQWIPAGI	106	HLA-C*07:01	1.394
WRQWIPAGIGITGII	RQWIPAGIGI	RQWPAGIGI	88	HLA-A*32:01	1.102

	WRQWIPAGI	WRQWIPAGI	88	HLA-C*07:01	1.394
	IPAGIGITGI	IPAGIGITGI	106	HLA-B*07:02	0.767
	IPAGIGITGII	IPAGIGITI	106	HLA-B*07:02	1.283
	IPAGIGITG	IPAGIGITG	106	HLA-B*07:02	1.768

Table S 11: Predicted binding of epitopes to participant MHC class II alleles for each recognised peptide within the pool spanning amino acid positions 33-200. Core: Binding core register. Rank of predicted affinity is compared to a set of 100.000 random natural peptides

Experimentally Determined Peptide	Predicted Peptide	Predicted Binding Core	Participant	Predicted Binding Allele	Rank score binding affinity (%)
AENCYNLEIKKPDGS	AENCYNLEIKKPDGS	YNLEIKKPD	82	DRB1_0801	0.13
PDGVRGFPRCRYVHK	PDGVRGFPRCRYVHK	VRGFPRCRY	82	DRB1_1302	1.6
AENCYNLEIKKPDGS	AENCYNLEIKKPDGS	YNLEIKKPD	60	DRB1_0801	0.15
	AENCYNLEIKKPDGS	YNLEIKKPD	60	DRB1_0801	0.19
	ENCYNLEIKKPDG	YNLEIKKPD	60	DRB1_0801	0.23
	AENCYNLEIKKPDG	YNLEIKKPD	60	DRB1_0801	0.24
	NCYNLEIKKPDGS	YNLEIKKPD	60	DRB1_0801	0.47
	NCYNLEIKKPDG	YNLEIKKPD	60	DRB1_0801	1.56
	AENCYNLEIKKPD	YNLEIKKPD	60	DRB1_0801	1.57
PDGVRGFPRCRYVHK	ENCYNLEIKKPD	YNLEIKKPD	60	DRB1_0801	2.87
	PDGVRGFPRCRYVHK	VRGFPRCRY	60	DRB1_1302	1.07
	PDGVRGFPRCRYVH	VRGFPRCRY	60	DRB1_1302	2.22
	DGVRGFPRCRYVHK	VRGFPRCRY	60	DRB1_1302	3.75
FLYDRLASTVIYR	PDGVRGFPRCRYV	VRGFPRCRY	60	DRB1_1302	3.89
	FLYDRLASTVIYR	YDRLASTVI	121	DRB1_0101	4.39

Table S 12: Predicted binding of epitopes to participant MHC class II alleles for recognised peptide within the pool spanning amino acid positions 190-362. Core: Binding core register. Rank of predicted affinity is compared to a set of 100.000 random natural peptides

Experimentally Determined Peptide	Predicted Peptide	Predicted Binding Core	Participant	Predicted Binding Allele	Rank Score Binding Value (%)
EYEIENFGAQHSTT L	EYEIENFGAQHSTT	IENFGAQH S	106	DRB1_040 3	3.13
	EYEIENFGAQHSTT L	IENFGAQH S	106	DRB1_040 3	3.27
	EYEIENFGAQHST	IENFGAQH S	106	DRB1_040 3	4.53

Table S 13: Predicted binding of epitopes to participant MHC class II alleles for recognised peptide within the pool spanning amino acid positions 515-676. Core: Binding core register. Rank of predicted affinity is compared to a set of 100.000 random natural peptides

Experimentally Determined Peptide	Predicted Peptide	Predicted Binding Core	Participant	Predicted Binding Allele	Rank Score Binding Value (%)
LRTYTILNRKAIDFL	LRTYTILNRKAID	YTILNRKAI	88	DRB1_1302	0.32
	LRTYTILNRKAIDF	YTILNRKAI	88	DRB1_1302	0.35
	RTYTILNRKAIDF	YTILNRKAI	88	DRB1_1302	0.41
	LRTYTILNRKAIDFL	YTILNRKAI	88	DRB1_1302	0.65
	RTYTILNRKAIDFL	YTILNRKAI	88	DRB1_1302	0.79
	RTYTILNRKAID	YTILNRKAI	88	DRB1_1302	1.06